SMITHSONIAN CONTRIBUTIONS TO THE EARTH SCIENCES • NUMBER 28

Field and Laboratory Investigations of Meteorites from Victoria Land and the Thiel Mountains Region, Antarctica, 1982–1983 and 1983–1984

Ursula B. Marvin
and Glenn J. MacPherson

EDITORS

SMITHSONIAN
MAR 0 3 1989
LIBRARIES

SMITHSONIAN INSTITUTION PRESS
Washington, D.C.
1989

AUTHENTICATED
U.S. GOVERNMENT
INFORMATION
GPO

ABSTRACT

Marvin, Ursula B., and Glenn J. MacPherson, editors. Field and Laboratory Investigations of Meteorites from Victoria Land and the Thiel Mountains Region, Antarctica, 1982–1983 and 1983–1984. *Smithsonian Contributions to the Earth Sciences,* number 28, 146 pages, frontispiece, 86 figures, 14 tables, 1989.—This monograph describes the meteorite collecting activities of the United States Antarctic Search for Meteorites (ANSMET) expeditions of the 1982–1983 and 1983–1984 field seasons. Descriptions and classifications are given of most specimens collected during the 1982–1983 season and some of those collected in the 1983–1984 season. Articles are included reviewing topics such as Antarctic achondrites, carbonaceous chondrites, meteorite weathering under polar conditions, trace element contents of Antarctic meteorites in comparison with those found elsewhere, and the meteorite pairing problem. One chapter describes the crystalline fabric of the ice surrounding a meteorite discovered emerging at the surface. The Appendix lists all ANSMET specimens classified as of June 1984, in numerical order for each locality and by meteorite class. The Appendix also includes a tentative list of paired specimens.

OFFICIAL PUBLICATION DATE is handstamped in a limited number of initial copies and is recorded in the Institution's annual report, *Smithsonian Year.* SERIES COVER DESIGN: Aerial view of Ulawun Volcano, New Britain.

Library of Congress Cataloging in Publication Data
Field and laboratory investigations of meteorites from Victoria Land and the Thiel Mountains Region, Antarctica, 1982–1983 and 1983–1984.
(Smithsonian contributions to the earth sciences ; no. 28)
"This monograph describes the meteorite collecting activities of the United States Antarctic Search for Meteorites (ANSMET) expeditions of the 1982–1983 and 1983–1984 field seasons"—P.
Bibliography: p.
1. Meteorites—Antarctic regions—Victoria Land. 2. Meteorites—Antarctic regions—Thiel Mountains Region. I. Marvin, Ursula B. II. MacPherson, Glenn J. III. Series.
QE1.S227 no. 28 550s 88-600361
[QB755.5.A6] [523.5'1]

Contents

Page

1. EDITOR'S INTRODUCTION, by Ursula B. Marvin and Glenn J. MacPherson . . . 1
2. THE 1982–1983 ANTARCTIC SEARCH FOR METEORITES (ANSMET) FIELD PROGRAM, by William A. Cassidy 5
3. THE EXPEDITION TO THE THIEL MOUNTAINS AND PECORA ESCARPMENT, 1982–1983, by John W. Schutt 9
4. EXTENSION OF THE ALLAN HILLS TRIANGULATION NETWORK SYSTEM, by John O. Annexstad and Kristine M. Annexstad 17
5. THE FIELD SEASON IN VICTORIA LAND, 1983–1984, by Robert F. Fudali and John W. Schutt 23
6. DESCRIPTIONS OF STONY METEORITES, by Brian Mason, Glenn J. MacPherson, Roberta Score, Carol Schwarz, and Jeremy S. Delaney 29
7. DESCRIPTIONS OF SOME ANTARCTIC IRON METEORITES, by Roy S. Clarke, Jr. . 61
8. OVERVIEW OF SOME ACHONDRITE GROUPS, by Jeremy S. Delaney and Martin Prinz 65
9. ANTARCTIC CARBONACEOUS CHONDRITES: NEW OPPORTUNITIES FOR RESEARCH, by Harry Y. McSween, Jr. 81
10. THE EMERGING METEORITE: CRYSTALLINE STRUCTURE OF THE ENCLOSING ICE, by Anthony J. Gow and William A. Cassidy 87
11. SIGNIFICANCE OF TERRESTRIAL WEATHERING EFFECTS IN ANTARCTIC METEORITES, by James L. Gooding 93
12. TRACE ELEMENT VARIATIONS BETWEEN ANTARCTIC (VICTORIA LAND) AND NON-ANTARCTIC METEORITES, by Michael E. Lipschutz 99
13. PAIRING OF METEORITES FROM VICTORIA LAND AND THE THIEL MOUNTAINS, ANTARCTICA, by Edward R.D. Scott 103
14. METEORITE DISTRIBUTIONS AT THE ALLAN HILLS MAIN ICEFIELD AND THE PAIRING PROBLEM, by Ursula B. Marvin 113

APPENDIX: Tables of ANSMET Meteorites 121

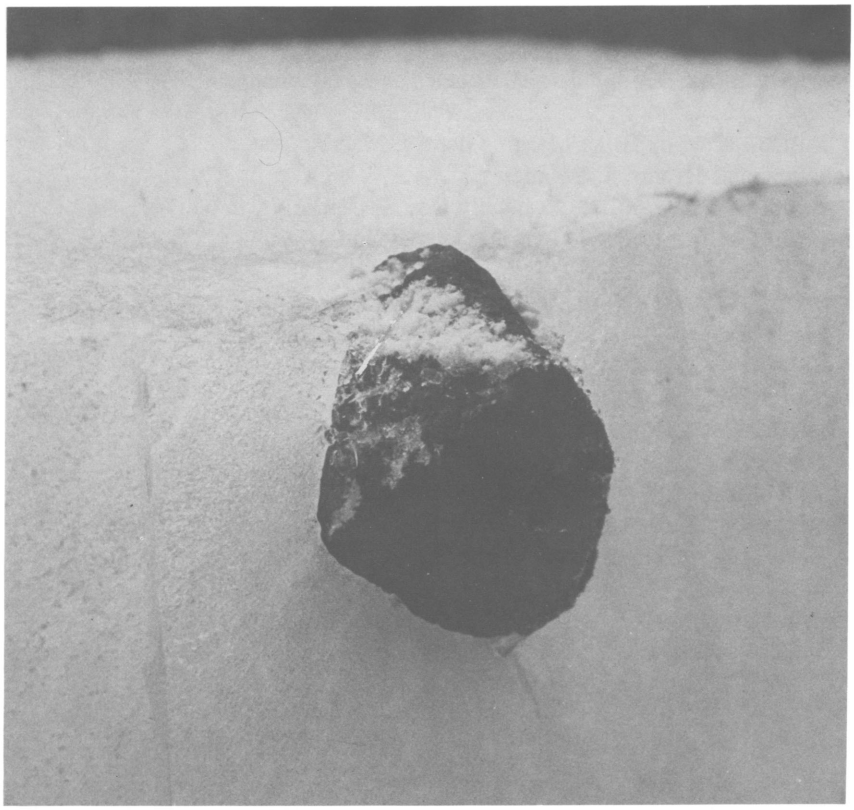

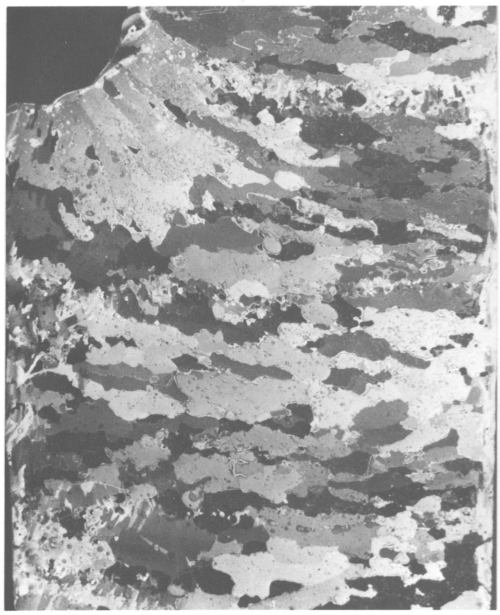

FRONTISPIECE.—The emerging meteorite, ALH82102. *Left:* The meteorite sitting in its enclosing ice after the block had been sawn in half. *Right:* A thin section of the enclosing ice shown in cross-polarized light. Flattened, horizontal ice crystals curve upwards toward the mold of the meteorite at top left of the photo. (Both photographs are at the same scale.)

Field and Laboratory Investigations of Meteorites from Victoria Land and the Thiel Mountains Region, Antarctica, 1982–1983 and 1983–1984

1. Editors' Introduction

Ursula B. Marvin and Glenn J. MacPherson

This is the fourth publication in the Smithsonian Contributions to the Earth Sciences series to present the results of the yearly United States Antarctic Search for Meteorites (ANSMET) expeditions to Antarctica. This issue describes the 1982–1983 and 1983–1984 field seasons in Victoria Land (at about 76°77′S, 159°E) and in the Thiel Mountains region, which lies nearer the South Pole at about 85°86′S, 90°W (Figure 1-1). It includes chapters describing and classifying the meteorites collected in these two seasons, and giving overviews of topics such as the range and character of Antarctic achondrites and carbonaceous chondrites, studies of meteorite weathering under polar conditions, and discussions of the difficult problem of pairing—identifying which specimens are fragments from the same meteorite fall. The first meteorite caught in the act of emerging at the surface of the ice is described, as is the crystalline fabric of the ice surrounding it. Appendix Table A lists all meteorites classified through June 1984 in numerical order for each locality; Appendix Table B lists specimens in consecutive order by meteorite class; and Appendix Table C lists those groups of paired specimens that are generally agreed upon at the present time. Paired groups should always be regarded as tentative because new analyses may identify specimens that do not belong to a group or additional specimens that do.

The numbers and main categories of meteorite specimens collected in the 1982–1983 and 1983–1984 seasons are listed in Table 1-1. Total numbers and aggregate weights of specimens of each meteorite class are given in Appendix Table B. The aggregate weights are of interest because of the inherent intractability of the pairing problem. We are unlikely ever to obtain secure counts of the number of falls of each meteorite class represented on the Antarctic stranding surfaces, and so we cannot compare numbers of Antarctic falls with those in the rest of the world. We can, however, obtain aggregate weights and, allowing for the vagaries of discovery, gain a general idea of how relative proportions of meteorite classes in the Antarctic collections compare with those found elsewhere.

The system for naming Antarctic meteorites was changed in 1982 by the dropping of a letter (A, for example) to designate the collecting expedition. When the system was originally adopted, some members of the Nomenclature Committee looked forward optimistically to a time when two or more expeditions, from different countries or organizations, might visit an area such as the Allan Hills during the same season. They foresaw the need for a letter (A, B, C) to identify each one. Hence, letters and numbers in a name such as ALHA76001 were chosen to indicate place, expedition, year, and specimen number: ALH (Allan Hills), A (Expedition A), 76 (1976), 001 (Specimen 1). In practice, however, meteoriticists viewed the expedition letter as incomprehensible and unnecessary. It has been dropped for all meteorites collected after the 1981 season; thus, the first Allan Hills specimen of 1982 was ALH82001.

The ANSMET program is governed by an interagency agreement between the National Science Foundation, the Smithsonian Institution, and the National Aeronautics and

Ursula B. Marvin, Smithsonian Astrophysical Observatory, Mail Stop 52, 60 Garden Street, Cambridge, Massachusetts 02138. Glenn J. MacPherson, Department of Mineral Sciences, National Museum of Natural History, Smithsonian Institution, Washington, D.C. 20560.

TABLE 1-1.—Numbers of classified meteorite specimens collected in the 1982–1983 and 1983–1984 (in parentheses) seasons.

Locality	Ordinary chondrites	Carbonaceous chondrites	Achondrites	Irons
Allan Hills	39 (77)	4 (3)	2 (3)	
Elephant Moraine	16 (183)	(3)	1 (15)	(3)
Pecora Escarpment	25	1	3	
Thiel Mountains*	14		2	
Taylor Glacier	1			
Inland Forts				1

*Thiel Mountains includes specimens collected at the Davies and Moulton Escarpments.

Space Administration. At the request of the scientific community, procedures (based on those used for lunar samples) were adopted for collecting specimens by sterile techniques and keeping them frozen until they are processed in nitrogen-filled cabinets at the Johnson Space Center at Houston. Details of the field and laboratory procedures are outlined in the first publication in this series (Marvin and Mason, 1980). In order to distribute research samples quickly and widely, all newly classified specimens are described in the *Antarctic Meteorite Newsletters;* these are mailed, on request, to investigators throughout the world. Any scientist wishing to obtain samples may submit a request, describing the proposed research and the numbers, weights, and types of samples required, to the Meteorite Working Group, a committee with a rotating membership responsible for monitoring the program and allocating samples. Requests for the *Antarctic Meteorite Newsletter* or for research materials should be addressed to the Secretary, Meteorite Working Group, Lunar and Planetary Institute, 3303 NASA Road 1, Houston, Texas 77058.

The Antarctic Meteorite Working Group meets twice each year, usually in April and September. Each issue of the newsletter publishes dates of meetings and deadlines for requests. Sample requests are welcome from all qualified scientists and are considered on the basis of their merit regardless of whether a scientist is funded for meteorite research. The allocation of Antarctic meteorite samples does not in any way commit a funding agency to support the proposed research.

For references on Antarctic meteorites, see the earlier publications in this series (Marvin and Mason, 1980, 1982, 1984) and the computerized lists of publications from the *Antarctic Meteorite Bibliography,* which may be obtained on request from the Lunar and Planetary Institute, 3303 NASA Road 1, Houston, Texas 77058. The *Antarctic Meteorite Bibliography* references articles in *Meteoritics,* in the annual proceedings of the Lunar and Planetary Science conferences at Houston, the symposia on Antarctic Meteorites held by the National Institute of Polar Research in Tokyo, and numerous other sources.

Libraries of polished thin sections are maintained in Washington, D.C., Houston, and Tokyo for the use of visitors who wish to make microscopic examinations. To obtain meteorite samples collected by parties sponsored by the Japanese Antarctic Research Expeditions, or to use the thin section library in Tokyo, contact Dr. Keizo Yanai, Curator, at the National Institute of Polar Research, 9-10 Kaga 1-chome, Itabashi-ku, Tokyo 173, Japan. To use the thin section library at the Johnson Space Center at Houston, contact the Secretary of the Meteorite Working Group at the address given above. To use the thin section library at the National Museum of Natural History, Smithsonian Institution, Washington, D.C. 20560, contact Roy S. Clarke, Jr., Curator.

Literature Cited

Marvin, Ursula B., and Brian Mason, editors

1980. Catalog of Antarctic Meteorites, 1977–1978. *Smithsonian Contributions to the Earth Sciences,* 23: 50 pages.

1982. Catalog of Meteorites from Victoria Land, Antarctica, 1978–1980. *Smithsonian Contributions to the Earth Sciences,* 24: 97 pages.

1984. Field and Laboratory Investigations of Meteorites from Victoria Land, Antarctica. *Smithsonian Contributions to the Earth Sciences,* 26: 138 pages.

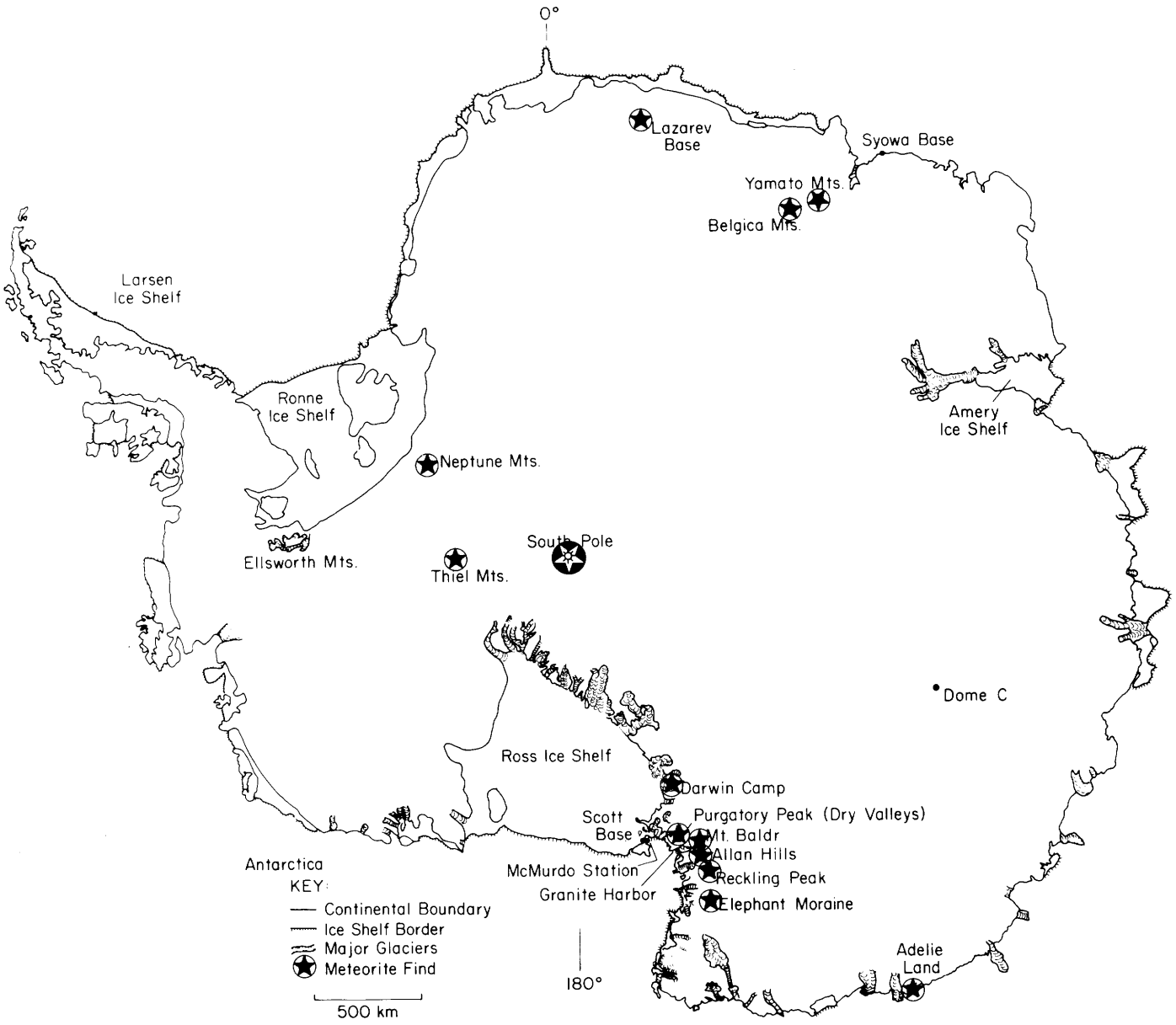

FIGURE 1-1.—Outline map of Antarctica showing sites of meteorite finds. Chance discoveries of four meteorites were made before deliberate searches began in 1973: Adelie Land, 1912, by Douglas Mawson; Lazarev, 1961, by a Soviet Union field party; Thiel Mountains, 1962, and Neptune Mountains, 1964, by U.S. field teams. The first concentration of different types of meteorites was found in 1969 on a blue icefield near the Yamato Mountains by Japanese scientists, who have since found thousands of specimens in the regions of the Yamato and Belgica mountains. ANSMET teams, working out of McMurdo Station, have found about 2000 specimens at the Allan Hills and other sites from Darwin Camp to Elephant Moraine and in the Thiel Mountains region. Individual meteorites have been found near Purgatory Peak, at Inland Forts in the Wright Dry Valley, and on the Taylor Glacier. These last two sites lie a short distance south of Purgatory Peak, too close to be distinguished on this map.

2. The 1982–1983 Antarctic Search for Meteorites (ANSMET) Field Program

William A. Cassidy

Introduction

During December 1982 and January 1983, the ANSMET program fielded three teams. One made reconnaissance searches in the Thiel Mountains (85°15′S, 91°00′W)–Pecora Escarpment (85°38′S, 68°42′W) area to locate previously unknown stranding surfaces (see Chapter 3). The second team carried out systematic searches and made meteorite recoveries at known concentration sites such as the Allan Hills (76°43′S, 159°40′E) and Elephant Moraine (76°11′S, 157°10′E). The third team remeasured and extended a previously set triangulation grid at the Allan Hills (see Chapter 4). The bilateral collecting effort was designed to insure recoveries this season and in future years. The Allan Hills party collected meteorites, as had been expected, and the reconnaissance party located new stranding surfaces, as had been hoped.

The Allan Hills–Elephant Moraine Excursion

Members of this group were Vagn F. Buchwald of the Instituttet for Metallaere Danmarks Tekniske Hojskole at Lyngby, Denmark, Tony Meunier of the United States Geological Survey at Reston, Virginia, Carl Thompson, an alpinist from Methuen, New Zealand, and the writer. Three of us set out by helicopter for the Middle Western Icefield (76°50′S, 158°26′E) where the lunar meteorite, ALHA81005, had been found the year before. Because of a lack of surface landmarks, however, we were unable to identify that icefield with certainty and landed, instead, at the Allan Hills Far Western Icefield (76°54′S, 157°01′E). This site is beyond the permitted limit for helicopter flights, but, at the time, we were unsure of our location. When we landed, the helicopter crewman hopped out and picked up a small meteorite, thereby establishing it as a site where meteorites could be found. (We believe he actually first saw the meteorite from the air and directed the pilot down to a landing alongside the specimen.) We had about half of our camp supplies with us and would have been able to stay, but we could not establish radio communications with McMurdo Station, and so we had to return, leaving our equipment and supplies at the site. Two days later we had another opportunity, and this time we succeeded in making radio contact with McMurdo and were allowed to stay.

Vagn Buchwald remained in McMurdo temporarily and traveled as a passenger on a helicopter run to the head of the Taylor Glacier. Walking around the landing site, he was both startled and highly pleased to pick up a meteorite he found lying on the glacier ice. Thus, the field season for this group began with two accidental discoveries. Meanwhile, at the Far Western Icefield we were finding that our accidental discovery there had placed us on a very large area of exposed ice with many meteorite specimens scattered on its surface.

The Far Western Icefield is a large, roughly W-shaped patch of ice about 75 km west of Allan Hills (Figure 2-1). Satellite photos show no areas of exposed ice farther west than this one. This site has a significant advantage in common with the Near and Middle Western Icefields, in that there is no source of terrestrial rocks upstream of it. Therefore, any rock found on its surface must be a meteorite. It appears to lie generally upstream of the Allan Hills Main Icefield. If so, any meteorites falling onto this surface, or being exposed here by ice ablation, should be transported to the Main Icefield over a period of time that would be measured by the horizontal flow rate of the ice. One would expect specimens recovered here to have younger terrestrial ages than those located closer to the Allan Hills barrier; one would expect also a more sparse distribution of specimens this far from the Allan Hills (cf. Whillans and Cassidy, 1983).

In the several weeks available we could not cover the entire surface of this large patch of bare ice, so we concentrated on its southeastern end and the central exposure near our campsite. We recovered 45 specimens in all, establishing the Far Western Icefield as a productive meteorite stranding surface. Among the specimens recovered was a walnut-sized meteorite "caught in the act" of weathering out of the underlying ice: a minor part of the meteorite was already exposed, but most of it was

William A. Cassidy, Department of Geology and Planetary Science, University of Pittsburgh, Pittsburgh, Pennsylvania 15260.

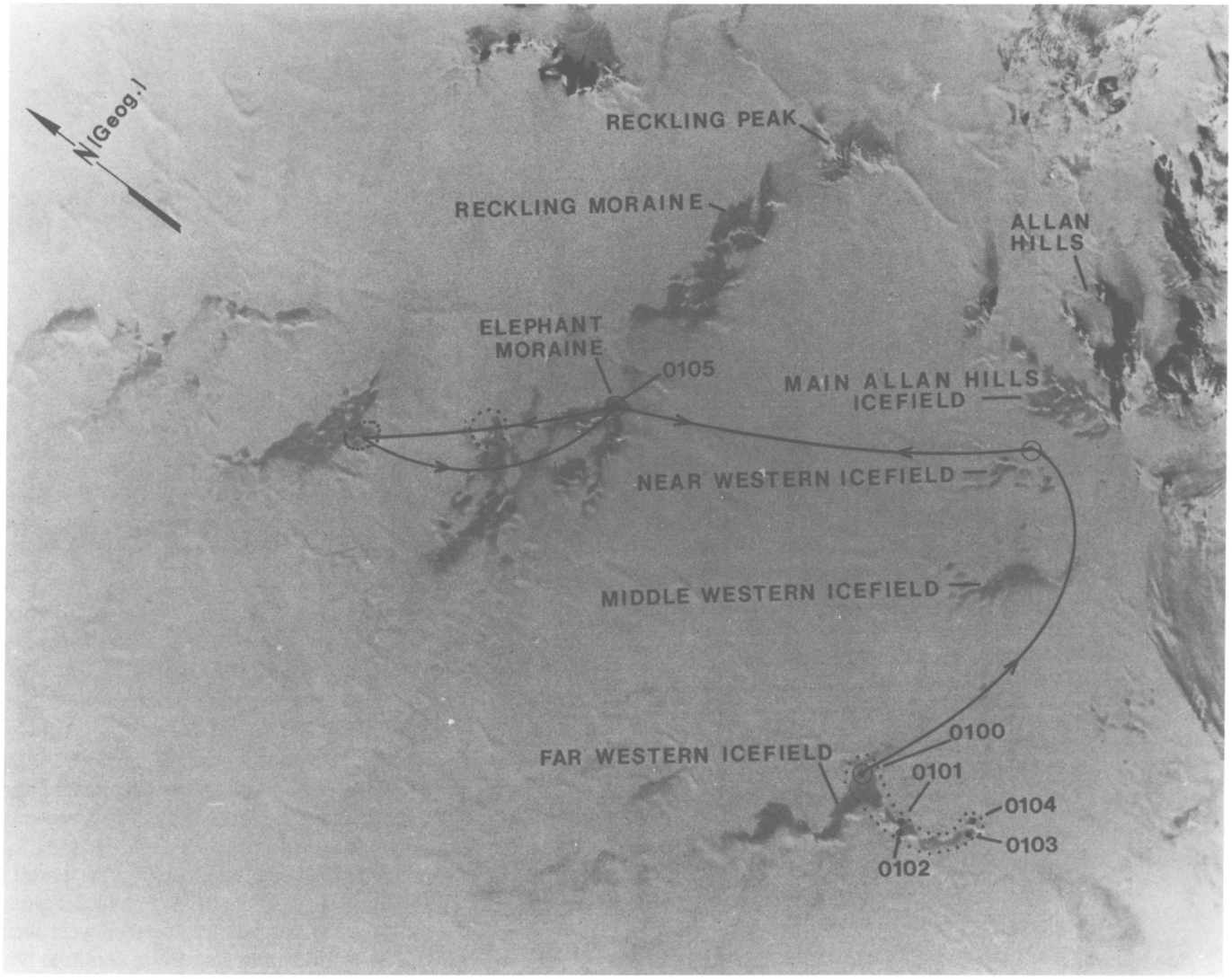

FIGURE 2-1.—Landsat photomap showing our field traverses, all meteorite stranding surfaces mentioned in this article, and the locations of six reference points determined by satellite Doppler positioning. (Illustration taken from 1972 NASA ERTS image E-1128-28293-7, near infra-red band.)

embedded in the ice. The significance of this occurrence and our treatment of the sample are described by Gow and Cassidy (Chapter 10).

The Far Western Icefield is so far from the Transantarctic Mountains that the only visible peak is Mt. Brooke in the Convoy Range, and this can be seen only from certain vantage points. Mapping of ice exposures and meteorite specimens is a problem here because reference points cannot be established by triangulation, and fixed points cannot be established because the ice is moving. Fortunately we had arranged the loan of two Magnavox model MX1502 geoceivers from the U.S. Bureau of Land Management; one was with the Thiel Mountains party and we had the other. With these instruments we were able to locate five points to use as references for mapping our meteorite finds. All of the five will be valuable as reference points for future finds, and three of them are precise enough to be useful in measuring ice flow vectors in this part of the East Antarctic Ice Sheet (see Table 2-1).

After using all the time we originally planned to devote to systematic searching on the Middle Western Icefield, we traversed eastward to John Annexstad's camp at the Main Icefield. Carl Thompson's snowmobile was running on only one cylinder at that time, so Tony Meunier and I each had to draw three loaded Nansen sledges behind our snowmobiles. We noticed very little difference between pulling two and pulling three sledges, and it is now a routine procedure to draw three sledges behind one snowmobile whenever that arrangement seems most convenient.

TABLE 2-1.—Best determinations of six geoceiver stations used in mapping meteorite finds. Locations and elevations of six stations were determined using satellite Doppler positioning procedures. Raw data determined in the field were refined later, using standardized computer programs for this purpose to arrive at the post-processed data given here. Stations 0100–0104 are located at the Far Western Allan Hills Icefield, and Station 0105 was located at our campsite at Elephant Moraine (Figure 2-1).

Station Number	Latitude S	Longitude E	Elevation (m)	Estimated error (in m)
0100	76°54′09.520″	157°01′26.511″	2117.54	1.5
0101	76°57′46.861″	156°54′40.164″	2145.01	2
0102	76°59′27.417″	156°53′46.806″	2190.95	2
0103*	77°02′50.954″	157°11′00.270″	2163.50	5–10
0104*	77°02′24.614″	157°15′33.896″	2142.87	5–10
0105†	76°17′34.910″	157°20′04.944″	2022.33	10

*Reference oscillator frequency offset was abnormally high but stable; data are good but a larger error is assigned.

†Broadcast solution (e.g., field data) not post-processed. Latitude and Longitude are referenced to the Naval Weapons Laboratory 10D system (Jenkins and Leroy, 1979).

Carl had a replacement machine waiting for him at John's camp, and we were joined there by Vagn Buchwald. We left for Elephant Moraine two days later, as a party of four. The traverse to a campsite at the far end of Elephant Moraine took exactly 11 hours, including about an hour of searching for the feature once we had arrived within a few miles of where we knew it to be.

During a week at Elephant Moraine, we collected 18 specimens and left the site, confident that more fragments will be recovered there in the future. High winds had prevented any but rather random reconnaissance searches, and, in areas where random searches give good recovery rates, systematic searching has always yielded many more specimens. During our one day of relatively good weather at Elephant Moraine we accomplished a round trip of 120 km, on which we visited some of the extensive ice exposures due west of Elephant Moraine (see photomap, Figure 2-1), and an isolated exposure to the northwest. Random-path searching at the latter site yielded two meteorites. As our four snowmobiles had covered a cumulative distance of 64 km, this seemed to be a low rate of discovery.

Because the weather had been consistently poor, and it was getting late in the season, we decided to return to the Allan Hills at the first opportunity. This came on 19 January. At 3:00 P.M. that day the wind dropped to 15 knots, so we broke camp and left by 7:00 P.M. The return to Annexstad's camp took only seven-and-one-half hours, despite steadily rising winds. These, combined with cold temperatures due to the lower sun angle during the night, stressed us more than I would have preferred, but the trip was made without incident. We were interested to find that we could easily follow our outward tracks made a week earlier, not because they were pressed into the snow but because they were now standing up several centimeters in relief, having offered some resistance to the erosive effects of the wind during the intervening week.

Results and Discussion

During the 1982–1983 field season unforeseen circumstances played a larger part in our results than in earlier years. Initially we landed at the wrong ice exposure west of the Allan Hills and discovered a previously unsuspected meteorite stranding surface. We had visited this site briefly by helicopter during the 1977–1978 season but had not found meteorites. We probably never would have returned to it had it not been for this lucky accident. Unforeseen also, however, was the spate of days with high winds, which greatly reduced our operating efficiency and turned our planned days of systematic searching at Elephant Moraine into days of reconnaissance trips, mostly near our field camp. In retrospect, these two circumstances may have offset one another.

Finally, by sheer coincidence we were able to borrow geoceivers for the very field season during which a put-in by mistake at an unplanned location left us at a site where we could benefit most from having a geoceiver orientation capability. If the effects of the first two factors offset each other, then this one gave us a distinct advantage.

The Whillans and Cassidy (1983) model for forming meteorite concentrations at a barrier such as the Allan Hills describes three mechanisms that may operate simultaneously: the direct fall of meteorites onto an exposed ice ablation surface, weathering out of meteorites that fell upstream and were transported at various depths to the ice ablation surface, and, once they emerged on that surface, ice-flow crowding of both sets of specimens toward the barrier. Given a constant infall rate of meteorites through time, and equal age for all parts of an ablation surface (and, for the moment, disregarding the crowding effect), all parts of the ablation surface should have a constant density of meteorites that fell directly onto that surface. Similarly, if ancient ice is being exposed by ablation close to the barrier at the same rate that less ancient ice is being exposed farther from the barrier, then the contribution of transported meteorites also should be constant.

Thus, any gradient in frequency of occurrence of meteorites on different parts of an ablation surface could be attributable only to the crowding effect, and this effect should act to increase the frequency of meteorite occurrences toward the barrier. Is such an increase observed? Because pairing estimates are so uncertain, it is difficult to judge in quantitative terms whether or not a regular increase in numbers of meteorites does occur as one traverses eastward from the Far Western Ice Field, over the Middle Western and Near Western Icefields, to the Main Icefield at the foot of the Allan Hills. Qualitatively, however, I can see no such variation, except within the Main Icefield itself. There, the frequency of meteorite occurrences is much higher on the ultimate downstream section of the ablation surface, below the step feature and closer to the barrier, than it is above the step feature. This suggests the possibility that the three icefields to the west actually are not located on a direct flowline toward the stranding surface at the Main Icefield. Future remeasurements of our geoceiver stations at the Far Western Icefield should help to resolve this question, since the ice will have moved in the interval.

Literature Cited

Jenkins, R.E., and C.F. Leroy
1979. "Broadcast" versus "Precise" Ephemeris-Apples and Oranges. *Proceedings of the Second International Geodetic Symposium on Satellite Doppler Positioning* (Austin, Texas, Jan 1979). Austin: University of Texas Press.

Whillans, I.M., and W.A. Cassidy
1983. Catch a Falling Star: Meteorites and Old Ice. *Science*, 222:55–57.

3. The Expedition to the Thiel Mountains and Pecora Escarpment, 1982–1983

John W. Schutt

Reconnaissance by C-130 Hercules

Two weeks of waiting in McMurdo at the end of the 1981–1982 season for aircraft availability and flying weather were over. William Cassidy and I were aboard a ski-equipped C-130 Hercules approaching the Thiel Mountains for a bird's-eye view of icefields selected as having a good probability of significant meteorite concentrations. Cassidy had looked at hundreds of aerial photographs of the Transantarctic Mountains, searching for expanses of ice with characteristics similar to those with known meteorite concentrations in southern Victoria Land. In West Antarctica, several areas in the Thiel Mountains region and at the Pecora Escarpment, 160 km to the east, appeared favorable (Figure 3-1). Two fragments of a pallasite had been found on blue ice in the Thiel Mountains in 1961 (Ford and Tabor, 1971). Could they signify a large meteorite concentration?

As the plane flew low over the Davies Escarpment we could see ice gleaming below. We passed over the precipitous Bermel Escarpment for a look at the icefields along the eastern side of the Thiel Mountains and then on to the Moulton Escarpment. Our excitement grew as we viewed these icefields. They did indeed have features in common with the concentration sites at the Allan Hills, Elephant Moraine, and Reckling Moraine. The aircraft turned from the Thiel Mountains, heading eastward for the Pecora Escarpment. Our excitement peaked as we circled low over these icefields and they, too, looked promising. Before leaving Antarctica we made plans to return to the Thiel Mountains and Pecora Escarpment for a reconnaissance traverse the following field season.

The Thiel Mountains–Pecora Escarpment Field Season

The field party of 1982–1983 consisted of Richard Crane, of the United States Navy, Urs Krahenbuhl, of the University of Bern, Switzerland, Louis Rancitelli, of Battelle Memorial Institute at Columbus, Ohio, and the writer. Our party spent thirty-five days in the field traveling roughly 1250 km on snowmobiles.

On 13 December 1982 we flew over the Thiel Mountains area to locate a landing site and to off-load equipment and drums of snowmobile fuel. We landed at 85°07′S, 88°02′W, approximately 23 km east of the Ford Massif. Two days later we flew a second mission to drop fuel at two points along our intended route and to put our party into the field.

Our first objective was a search of the icefields east of Mt. Walcott and Mt. Wrather in the southern Thiel Mountains, where the pallasite had been found (Figure 3-2). We discovered no meteorites there. We then proceeded to the Pecora Escarpment, a traverse of nearly 200 km requiring three days.

The Pecora Escarpment is a rocky mountainside, approximately 23 km long. It trends SW–NE and forms an absolute barrier to ice flow. Roughly 125 square km of ice is exposed upstream (Figure 3-3). Several less extensive icefields associated with ice escarpments are present within a radius of about 50 km. Upon arriving at the Pecora Escarpment we found snow from recent storms covering a considerable area of the icefield. Nevertheless, we began finding meteorites there soon after beginning our search. Two days of high katabatic winds interrupted our reconnaissance, but the winds removed much of the snow and allowed us to search more effectively. We found meteorites in greater numbers as we worked our way toward the southwest end of the Pecora Escarpment. Many of the specimens lay upstream of the rock barrier, as would be expected. However, many others were found on ice that appears to be downstream of the absolute barrier to ice flow; this has not yet been explained. From the icefields in the immediate vicinity of the Pecora Escarpment, we recovered 32 meteorite specimens and took one sample of ice to be used for age determination and ice chemistry studies. Because time did not allow for both thorough searching and collection, we left at least 50 meteorites in the field to be picked up in future seasons. We did not explore ice patches outside the immediate vicinity of the Pecora Escarpment, where we hope that additional meteorites will be found.

Once we had determined that a significant meteorite

John W. Schutt, Department of Geology and Planetary Sciences, University of Pittsburgh, Pittsburgh, Pennsylvania, 15260.

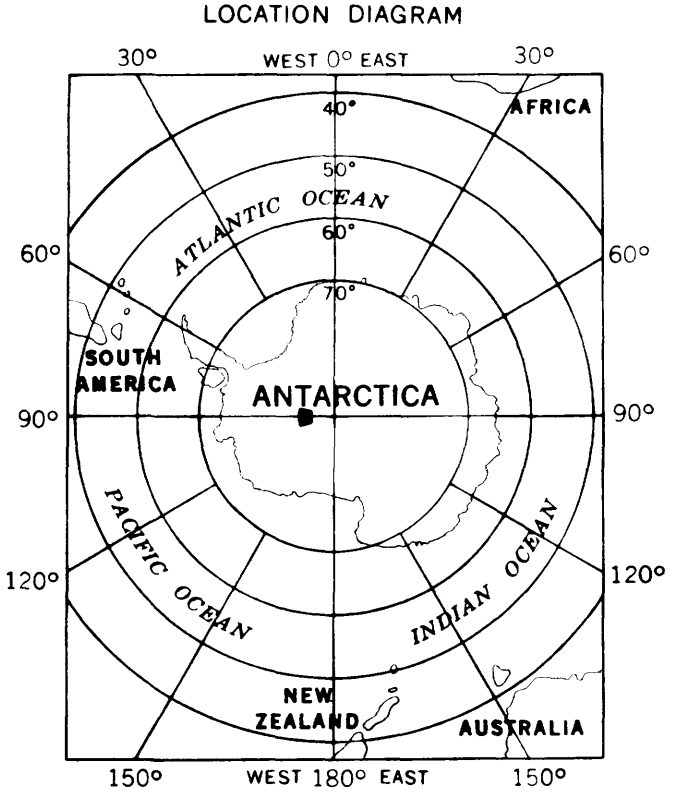

FIGURE 3-1.—Location of the Thiel Mountains–Pecora Escarpment Region, West Antarctica.

concentration existed at the Pecora Escarpment and that systematic searching would be required there, we resumed our reconnaissance traverse. Our next objective was the Davies Escarpment, 160 km to the west. We followed our outward trail back for a distance, then broke off and headed for Lewis Nunatak, near the southern end of the Davies Escarpment. Extending southward from the Thiel Mountains nearly 55 km, the Davies Escarpment presents no absolute barrier to ice flow. Ice cliffs and heavily crevassed areas are common along its length with only a couple of small, isolated rock exposures. Blue ice areas are of limited extent there and are present only at the base of the escarpment (Figure 3-4).

Upon reaching the Davies Escarpment we found considerable snow on the icefields; however, there was sufficient exposure to determine the extent of any meteorite concentrations. Our search of icefields along the Davies Escarpment yielded seven meteorite specimens. We found no meteorites on the small ice patches near Lewis Nunatak, but we picked up one specimen on the ice approximately 8 km SSW of Lewis Nunatak and six specimens during a thorough search of the largest and northernmost icefield. We concluded that large meteorite concentrations are not present in the vicinity of the Davies Escarpment.

Proceeding from the Davies Escarpment, we traversed to the Moulton Escarpment, an isolated nunatak 15 km west of the Ford Massif. This east–west trending escarpment is approximately 20 km in length. A bedrock ridge standing above the ice cap forms an apparent absolute barrier to ice flow along 7 km of the escarpment. At least seven distinct bouldery, ice-cored moraines, with no exposed bedrock, are situated below the escarpment (Figure 3-5).

Conventional thought on meteorite concentrations dictates that the icefields upstream of a bedrock barrier should have the greatest potential as stranding surfaces. Our first search upstream at the Moulton Escarpment resulted in no meteorite finds. A search of the second most likely area, 6 km east of Chastain Peak, produced only one specimen. After our successes at the Pecora and Davies escarpments, we had felt confident of success at the Moulton Escarpment as well, and were disappointed by the absence of any concentrations. We expected the ice downstream of the bedrock to lack meteorites, and we probably would not have visited that area except that we had to cross it to reach our air drop of fuel. On the last trip to the drop site, we spotted a small meteorite, distinguished by its anomalous shape, lying amongst the abundant dark-gray and black terrestrial rocks. We returned the next day in better weather and lighting conditions. We found no additional specimens at the easternmost ice-cored moraine, but, as we moved southward past the moraine, we found nine meteorites concentrated in a small area between the moraine and the escarpment (Figure 3-6). We recovered a total of 11 meteorite specimens from the Moulton Escarpment icefields.

Our party found three new meteorite concentration sites and recovered a total of 50 specimens as a result of reconnaissance searches of the Pecora, Davies, and Moulton escarpments. Forty-two of the specimens are classified as ordinary chondrites, seven as achondrites, and one as a carbonaceous chondrite (see Table 3-1).

The meteorite concentration at the Moulton Escarpment is unusual in that all meteorites, except one, were located on ice that is apparently downstream of an absolute barrier to ice flow. We also found meteorites on what may be downstream ice at the Pecora Escarpment. The discovery of these "unusual" concentrations, which contradict previous experience and

TABLE 3-1.—Classification of meteorite specimens recovered from the Thiel Mountains/Pecora Escarpment region, 1982–1983. (See *Antarctic Meteorite Newsletter*, 6(2), 7(1), 7(2).)

Location	Classification			
	Ordinary chondrite	Carbonaceous chondrite	Achondrite	Total
Pecora Escarpment	26	1	5	32
Davies Escarpment	6	0	1	7
Moulton Escarpment	10	0	1	11
Total	42	1	7	50

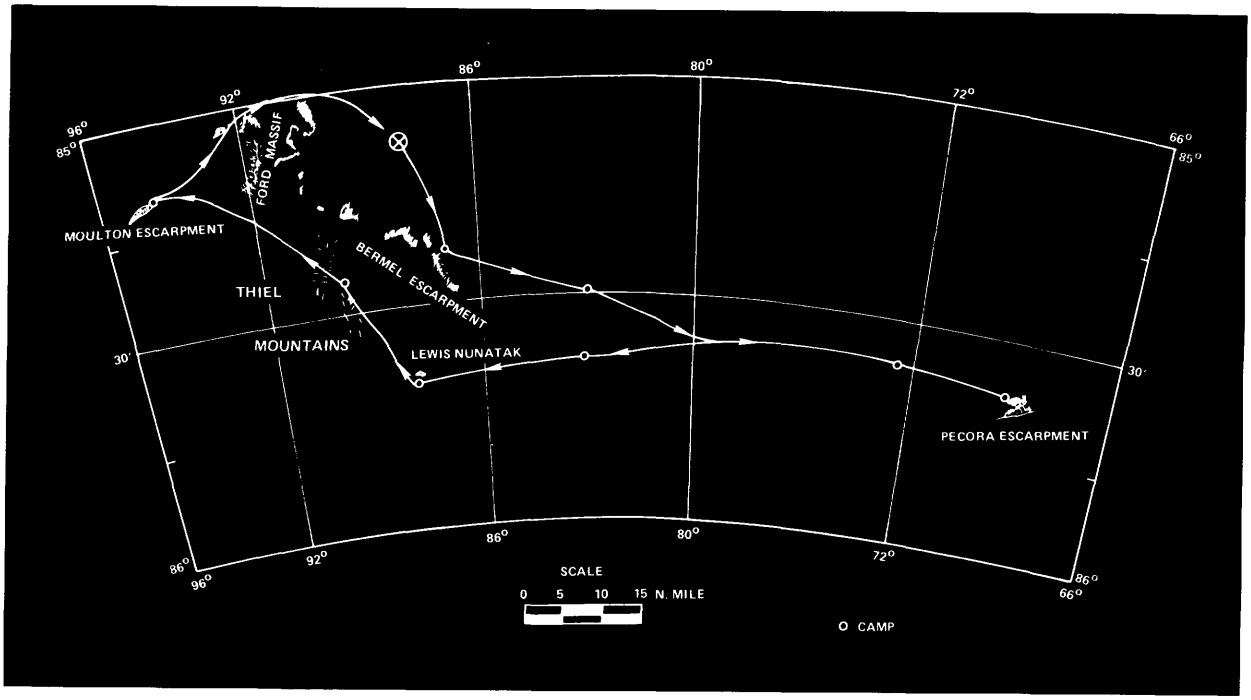

FIGURE 3-2.—Route of the 1982–1983 reconnaissance traverse in the Thiel Mountains–Pecora Escarpment region.

FIGURE 3-3.—Camp near the base of Mount Wrather, Thiel Mountains.

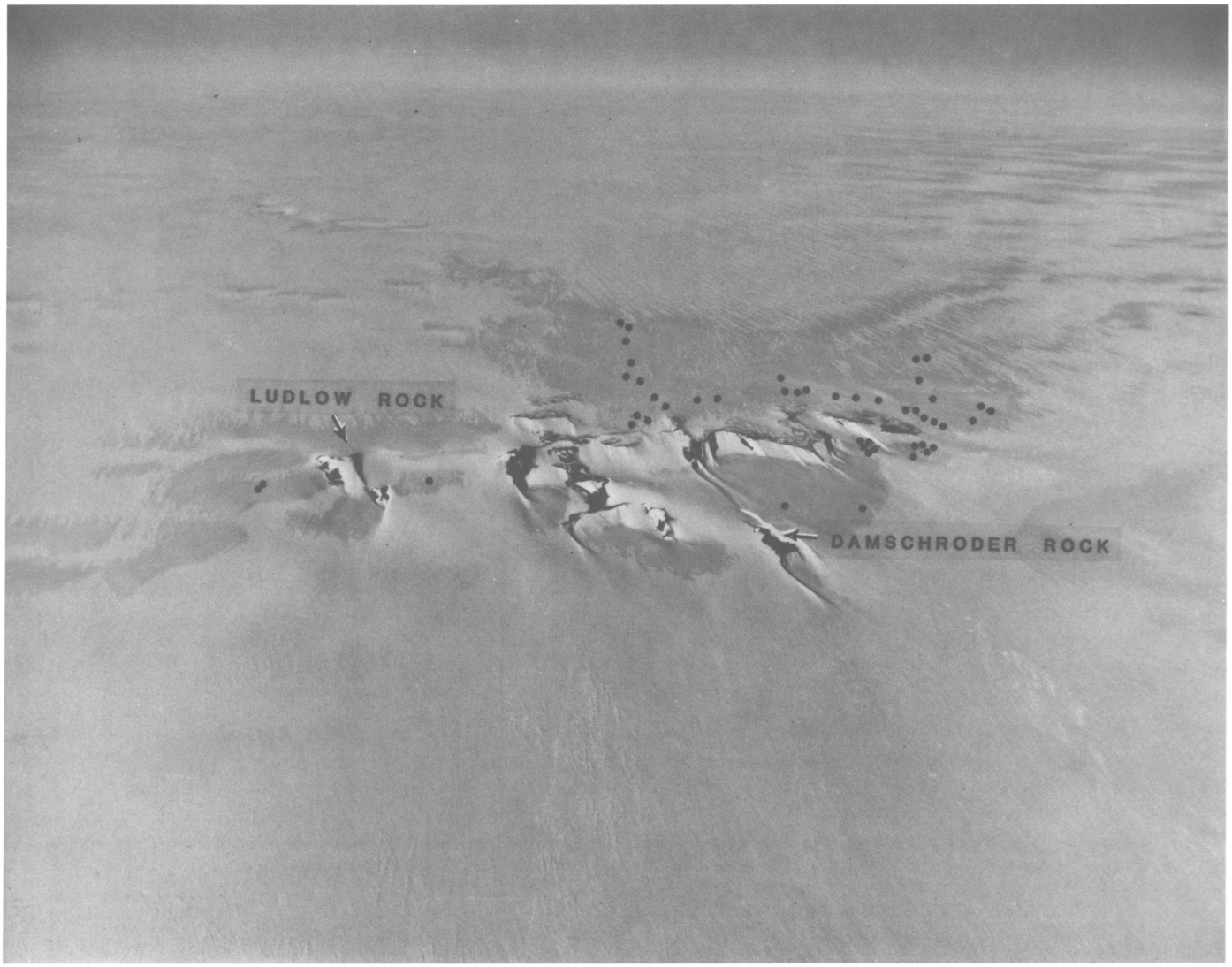

FIGURE 3-4.—Aerial view looking southward over Pecora Escarpment. The large icefield, covering about 125 square km upstream (south) of the barrier yielded an abundance of meteorite specimens (dots), but specimens were also found on smaller icefields downstream of the Escarpment in the vicinity of Ludlow Rock and west of Damschroder Rock.

conventional thought on the concentration mechanism, have increased the prospects for finding concentrations in areas that previously would not have been searched.

NOTE: A Magnavox MX-1502 Satellite Surveyor, on loan from the U.S. Bureau of Land Management, was used to determine the geodetic positions of several meteorites (Figure 3-7) at the Pecora Escarpment. Doppler base stations were established on Lulow Rock at the Pecora Escarpment and at Chastain Peak (Figure 3-8) at the Moulton Escarpment. These data have been used by the U.S.G.S. to improve the WGS-72 survey net in Antarctica.

Literature Cited

Antarctic Meteorite Newsletter, 6(2), August 1983.
Antarctic Meteorite Newsletter, 7(1), February 1984.
Antarctic Meteorite Newsletter, 7(2), July 1984.
Ford, A.B., and R.W. Tabor
1971. The Thiel Mountains Pallasite. *United States Geological Survey Professional Paper*, 750-D. Washington, D.C.: United States Government Printing Office.

FIGURE 3-5.—Aerial view looking southward along the Davies Escarpment (right center). Dots indicate locations of the seven meteorite specimens found in this area: six on the northernmost icefields at the foot of the Escarpment, and one about 8 km SSW of Lewis Nunatak.

FIGURE 3-6.—Aerial view looking southward over the Moulton Escarpment with Chastain Peak near the eastern end.

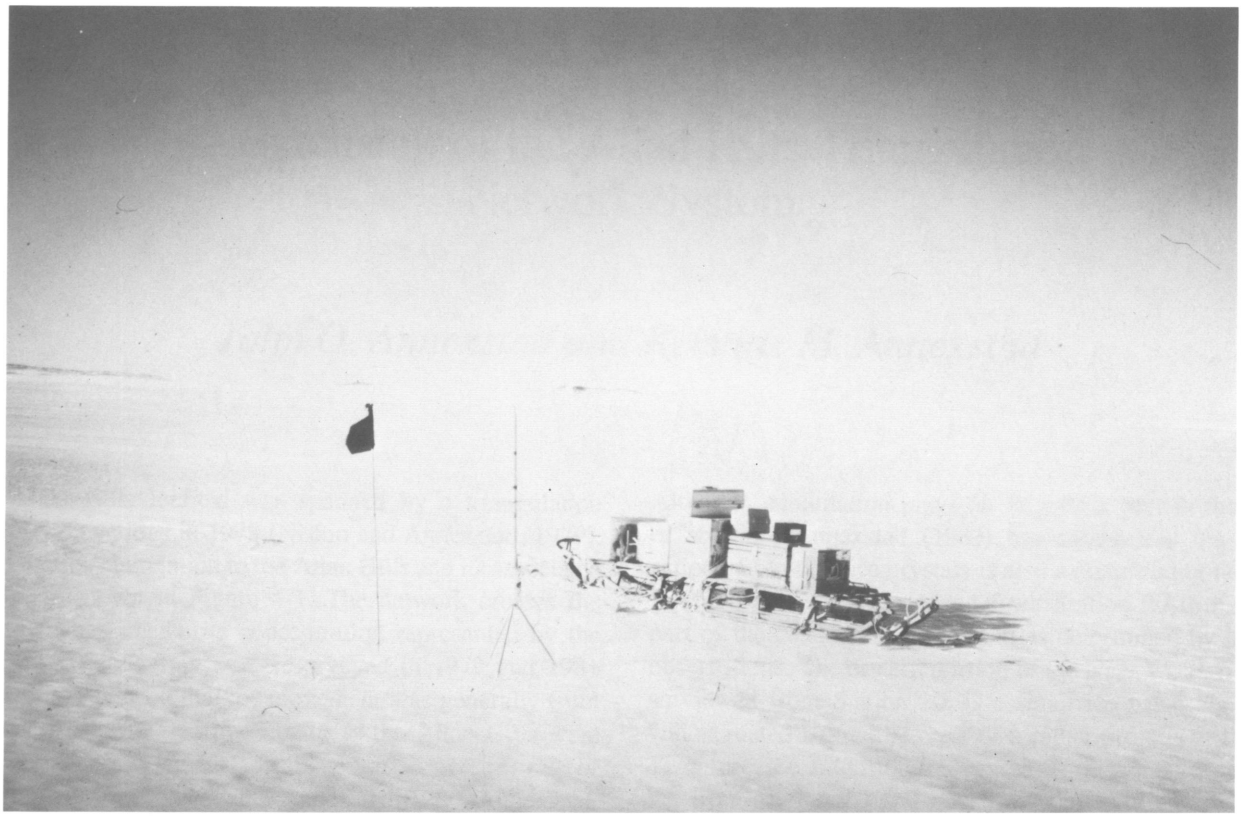

FIGURE 3-7.—Satellite surveying of meteorite locations at the Pecora Escarpment.

FIGURE 3-8.—Satellite surveying at Chastain Peak survey point in the Moulton Escarpment.

4. Extension of the Allan Hills Triangulation Network System

John O. Annexstad and Kristine M. Annexstad

The Allan Hills Icefield was spanned by a triangulation network of 20 stations in 1978 (Nishio and Annexstad, 1979). Station locations in relation to the Allan Hills and its associated icefields are shown in Figure 4-1. The network crosses the region of highest meteorite concentration represented by the dotted area. The stations were resurveyed in 1979 and 1981 and the results showed that ice movement was generally from west to east, it decreased in velocity as the Allan Hills were approached, and the ice surface ablated at an average rate of about 5 cm per year (Nishio and Annexstad, 1980; Annexstad, 1983; Schultz and Annexstad, 1984).

During the 1982/1983 austral summer field season the authors extended the original triangulation network from the Allan Hills Main Icefield to the Near Western Icefield (Figure 4-2) and attempted to locate station positions with an astronomical theodolite. Inclement weather forced an early end to the field season and frustrated attempts to accurately survey the newly established stations.

The network as it now appears is shown in Figure 4-3 extending in a westerly direction from the baseline (Stations 1 and 2). Stations 25 to 38 were added to the original line. Station numbers are not sequential because the strain flower (Stations 21–24) was established after the initial survey of the original network (Stations 1–20).

Ablation was measured at each station of the original network prior to installing the line extension. This measurement consists of obtaining the distance to 0.1 cm from the top of the pole to the surface of the ice. An east side and west side reading is taken at each station and the measurements averaged, because the ice surface can be quite uneven near the base of the poles.

Table 4-1 lists the annual rates of ablation from 1978 to 1982 with the four year average and standard deviation (from Annexstad, 1983). From this table it can be seen that the rate of ablation varies from year to year and from station to station. Although sublimation plays an important part in the process of ablation, Annexstad (1983) has shown that the abrasive action of blowing ice crystals is also a contributing factor.

The network was extended from Station 20 to the visible part of the Near Western Icefield as determined by binocular observations. The eastern portion of the Near Western Icefield, as viewed from Station 20, is a small ice patch about 1 km wide situated below the crest of a rather prominent firn field. Therefore, the extension line was constructed as two legs, one leg from Station 20 and one leg about a kilometer south of Station 20, each of which intercepted one edge of the visible portion of the eastern section of the Near Western Icefield.

Stations 20–36 (even numbered) were positioned about 1.5 km apart unless a closer spacing was needed for visual contact. Each station was placed so that a lower numbered and a higher numbered station were visible with binoculars.

Stations 25 to 37 were positioned along a line 1 km to the south of the even-numbered leg. Each individual station was placed as close as possible to a point on the perpendicular bisecting the line between two even-numbered stations and visible from a lower and higher numbered station on the same leg. This method of positioning ensures that the surveyor at each station has clear visibility of at least three other stations.

Each station consists of a 3 m bamboo pole placed into a 7.5 cm diameter hole drilled 70–100 cm deep in the ice or firn. The base of the pole is wrapped in a layer of fiberglass insulation to decrease ablation effects from conduction and to ease pole removal for the survey. The poles were numbered appropriately and a red trail flag attached 2–3 centimeters below the top. Measurements were taken of the depth of the hole and the height of the pole from the surface.

Figure 4-4 shows one of us (KMA) using a fiberglass-bodied drill to establish one of the stations. The drill is operated by hand and the operator is protected from the prevailing winds by a snowmobile-mounted, triangularly shaped windbreak. The fiberglass-bodied drill is considerably easier to use than the steel SIPRE drill, formerly used on this project, but its lack of weight requires some downward pressure by the operator.

Numerous attempts were made to establish station positions

John O. Annexstad, NASA Johnson Space Center, Houston, Texas 77058. Kristine M. Annexstad, Frank Welch and Associates, Dallas, Texas 75205.

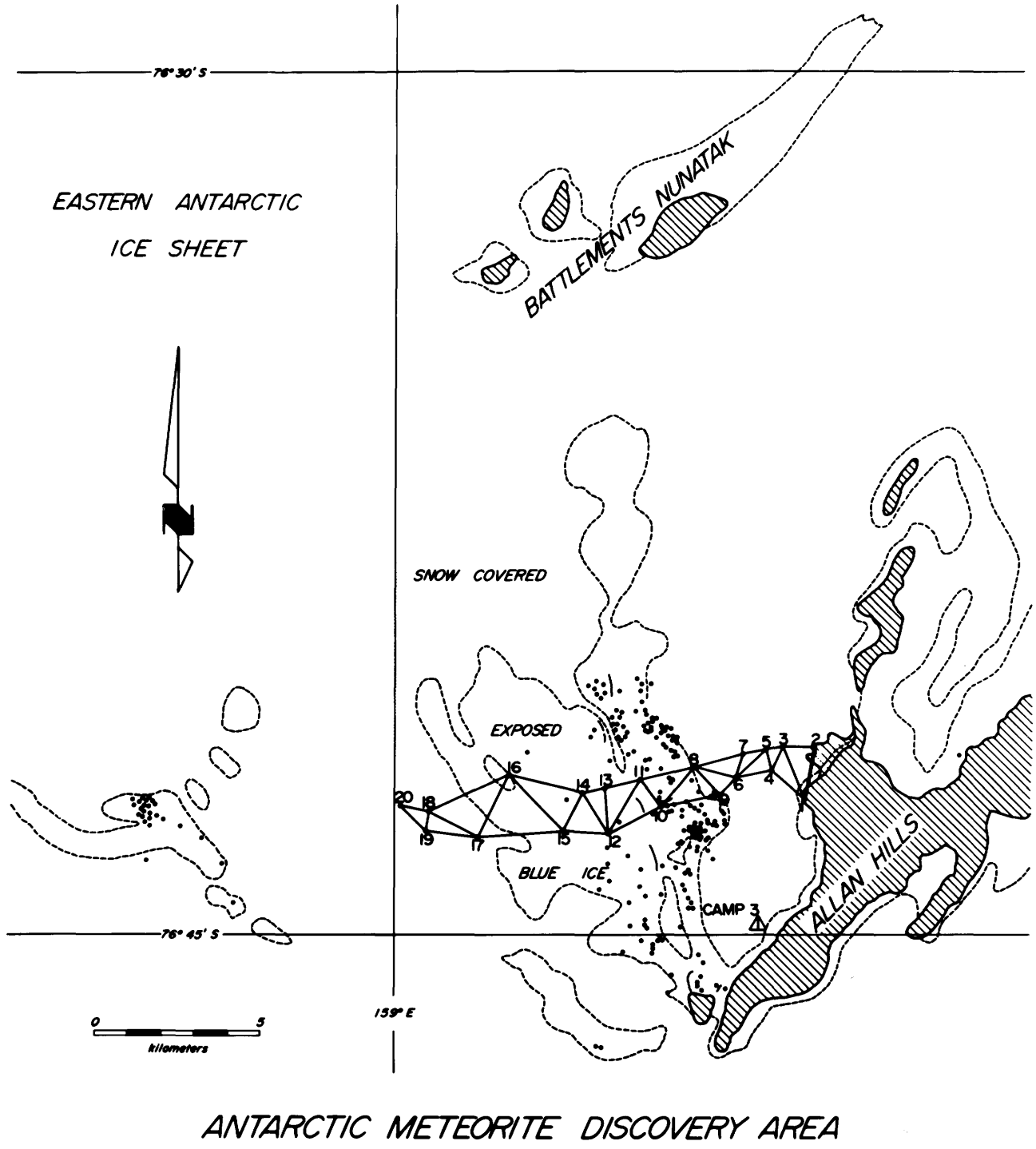

FIGURE 4-1.—The original triangulation network across the Allan Hills Main Icefield.

and distances from known points by triangulation survey methods. A Wild T-2 theodolite and the triangular windbreak pictured in Figure 4-4 were used in these attempts. Unfortunately, the Antarctic weather did not cooperate and only two stations (20 and 19) were successfully occupied. It should be noted that conditions varied between whiteouts and severe blowing snow, which made theodolite observations all but impossible in this area. The network extension is constructed primarily in firn so that even moderate winds will obscure the survey targets with blowing snow.

The distances between Stations 20–38, shown in Figure 4-1, are snowmobile odometer readings, because the triangulation

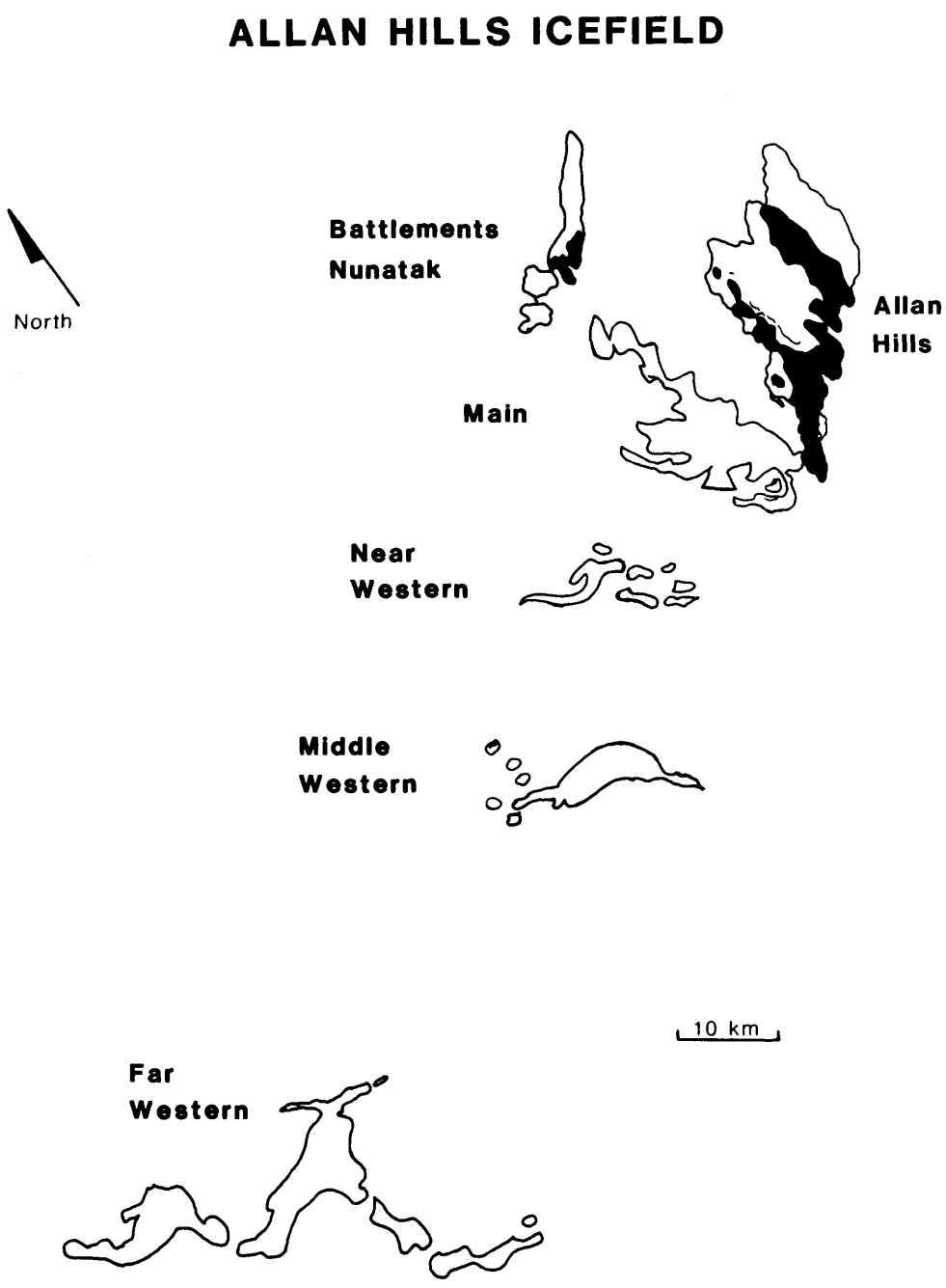

FIGURE 4-2.—The four icefields lying west of the Allan Hills.

survey was not completed. These distances are subject to the errors due to surface undulations of the firn and the notorious inaccuracies of snowmobile odometers.

Although a precise determination of position and movement of the stations must await future surveys, some visual observations of surface conditions were noted at the Near Western Icefield. A wave-like step feature at the eastern edge of the Near Western Icefield is the most prominent topographic feature. This step feature resembles the one in the immediate vicinity of the Allan Hills that Yanai et al. (1978) described as a monocline. On the eastern slope of the step the blue ice has reached the surface and the high winds in that area keep it free of snow. The ice surface is interlaced with small crevasses and tensional cracks, which are common features in blue ice areas. The general alignment of the crevasses is with the long axis perpendicular to a northeast ice flow direction. The crevasse patterns indicate that the surface ice in this vicinity will bypass the Allan Hills Main Icefield, which lies to the east.

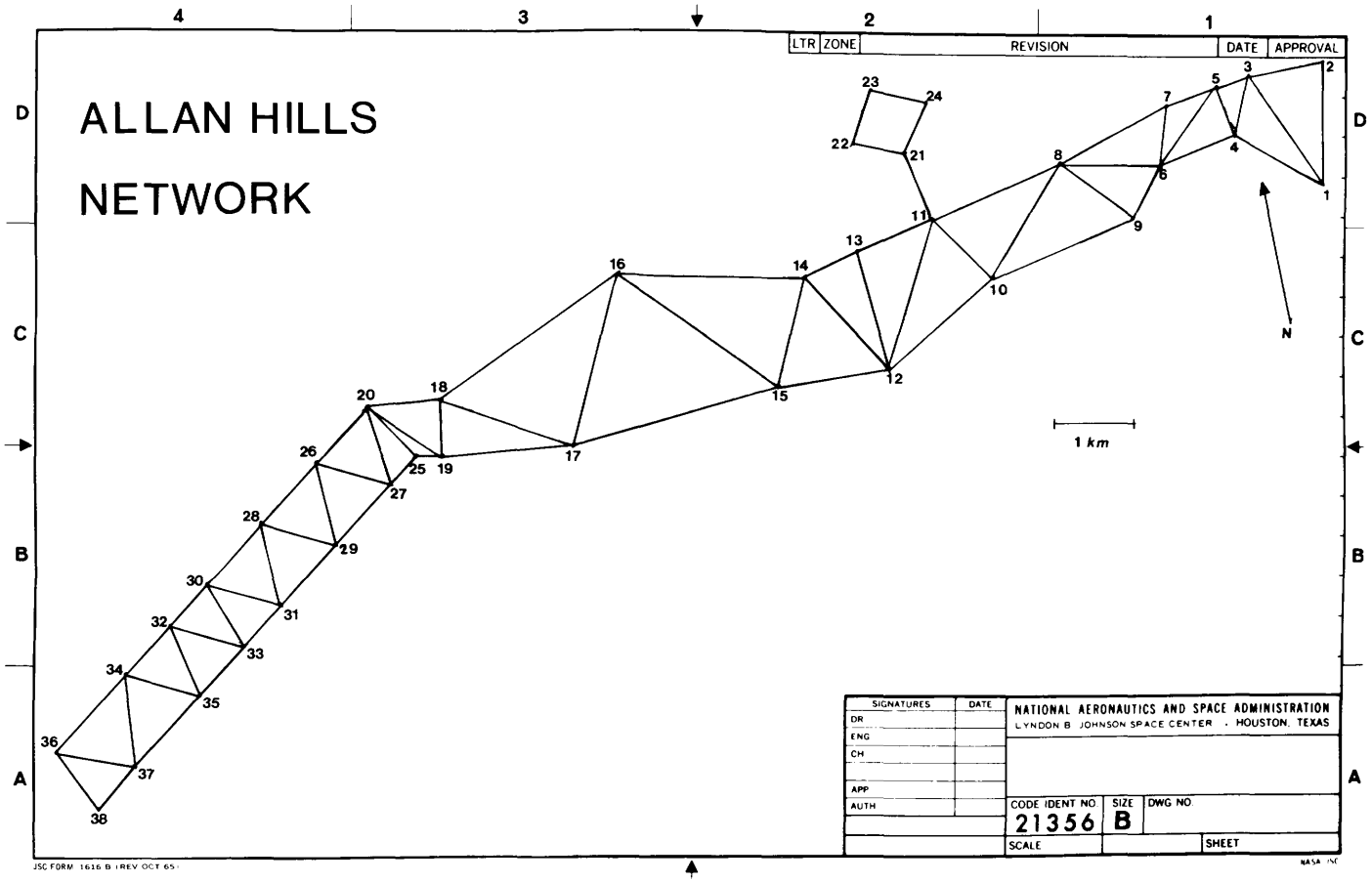

FIGURE 4-3.—The triangulation network with recent extensions: the strain flower (Stations 21 to 24) and the southwest extension (Stations 25–38).

In a description of the four icefields that are upstream of the Allan Hills, Schutt et al. (1983) suggested that they are all interconnected and part of the main Allan Hills Icefield. The locations of these ice fields are shown in Figure 4-2 relative to the Allan Hills and Battlements Nunatak (Annexstad, 1983). The assumption that the four icefields are interconnected may be a premature guess if the direction of motion indicated by crevasse alignment at the Near Western Icefield is correct. If the icefields are interconnected, it should follow that surface crevasse patterns should indicate an easterly flow direction, toward the Allan Hills. A positive determination of the direction of flow and its velocity must await further survey data. Until those data are available it does appear that the meteorite concentration areas in the main Allan Hills Icefield represent the convergence of a diverse set of flow patterns emanating from a number of widely spaced sources.

Literature Cited

Annexstad, J. O.
1983. Meteorite Concentrations and Glaciological Parameters in the Allan Hills Icefield, Victoria Land, Antarctica. Doctoral dissertation, Doktor der Naturwissenschaft, Johannes Gutenberg Universitat, Mainz, Federal Republic of Germany.

Nishio, F., and J. O. Annexstad
1979. Glaciological Survey in the Bare Ice Area near the Allan Hills in Victoria Land, Antarctica. *Memoirs of the National Institute of Polar Research* (Japan), special issue, 15:13–23.
1980. Studies on the Ice Flow in the Bare Ice Area near the Allan Hills in Victoria Land, Antarctica. *Memoirs of the National Institute of Polar Research* (Japan), special issue, 17:1–13.

Schultz, L., and J. O. Annexstad
1984. Ablation and Ice Movement at the Allan Hills Main Icefield between 1978 and 1981. *In* U.B. Marvin and B. Mason, editors, Field and Laboratory Investigations of Meteorites from Victoria Land, Antarctica. *Smithsonian Contributions to the Earth Sciences,* 26:17–22.

Schutt, J.W., W.A. Cassidy, G. Crozaz, R.F. Fudali, and U.B. Marvin
1983. Results of Meteorite Search and Recovery Activities in the Vicinity of the Allan Hills, Antarctica, Dec. 1981–Jan. 1982. *In* R.L. Oliver, P.R. James, and J.B. Jago, editors, *Antarctic Earth Science.* Canberra: Australian Academy of Science.

Yanai, K., W.A. Cassidy, M. Funaki, and B.P. Glass
1978. Meteorite Recoveries in Antarctica During Field Season 1977–78. *Proceedings of the 9th Lunar and Planetary Science Conference,* pages 977–987.

TABLE 4-1.—Rates of ablation (–) and accumulation (+) measured in centimeters per year at survey stations on the Allan Hills Icefield.

Station	1978–1979	1979–1980	1980–1981	1981–1982	1978–1982 Average ± Std. Dev.
3	– 2.2	+ 1.8	– 2.0	+ 2.8	+ 0.1 ± 2.6
4	– 2.3	– 0.9	+ 18.1	– 2.9	+ 3.0 ± 10.1
5	– 1.1	– 2.1	+ 1.4	– 0.1	– 0.5 ± 1.5
6	– 1.7	– 2.5	– 2.8	– 3.2	– 2.6 ± 0.6
7	– 2.6	– 2.8	+ 2.6	– 0.4	– 0.8 ± 2.5
8	– 3.8	– 1.7	– 1.9	– 1.3	– 2.2 ± 1.1
9	– 4.3	– 2.0	– 3.3	– 4.7	– 3.6 ± 1.2
10	– 6.6	– 3.7	– 5.7	– 0.2	– 4.0 ± 2.8
11	– 5.7	– 2.7	– 5.8	– 7.1	– 5.3 ± 1.9
12	– 4.5	– 2.9	– 5.1	– 2.4	– 3.7 ± 1.3
13	– 5.7	– 6.5	– 6.2	– 5.8	– 6.0 ± 0.4
14	– 7.2	– 2.6	– 4.3	– 4.8	– 4.7 ± 1.9
15	– 5.8	– 2.1	– 4.9	– 4.2	– 4.2 ± 1.6
16	– 4.3	– 0.1	– 1.6	– 1.8	– 2.0 ± 1.7
17	– 5.4	– 3.5	– 2.9	– 7.2	– 4.8 ± 2.0
18	– 4.7	– 4.2	– 3.5	– 5.7	– 4.5 ± 0.9
19	– 3.2	– 1.1	– 2.0	– 2.5	– 2.2 ± 0.9
20	– 1.8	– 1.3	– 1.7	+ 0.4	– 1.1 ± 1.0
21	– 6.5	– 2.6	– 4.9	+ 5.1	– 2.2 ± 5.1
22	– 5.8	– 1.4	– 2.8	– 8.4	– 4.6 ± 3.1
23	– 6.1	– 3.0	– 5.6	– 3.3	– 4.5 ± 1.6
24	– 0.5	– 3.7	– 4.8	– 5.6	– 4.8 ± 0.8

FIGURE 4-4.—Kristine Annexstad drilling a station hole with the fiberglass-bodied drill. The triangular windshield is attached to the snowmobile.

5. The Field Season in Victoria Land, 1983–1984

Robert F. Fudali and John W. Schutt

The 1983–1984 season marked the eighth consecutive year of Antarctic Search for Meteorites fieldwork on the South Polar Plateau. This ANSMET team was the largest single field party to date, consisting of eight people equipped with eight steel-cleated snowmobiles and 12 Nansen sleds. The team was led by William A. Cassidy of the University of Pittsburgh. Other participants were A.C. Hitch, of Ferndale, Washington, K. Nishiizumi, of the University of California at San Diego, Paul Pellas, of the Museum of Natural History in Paris, Ludolf Schultz, Max Planck Institute for Chemistry in Mainz, West Germany, Paul Sipiera, Harper College, Illinois, and the authors.

Despite some annoying equipment malfunctions involving the snowmobiles, Nansen sleds, and field radios, and two potentially serious mishaps caused by a parachute that failed to open during a fuel drop at Elephant Moraine, plus a bad tent fire late in the season, our overall accomplishments rank with the best of those of previous seasons. Our provisional field count of meteorites, meteorite fragments, and possible meteorites was 367, and 40 to 50 more small fragments were not bagged individually. One iron meteorite was found in the Wright Valley by a member of George Denton's University of Maine field party and turned over to us at the end of the season.

For the first time, many of the meteorite find locations were determined using a theodolite and an electronic distance measuring device. These locations were also determined absolutely, with accuracy on the order of a few meters, by tying them to geoceiver stations positioned at Elephant Moraine and the Far Western Icefield the previous season by satellite doppler tracking. This surveying equipment was also used to emplace a series of survey stations between the Far Western Icefield and the Main Icefield in the Allan Hills region. These stations were tied to the previously established triangulation network on the Main Icefield and to the geoceiver stations on the Far Western Icefield. Gravity measurements were made at all these stations and tied to the previous gravity measurements over the triangulation network (Fudali, 1982). The gravity data are now sufficient to give us a general idea of the depth and configuration of the ice/bedrock interface out to a distance of 70 km WSW of the Allan Hills. Finally, we collected large blocks of ice from five icefields, using a power chain saw, for a number of isotopic studies that we hope will lead to a better understanding of the ice ages and ice dynamics in the collecting areas.

Our original plan called for a Hercules C-130 put-in of our party at the Far Western Icefield, 70 km WSW of the Allan Hills, which we would search systematically and then move to the Mid and Near Western Icefields for similar work. The four separate blue icefields WSW of the Allan Hills have been described in some detail by Fudali and Schutt (1984) and are shown in Figure 4-2 (Chapter 4). However, C-130 reconnaissance flights were unable to find a suitable landing site anywhere in the vicinity of the Far Western Field. The only suitable landing site we found was in the vicinity of Griffin and Outpost Nunataks, which held no promise of meteorites. Under those circumstances, we decided to revise our plans and devote a major effort to systematically searching Elephant Moraine and its adjacent blue ice fields, and then to traverse overland to the ice fields west of Allan Hill (Figure 5-1).

To find a suitable landing site for a ski-equipped C-130 on the South Polar Plateau is an interesting task. The preferred test is to drive the C-130 onto the snowfield under flying power and observe the effects of this maneuver, both on the aircraft and on the snow surface. Those of us who participated in such reconnaissance flights can attest to the adrenalin-pumping nature of such maneuvers. We commend C-130 Commander Brian Rich and his crew for their competence and their "cool."

On 9 and 10 December, two C-130 flights put in our party, equipment, and supplies, 60 km north of Elephant Moraine (Figure 5-2). Strong katabatic winds made overland travel difficult and, indeed, kept us tentbound at the landing site for two days. We reached the moraine (Figure 5-3) on the morning of 15 December.

We spent 13 days at Elephant Moraine, systematically searching the blue ice fields, east, west, and south of the moraine with snowmobile sweeps. We also spent considerable

Robert F. Fudali, Department of Mineral Sciences, National Museum of Natural History, Smithsonian Institution, Washington, D.C. 20560. John W. Schutt, Department of Geology and Planetary Sciences, University of Pittsburgh, Pittsburgh, Pennsylvania 15260.

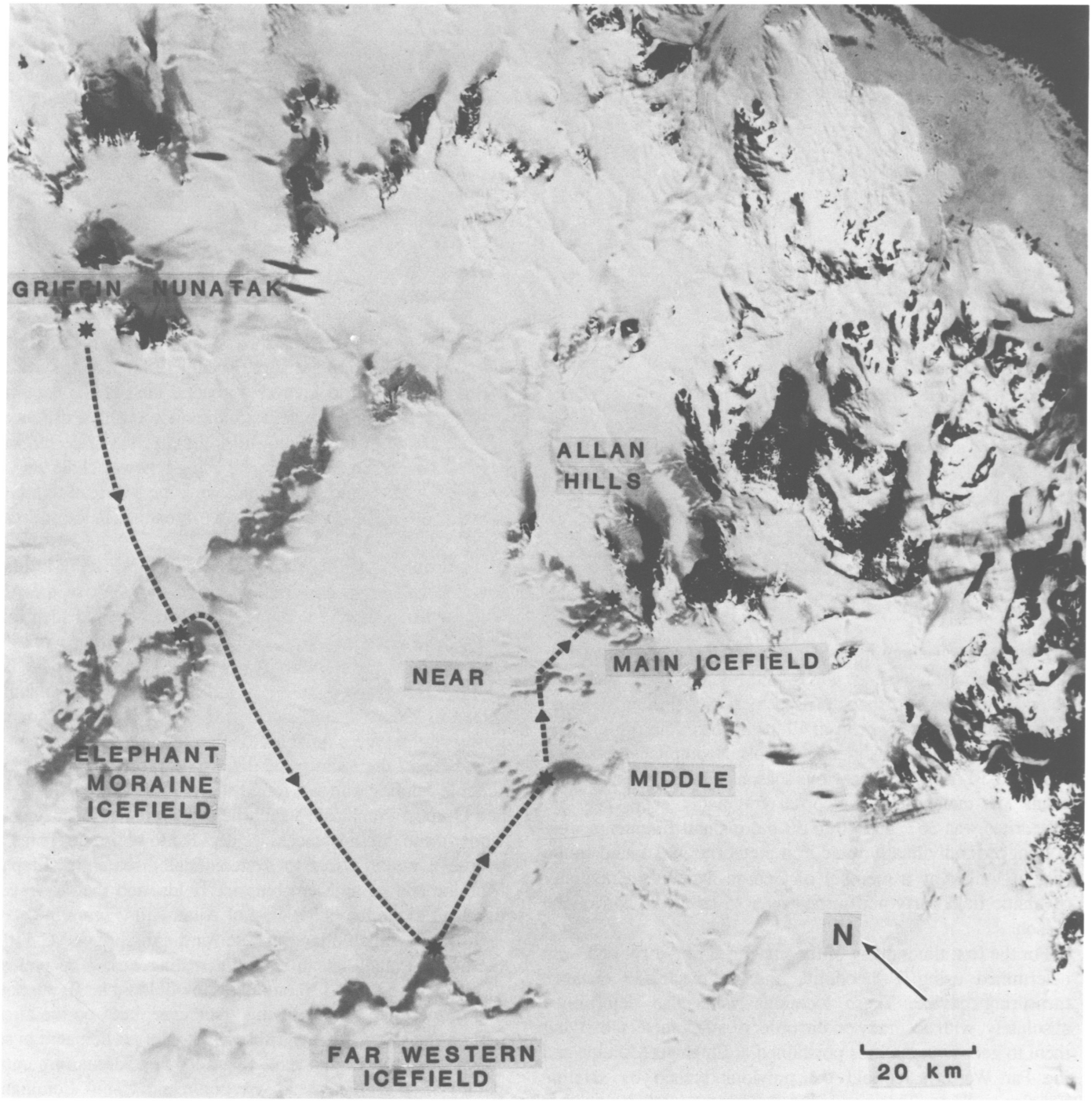

FIGURE 5-1.—Camps and route of the season's snowmobile traverse that logged 1250 km in 45 days.

time searching, on foot, within the moraine. Meteorites do occur in the moraine and can be distinguished from the terrestrial rock litter (Figure 5-4), but the bulk of the meteorites were recovered from the blue ice surfaces, and it is questionable whether persistent moraine searches on foot is a time-effective way to recover Antarctic meteorites. We continued to find meteorites on blue ice until the day we left and there are surely additional meteorites on the icefields there. A total of 207 field numbers were issued at Elephant Moraine, with provisional field identifications as shown in Table 5-1.

On 26 December, a C-130 air drop at the moraine provided us with a spectacular cratering experiment. One of the three pallets failed to deploy its parachute and four 55-gallon drums of fuel impacted the snow with undiminished velocity. All

FIGURE 5-2.—Unloading a ski-equipped C-130 Hercules near Griffin and Outpost Nunataks.

FIGURE 5-3.—The southern part of Elephant Moraine, looking south.

four drums were breached by the impact but we managed to salvage three of the four with minimal fuel loss. The fourth drum provided us with 55 gallons of fuel-soaked snow in which to burn our trash before breaking camp.

Elephant Moraine is an interesting feature that deserves further study. It is unrelated to any bedrock outcrop and consists of a complexly configured ice ridge littered with a thin surface veneer of rocks of diverse sizes and types. Similar moraines elsewhere in Antarctica have been assumed to signal the presence of bedrock at shallow depth beneath them. The meteorite concentration provides indirect evidence of a subsurface, partial barrier to ice movement, but we have no direct information on this postulated barrier.

The weather during the 15–28 December period was almost entirely dominated by temperatures well below freezing and strong katabatic winds. Nevertheless, on several occasions liquid water was observed on the lee and sunny side of rock surfaces in the moraine (Figure 5-5). Almost all Antarctic meteorites show some weathering effects and many are badly oxidized. Meteorite weathering has generally been regarded as an extremely slow process on the Polar Plateau, characterized by only infrequent contact with liquid water on warm, sunny, windless days. Our observations at Elephant Moraine suggest that liquid water may be a more pervasive weathering agent than previously supposed.

We departed Elephant Moraine on 29 December (Figure 5-6) and proceeded to the camp site of the 1982–1983 season on the Far Western Icefield. Aside from the partial disintegration of one Nansen sled, carrying two 55-gallon drums of fuel, this leg was made in two days without significant incident.

We did not intend to collect meteorites systematically at the Far Western Icefield, as the field season was drawing to a close and we had much else still to do. We were primarily interested in collecting ice samples for isotopic studies, especially from the site of a meteorite found embedded in the ice last year (see Chapter 10), and in tying together the geoceiver stations emplaced the previous season with a view toward extending ground-surveyed stations from the Far Western Field all the way to the Allan Hills network. At the expense of leaving a number of observed but uncollected meteorites on the ice, we achieved these goals. We could not, however, resist collecting a few meteorites, including 76 individual fragments of a carbonaceous chondrite (Figures 5-7 and 5-8) that Paul Pellas caught sight of as we were proceeding toward the ice-embedded meteorite site. These fragments appeared to be entirely fresh and were scattered on both ice and snow surfaces, leading us to believe we might be collecting a very recent fall. ^{26}Al measurements have subsequently shown this supposition to be incorrect (W.A. Cassidy, personal communication).

On 6 January we broke camp and proceeded to the Middle Western Icefield, putting in survey and gravity stations along the way. We intended to systematically and thoroughly sweep that entire icefield for meteorites but were hampered by high winds during virtually our entire nine-day stay. In fact high winds kept us tentbound for seven straight days. Nevertheless, we did manage to collect a few meteorites and extend the survey and gravity stations half way to the Near Western Icefield before leaving for the Main Icefield.

On 14 January a bad tent fire resulted in burns to Paul Sipiera's hands and face. He was evacuated by helicopter within two hours and, upon landing at McMurdo, was put directly on a C-130 flight to New Zealand. The same helicopter returned Paul Pellas and Ludolf Schutz to McMurdo, leaving five of us in the field.

On 16 January we moved camp for the last time, extending survey and gravity stations to the Near Western Icefield and then traversing directly to the Main Icefield for our final few days. On the 17th a three-man crew from the British Broadcasting Corporation joined us for several days of filming and thereby severely curtailed our collecting activities. In just a few hours of searching, however, we found 29 meteorites on ice surfaces that have been searched and researched in past

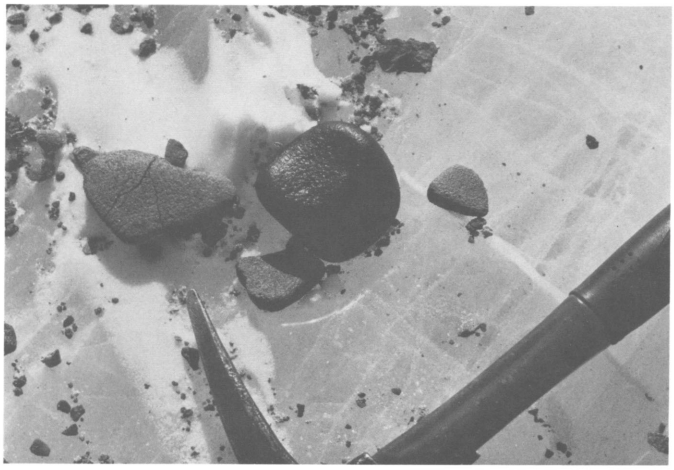

FIGURE 5-4.—Small iron meteorite (dark and shiny) found among the rocks of Elephant Moraine.

FIGURE 5-5.—Liquid water and icicle on the sun-facing side of a boulder in Elephant Moraine.

FIGURE 5-6.—ANSMET on the move.

FIGURE 5-7.—Paul Pellas and the first three carbonaceous chondrite fragments found at the northernmost extension of a small strewnfield containing a total of 56 fragments (see also Figure 5-8).

seasons. This probably reflects the fact that snow cover was remarkable for its virtual absence on the Main Icefield, in contrast to previous seasons. A few meteorites were also incidentally picked up by a two-person party working to extend the survey stations from the Near Western Field to the triangulation network on the Main Field.

On 21 January, meteorites, ice blocks, and three team members were flown to McMurdo. Three days later the last two people were returned safely, bringing to a close what was arguably the most ambitious ANSMET field season to date. Our snowmobile odometers logged over 1250 km during 45 days on the Polar Plateau. In addition to the large number of meteorites returned from five separate locations, an ice sampling program was carried out, and survey and gravity stations now extend from exposed bedrock at Allan Hills to the Far Western Icefield.

Literature Cited

Fudali, Robert F.

1982. Gravity Measurements across the Allan Hills Main Meteorite Collecting Area. *Antarctic Journal of the United States, XVIII,* 5:58–60.

Fudali, Robert F., and John W. Schutt

1984. The Field Season in Victoria Land, 1981–1982. *In* U.B. Marvin and B. Mason, editors, Field and Laboratory Investigations of Meteorites from Victoria Land, Antarctica. *Smithsonian Contributions to the Earth Sciences,* 26:9–16.

Table 5-1.—Tentative classification of meteorite specimens found at Elephant Moraine and the Allan Hills icefields during the 1983–1984 season.

Specimens	Icefield					
	Elephant Moraine	Allan Hills Far West	Allan Hills Mid West	Allan Hills Near West	Allan Hills Main	Total
Ordinary chondrites	179	7	31	13	29	259
Carbonaceous chondrites	4	76	2			82
Acondrites	12		2			14
Stony-Irons	1					1
Irons	3					3
Possible meteorites	8					8
Total	207	83	35	13	29	367

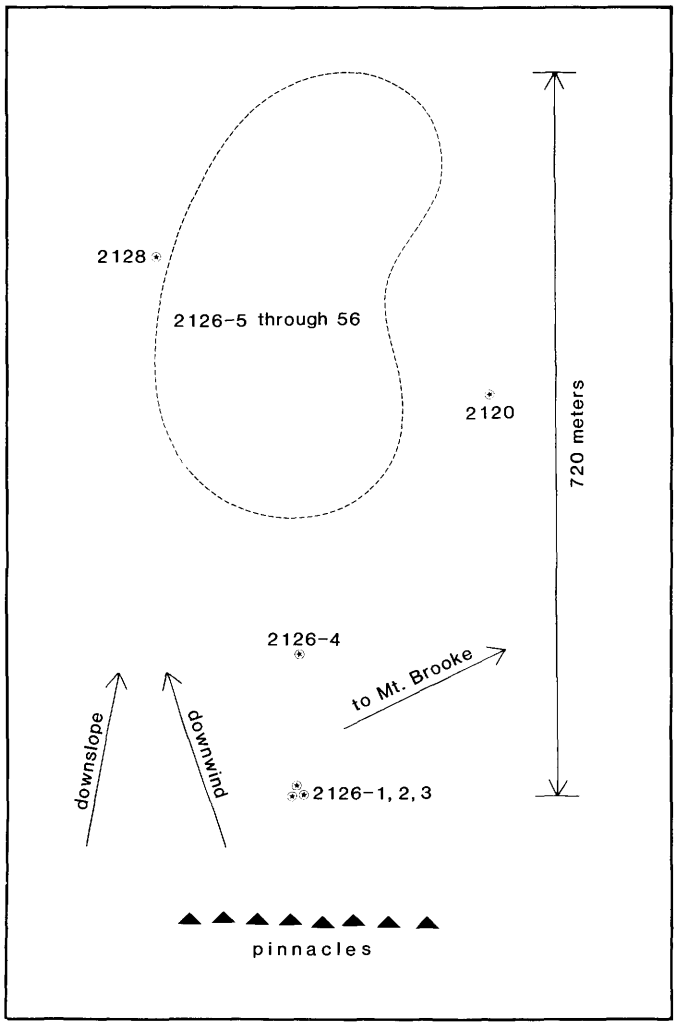

FIGURE 5-8.—Sketch map of carbonaceous chondrite strewnfield of 56 fragments (field numbers 2126-1 to 2126-56) on the Allan Hills Far Western Icefield. Numbers 2120 and 2128 are other types of meteorites in the same area.

6. Descriptions of Stony Meteorites

Brian Mason, Glenn J. MacPherson, Roberta Score, Carol Schwarz, and Jeremy S. Delaney

This chapter provides descriptions of some of the individual meteorite specimens collected during the 1982–1983 and 1983–1984 field seasons. The descriptions are based largely on those published in the *Antarctic Meteorite Newsletter*, with additional information as available. Also included here are previously unpublished data on small specimens of special interest from the 1978–1979 and 1981–1982 field seasons. The Appendix contains a complete list of Antarctic meteorites recovered to date, along with their type, weathering grade, mass, etc. Specimens weighing less than 100 grams that do not show distinctive features are listed in the Appendix, but are not described in the text.

Descriptions are arranged according to meteorite classification. Within the chondrites the specimens are grouped according to the Van Schmus and Wood (1967) classification, and the descriptions follow the order of increasing petrographic type.

The letter-number designations concur with guidelines recommended by the Committee on Nomenclature of the Meteoritical Society; each carries the following information: location, e.g., ALH (Allan Hills); expedition and year, e.g., A81 (Expedition A, 1981); sample number, xxx (e.g., 213). After 1981 the "A" preceding the year was dropped. The original weight of the specimen is given to the nearest gram (nearest 0.1 gram for specimens weighing less than 100 grams).

Chondrites

CLASS C2

FIGURES 6-1, 6-2

ALHA81312 (0.7 g).—This small specimen (1.0 × 0.8 × 0.5 cm) was tentatively identified as a carbonaceous chondrite from its exterior features, and this has been confirmed by examination of the thin section. The section shows several small chondrules (maximum diameter 0.5 mm) and numerous colorless mineral grains in a translucent brown to opaque black matrix. McSween (personal communication) reports the following modal analysis of this section (vol. %): matrix, 60.3; monomineralic grains, 14.1; chondrules and polymineralic fragments, 22.8; inclusions, 2.8. Microprobe analyses show the following wide ranges in composition for olivine and pyroxene: olivine, Fa_{1-35}, with a mean of Fa_6; pyroxene generally close to clinoenstatite in composition, but individual grains range up to Fs_{31}. Small refractory (spinel-rich) inclusions are present, some of which contain pleochroic (deep blue to colorless) hibonite.

ALH82100 (24.3 g).—Patches of fusion crust are preserved mainly on one side of this small stone (3.5 × 3.5 × 2.5 cm). Small submillimeter inclusions are visible on the exposed interior surfaces. The stone is unfractured and one face has a rough texture from weathering. The thin section shows numerous small colorless grains (up to 0.3 mm) and irregular aggregates (up to 0.6 mm, and mainly of olivine), and sparse chondrules, in a black matrix that is translucent brown in thinned areas. A few small spinel- and perovskite-bearing refractory inclusions and spherules are present. Trace amounts of nickel-iron and troilite occur as widely dispersed minute grains. Microprobe analyses show olivine compositions in the range Fa_{1-47}, but most grains are iron-poor and the mean composition is Fa_5; pyroxene is rare, and only two grains of clinoenstatite (Fs_{1-2}) were analyzed. McSween (personal communication) reports the following modal analysis of this section (vol.%): matrix, 77.1; monomineralic grains, 7.5; chondrules and polymineralic fragments, 13.9; inclusions, 1.5.

ALH82131 (1.0 g).—One small patch of blistery fusion crust remains on this tiny specimen (1 × 1 × 0.5 cm). The exposed underlying surface is black with a greenish tinge. The interior is black and contains many submillimeter-size white inclusions. A green weathering rind extends approximately 1 mm into the stone. The very small thin section shows a single chondrule in a black (brown on thin edges) opaque matrix. Microprobe analyses show that the matrix has the composition

Brian Mason and Glenn J. MacPherson, Department of Mineral Sciences, National Museum of Natural History, Smithsonian Institution, Washington, D.C. 20560. Roberta Score and Carol Schwarz, Northrop-Houston, Johnson Space Center, Houston, Texas, 77058. Jeremy S. Delaney, Department of Mineral Sciences, American Museum of Natural History, New York, N.Y. 10024.

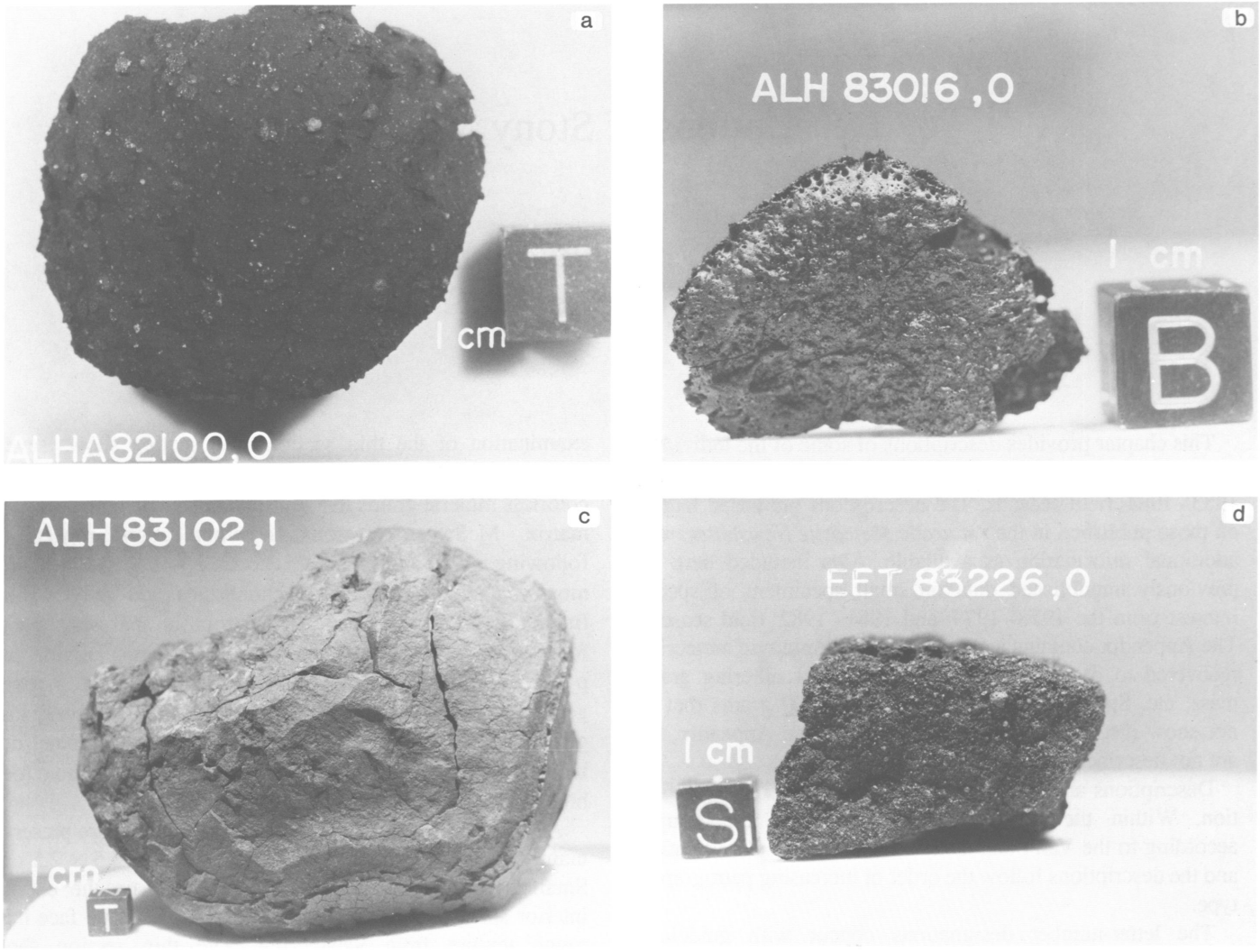

FIGURE 6-1.—C2 chondrites; note the blistery fusion crust on ALH83016.

characteristic of C2 chondrites. Clasts and inclusions are largely replaced by green to brown phyllosilicate material. Olivine in the chondrule is almost pure forsterite (FeO 0.3%; CaO 0.3%–0.4%).

ALH83016 (4.1 g).—A brown to black fusion crust covers part of this small stone (3 × 2 × 0.8 cm). The interior is black with abundant irregular white inclusions and some chondrules. The thin section shows a few poorly defined chondrules up to 1.8 mm across, consisting of granular or barred olivine with minor polysynthetically twinned clinopyroxene. A few small spinel-rich inclusions are present. The bulk of the meteorite consists of translucent brown to opaque black matrix. Scattered through the matrix are colorless, birefringent grains, mostly olivine, up to 0.3 mm but usually less than 0.1 mm across. Trace amounts of nickel-iron and sulfides are dispersed throughout the section as minute grains. Well-preserved fusion crust rims part of the section. Microprobe analyses show that olivine varies widely in composition, ranging from $Fa_{0.3}$ to Fa_{30} (with a mean of Fa_{11}); it also has a notable chromium content, 0.1–0.5 weight percent Cr_2O_3. Pyroxene is generally close to clinoenstatite in composition. McSween (personal communication) reports the following modal analysis of this section (vol.%): matrix, 65.6; monomineralic grains, 7.1; chondrules and polymineralic fragments, 22.6; inclusions, 3.7.

ALH83100 (2293 g).—Since the initial description of this stone, many other specimens have been paired with it (e.g., see *Antarctic Meteorite Newsletter*, 8(2), and the cumulative weight for 55 pieces is 2293 g. ALH83100 itself is an angular fragment, and is so highly fractured that several pieces fell off during handling. The surface is dull black with a few barely discernible clasts or chondrules. White "evaporite" deposits are present locally; these are apparently weathering products formed in the Antarctic, but they only became visible in the receiving laboratory as water in the interior of the meteorite worked its way to the surface carrying soluble salts along with it. The thin section shows a large number of clasts (up to 1

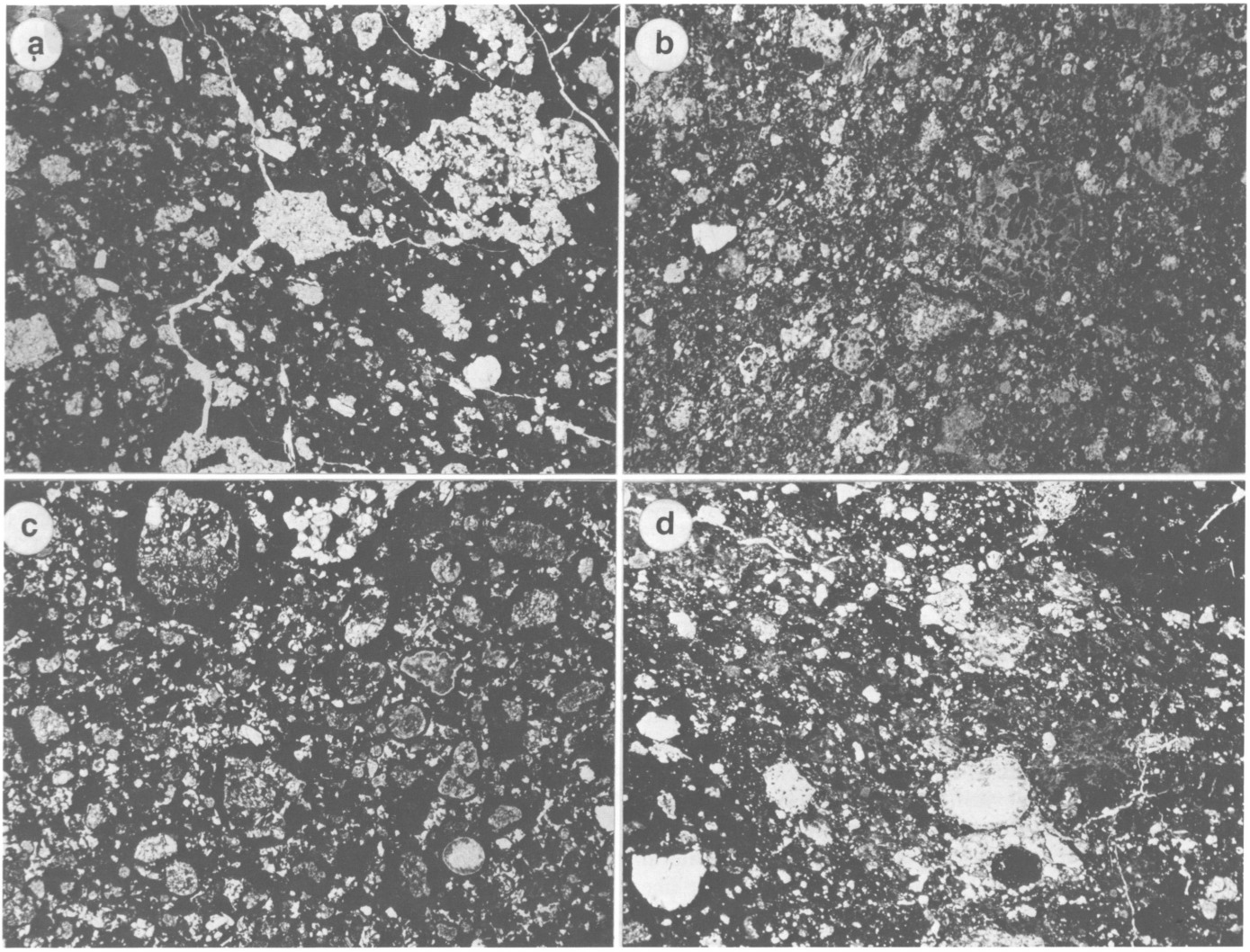

FIGURE 6-2.—Photomicrographs of thin sections of C2 chondrites (each field of view is 3 × 2 mm): *a*, ALHA81312; *b*, ALH83100; *c*, EET83226; *d*, EET83250. Irregular aggregates, grains, and rare chondrules, mainly of olivine (white to gray) in translucent to opaque matrix (black).

mm across) and mineral grains, and a few chondrules, in a dark matrix. A little (about 1%) sulfide is present as minute grains, some of which are concentrated at the margins of chondrules. Nickel-iron occurs in trace amounts, some as small spherules. The clasts, inclusions, and most of the mineral grains consist of phyllosilicate and, in many places, calcite, that are probably alteration products of the original phases. Microprobe analyses shows that a few preserved primary grains are forsteritic olivine.

ALH83102 (1786 g).—This meteorite consists of 20 or more pieces; only two of the larger pieces have been examined to date. Both pieces are extensively fractured and extremely friable. Small patches of fusion crust are present. White evaporite deposits (see above) are present on both interior and exterior surfaces. Small white inclusions are visible in a greenish black to black matrix that locally shows signs of heavy oxidation. The thin sections show that the two fragments are identical. Both are intensely altered, with the matrix, inclusions, and chondrules being almost completely replaced by iron-rich phyllosilicates, calcite, and iron oxides. The matrix is opaque and black except where the sections are unusually thin. Olivine grains are sporadically preserved, with compositions that are mostly $Fa_{0\text{-}2}$, although some range up to Fa_{42}. One small spinel-rich refractory spherule was found, in which the spinel is nearly pure $MgAl_2O_4$. No other primary phases were found in this spherule.

This meteorite can confidently be paired with ALH83100, because of the identical and unusual petrographic features of both specimens and because of their geographic proximity on the ice field where they were found (see Chapter 5).

EET83224 (8.6 g).—A dull and fractured fusion crust covers about one-quarter of this small specimen (2.5 × 2.5 × 1.5 cm).

Some of the uncrusted surface is jet black, but in places it has weathered to a brown color. Chondrules and small irregular white inclusions are visible in the jet black interior. The thin section shows a few chondrules (up to 0.8 mm in diameter), small (0.1 mm or less), colorless, and birefringent grains (mostly olivine), and what appear to be chondrule or clast fragments, all in a transparent brown to opaque black matrix. Chondrules consist mostly of granular olivine, but a few have minor polysynthetically twinned clinopyroxene as well. A few small spinel-bearing refractory inclusions are present. Accessory nickel-iron and trace amounts of sulfide are dispersed throughout the section as minute grains. Microprobe analyses gave the following compositions: olivine ranges from $Fa_{0.2}$ to Fa_{41}, with a mean of Fa_8; pyroxene is generally near enstatite in composition (FeO 0.4%–1.0%). McSween (personal communication) reports the following modal analysis of this section (vol.%): matrix, 63.8; monomineralic grains, 12.4; chondrules and polymineralic fragments, 21.3; inclusions, 2.5.

EET83226 (33.1 g).—No fusion crust remains on this angular fragment (4 × 2.5 × 3 cm). The exposed surface is jet black with a granular texture and shows abundant chondrules and inclusions. The thin section shows abundant small chondrules, averaging about 0.3 mm in diameter, and numerous mineral aggregates and mineral grains, set in a moderate amount of dark brown to black opaque matrix. Chondrule types include granular and barred olivine, some of which contain pale brown and partly devitrified glass. Accessory amounts of finely dispersed nickel-iron and sulfide are present. Microprobe analyses show that much of the olivine is near forsterite in composition, but occasional iron-rich grains are present (the overall range is $Fa_{0.5\text{-}69}$, with a mean of Fa_{12}). Pyroxene grains are rare; their composition range is $Fs_{0.6\text{-}10}$. McSween (personal communication) reports the following modal analysis of this section (vol.%): matrix, 39.6; monomineralic grains, 14.5; chondrules and polymineralic fragments, 36.1; inclusions, 9.8.

EET83250 (11.5 g).—This specimen broke into many fragments during transport from Antarctica. Both fusion crust and white evaporite deposits cover much of the exterior surface. Interior surfaces are black and speckled with white inclusions. In thin section only a few chondrules and chondrule fragments are seen; the bulk of the meteorite consists of brown to black semi-opaque matrix, enclosing numerous small (0.1 mm and less), colorless, birefringent grains, mostly olivine. A few small spinel-rich inclusions are present. The matrix also contains trace amounts of finely dispersed nickel-iron and sulfides. Well-preserved fusion crust rims part of the section. Microprobe analyses show most of the olivine is close to forsterite in composition, with a few iron-rich grains (the range is $Fa_{0.3\text{-}22}$, with a mean of Fa_4). Pyroxene grains are rare; their composition range is $Fs_{2\text{-}14}$. McSween (personal communication) reports the following modal analysis of this section (vol.%): matrix, 71.2; monomineralic grains, 14.5; chondrules and polymineralic fragments, 12.1; inclusions, 2.2.

CLASS C3

FIGURES 6-3, 6-4

ALHA81258 (1.1 g).—This small stone (1 × 1 × 0.5 cm) is mostly covered by vesicular black fusion crust; chondrules are visible on interior surfaces. The thin section shows numerous chondrules up to 2 mm across and irregular crystalline aggregates up to 3 mm in maximum dimension, set in a minor amount of dark brown to black semi-opaque matrix. The chondrules and aggregates consist mainly of granular olivine with minor amounts of polysynthetically twinned pyroxene. Trace amounts of nickel-iron are present as minute grains. Sulfide is present in small amounts, finely dispersed throughout the matrix and sometimes concentrated in chondrule rims. Microprobe analyses of chondrule olivines show a wide composition range: $Fa_{0\text{-}28}$, mean Fa_{11}; the matrix appears to consist largely of fine-grained iron-rich olivine, $Fa_{40\text{-}60}$. Pyroxene in the chondrules is clinoenstatite, mostly near Fs_1, but with occasional Fe-rich grains. The meteorite is a C3V chondrite, very similar to ALHA81003; the possibility of pairing should be considered.

ALH82101 (29.1 g).—The exterior surfaces of this stone (3 × 2.7 × 2.7 cm) are mostly covered with a shiny, blistery fusion crust. Broken surfaces reveal a gray-beige interior with an outer, 1 mm thick, discontinuous weathering rind. The matrix is fine-grained, with metal and a few white to gray inclusions being visible. The thin section shows an aggregate of small chondrules (average diameter ~0.5 mm), chondrule fragments, and mineral grains set in an extremely fine-grained, translucent tan to yellow-brown matrix. The chondrules show a wide variety of textures; in barred olivine chondrules the material interstitial to the bars is pale brown isotropic glass. Minor amounts of nickel-iron and sulfide are present, as small grains

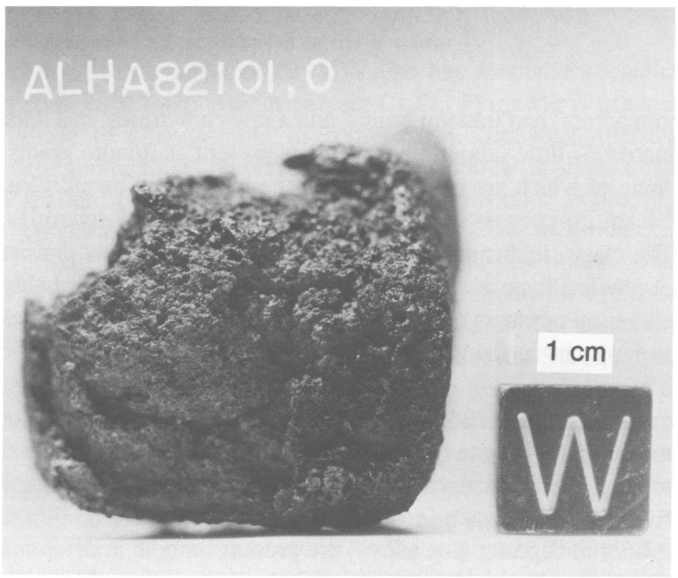

FIGURE 6-3.—C3 chondrite ALH82101.

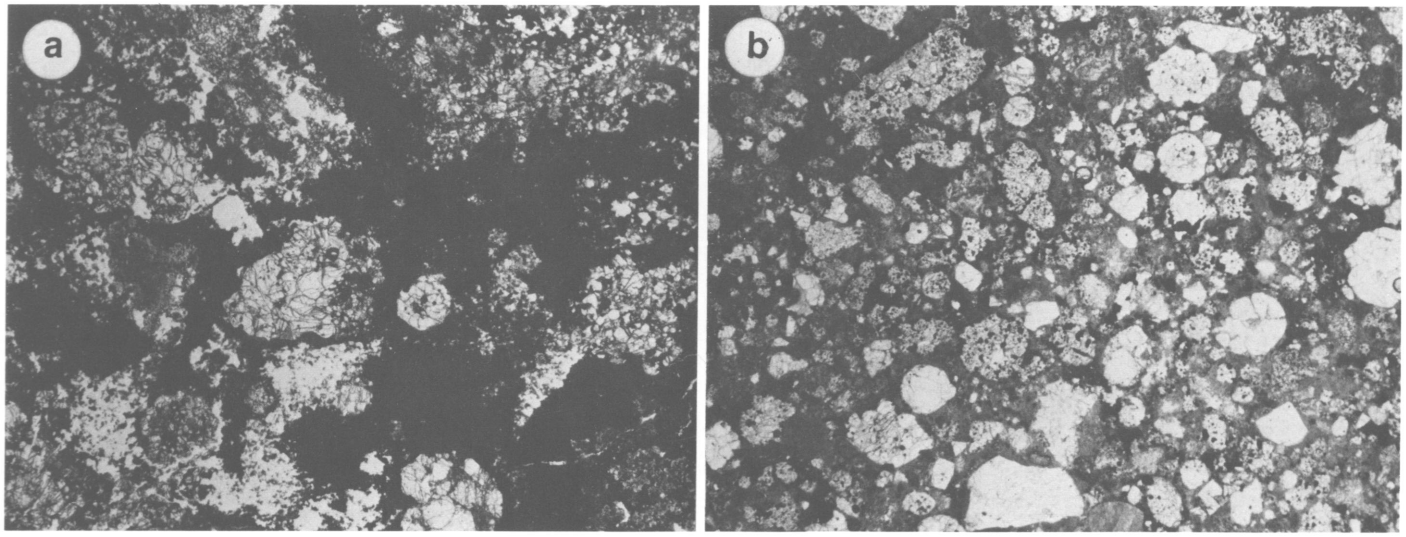

FIGURE 6-4.—Photomicrographs of thin sections of C3 chondrites (each field of view is 3 × 2 mm). *a*, ALHA81258; *b*, ALH82101. Note the textural differences between ALHA81258 (C3V) and ALH82101 (C3O).

within some chondrules and also concentrated around their margins. Numerous small refractory inclusions are present; identified phases include melilite, deep pink spinel, and colorless hibonite. Microprobe analyses of olivine show a wide composition range: $Fa_{1\text{-}50}$, with a mean of Fa_{22}; only a few grains of pyroxene were found, having a composition range of $Fs_{1\text{-}10}$. The meteorite is classified as a C3 chondrite of the Ornans subtype; it is possibly paired with ALHA77003.

Wieler et al. (1985) have reported abundances and isotopic compositions of He, Ne, and Ar in ALH82101.

CLASS H3

FIGURE 6-5

ALH82110 (39.3 g).—Fusion crust totally covers this small stone (4.5 × 2.5 × 2.0 cm). Chipping has exposed a weathered interior with some obvious inclusions. The thin section shows a close-packed aggregate of chondrules and chondrule fragments in a minor amount of opaque matrix. Nickel-iron grains are abundant in the matrix, sometimes concentrated in chondrule rims; troilite is present in lesser amount. A wide variety of chondrules is present, ranging up to 2 mm in diameter; the most common types are porphyritic and granular olivine and olivine-pyroxene. Microprobe analyses show the following wide composition ranges in olivine and pyroxene: olivine, $Fa_{0.6\text{-}24}$, with a mean of Fa_{14} (% mean deviation of FeO is 52; see Dodd et al., 1967, for definition of % mean deviation); pyroxene, $Fs_{3\text{-}28}$, with a mean of Fs_{13} (% mean deviation of FeO is 48).

PCA82520 (22.7 g).—Dull black fusion crust covers 80% of the surface of this pyramidal stone (3 × 2 × 1.5 cm), the remainder being covered with a shiny reddish brown crust. Extensive weathering has given the matrix a yellowish to reddish brown color, but some metal is nonetheless preserved. The thin section shows a close-packed aggregate of chondrules (up to 1.5 mm in diameter), chondrule fragments, and a few clasts, with interstitial nickel-iron and troilite and a relatively small amount of dark matrix. A considerable variety of chondrules is present, the majority being granular or porphyritic olivine types with transparent to turbid interstitial glass; other types include fine-grained pyroxene, medium-grained olivine plus polysynthetically twinned clinopyroxene, and barred olivine. Brown limonitic staining pervades the section.

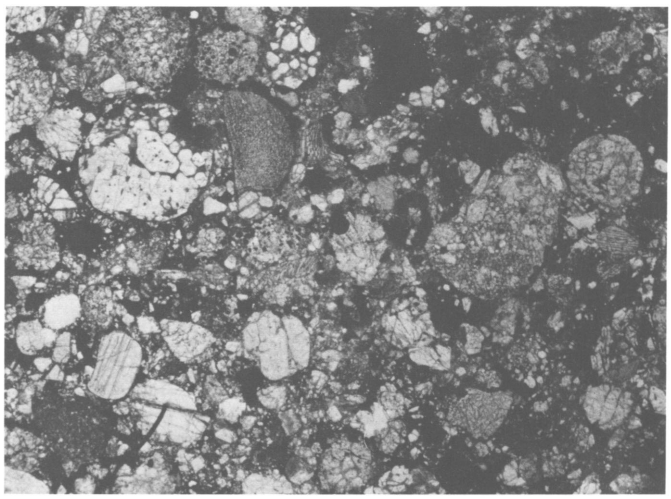

FIGURE 6-5.—Photomicrograph of thin section of H3 chondrite ALH82110 (field of view is 3 × 2 mm). A closely packed aggregate of chondrules, irregular fragments, and mineral grains is set in a minor amount of dark matrix.

Microprobe analyses show olivine mainly in the range Fa_{15-22}, but one clast has olivine Fa_6; the mean composition is Fa_{17} (% mean deviation of FeO is 27). Pyroxene ranges in composition from Fs_2 to Fs_{19} with a mean of Fs 14 (% mean deviation of FeO is 24).

CLASS L3

FIGURES 6-6, 6-7

ALHA78013 (4.1 g), 78186 (3.1 g), 78236 (14.4 g), 78238 (9.8 g), 78243 (1.9 g), 81145 (21.1 g), 81156 (19.7 g), 81162 (59.4 g), 81190 (48.3 g), 81191 (30.4 g), 81214 (4.4 g), 81229 (40.0 g), 81243 (15.0 g), 81259 (9.9 g), 81272 (22.9 g), 81280 (54.9 g), 81292 (12.9 g), 81299 (0.5 g).—Examination of thin sections and microprobe analyses of the minerals in these meteorites show that they are essentially identical to ALHA77011, and can confidently be paired with it. E.R.D. Scott (personal communication) has also examined the sections and supports this interpretation.

ALHA78046 (70.0 g).—Thin section examination shows that this stone consists almost entirely of a close-packed aggregate of chondrules and chondrule fragments; most of the interstitial material consists of nickel-iron and troilite grains, in places forming rims on the chondrules. Weathering is extensive, with limonitic staining and small areas of brown limonite throughout the section. Chondrules range from 0.3 to 3.6 mm in diameter; a variety of types is present, the most common being granular and porphyritic olivine and olivine-pyroxene. Microprobe analyses show considerable variability in mineral compositions. Olivine compositions range from Fa_8 to Fa_{25}, with a mean of Fa_{19} (% mean deviation of FeO is 20). Pyroxene compositions range from Fs_8 to Fs_{20}, with a mean of Fs_{16}. The % mean deviation of FeO in olivine is much lower than that for olivine in the ALHA77011 group, suggesting that this meteorite is more equilibrated and hence different from the 77011 group.

ALHA78133 (59.9 g).—Thin section examination shows that this stone is largely made up of chondrules and chondrule fragments set in a minor amount of dark matrix. Nickel-iron and troilite are present in subequal amounts, dispersed through the matrix as small grains and sometimes forming rims on the chondrules. A moderate amount of weathering is indicated by brown limonitic staining throughout the matrix. Chondrules range in diameter from 0.3 to 1.5 mm; types seen include porphyritic olivine and olivine-pyroxene, granular olivine and olivine-pyroxene, devitrified glass, and radiating pyroxene. Microprobe analyses show olivine ranging in composition from Fa_1 to Fa_{34} with a mean of Fa_{16} (% mean deviation of FeO is 52); pyroxene ranges in composition from Fs_1 to Fs_{16} with a mean of Fs_8 (% mean deviation of FeO is 69). In mineral composition this meteorite is similar to those in the ALHA 77011 group, but E.R.D. Scott (personal communication) states that it appears to lack the graphite-magnetite intergrowths characteristic of that group.

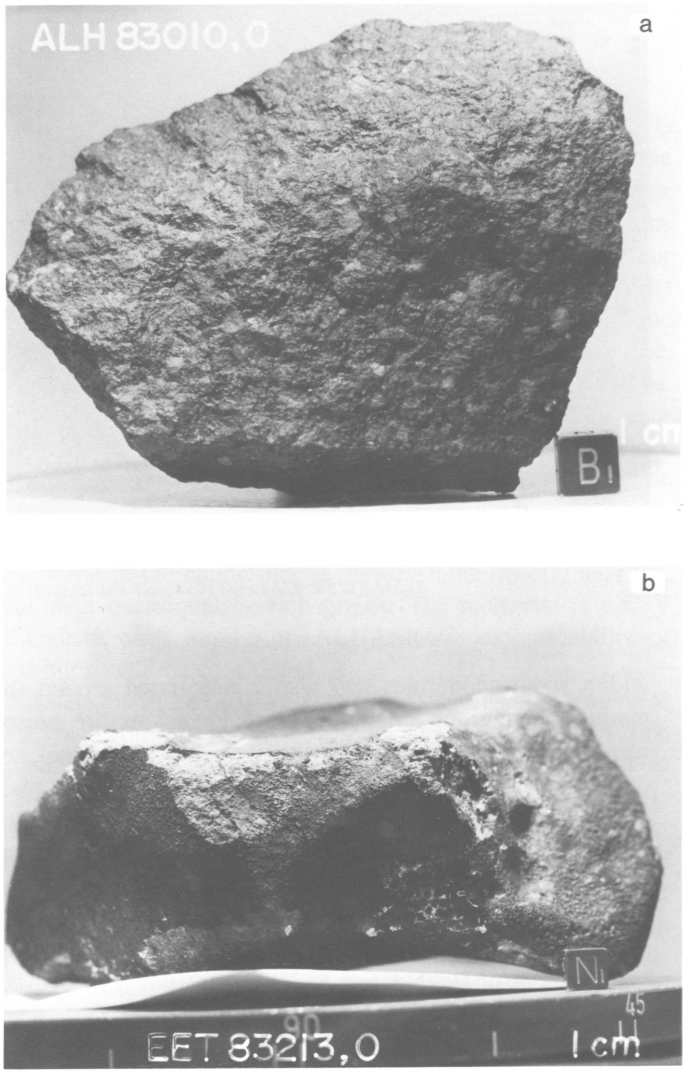

FIGURE 6-6.—L3 chondrites.

ALH83010 (395 g).—A black iridescent fusion crust is present on one side of this meteorite fragment (10.5 × 8 × 2 cm). The other surfaces are dark greenish gray with iridescent reddish brown areas. Numerous chondrules (1–4 mm in diameter) and large clasts (the largest is 1.0 × 0.5 cm) are visible on the exposed interior surfaces. The stone is extremely coherent. The interior consists of dark matrix with numerous millimeter-sized, gray to yellowish colored chondrules. Nickel-iron is clearly visible. The thin section shows sharply defined chondrules up to 2.5 mm in diameter, many of which contain clear brown isotropic glass. Pyroxene is mostly monoclinic and has a composition range of Fs_{2-28}. Olivine compositions are in the range Fa_{4-31}. Metal (two phases present) is subequal with troilite in abundance. There are well-defined sulfide rims around many chondrules. Chromite is accessory and is

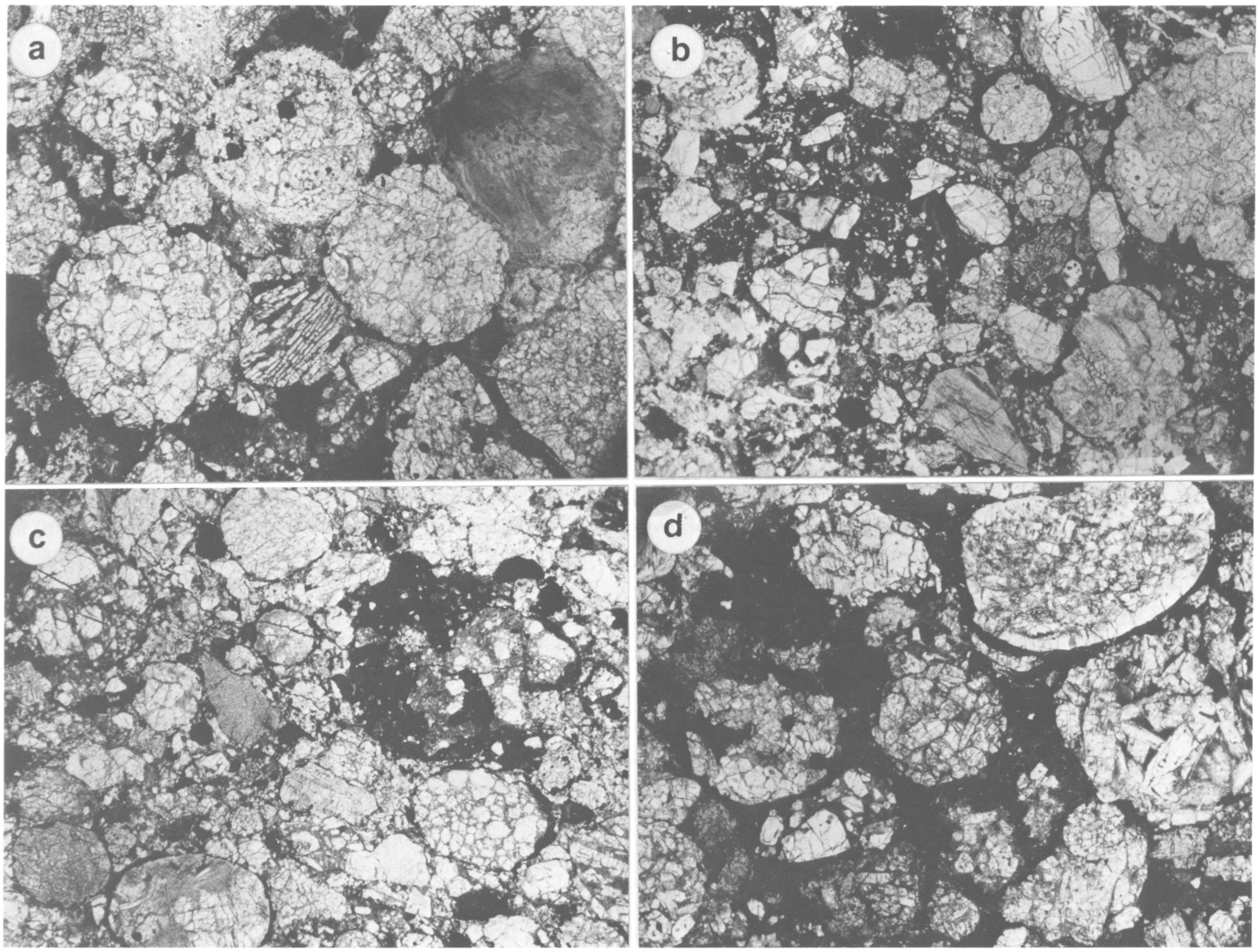

FIGURE 6-7.—Photomicrographs of thin section of L3 chondrites (each field of view is 3 × 2 mm): *a*, ALHA78046; *b*, ALHA78133; *c*, EET82601; *d*, EET83213. A closely packed aggregate of chondrules, irregular fragments, and mineral grains set in dark matrix.

generally very fine-grained.

EET82601 (149 g).—This angular to subrounded specimen is covered with patchy remnants of fusion crust. Chondrules 1–4 mm in diameter are visible on the surfaces where fusion crust is missing. The interior is very dark with weathered, millimeter-sized chondrules visible. The thin section shows a close-packed aggregate of chondrules, ranging up to 1.5 mm in maximum dimension. A variety of types is present, the most common being granular olivine and olivine-pyroxene, porphyritic olivine and olivine-pyroxene, and cryptocrystalline pyroxene. The small amount of matrix is fine-grained and opaque, and contains a few grains of nickel-iron and troilite. The meteorite is considerably weathered, with brown limonitic staining throughout the section. Olivine and pyroxene show the following wide ranges of compositions: olivine, Fa_2 to Fa_{39}, with a mean of Fa_{22} (% mean deviation of FeO is 36); pyroxene, Fs_1 to Fs_{35}, with a mean of Fs_{13} (% mean deviation of FeO is 45).

EET83213 (2727 g).—A dull, fractured fusion crust covers most of this stone (16 × 15 × 7 cm); evaporite deposits are present on several surfaces. The interior is greenish gray with numerous white, cream, and darker gray inclusions or chondrules. Some metal is present. The thin section shows sharply defined chondrules up to 3 mm in diameter set in a brown matrix. Isotropic clear brown glass is preserved in some chondrules. Moderate limonitic staining is locally present, indicating mild to moderate weathering. Monoclinic pyroxene is very common, with a composition range of $Fs_{3\text{-}26}$. Olivine

ranges in composition from Fa_{13} to Fa_{30}. Minor metal and troilite are present in subequal amounts; two metal phases are present, locally in plessitic intergrowths.

This meteorite is very similar in texture and mineral compositions to EET82601, and the possibility of pairing should be considered.

CLASS LL3

FIGURE 6-8

TIL82408 (80.1 g).—A polygonally fractured, black fusion crust coats much of this stone (4.5 × 4 × 2.5 cm). Areas without fusion crust are somewhat friable. The meteorite is clast-rich, with a very dark gray to black matrix. Oxidation is evenly distributed throughout the interior. The thin section shows a close-packed aggregate of chondrules and chondrule fragments, up to 4 mm across. The matrix is black and opaque, much of it forming rims to the chondrules; the matrix contains much sulfide and a little nickel-iron (largely weathered to limonite). A wide variety of chondrule types is present, including porphyritic olivine and olivine-pyroxene, granular olivine and olivine-pyroxene, barred olivine, and fine-grained pyroxene. Some of the chondrules preserve clear, isotropic, interstitial glass. Microprobe analyses show the following wide ranges of compositions for olivine and pyroxene: olivine, $Fa_{1\text{-}29}$, with a mean of Fa_{15} (% mean deviation of FeO is 41); pyroxene, $Fs_{2\text{-}21}$, with a mean of Fs_9. The highly variable compositions of olivine and pyroxene and the presence of isotropic glass indicate type 3, and the small amount of nickel-iron suggests the LL group; the meteorite is thus tentatively classified as an LL3 chondrite.

Wieler et al. (1985) have reported abundances and isotopic compositions of He, Ne, and Ar in TIL82408.

CLASS C4

FIGURES 6-9, 6-10

ALH82135 (12.1 g).—Black fusion crust covers most of this triangular-shaped stone (3 × 2.5 × 1 cm). Freshly broken surfaces expose a dark bluish gray matrix with signs of some oxidation. In thin section the meteorite consists largely of finely granular olivine (grains ranging up to 0.1 mm), minor pyroxene, plagioclase, and opaques. A few relatively coarse-grained olivine chondrules are present. Microprobe analyses give the following compositions: olivine, Fa_{27} (a few grains are more iron-rich); pyroxene, Fs_{25}; plagioclase, $An_{20\text{-}75}$. This meteorite is similiar to Karoonda and PCA82500 in texture and mineral compositions.

Wieler et al. (1985) have reported abundances and isotopic compositions of He, Ne, and Ar in ALH82135. Scott (1985) has discussed its petrology.

PCA82500 (90.9 g).—This specimen (7 × 5 × 2.8 cm) has a very unusual external appearance. It is extremely fragmented and has numerous rounded cavities, some of which extend through the thickness of the specimen to give it a "swiss cheese" appearance. The cavities were filled with ice and snow when the meteorite was found. Several patches of fusion crust are present. The exterior surfaces vary in color from dark gray to lighter gray and yellowish gray, the lighter colors being characteristic of the less weathered areas. Inclusions (chondrules?) are exposed on those portions of the exterior surface that lack fusion crust. White evaporite deposits and yellow-colored weathering residues are abundant on interior surfaces; the white material is an unusual nickel-rich magnesium sulfate (J. Gooding, personal communication, 1986). In spite of the weathering and evaporite deposits, the interior surfaces reveal a fine-grained matrix with minute metal flecks and a few

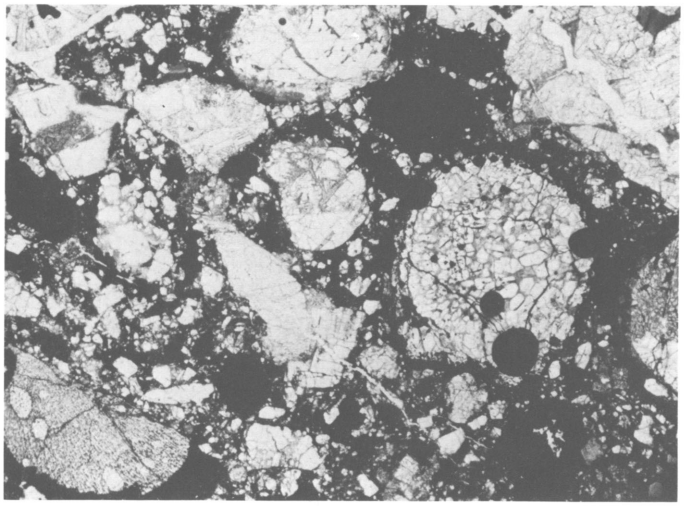

FIGURE 6-8.—Photomicrograph of thin section of LL3 chondrite TIL82408 (field of view is 3 × 2 mm). Chondrules, chondrule fragments, irregular fragments, and mineral grains are set in a dark matrix.

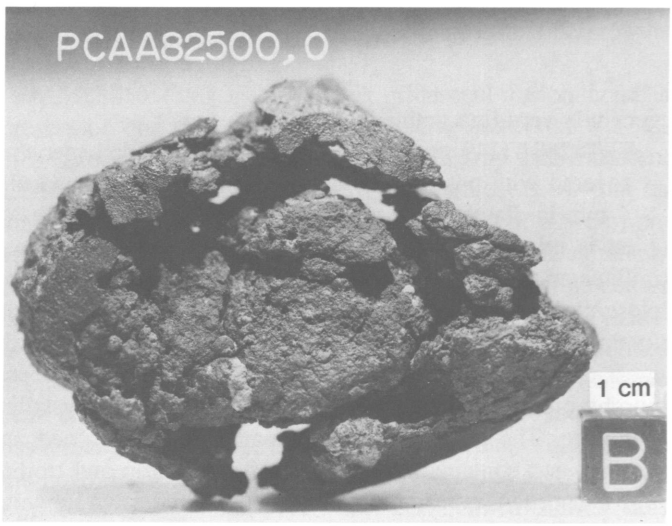

FIGURE 6-9.—C4 chondrite PCA82500.

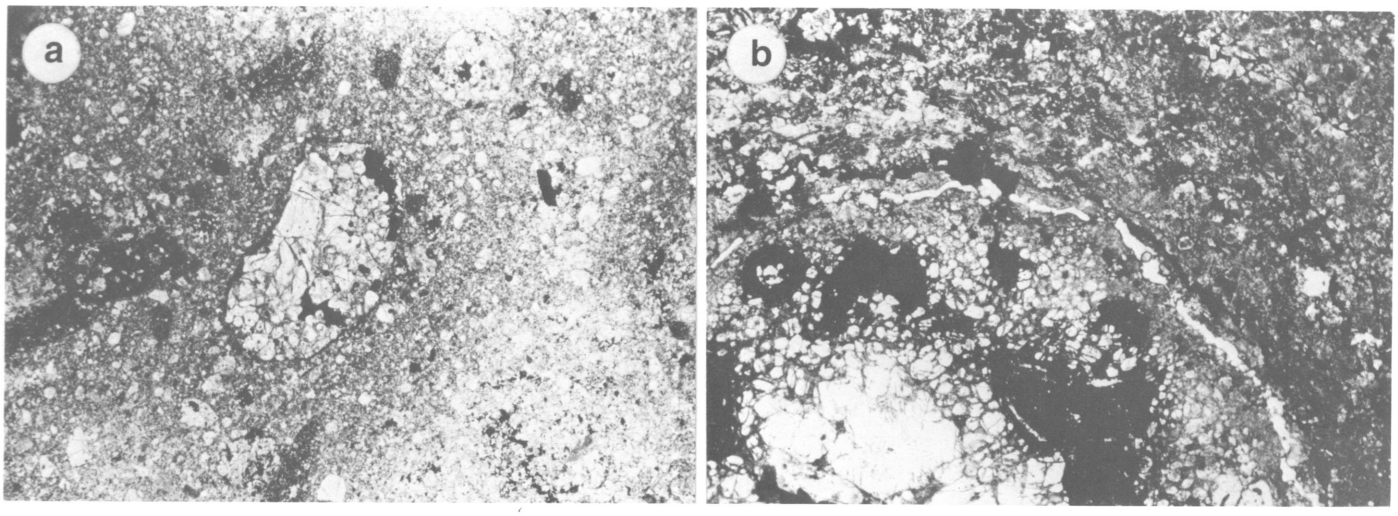

FIGURE 6-10.—Photomicrographs of thin section of C4 chondrites (each field of view is 3 × 2 mm): *a*, ALH82135; *b*, PCA82500. In ALH82135, sparse chondrules are set in a matrix consisting largely of fine-grained olivine. In PCA82500, the lower left area shows a segment of a large (3.6 mm diameter) chondrule.

yellowish dots of oxidation. The thin section contains a single porphyritic olivine chondrule, diameter 3.6 mm, in an aggregate of turbid anhedral olivine grains averaging 0.1 mm. Small amounts of troilite and nickel-iron are present, the metal being largely weathered to brown limonite. Microprobe analyses show a uniform olivine composition of Fa_{31}, and variable plagioclase in the range An_{20} to An_{40}. No pyroxene was found. This meteorite was classified in the *Antarctic Meteorite Newsletter*, 6(2), as an LL6 chondrite, but has since been recognized as a C4 chondrite that is very similar to Karoonda (Scott, 1985).

Wieler et al. (1985) have reported abundances and isotopic compositions of He, Ne, and Ar in PCA 82500. Scott (1985) concludes that Karoonda, PCA 82500, Yamato 6903, and Mulga (West) are very similar and may have come from the same body.

CLASS E4

FIGURE 6-11

ALHA81189 (2.6 g).—No fusion crust remains on this fractured reddish brown stone (2 × 1.5 × 0.5 cm). The thin section shows an aggregate of chondrules, chondrule fragments, and mineral grains set in an opaque matrix. The chondrules range up to 0.9 mm in diameter; most of them consist of granular pyroxene (sometimes with a little olivine), but a few are made up of nickel-iron and troilite. The matrix consists largely of nickel-iron and troilite, with a considerable amount of secondary limonite. Microprobe analyses show that the pyroxene is close to $MgSiO_3$ in composition (FeO 0.5%–4.5%, with a mean of 1.9%; Al_2O_3 0.02%–2.4%, mean 0.7%; CaO 0.1%–0.7%, mean 0.3%; TiO_2 0%–0.13%, mean 0.08%; MnO 0.07%–0.22%, mean 0.15%). Most of the olivine grains are close to Mg_2SiO_4 in composition (FeO 0.7%–6.4%). One grain of a silica polymorph was analyzed. The metal contains approximately 2.5% Si. Because some of the pyroxene is polysynthetically twinned clinoenstatite, the meteorite is tentatively classified as an E4 chondrite.

ALH82132 (5.9 g).—No fusion crust remains on this iridescent, reddish brown, highly oxidized stone (2 × 2 × 1 cm). A thin coating of evaporite deposits are present on some of the extensively weathered interior surfaces. Thin section examination shows that chondrules are relatively abundant but small, ranging up to 0.6 mm in diameter. Most of them consist of pyroxene, but some are made up almost entirely of nickel-iron and troilite. The matrix consists largely of granular pyroxene, with lesser amounts of nickel-iron and sulfides, a little plagioclase and a silica polymorph. The meteorite is considerably weathered, with brown limonitic staining throughout the section. Microprobe analyses show that the pyroxene is almost pure $MgSiO_3$ (FeO 0.06%–0.7%, mean 0.3%; Al_2O_3 0–0.3%, mean 0.04%; CaO 0.02%–0.6%, mean 0.16%; TiO_2 and MnO each less than 0.05%). Plagioclase is almost pure albite (CaO 0.2%, K_2O 0.11%). The meteorite is an enstatite chondrite and, since some of the pyroxene is polysynthetically twinned clinoenstatite, it is classified as an E4 chondrite.

E.R.D. Scott (personal communication) has examined the thin sections of the E4 chondrites from the Allan Hills, and comments that 81189 and 82132 are definitely not paired, 82132 appearing more equilibrated than 81189; 81189 does resemble 77156 and 77295, and may tentatively be paired with them.

PCA82518 (21.9 g).—The fusion crust coating this stone (3 × 2.5 × 2 cm) is shiny, iridescent, and ranges in color from orange-red to brown to black. The exterior is dotted with numerous vugs that are lined with fusion crust. Exposed interior surfaces reveal a dark brown matrix with abundant chondrules (as large as 3 mm in diameter) and metal. Thin

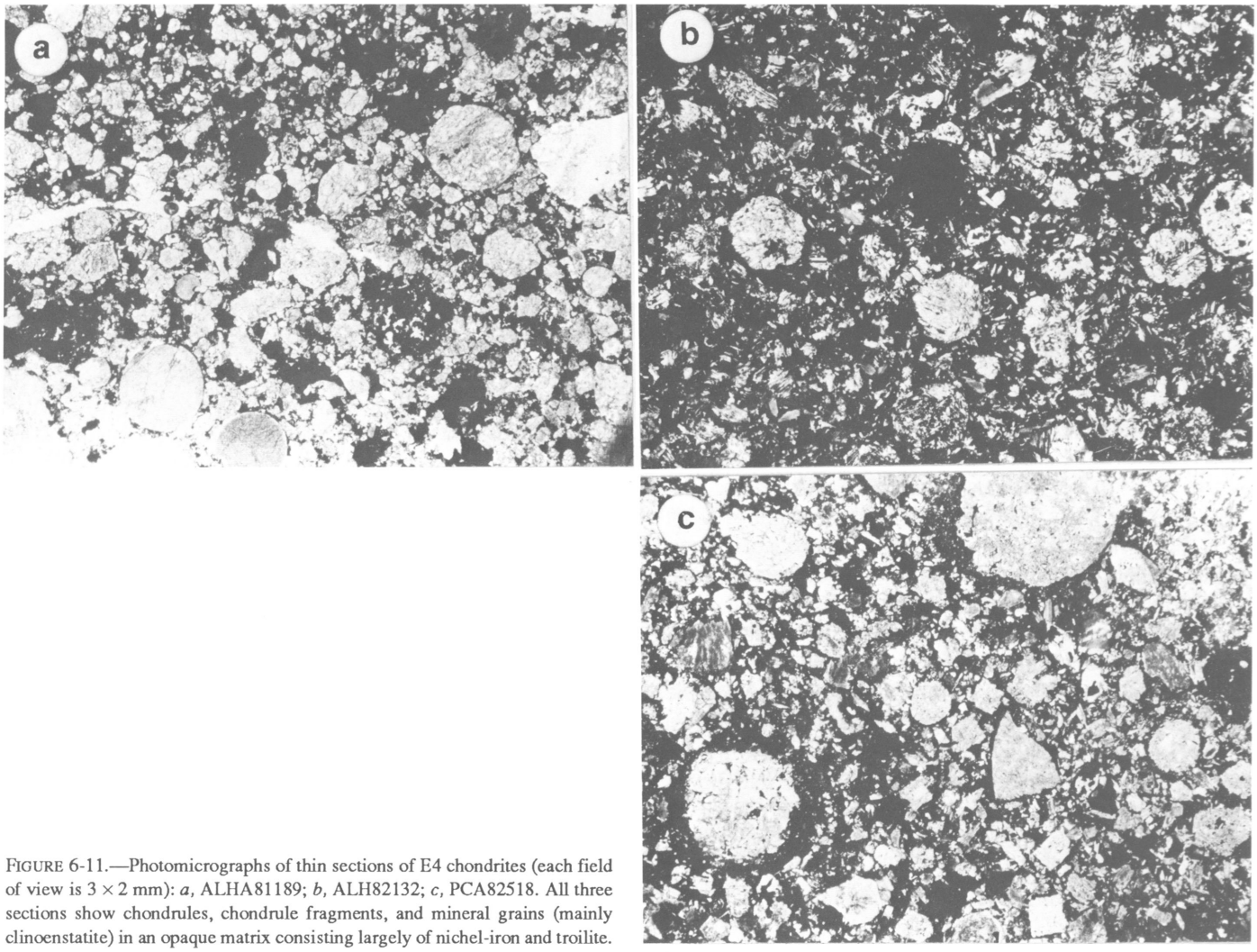

FIGURE 6-11.—Photomicrographs of thin sections of E4 chondrites (each field of view is 3 × 2 mm): *a*, ALHA81189; *b*, ALH82132; *c*, PCA82518. All three sections show chondrules, chondrule fragments, and mineral grains (mainly clinoenstatite) in an opaque matrix consisting largely of nichel-iron and troilite.

section examination shows that the chondrules are abundant but generally small, ranging from 0.3 to 0.9 mm in diameter; they consist of granular or fine-grained pyroxene. The matrix consists largely of granular pyroxene, with lesser amounts of nickel-iron and sulfides, and a little plagioclase. The meteorite is considerably weathered, with brown limonitic staining throughout the section. Microprobe analyses show that the pyroxene is almost pure $MgSiO_3$ (FeO 0.2%–0.8%, mean 0.5%; Al_2O_3 0.07%–0.7%, mean 0.5%; CaO 0.04%–0.7%, mean 0.2%; TiO_2 and MnO each less than 0.1%). Plagioclase is almost pure albite (K_2O 0.6%, CaO less than 0.1%). One grain of forsteritic olivine was analyzed. The meteorite is an enstatite chondrite and, since part of the pyroxene is polysynthetically twinned clinoenstatite, it is classified as E4.

CLASS H4

FIGURES 6-12, 6-13

ALHA78051 (119 g).—In thin section this stone is seen to consist of numerous chondrules, up to 1.5 mm in diameter, set in finely granular matrix of olivine, pyroxene, nickel-iron, and troilite. Moderate weathering is indicated by brown limonitic staining concentrated around metal grains. Well-preserved fusion crust borders one edge of the section. Microprobe analyses show olivine to be uniformly Fa_{18} in composition; the pyroxene composition is somewhat variable, $Fs_{15\text{-}18}$.

ALH82126 (139 g).—This stone (7 × 4 × 2.5 cm) was completely covered with dull brown fusion crust. Chipping revealed some inclusions in the heavily weathered interior. The thin section shows numerous chondrules, up to 2 mm in diameter, in a granular groundmass of olivine and pyroxene, with minor nickel-iron and lesser amounts of troilite. Brown limonitic staining pervades the section. Remnants of fusion crust are present on one edge. Microprobe analyses give the following compositions: olivine, Fa_{18}; pyroxene is somewhat variable, $Fs_{14\text{-}18}$.

EET82602 (1824 g).— An extremely thin, black fusion crust completely covers the regmaglypted surface of this meteorite

(10 × 14 × 8 cm). The stone broke along a pre-existing fracture, exposing both weathered and unweathered material. The material exposed is orange-brown with abundant visible metal (this may not be representative of the entire specimen). Chondritic structure is well developed in thin section, with chondrules ranging up to 1.5 mm in diameter. A variety of chondrule types is present, including porphyritic and barred olivine (with turbid, devitrified glass between the olivine crystals), granular olivine, olivine-pyroxene, and fine-grained pyroxene. Some of the pyroxene is polysynthetically twinned clinobronzite. The chondrules are set in a fine-grained granular groundmass of olivine and pyroxene, with minor amounts of nickel-iron and troilite. Brown limonitic staining pervades the section, and veinlets of red-brown limonite are present. Microprobe analyses give the following compositions: olivine, Fa_{19}; pyroxene, Fs_{16}.

EET82609 (325 g).—This stone (7.5 × 5 × 3.5 cm) is angular with rounded corners. Brownish black fusion crust or remnant fusion crust covers the entire specimen. The interior has a dark matrix with reddish brown oxidation disseminated throughout. The thin section shows a close-packed aggregate of small chondrules, ranging up to 0.6 mm in diameter, set in a granular groundmass consisting largely of olivine and pyroxene, with minor amounts of nickel-iron and troilite. Some of the pyroxene is polysynthetically twinned clinobronzite. Brown limonitic staining pervades the section. Microprobe analyses give the following compositions: olivine, Fa_{18}; pyroxene Fs_{17} (the pyroxene is somewhat variable in composition).

EET83207 (1238 g).—A black to reddish brown fusion crust covers this oblong meteorite (15 × 7.5 × 6 cm). Several deep fractures penetrate the interior, one splitting the stone almost in half. The interior is mostly dark reddish brown, although small areas of less-weathered yellowish matrix are still present. The thin section shows well-defined chondrules up to 2 mm in diameter. Microcrystalline structure is preserved in some chondrules , but glass is devitrified. Olivine is uniformly Fa_{18} in composition. Monoclinic pyroxene ($Fs_{16\text{-}18}$) is common. Two metal phases are present, and tetrataenite (Ni 55%) is also present locally. Troilite is subordinate to metal in abundance. Chromite is accessory. This meteorite was originally classified as H4-5 in the *Antarctic Meteorite Newsletter*, 8(1).

EET83211 (542 g).—A weathered, polygonally fractured fusion crust covers 75% of this meteorite fragment (10 × 7 3.5 cm). The surface is iridescent in places, and a minor amount of evaporite deposit is present. The interior of the stone is also very fractured; broken surfaces are reddish brown and quite smooth. The interior is extremely weathered, but some metal is nonetheless visible. The thin section shows sharply defined chondrules up to approximately 0.6 mm in diameter in a microcrystalline groundmass. Metal is abundant and exceeds troilite in amount. Intense limonitic staining, together with hematite veins, indicate heavy weathering. The olivine composition is relatively uniform, $Fa_{18\text{-}20}$. Pyroxene is commonly monoclinic, with a narrow composition range of

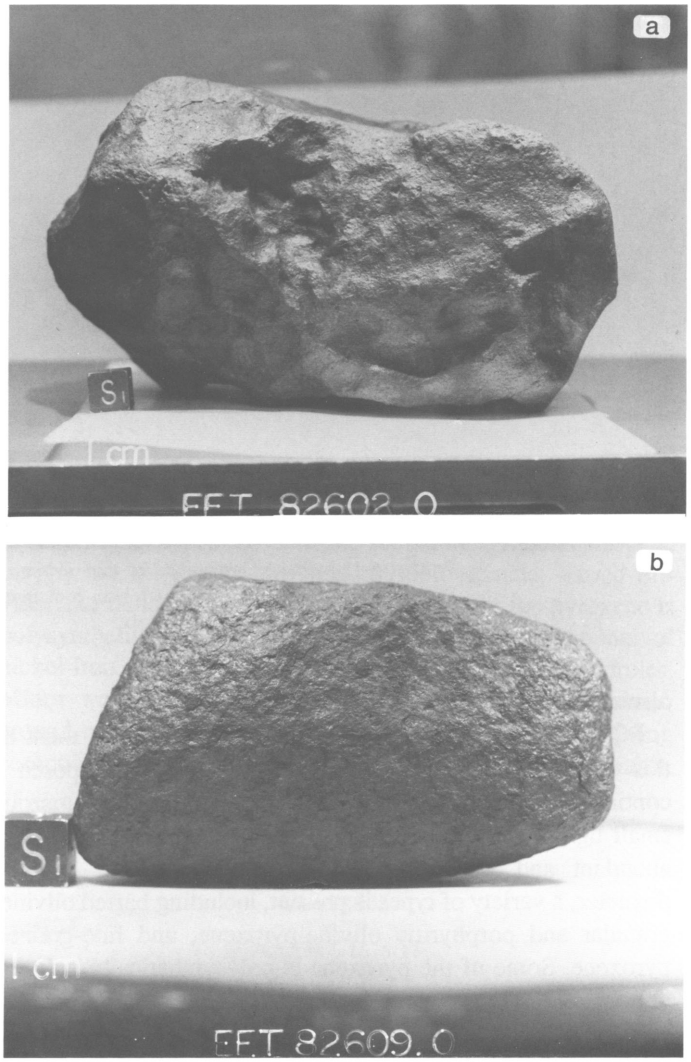

FIGURE 6-12.—H4 chondrites.

$Fs_{16\text{-}20}$. Some very fine-grained plagioclase ($An_{12}Or_5$) was found.

PCA82511 (149 g).—Flow marks are apparent in the iridescent brown to black fusion crust on the top surface (as oriented on the ice) of this stone (5.5 × 6 × 3.5 cm). The bottom surface shows several fractures and the fusion crust is extensively weathered, having an orange tinge. The interior that was exposed by chipping may not be representative of the entire stone; it is heavily weathered with only small areas of unweathered light gray material. In thin section, chondrules are abundant and well-developed. A variety of types is present, the commonest being porphyritic olivine, porphyritic olivine-pyroxene, and radiating pyroxene. Much of the pyroxene is polysynthetically-twinned clinobronzite. The matrix consists of fine-grained olivine and pyroxene, with minor amounts of nickel-iron and troilite; it is heavily stained with limonite. Well-preserved fusion crust is present along one edge of the section. Microprobe analyses give the following compositions:

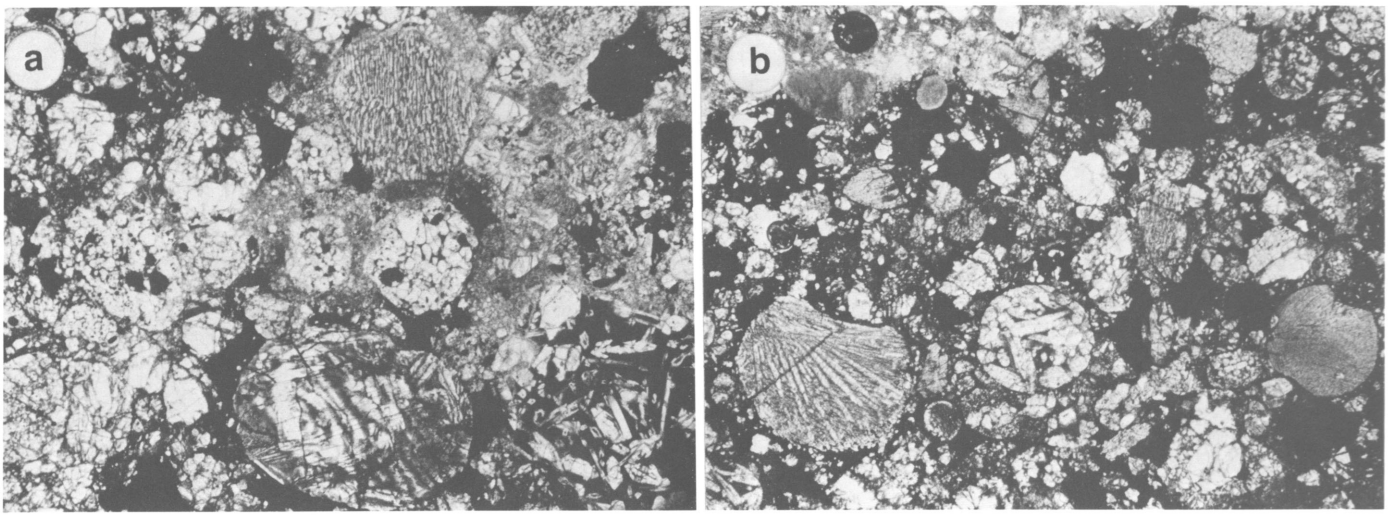

FIGURE 6-13.—Photomicrographs of thin sections of H4 chondrites (each field of view is 3 × 2 mm): *a*, PCA82524; *b*, PCA82511. Although both contain numerous well-defined chondrules, some chondrule margins tend to merge with the granular matrix.

olivine, Fa_{17}; pyroxene, Fs_{15}.

PCA82524 (113 g).—A black fusion crust covers most of this cuboidal stone (5 × 4 × 3.5 mm). Chipping exposed a continuous weathering rind, light gray matrix and numerous small light and dark inclusions. In thin section chondrules are abundant and well-developed, ranging up to 1.2 mm in diameter; a variety of types is present, including barred olivine, granular and porphyritic olivine-pyroxene, and fine-grained pyroxene. Some of the pyroxene is polysynthetically twinned clinobronzite. The groundmass consists largely of fine-grained olivine and pyroxene, with minor amounts of nickel-iron and troilite. A minor degree of weathering is indicated by brown limonitic staining around metal grains. Microprobe analyses give the following compositions: olivine, Fa_{18}; pyroxene, Fs_{16}.

CLASS L4

FIGURES 6-14, 6-15

ALH83001 (1568 g).—Shallow regmaglypts are present on this fusion-crusted stone (17.5 × 9 × 6.5 cm). Most of the interior that has been exposed by chipping is weathered, but it may not be representative of the entire stone. The less weathered material is medium gray and contains chondrules. The thin section shows sharply defined chondrules up to 2.5 mm in diameter, in which original brown glass is now turbid and birefringent. Metal (mostly one-phase) and troilite are subequal in amount. Light to moderate limonitic staining indicates mild weathering. Olivine composition is somewhat variable, $Fa_{23\text{-}28}$. Monoclinic pyroxene is abundant, and has a composition range of $Fs_{20\text{-}32}$.

PCA82514 (129 g).—A dull black fusion crust is present on one surface of this stone (6 × 3 × 3 cm), the other surfaces having weathered to reddish brown. The interior is medium gray and shows dark and light inclusions. A partial weathering rind was exposed when the stone was chipped. In thin section chondrules are abundant and well-developed, ranging up to 2 mm in diameter; a variety of types is present, including porphyritic olivine, porphyritic olivine-pyroxene, barred olivine, and fine-grained olivine and pyroxene. Much of the pyroxene is polysynthetically-twinned clinobronzite. The matrix consists of fine-grained olivine and pyroxene, with coarser grains of nickel-iron and troilite. Brown limonitic staining surrounds the metal grains. Microprobe analyses give the following compositions: olivine, Fa_{23}; pyroxene somewhat variable, $Fs_{11\text{-}22}$, mean Fs_{18}.

The following four specimens are L4 chondrites from the Thiel Mountains that are possibly paired. All are very similar in their textures, mineral compositions, and degree of weathering. The thin sections all show a close-packed aggregate of chondrules, up to 3 mm in diameter, in a minor amount of granular groundmass that consists of olivine, pyroxene and minor amounts of nickel-iron and troilite. Brown limonitic staining pervades the sections. Microprobe analyses give the following compositions: olivine $Fa_{23\text{-}24}$; pyroxene is somewhat variable, with a mean of $Fs_{20\text{-}21}$.

TIL82404 (321 g).—This stone (7 × 7.5 × 3 cm) is partly covered with brownish black fusion crust; many inclusions are visible in areas devoid of crust. Chipping has exposed a dark gray matrix that is inclusion- and metal-rich, with evenly distributed oxidation.

TIL82406 (152 g).—This stone (5.5 × 5.0 × 3.5 cm) is angular with subrounded edges, and most of it is covered with dull black fusion crust. The dark gray interior shows numerous inclusions, and oxidation is evenly scattered throughout.

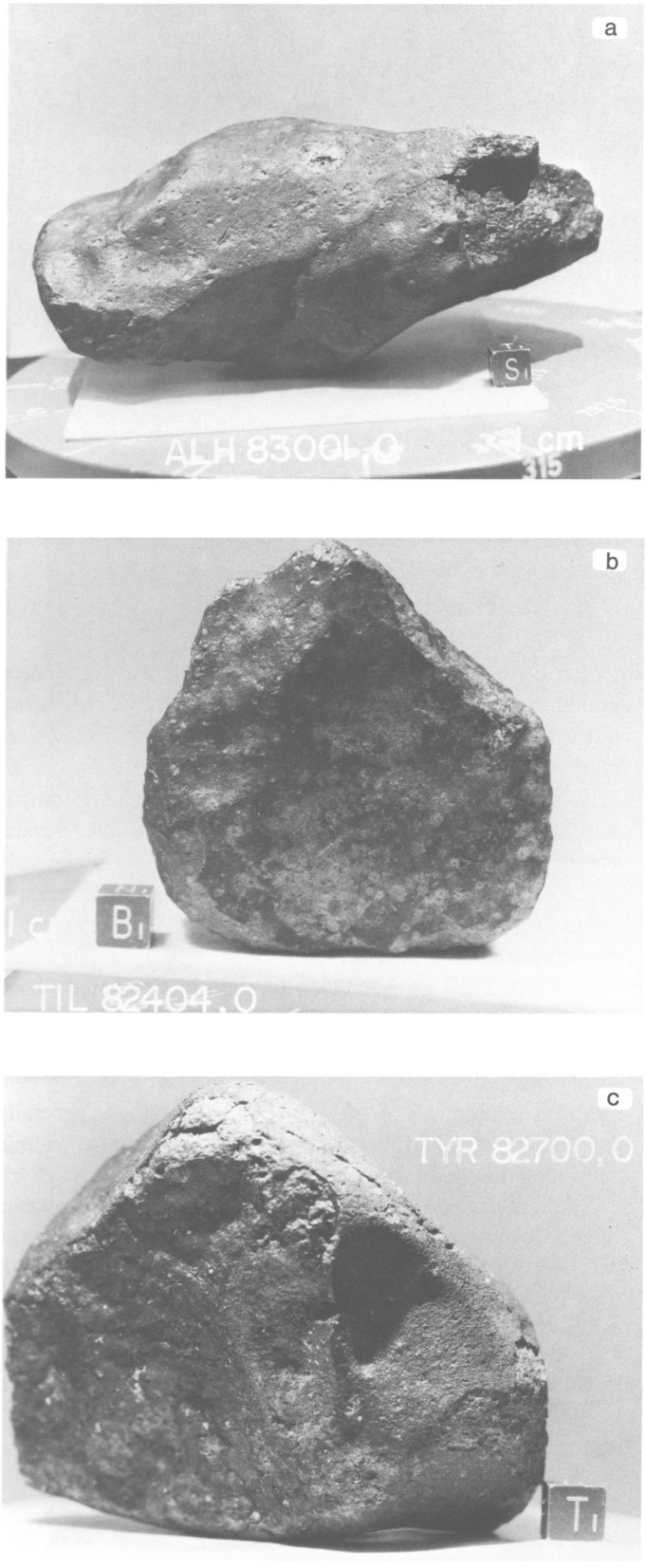

FIGURE 6-14.—L4 chondrites.

TIL82407 (220 g).—This is an angular oblong stone (9.5 × 4.5 × 3 cm) with three flat sides, completely covered with brownish black fusion crust. Abundant oxidation haloes are obvious on the surface. Most of the interior has weathered to a deep reddish brown, but fresh material is dark gray.

TIL82411 (179 g).—This meteorite (6.5 × 4.5 × 3 cm) is covered with slightly weathered fusion crust. No fractures are present. The interior is dark and slightly weathered, and contains abundant chondrules 1–2 mm in diameter.

TYR82700 (892 g).—Black to brown fusion crust covers 60% of this stone (10 × 8.5 × 7 cm). Other surfaces are brown with light inclusions. A white evaporite deposit dots the surface. The interior is extensively oxidized. The thin section shows a close-packed aggregate of chondrules and chondrule fragments, set in a minor amount of granular matrix. A variety of chondrule types is present, including granular olivine, porphyritic olivine, porphyritic olivine-pyroxene, barred olivine, and radiating fibrous pyroxene. Much of the pyroxene is polysynthetically twinned clinobronzite. Minor amounts of nickel-iron and troilite are present, interstitial to the chondrules. Minor weathering is indicated by brown limonitic staining around metal grains. Microprobe analyses give the following compositions: olivine, Fa_{24}; pyroxene somewhat variable, $Fs_{15\text{-}23}$, mean Fs_{18}.

CLASS H5

FIGURES 6-16, 6-17

ALHA81161 (122 g).—This stone (6.5 × 4 × 2.8 cm) has thin fusion crust on one side. It is extremely fractured and brown to iridescent brown. Chipping exposed a totally weathered interior.

ALHA81183 (104 g).—Dull fusion crust covers most of this stone (6 × 3.5 × 3 cm); areas without fusion crust have an iridescent red-brown color. Several fractures penetrate the interior, which has a deep reddish brown color.

ALHA81295 (105 g).—Some very thin fusion crust is preserved on one surface of this meteorite (7 × 4.5 × 2 cm). The surface color is iridescent reddish brown. Many fractures penetrate the interior, which is extensively weathered.

ALH82102 (48 g).—This stone was found weathering out of the ice in the Far Western Icefield. It was collected in situ inside of a large block of encasing ice (see Frontispiece). The ice block was sent to an ice coring lab in New Hampshire and determined to be original (not refrozen) ice; see Chapter 10. The dull black, polygonally fractured fusion crust of the meteorite contains many centimeter-size oxidation haloes that are orange-red. One fracture surface is reddish brown. The interior of the meteorite is uniformly very weathered.

ALH82103 (2529 g).—A slightly weathered fusion crust covers nearly all of this meteorite (14 × 11 × 9 cm). Regmaglypts occur on several faces. Surfaces without fusion

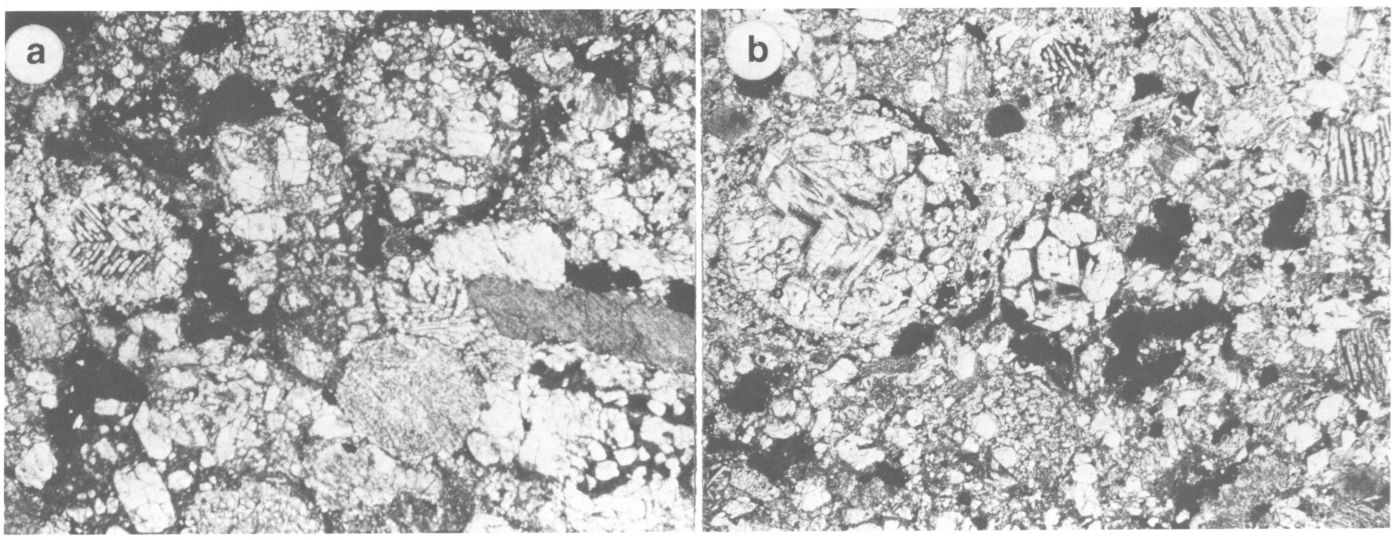

FIGURE 6-15.—Photomicrographs of thin sections of L4 chondrites (each field of view is 3 × 2 mm): *a*, TIL82406; *b*, PCA82514. Chondritic structure is prominent, but some chondrules show partial integration with the granular matrix.

crust show a 1–2 mm thick weathering rind, but a few small clasts are visible. The interior consists of gray matrix dotted with oxidation.

ALH82122 (142 g).—A thin fusion crust covers this rectangular meteorite (4.5 × 4 × 2.5 cm). The interior is light to dark gray with oxidation haloes around metal grains.

EET82603 (8210 g).—This large stone (18 × 19 × 14 cm) is almost completely covered with a black, polygonally fractured fusion crust. White evaporite deposits occur on four of the six sides of the meteorite and are quite thick in some places. As in the cases of other Antarctic meteorites having evaporite deposits (see description for ALH83100), the deposits on EET82603 formed while the sample was drying in the gaseous nitrogen atmosphere of the storage cabinets in Houston. Chipping of the meteorite revealed that a weathering rind is also present. The interior matrix is gray with large areas having a dark gray to deep reddish brown color. Extensive weathering has occurred along internal cracks.

EET82604 (1570 g).—A thin black fusion crust coats most of this blocky meteorite (11 × 11 × 8.5 cm). The stone broke along a pre-existing fracture, exposing mostly weathered material, though metal is still obvious, as is a small amount of less-weathered material.

EET83200 (778 g).—This angular chondrite (10 × 8 × 5 cm) is covered with weathered black fusion crust that is pitted with oxidation. Flow lines are present on part of one surface. The stone is broken, and the exposed surface is weathered to a shiny dark brown. The interior is a dark reddish brown with a small band of relatively unweathered material. This meteorite was originally classified H4-5 in the *Antarctic Meteorite Newsletter*, 8(1).

EET83203 (545 g).—No fusion crust remains on this smooth reddish brown chondrite (6.5 × 7.5 × 6 cm). Several deep parallel fractures penetrate the interior, which is reddish brown with some areas less weathered than others. Metal flecks are visible.

EET83208 (263 g).—This meteorite (11 × 5.5 × 3 cm) is totally covered by a smooth black fusion crust. Several penetrating fractures and a number of regmaglypts are present. The stone broke in half along a fracture, and the interior is extensively weathered. Further chipping has revealed a less-weathered dark interior.

TIL82409 (230 g).—A black to slightly weathered fusion crust covers nearly all the meteorite (6.5 × 4.5 × 4.5 cm). The interior has a yellowish tinge and large dark haloes from weathering.

In thin section, all of the H5 chondrites show a generally well-developed chondritic structure with a variety of chondrule types, including granular olivine, porphyritic olivine, porphyritic olivine-pyroxene, barred olivine, and fine-grained pyroxene. Chondrule margins may be somewhat diffuse, tending to merge with the granular groundmass. The latter consists largely of olivine and pyroxene, with minor amounts of 2-phase nickel-iron, troilite, and chromite; minute grains of sodic plagioclase can sometimes be detected. The compositions of the olivine (Fa_{16-19}) and pyroxene (Fs_{14-17}) are uniform within the individual specimens.

CLASS L5

FIGURES 6-18, 6-19

ALH82104 (398 g).—This stone (6 × 6 × 6 cm) is mostly covered with a thin black fusion crust. The exposed underlying

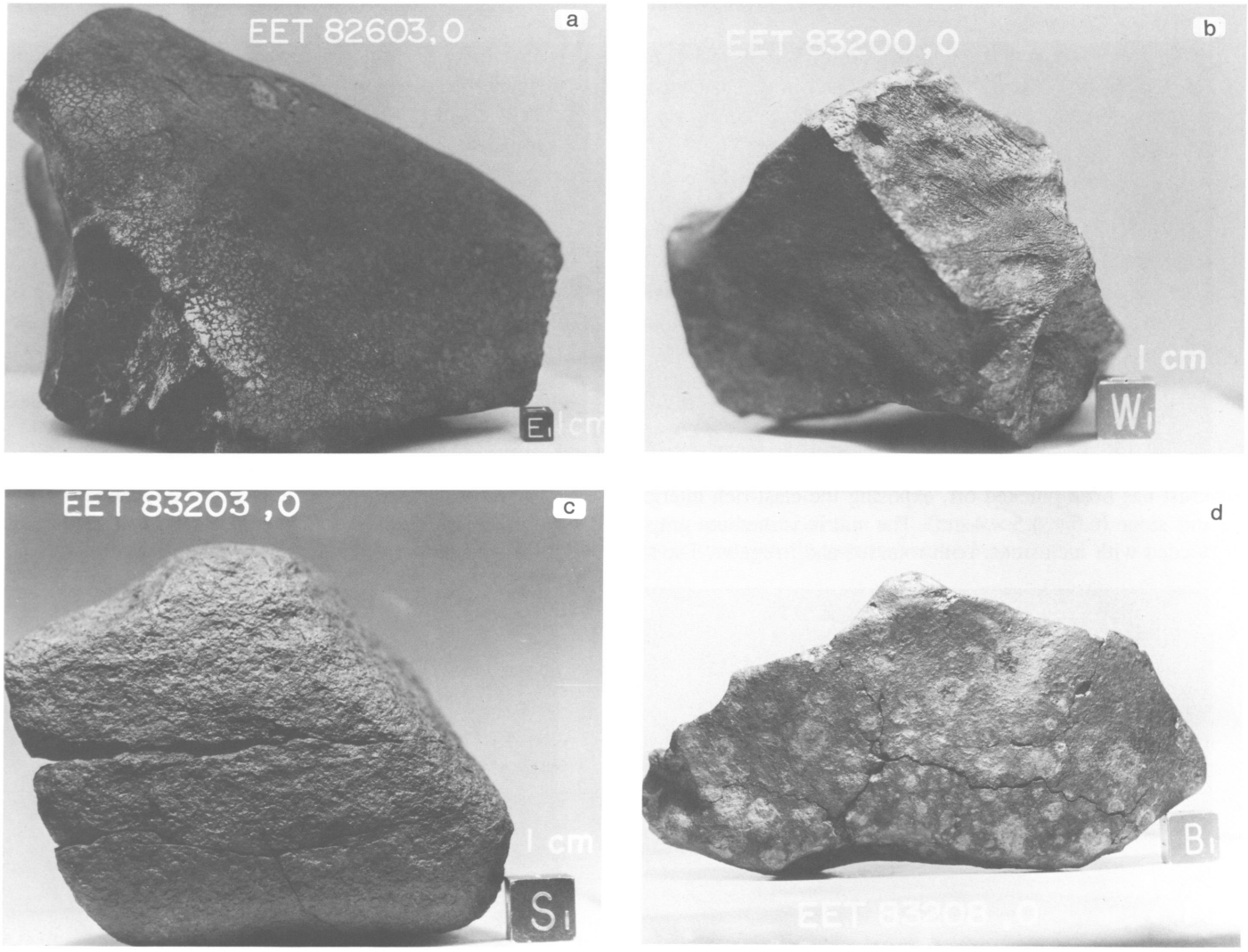

FIGURE 6-16.—H5 chondrites. Note the flow lines on the fusion crust of EET83200.

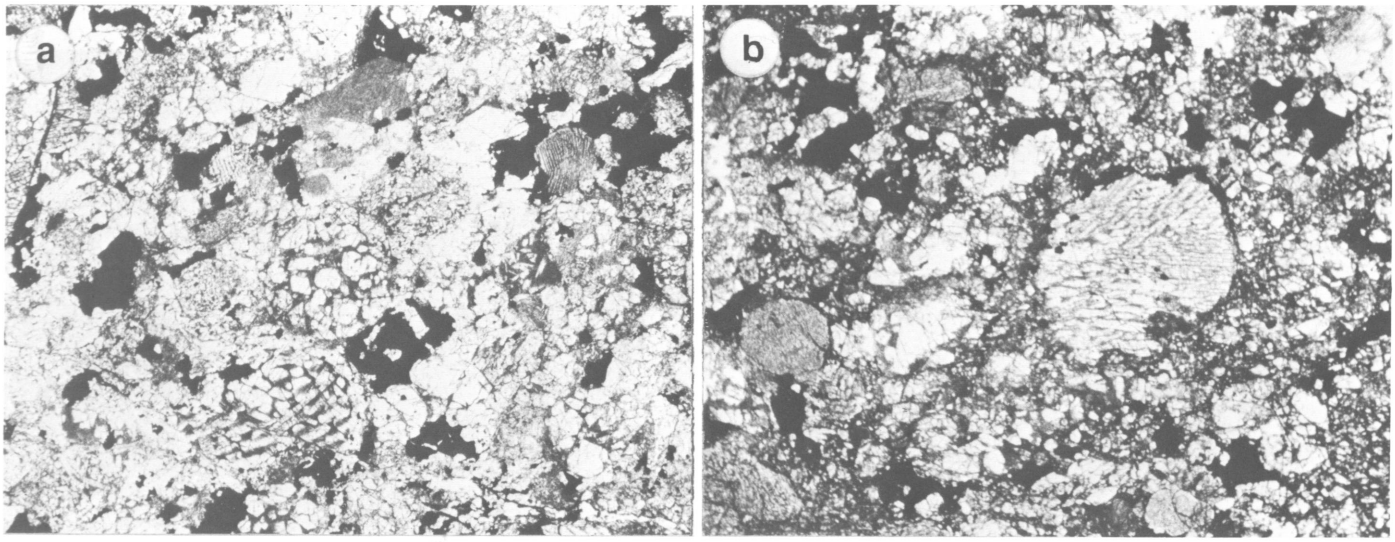

FIGURE 6-17.—Photomicrographs of thin sections of H5 chondrites (each field of view is 3 × 2 mm): *a*, EET82603; *b*, TIL82409. Chondritic structure is well-developed, but chondrule margins tend to merge with the granular groundmass.

surfaces are brown and rough in texture. The interior is made up of light gray matrix with rounded and irregular inclusions. A few oxidation haloes and a continuous weathering rind are present.

PCA82504 (3093 g).—Fusion crust covers 80% of the surface of this meteorite (18 × 12 × 9 cm), and is dotted with oxidation. Areas not covered with fusion crust are somewhat weathered but still reveal a grayish matrix. The interior is gray, contains small inclusions, and is dotted with oxidation haloes.

PCA82505 (3085 g).—Patches of fusion crust remain on this meteorite (16 × 11 × 11 cm). Exposed underlying surfaces are generally reddish brown, with lighter colored inclusions evident. A major fracture divides the stone in half. The interior is dark with reddish oxidation.

PCA82510 (254 g).—Some of the blackish brown fusion crust has been plucked off, exposing the clast-rich interior of this stone (6.5 × 4.5 × 4 cm). The matrix is medium gray and loaded with inclusions, both rounded and irregular. The stone is amazingly fresh; minor pockets of oxidation are present, but they are the exception.

PCA82513 (239 g).—One face of this stone (6 × 5 × 4 cm) is rounded and smooth, with a shiny black to weathered fusion crust. The other faces have a dull fractured fusion crust that is slightly blistery in places. Flow lines are present. The interior is light gray with occasional dark gray inclusions or chondrules. Metal flecks are visible, and are commonly surrounded by oxidation haloes. A discontinuous weathering rind is present.

PCA82519 (125 g).—A dull brownish black fusion crust covers 80% of this meteorite fragment (4 × 6 × 3 cm). Oxidation is evenly disseminated throughout the interior. Unweathered matrix is dark gray and inclusion-rich.

TIL82400 (220 g).—This meteorite (8 × 5 × 5 cm) has only a few remnant patches of fusion crust. The exposed underlying meteorite is friable, has a rough texture and reddish brown color, and shows numerous gray-green chondrules (1–3 mm

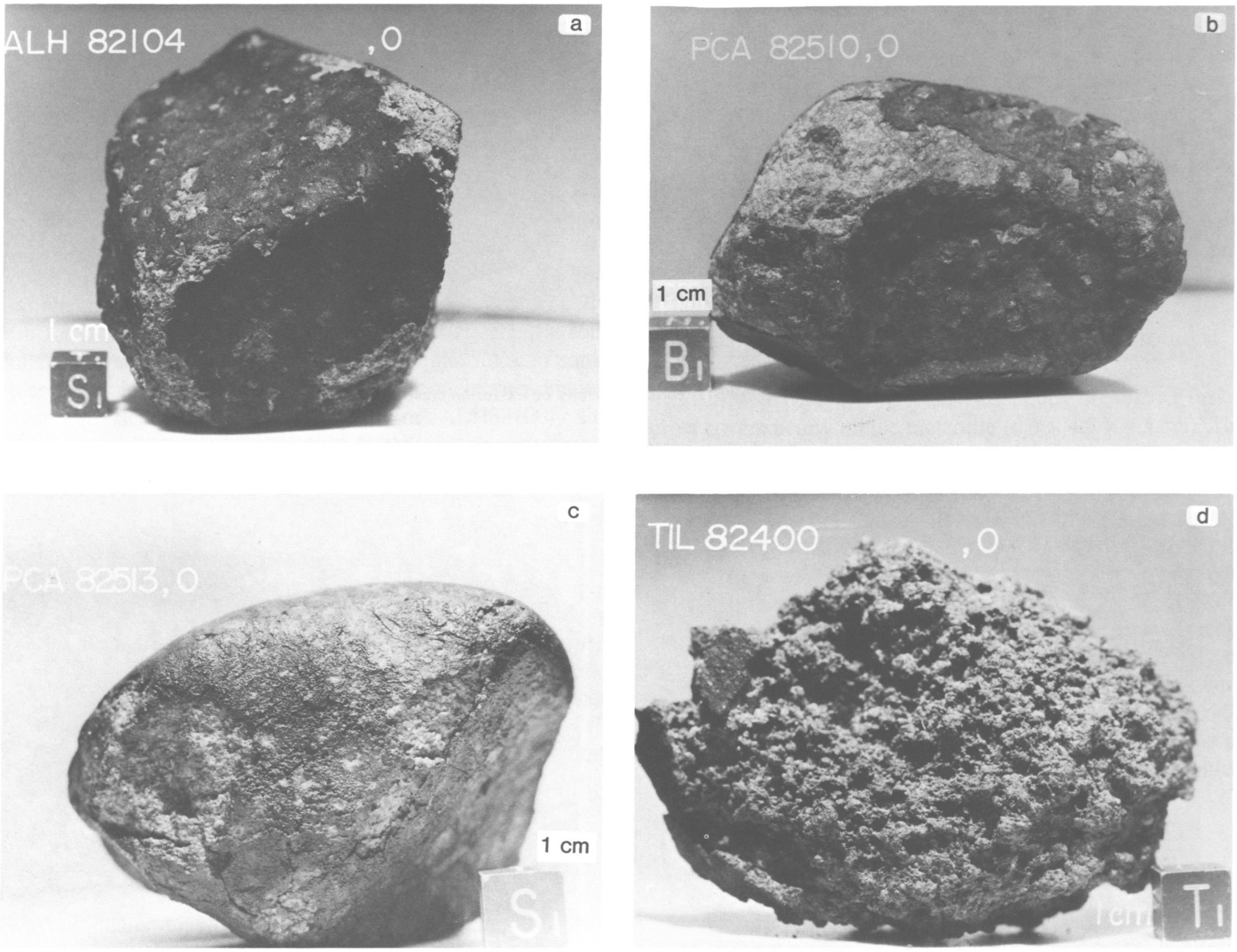

FIGURE 6-18.—L5 chondrites.

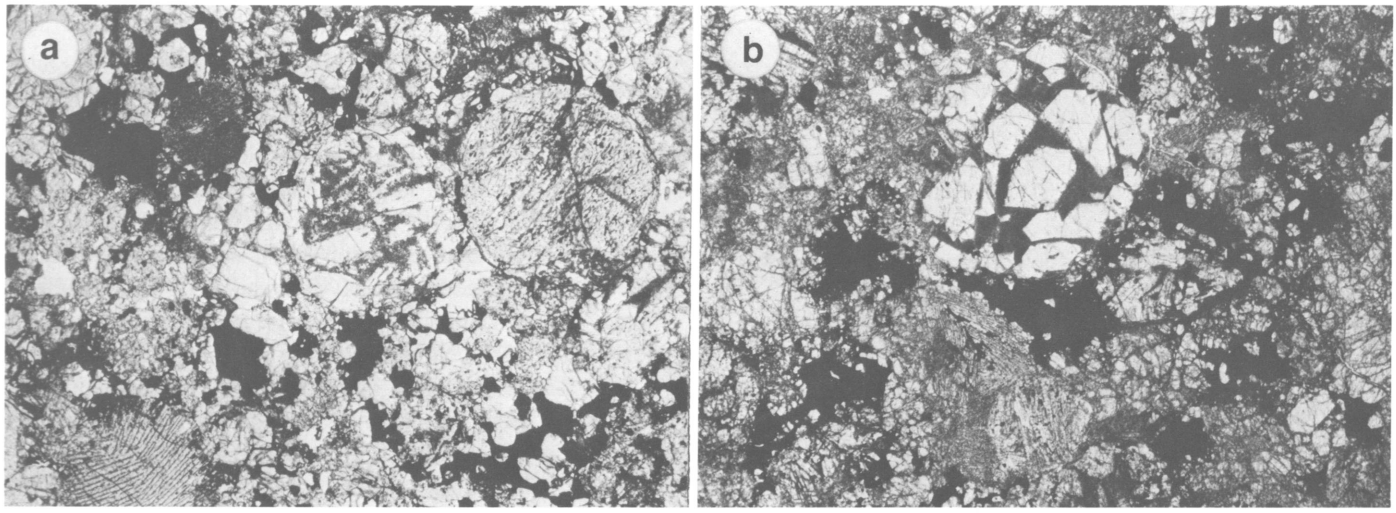

FIGURE 6-19.—Photomicrographs of thin section of L5 chondrites (each field of view is 3 × 2 mm): *a*, PCA82505; *b*, TIL82400. Chondrules are prominent, but show some integration with the granular groundmass.

diameter). The interior is light gray with some oxidation.

In thin section the L5 chondrites show a generally well-developed chondritic structure, with a variety of chondrule types, including porphyritic olivine, granular olivine, granular olivine-pyroxene, and radiating pyroxene. Chondrule margins are commonly diffuse, tending to merge with the granular groundmass. The latter consists largely of olivine and pyroxene with minor subequal amounts of nickel-iron and troilite. The compositions of the olivine (Fa_{23-25}) and largely-orthorhombic pyroxene (Fs_{19-21}) are essentially uniform within individual specimens.

CLASS E6

FIGURE 6-20

ALHA81260 (124.1 g).—A weathered fusion crust covers about 80% of this stone (4.5 × 5 × 3 cm). The one fracture surface has weathered to a deep reddish brown. A minute amount of evaporite deposit is present and is most abundant immediately underneath the fusion crust. The stone is extremely hard to break. The interior matrix is bluish black, with black and white crystal faces being obvious under a binocular microscope. Only vague traces of chondritic structure are visible in the thin section, which shows the meteorite to consist largely of granular enstatite, a considerable amount of nickel-iron (~20%) and minor amounts of sulfides and plagioclase. Remnants of fusion crust are present in the section. Weathering is minor, with a little limonitic staining around some metal grains. Microprobe analyses show the enstatite is almost pure $MgSiO_3$ (CaO 0.8%; FeO 0.2%; Al_2O_3, TiO_2, and MnO each <0.1%); plagioclase is somewhat variable in composition, An_{13-19}. The meteorite is an E6 chondrite; the only other E6 chondrite from the Allan Hills, ALHA 81021, is similar but appears to be more weathered. The possibility of pairing should be considered.

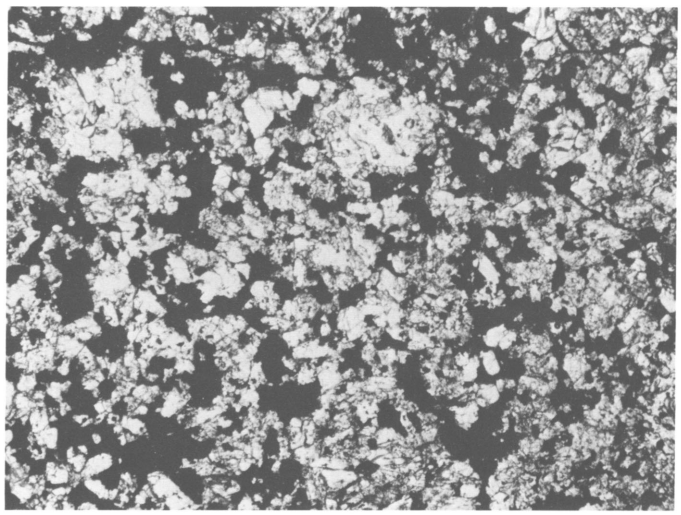

FIGURE 6-20.—Micrograph of thin section of the E6 chondrite ALHA81260 (Field of view is 3 × 2 mm). Chondritic structure is barely perceptible, the section showing a granular aggregate consisting largely of enstatite (white to gray) and nickel-iron and troilite (black).

CLASS H6

FIGURES 6-21, 6-22

EET83201 (1059 g).—No fusion crust remains on this polished and rounded stone (10 × 8 × 7 cm). It was chipped along a crack, exposing a reddish brown interior with metal flecks. Thin section examination shows well-preserved chondrules up to 2 mm in diameter, enclosed in a matrix that is intensely recrystallized to a coarse polygonal-granular texture.

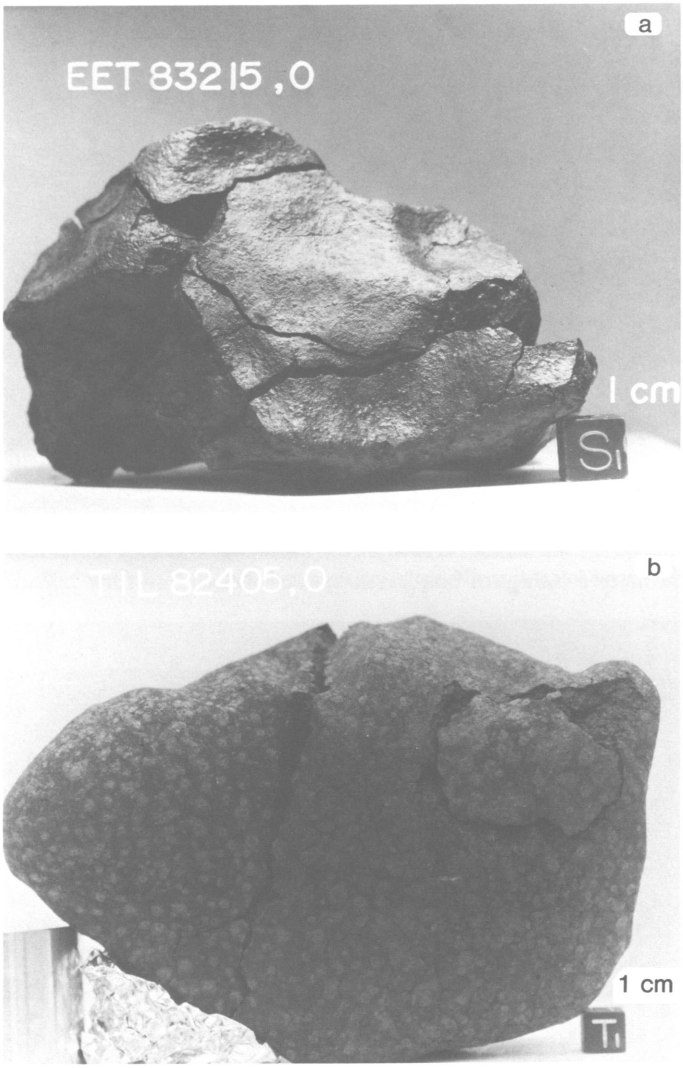

FIGURE 6-21.—H6 chondrites. Note the oxidation haloes on the surface of TIL82405.

Plagioclase ($An_{13-14}Ab_{80-81}Or_6$) is well-developed and abundant. Orthorhombic pyroxene (Fs 18) and olivine (Fa_{18-20}) are uniform in composition. Metal and troilite are subequal in abundance. Chromite is an accessory phase.

EET83215 (510 g).—This meteorite (9 × 7 × 6 cm) consists of three pieces (one large and two small) that fit together perfectly. The exterior is shiny, smooth, and reddish brown with some remnants of fusion crust. Fracturing is extensive. The interior surfaces are heavily weathered; some metal was noted. In thin section, chondrules up to 2 mm in diameter are fairly well-preserved; some retain microcrystalline structure. Plagioclase is abundant and coarse but is highly maskelynetized. Olivine and mostly-orthorhombic pyroxene are very uniform in composition, Fa_{18} and Fs_{19} respectively. Metal is more abundant than troilite; at least two metal phases are present, including some tetrataenite (approximately 52% Ni). This meteorite was originally classified as H5-6 in the *Antarctic Meteorite Newsletter*, 8(1).

TIL82405 (1001 g).—Three perfectly fitting pieces make up this specimen (15 × 10 × 14 cm). The fusion crust is polygonally fractured and shows oxidation haloes. The interior is gray with small specks of oxidation. A 1–4 mm thick weathering rind is present. In thin section chondrules are sparse and poorly defined, tending to merge with the granular groundmass. The latter consists largely of olivine and pyroxene, with minor amounts of nickel-iron, plagioclase, and troilite. Brown limonitic staining surrounds the metal grains. Microprobe analyses give the following compositions: olivine, Fa_{19}; pyroxene, Fs_{17}; plagioclase, An_{13}.

FIGURE 6-22 (*Below*).—Photomicrographs of thin sections of H6 chondrites (each field of view is 3 × 2 mm). *a*, TIL82405; *b*, EET83201. Chondrules are present, but tend to merge with the granular groundmass.

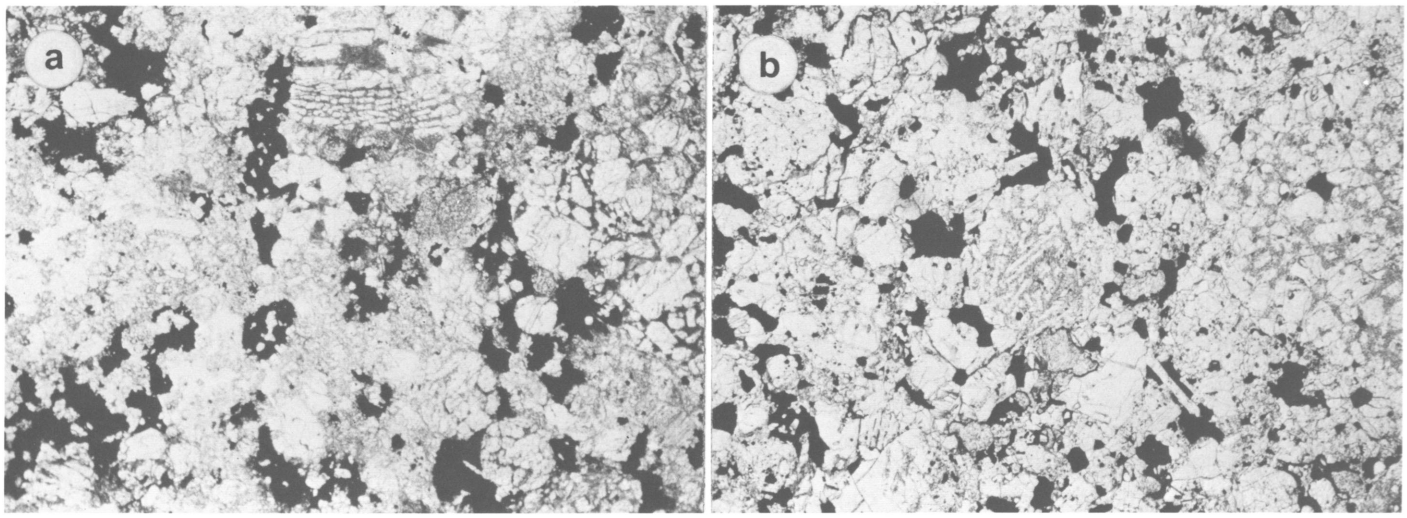

CLASS L6

FIGURES 6-23, 6-24

ALH81247 (104 g).—This stone (5.5 × 4 × 3 cm) is covered with a dull, blistery fusion crust. Numerous fractures criss-cross the surface but do not extend far into the interior. A minute amount of evaporite deposit is present. The interior is light gray with numerous inclusions, some more than 1 mm in largest dimension. A weathering rind 1–9 mm thick is present.

ALH82105 (363 g).—This stone (8 × 7.5 × 3 cm) is flat with well-rounded edges and is totally covered with a brown to black, polygonally fractured fusion crust showing many oxidation haloes. A continuous weathering rind, 1–5 mm thick, was exposed on chipping. The interior is whitish gray with a few areas of oxidation. Abundant metal is obvious.

ALH82118 (110 g).—Remnants of black fusion crust are present on this meteorite (5 × 4.5 × 3 cm). Elsewhere the surface is rough and friable, with a light gray matrix dotted with oxidation haloes around metal grains. One deep fracture penetrates the stone.

ALH82123 (110 g).—Fusion crust covers most of this stone (6 × 4 × 3 cm). Chondrules up to 5 mm in diameter are visible on a fracture surface. A 5 mm thick weathering rind was exposed when the meteorite was chipped.

ALH82125 (178 g).—A dull to lustrous fusion crust covers this dumbbell-shaped meteorite (8 × 3.5 × 2.5 cm). The interior is highly weathered.

ALH83101 (639 g).—This smooth rounded stone (9 × 8 × 5.5 cm) is covered with a black, polygonally fractured fusion crust. One surface is flat and iridescent. Areas where fusion crust has weathered away reveal a rough reddish surface with areas of gray matrix. The interior is light gray and sparsely dotted with oxidation. Metal flecks are numerous.

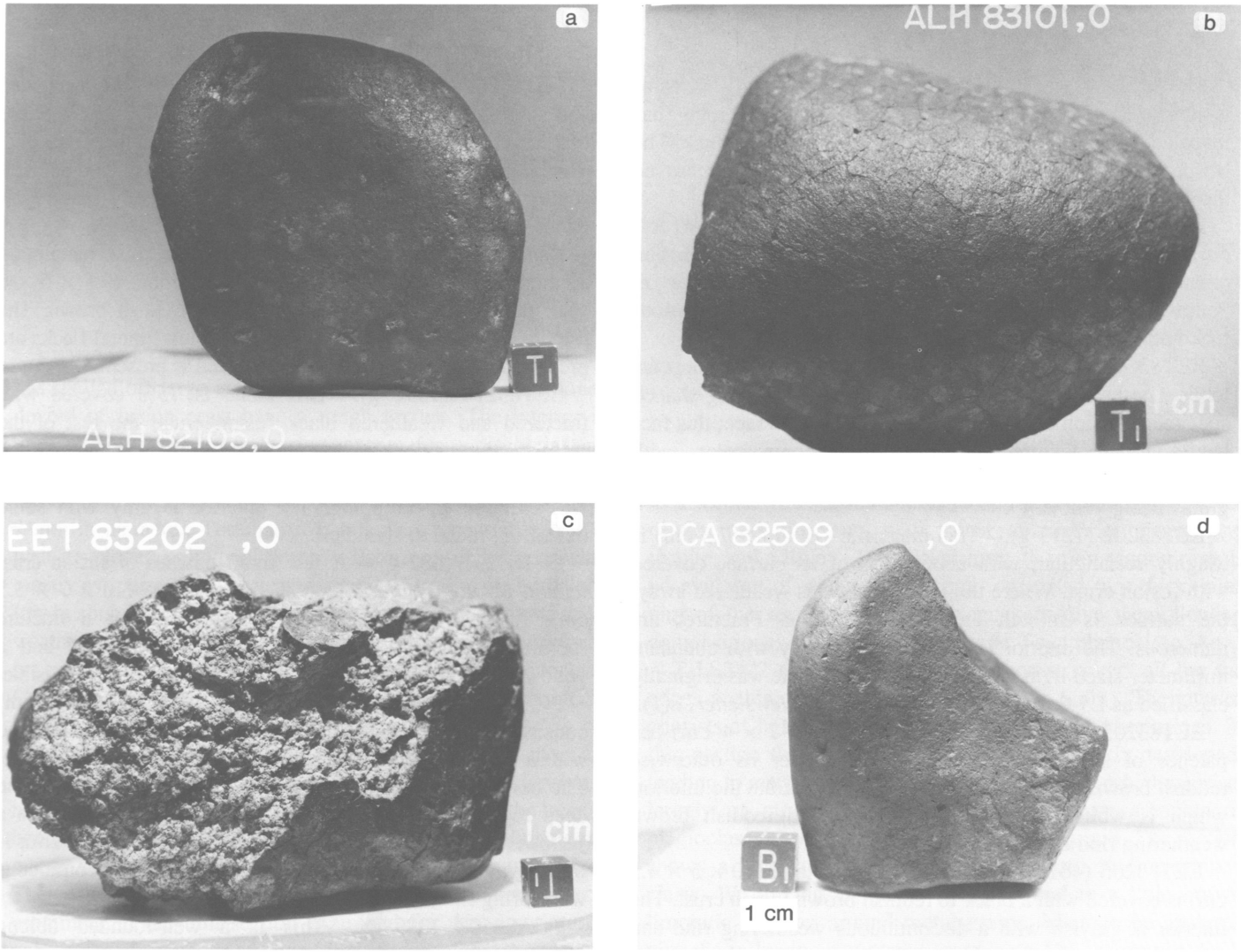

FIGURE 6-23.—L6 chondrites.

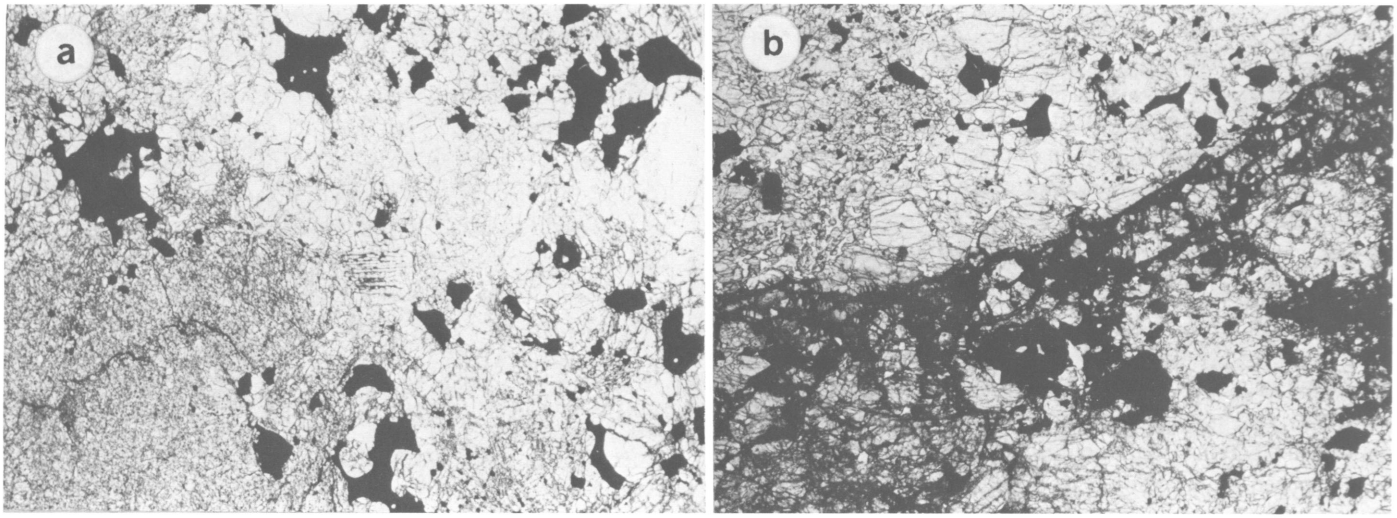

FIGURE 6-24.—Micrographs of thin sections of L6 chondrites (each field of view is 3 × 2 mm): *a*, EET83214; *b*, EET83206. Chondritic structure is barely discernible in these samples, the chondrules merging with granular groundmass. Note the dark glassy shock veining in EET83206.

EET82605 (624 g).—This angular stone (9 × 7.5 × 5.5 cm) is mostly covered with a black fusion crust. Chipping has revealed a discontinuous weathering rind 1.7–2 mm thick. The fresher interior is light in color with oxidation scattered throughout. Several inclusions were noted.

EET82606 (981 g).—This angular meteorite (11.5 × 9 × 7 cm) is smooth and dark reddish brown with remnants of fusion crust. Several fractures penetrate the stone. Light grayish yellow matrix with numerous inclusions and oxidation haloes make up the interior.

EET82607 (165 g).—This stone (5.5 × 4 × 4 cm) appears to be one-half of what was formerly a thin oblong-shaped specimen. Fusion crust is present on all but one face; this face has a rough texture and a reddish brown color, with lighter-colored inclusions or chondrules and some tiny metal grains being visible.

EET83202 (1213 g).—This meteorite (12 × 7 × 7.5 cm) is roughly rectangular, with about 50% of its surface covered with fusion crust. Where the fusion crust has weathered away, the surface is smooth and reddish brown. Fractures are numerous. The interior is light and dark gray with abundant millimeter-sized light inclusions. This meteorite was originally classified as L5-6 in the *Antarctic Meteorite Newsletter*, 8(1).

EET83205 (470 g).—This chondrite (8 × 7 × 4 cm) has patches of shiny fusion crust scattered over its otherwise reddish brown surface. Several fractures penetrate the interior, which is white to yellow-gray. A gray to reddish brown weathering rind is present.

EET83206 (461 g).—This rectangular stone (10 × 5 × 4.5 cm) is covered with a black to reddish brown fusion crust. The interior is grayish with a discontinuous weathering rind and some large oxidation haloes. Glassy veins crisscross the interior.

EET83209 (520 g).—This stone (8 × 7 × 6 cm) is rounded and smooth with scattered remnants of fusion crust; surfaces that lack fusion crust are reddish brown and slightly polished. The interior is reddish to yellowish, heavily weathered but with some visible metal flecks. Plagioclase is locally maskelynitized.

EET83210 (425 g).—Patches of fusion crust remain on approximately 30% of this meteorite fragment (9.5 × 6 × 6 cm); the other surfaces are smooth and reddish brown. The interior is gray with some oxidation staining; metal flecks are present. A discontinuous weathering rind is present.

EET83214 (1397 g).—This stone is 75% covered with fractured and weathered black fusion crust; the rest of the surface is reddish brown, has a rough texture, and shows some yellowish matrix. A 5 mm thick reddish brown weathering rind was exposed by chipping. The interior is gray with some oxidation; metal is abundant.

EET83237 (882 g).—A few small patches of fusion crust remain on this rounded reddish brown stone (10 × 7 × 5.5 cm). A small area was chipped off, exposing a fracture (possibly annealed) that is preferentially weathered and a yellowish matrix. Metal flecks and a few inclusions are visible.

PCA82503 (8308 g).—This large stone (27 × 17 × 12 cm) consists of two pieces that fit together perfectly, each covered with a thin black fusion crust except for the fracture surface. The bottom (as oriented on the ice) is smooth and has some deep regmaglypts. The fracture surface has weathered to a yellowish brown color and has a rough texture. The interior is light gray with some oxidation haloes. A discontinuous weathering rind, 1–2 mm thick, is present.

PCA82508 (389 g).—This is a well-rounded oblong meteorite (9 × 5 × 4 cm) with a black fusion crust coating all but one corner. This exposed area is somewhat weathered to a

reddish brown color. The interior is light gray with light and dark inclusions (chondrules?), and shows some oxidation haloes.

PCA82509 (285 g).—A brownish black fusion crust completely covers this cuboidal meteorite (5 × 5 × 4 cm). Chipping has exposed an area that is mostly oxidized but probably not representative of the entire specimen. Fresh material is light gray with abundant fresh metal visible.

TIL82401 (281 g).—A thin, dull black fusion crust coats parts of three surfaces of this fragment (6.5 × 6 × 5.5 cm). The other surfaces are smooth and reddish brown. Chondrules (1–6 mm diameter) are visible. A wide discontinuous weathering rind was exposed on chipping, as was fresh gray matrix with a minor amount of oxidation.

The L6 chondrites are all very similiar in their petrographic characteristics. The thin sections show sparse, poorly defined chondrules that tend to merge with the granular groundmass. Principal minerals are olivine and pyroxene in subequal amounts, together with minor quantities of plagioclase (or maskelynite), nickel-iron, troilite, diopside, and accessory chromite and merrillite. Microprobe analyses (see Appendix, Table A) show essentially uniform compositions for the principal minerals: olivine, Fa_{23-25}; orthopyroxene, Fs_{19-21}; plagioclase, An_{10-12}. The following meteorites contain maskelynite: EET82605, EET82606, PCA82503, PCA82509, EET83209.

Class LL6

Figures 6-25, 6-26

EET83204 (376 g).—A polygonally fractured fusion crust has spalled off large areas of this stone (8 × 6 × 5 cm). Areas devoid of fusion crust have a rough texture. The interior is gray without visible weathering, except for a discontinuous darker gray rind and several reddish haloes. Metal flecks are present. A thin section shows poorly defined chondrules up to 2 mm in diameter. The matrix is intensely recrystallized to a well-developed polygonal granular texture. Metal (two-phase, mostly as coarse patchy intergrowths) and troilite are both very low in abundance. Minor local limonitic staining suggests mild weathering. Olivine and orthopyroxene are essentially uniform in composition, Fa_{29-31} and Fs_{27}, respectively. Plagioclase ($An_{11}Or_{5-13}$) is coarse and abundant; the reason for the variation in the orthoclase content is not known.

PCA82507 (479 g).—A black fusion crust covers most of this stone (6 × 6 × 6.5 cm). Areas not covered by fusion crust have a brownish color. Many chondrules are visible, the largest being 5 mm in diameter. The interior consists of a bluish gray matrix with white and dark gray inclusions up to 1 mm in size. There is little obvious metal. Chondritic structure is not prominent in the thin section examined for this description: only a few fragments of individual chondrules are present. This section thus may not be representative of the meteorite as a whole. The section shows mostly a granular aggregate of olivine and pyroxene, with minor amounts of plagioclase, troilite, and a little (~1%) nickel-iron. The thin section reveals no evidence of weathering. Fusion crust (0.4 mm thick) rims part of the section. Microprobe analyses give the following compositions: olivine, Fa_{30}; pyroxene, Fs_{25}; plagioclase, An_{11}.

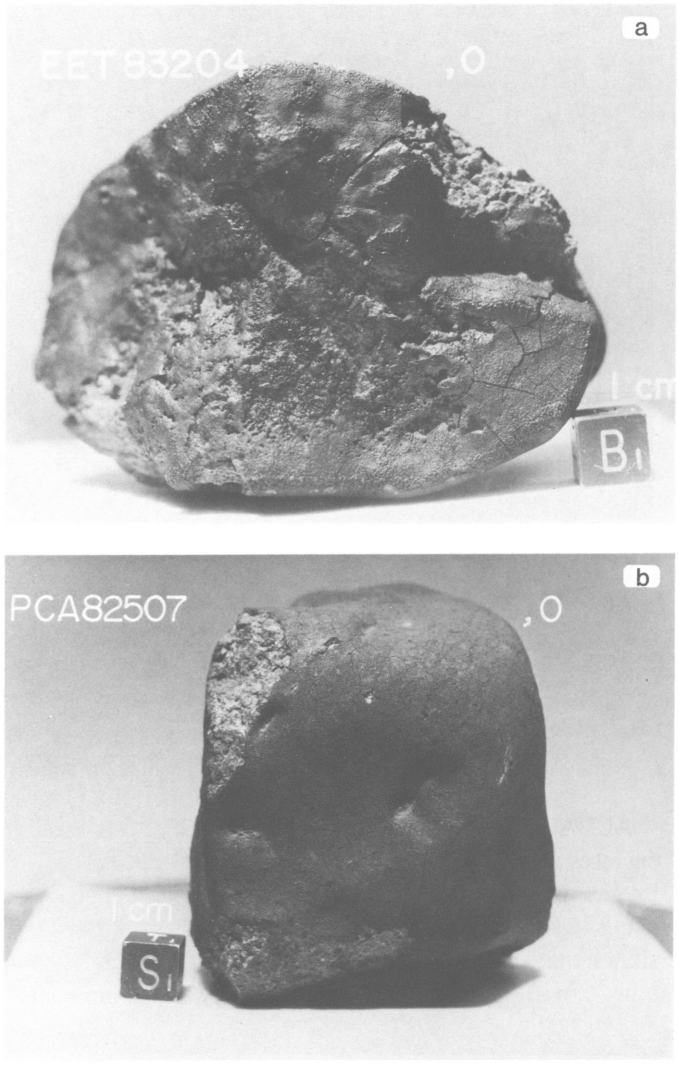

Figure 6-25.—LL6 chondrites.

TIL82402 (476 g).—Black fusion crust covers all but the edges of this cuboidal meteorite (7 × 6 × 6 cm). The interior consists of light gray matrix with dark and light inclusions. In thin section the chondrules are sparse and poorly developed, tending to merge with the granular groundmass, which consists largely of olivine and pyroxene, with minor amounts of plagioclase, troilite, and a little (~2%) nickel-iron. The section shows a brecciated structure, with medium- to fine-grained clasts. Weathering is minor, being limited to a little brown limonitic staining around metal grains. Microprobe analyses give the following compositions: olivine, Fa_{29}; pyroxene, Fs_{24}; plagioclase, An_{10}.

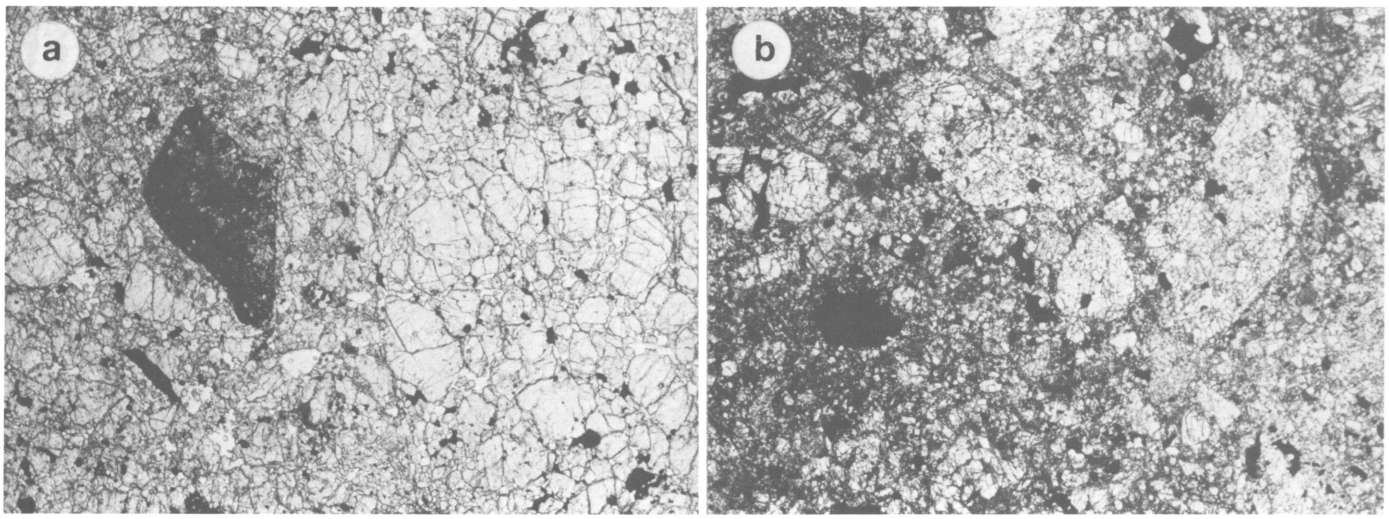

FIGURE 6-26.—Photomicrographs of thin sections of LL6 chondrites (each field of view is 3 × 2 mm): *a*, PCA82607; *b*, TIL82402. The chondritic structure is almost completely erased by extensive brecciation and integration with the granular matrix.

CLASS "H?" ACAPULCO-LIKE

FIGURE 6-27

ALHA81261 (11.8 g).—A brown and black fusion crust encloses about 50% of this small stone (2 × 1.5 × 1.5 cm). The interior is light to medium gray, with abundant metal grains being visible. A weathering rind is present. The thin section shows that this meteorite is an equigranular (grains 0.1–0.4 mm across) aggregate of approximately equal amounts of olivine and orthopyroxene, with minor amounts of nickel-iron, plagioclase, troilite, diopside, and accessory chromite. A little limonitic staining is present around metal grains. Microprobe analyses show that the mineral are uniform in composition: olivine, Fa_{11}; orthopyroxene, $Wo_2En_{87}Fs_{11}$; plagioclase, $An_{14}Or_4$. This specimen is identical in all respects with ALHA 77081, classed as an H? meteorite, and the two are almost certainly paired. The mineral analyses are indistinguishable from those of Acapulco (Palme et al., 1981).

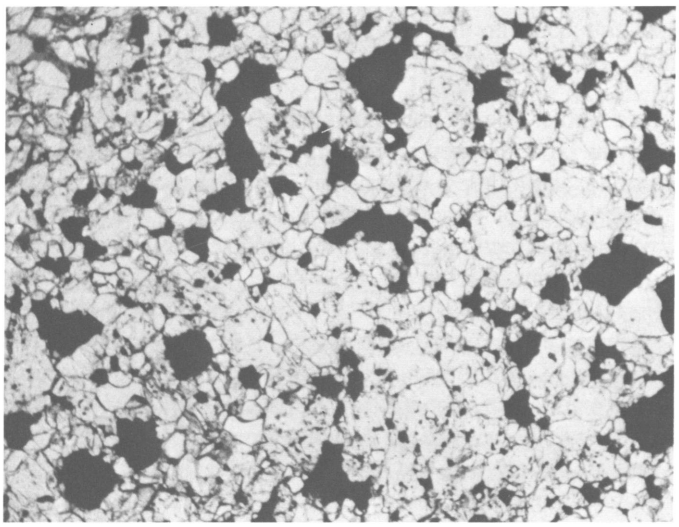

FIGURE 6-27.—Photomicrograph of thin section of the "H?" Acapulco-like chondrite ALHA81261 (field of view is 3 × 2 mm). This meteorite is an equigranular aggregate consisting mainly of olivine, orthopyroxene, and plagioclase (white to gray), with minor amounts of nickel-iron, troilite, and chromite.

ALHA81315 (2.5 g) is identical with ALHA 81261 in all respects.

In the future we will refer to these meteorites, and ALHA77081, as Class "H?" Acapulco-like.

Achondrites

EUCRITES

FIGURES 6-28, 6-29

ALHA81313 (0.5 g).—The classification of this very small (0.8 × 0.7 × 0.4 cm) and completely crusted stone as a eucrite is tentative as of this writing. It is either an unusual eucrite or, alternatively, it could be related to the shergottites. Unfortunately, most of the specimen was consumed in producing a thin section. The section shows a granular aggregate (grains 1–3 mm in maximum dimension) of colorless plagioclase (maskelynite) and pale gray, weakly pleochroic pyroxene with trace amounts of nickel-iron, troilite, and chromite. A vague impression of pyroxene-rich and plagioclase-rich layers is present, possibly suggesting a cumulate. The pyroxene appears to be an inverted pigeonite: orthopyroxene with small blebs of exsolved augite. Point counting gives the following volume

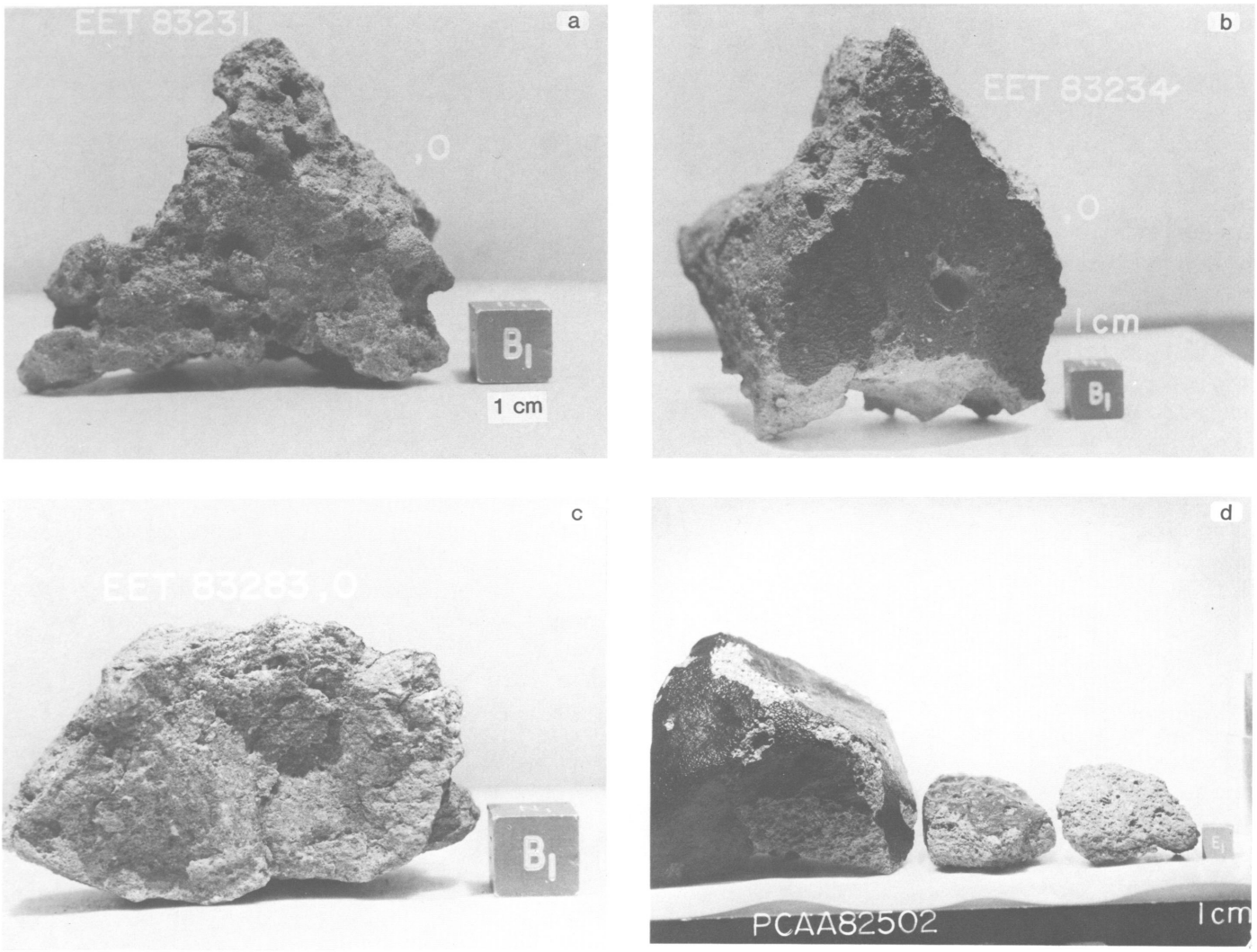

FIGURE 6-28.—Eucrites.

percentages: pyroxene, 54; plagioclase, 46. Microprobe analyses show the maskelynite to be essentially stoichiometric and fairly uniform in composition, averaging An_{93} (Na_2O 0.6%–1.4%, K_20 <0.4%). The orthopyroxene composition is also fairly uniform, averaging $Wo_3En_{59}Fs_{38}$; Al_2O_3 0.4%, MnO 0.9%, TiO_2 0.2%, Cr_2O_3 0.3%. The composition of a single augite bleb is $Wo_{38}En_{42}Fs_{20}$. In texture and mineral chemistry this meteorite closely resembles the Moama monomict eucrite (Lovering, 1975). For this reason, and because its mineral chemistry is different from that of the shergotites, Delaney and Prinz (Chapter 8) conclude that 81313 is a eucrite and not a shergotite as originally suggested.

TIL82403 (49.8 g).—A shiny black fusion crust encloses 70% of this achondrite (4.7 × 4 × 2 cm). The exposed underlying surface is gray with some white and black-and-white clasts being visible. The top surface (as oriented on the ice) contains numerous vugs, some as large as 5 mm in diameter. The interior matrix is light gray with small white and darker gray clasts. One large, coarse-grained, black-and-white clast was exposed when the meteorite was chipped. The thin section shows a microbreccia of angular fragments (grains up to 1.2 mm across) of pyroxene (orthopyroxene and pigeonite) and plagioclase, in a matrix of comminuted pyroxene and plagioclase. Plagioclase and pigeonite locally form coarse to fine-grained ophitic intergrowths. Trace amounts of troilite and nickel-iron are present as minute grains. Microprobe analyses show a considerable range of pyroxene compositions, overlapping both the orthopyroxene and pigeonite fields: $Wo_{3-22}En_{30-40}Fs_{43-58}$. Plagioclase shows a considerable range of composition, An_{77-93}.

PCA82501 (54.4 g).— This achondrite (4.5 × 3 × 3 cm) has areas of shiny fusion crust remaining on all surfaces. Some sides are smooth, while others are rough and contain numerous vugs. Areas lacking fusion crust reveal the specimen to be coarse grained, white to dark gray in color, and with some yellowish oxidation. No individual clasts are visible. A very

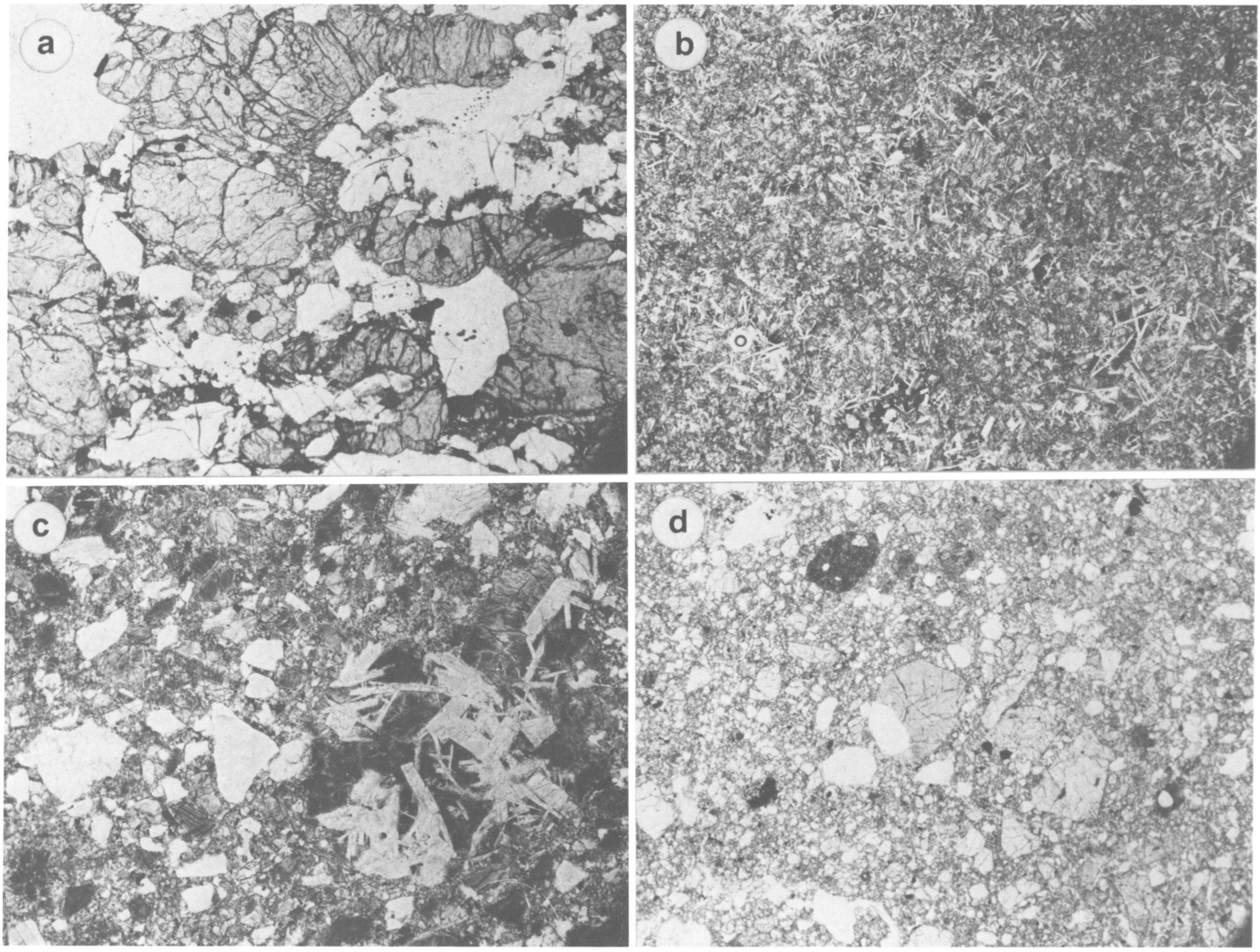

FIGURE 6-29.—Micrographs of thin sections of eucrites (each field of view is 3 × 2 mm): *a*, PCA81313 (white is maskelynite, the gray is pyroxene); *b*, PCA82502. Note the fine-grained unbrecciated texture; *c*, TIL82403. This is a microbreccia of angular fragments of pyroxene and plagioclase, in a matrix of comminuted matrix of the same phases; note the ophitic clast; *d*, EET 83234. This is a microbreccia of angular fragments of pyroxene (pale gray) and plagioclase (white); note the dark glassy clasts.

small amount of oxidation is present in the interior. The thin section shows an ophitic intergrowth of plagioclase and pigeonite; the plagioclase laths average about 1 mm long. Trace amounts of troilite and nickel-iron are present as minute grains, the metal grains commonly being surrounded by rusty limonitic haloes. Microprobe analyses show pyroxene compositions ranging fairly continuously from Wo_4Fs_{57} (orthopyroxene) to $Wo_{21}Fs_{41}$ (pigeonite), the range in En content being quite limited. Plagioclase compositions are in the range $An_{80\text{-}92}$. The meteorite is unbrecciated in the thin section.

PCA82502 (890 g).—This meteorite consists of 3 pieces (6 × 4.5 × 2.8 cm; 4.5 × 4.3 × 3 cm; 11 × 8.5 × 8 cm) that have areas of extremely shiny fusion crust. These 3 pieces do not fit together, but their field relationships and their megascopic appearances suggest they may be paired. The interiors of the fragments have a light gray matrix with darker gray inclusions up to several mm across. No weathering is evident, except that the exterior surfaces are darker gray than the interior surfaces. The thin section shows a fine-grained ophitic intergrowth of pigeonite and plagioclase (average length of plagioclase laths is about 0.1 mm). Small areas of somewhat coarser material may be partly resorbed clasts of similar composition. Trace amounts of nickel-iron and troilite are present, as minute grains. Microprobe analyses show pyroxene compositions ranging fairly continuously from Wo_5Fs_{61} to $Wo_{34}Fs_{36}$, the range in En content being quite limited. The plagioclase composition is $An_{77\text{-}92}$. The meteorite is a eucrite and is unbrecciated in thin section; it is possibly a fine-grained variant

of PCA80501.

EET83229 (312 g).—This meteorite (8 × 6 × 4 cm) is macroscopically similar to other 1983 Elephant Moraine eucrites, with the exception of one large (4 × 3 × 0.2 cm) brown crystalline clast. The thin section shows a typical polymict eucrite breccia with many pyroxene, plagioclase, and opaque mineral clasts, and a few small lithic clasts. One lithic clast has a feldspar phenocryst, an unusual feature for a eucritic clast. Pyroxene clasts show various degrees of exsolution, clouding, and compositional dispersion. Feldspar clasts show variable amounts of shock modification. Many cracks filled with dark weathering material crosscut the section. Microprobe analyses give the following compositions: pyroxene $Wo_{4-39}En_{26-60}Fs_{31-55}$; plagioclase An_{74-93}.

EET83231 (66.4 g).—This stone (5.5 × 4 × 4.5 cm) is very angular and contains numerous vesicles; no fusion crust is present. The thin section shows a polymict achondritic breccia containing several fine- and very fine-grained mafic clasts. Numerous orthopyroxene crystal fragments similar to diogenitic pyroxene are present; however, microprobe analyses showed no pyroxenes of diogenitic composition. Mafic clasts vary from coarse-grained subophitic basalts, with and without optically-zoned pyroxene and feldspar, to uncommon glassy clasts with fine crystallites. Microprobe analyses give the following compositions: pyroxene $Wo_{1-20}En_{40-49}Fs_{37-51}$; plagioclase An_{80-92}.

EET83232 (211 g).—This meteorite (7 × 8 × 4.5 cm) is macroscopically similar to the other 1983 Elephant Moraine eucrites. In thin section it is a typical polymict eucrite breccia with a variety of lithic clasts. Pyroxene clasts include pigeonites with μm scale exsolution lamellae, and both clouded and unclouded grains are present. Some pyroxene clasts have clear zoning that mimics the irregular clast outlines, suggesting that they were metamorphosed after brecciation. Feldspar clasts have shock features, and some may be recrystallized. A few feldspar clasts have abundant inclusions of clinopyroxene up to 20 μm in size. Mafic clasts vary from coarse to very fine-grained, and contain cloudy exsolved pyroxene. Silica minerals in these clasts appear both as interstitial space fillings and as coarse lath-shaped crystals that appear to crosscut the earlier texture. No orthopyroxene was recognized. Microprobe analyses give the following compositions: pyroxene $Wo_{1-25}En_{42-48}Fs_{43-52}$; plagioclase An_{86-93}. This meteorite is a polymict eucrite similar to EETA79004 and 79011.

EET83234 (180 g).—This specimen (7.5 × 7.5 × 3 cm) is a fragment similar to other 1983 Elephant Moraine eucrites. It contains a corner of a brown crystalline clast similar to that in EET 83229, and may be a piece of that stone. The thin section shows a typical polymict eucrite with a variety of small mafic clasts, including extremely fine-grained and glassy ones. Most pyroxene clasts are pigeonitic. Microprobe analyses give the following compositions: pyroxene $Wo_{1-33}En_{38-64}Fs_{29-59}$; plagioclase An_{78-96}. An unusual feature of this stone is the presence of pyroxene clasts with blebby rather than lamellar exsolution. These clasts (Wo_6En_{58-62}) may be similar to pyroxene in Binda and are rare in Elephant Moraine eucrites.

EET83236 (6.4 g).—A shiny black fusion crust with flow marks covers 60% of this stone (2 × 2 × 1 cm). The interior is bluish gray with numerous white and dark clasts. Several oxidation haloes were noted. The thin section shows a lightly brecciated medium-grained eucrite containing pyroxene in an ophitic to subradiate texture with generally lath-like feldspar. The pyroxene is generally inverted pigeonite, with herringbone textures preserved locally. Both pyroxene and plagioclase crystals are generally clouded, although a few pyroxene grains are quite clear. The feldspar is commonly clouded in patches and has a mottled extinction. In places it is nearly isotropic; it therefore has been substantially shocked. Interstitial silica minerals, troilite, chromite, and ilmenite are accessory phases. Microprobe analyses give the following compositions: pyroxene, $Wo_{1-42}En_{31-39}Fs_{25-59}$; plagioclase, An_{89-93}.

EET83283 (57.3 g).—This stone (6 × 2.5 × 3 cm) is typical of the other 1983 Elephant Moraine eucrites. The thin section shows a typical polymict achondrite with lithic and mineral clasts similar to the other Elephant Moraine polymict eucrites. Lithic clasts are generally fine-grained basalts and breccia fragments. The matrix is very dark and full of holes and cracks, suggesting that it has been severely weathered. Microprobe analyses give the following compositions: pyroxene $Wo_{2-16}En_{41-61}Fs_{33-48}$; plagioclase An_{82-95}. Some pyroxene clasts are shocked orthopyroxene (En_{55-65}), but most are pigeonitic with fine exsolution lamellae; none are as magnesian as diogenetic pyroxene. This meteorite is generally similar to EETA79004 and 79011.

HOWARDITES

FIGURES 6-30, 6-31

EET82600 (247 g).—Some black pitted fusion crust is present on one surface of this stone (7 × 5 × 5 cm). The other surfaces are smooth and gray with small white and dark gray inclusions. Chipping has revealed a gray interior with an indistinct whitish weathering rind. Inclusions are small and not very obvious. The thin section shows a microbreccia of angular fragments (grains up to 2 mm across) of pyroxene (orthopyroxene and pigeonite) and plagioclase, and rare plagioclase-pigeonite clasts up to 1.5 mm across, in a matrix of comminuted pyroxene and plagioclase. Trace amounts of troilite and nickel-iron are present. Microprobe analyses show a wide range in pyroxene compositions: $Wo_{1-24}En_{33-77}Fs_{22-53}$; the grains with En >70 indicate the presence of a diogenitic component. Plagioclase shows a considerable range of compositions, An_{79-93}. The meteorite is possibly paired with EETA79006.

EET83212 (402 g).—The exterior color of this achondrite (7 × 6 × 7 cm) ranges from medium gray to brown-gray, except for a thin, dull-black fusion crust on two surfaces. The interior

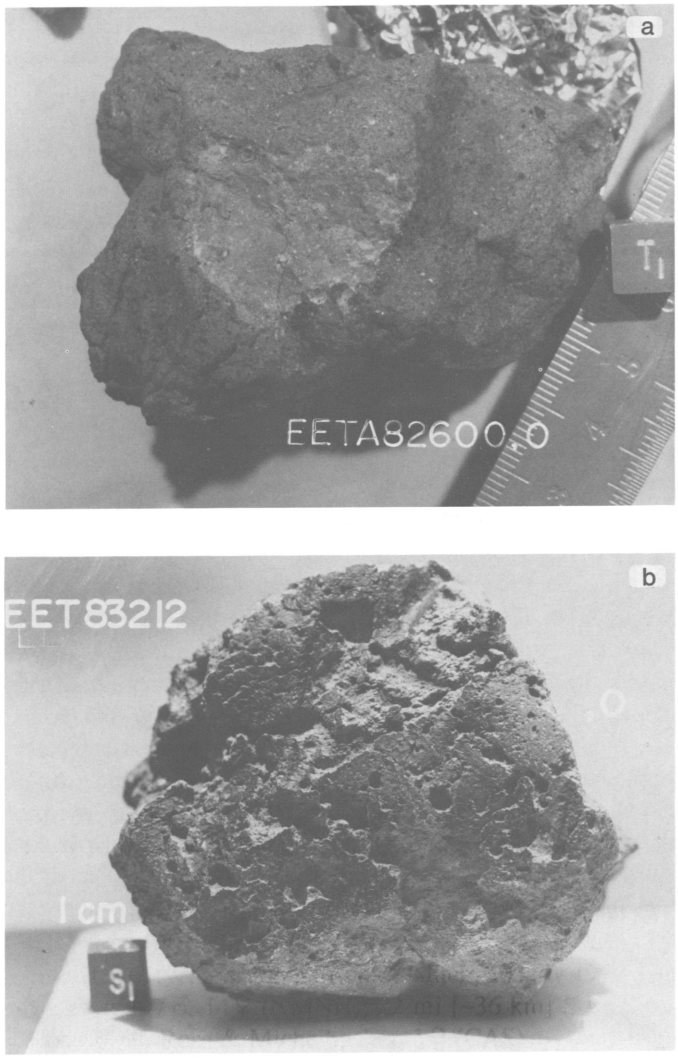

FIGURE 6-30.—Howardites.

is gray and rich in clasts; the latter include black fine-grained varieties and possibly some eucritic ones. A 1 cm thick weathering rind was exposed when the stone was chipped. The thin section is dominated by a single, very fine-grained mafic clast of the type common in both Allan Hills and Elephant Moraine polymict eucrites. Numerous smaller mineral clasts are enclosed within this large clast. Several outer parts of this fine-grained clast that border the coarser-grained matrix are darker than the clast interior, either because the border region is finer-grained or because of the presence of iron oxide weathering products. Some mineral clasts have dark fine-grained "chill zones" around them. Pyroxene grains within this dark clast have a variety of fine- and coarse-scale exsolution lamellae. Feldspar grains are partly maskelynitized. One feldspar clast has a glassy core with a feldspar rim that mimics the shape of the clast. Heating by the mafic melt that quenched to form the dark clast apparently caused devitrification of the previously-shocked feldspar grains. The "normal" breccia of 83212 contains breccia clasts, basaltic clasts with clouded pyroxenes and intergranular textures, granular mafic clasts with recrystallized pyroxene, and some glassy material. One clast of diogenetic orthopyroxene was observed. Microprobe analyses give the following compositions: pyroxene $Wo_{1-35}En_{33-80}Fs_{18-53}$; plagioclase An_{84-96}.

EET83227 (1973 g).—This meteorite (13 × 10 × 9 cm) has a rounded shape, and the outer surfaces contain numerous deep vugs. A few millimeter-sized patches of fusion crust remain on the gray exterior. Several different kinds of clasts are visible, the largest being 2 cm in length; they include eucritic clasts, black fine-grained clasts, pinkish brown fine-grained clasts, and black and white clasts. Both interior and exterior surfaces show numerous oxidation haloes up to 1 cm in diameter. Interior surfaces are lighter gray than the exterior ones. The thin section reveals a typical polymict achondrite, with one large medium-grained mafic clast containing ophitic to radial pyroxene/plagioclase intergrowths. The pyroxene and plagioclase in this clast are zoned and show little clouding. Other clasts include breccia, shocked pyroxene, and twinned feldspar. No maskelynite was observed. Coarse-grained lithic fragments, fine-grained granular mafic clasts and rare glassy fragments are also present. Microprobe analyses give the following compositions: pyroxene, $Wo_{1-39}En_{30-73}Fs_{23-54}$; plagioclase, An_{78-98}. The occurrence of pyroxene grains with En >70 indicates the presence of a diogenitic component in this meteorite.

EET83228 (1206 g).—One small patch of black fusion crust remains on this moderately fractured meteorite (12.5 × 11.5 × 8.5 cm). Exterior surfaces are darker gray than interior ones; many areas are heavily oxidized. Numerous deep vugs are present on all of the exterior surfaces. Abundant clasts of various types are readily apparent. The thin section shows a polymict eucrite with a variety of generally small lithic clasts. These latter include types seen in both howardites and polymict eucrites, ranging from medium- and coarse-granular clasts to interstitial basalts. Microprobe analyses give the following compositions: pyroxene, $Wo_{1-25}En_{32-80}Fs_{18-54}$; plagioclase, An_{82-94}. A few large orthopyroxene clasts have concentric zoning (cores are En_{70-75}), suggesting exchange reactions with the surrounding breccia. These modified clasts are similar to clasts in EETA 79004, with which this meteorite may be paired.

EET83235 (254 g).—This meteorite (7 × 6 × 4 cm) looks similar to the other 1983 Elephant Moraine eucrites except that it appears to be more heavily weathered, as indicated by the presence of a thick dark gray weathering rind. The thin section shows a very dark gray matrix that appears to have been modified by this weathering, as sulfate is present. One pyroxenite clast contains two large (~1 mm) pyroxene crystals showing no exsolution; this may be a fragment of an orthopyroxenite, but shock modification has produced inclined extinction in the pyroxene. Feldspar clasts also show abundant evidence of shock. Pigeonite clasts are abundant, in which the

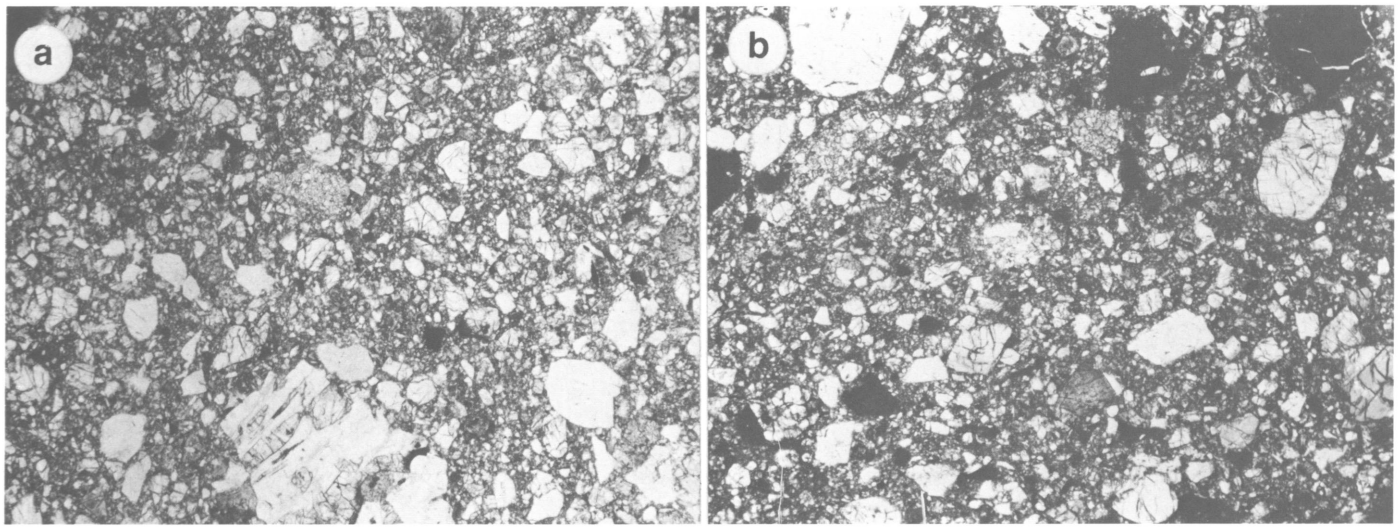

FIGURE 6-31.—Photomicrographs of thin sections of howardites (each field of view is 3 × 2 mm): *a*, EET82600. This is a microbreccia of orthopyroxene, pigeonite, and plagioclase in a comminuted matrix of pyroxene and plagioclase. Note the small gabbroic clast. *b*, EET83228. This is similar to 82600; note the dark glassy clasts.

pyroxene shows μm-scale exsolution. One mafic clast has a gabbroic texture and contains lath-shaped tridymite (?) crystals over 1 mm in length. Other clasts are extremely fine-grained or glassy. Microprobe analyses give the following compositions: pyroxene, $Wo_{1\text{-}38}En_{22\text{-}72}Fs_{26\text{-}54}$; plagioclase, $An_{86\text{-}96}$. One large diogenitic clast was analyzed in which the pyroxene is Wo_2, En_{72}, Fs_{26}.

EET83251 (261 g).—This stone (7 × 5.5 × 4 cm) is another typical example of the 1983 Elephant Moraine polymict achondrites. The thin section shows a wide variety of clast types, including medium- to coarse-grained gabbroic clasts with zoned pyroxene and plagioclase crystals, fine-grained basaltic clasts, glassy (or devitrified) clasts, breccia and recrystallized breccia clasts, pyroxene-rich mafic and breccia clasts, and orthopyroxene clasts (some containing orthopyroxene as magnesium-rich as En_{85}). One coarse-grained mafic clast contains anhedral feldspar crystals (>200 μm in size) with 1–10 μm-sized inclusions of clinopyroxene, a feature generally seen only in monomineralic feldspar clasts in Victoria Land achondrites. Microprobe analyses give the following compositions: pyroxene, $Wo_{1\text{-}28}En_{37\text{-}85}Fs_{14\text{-}58}$; plagioclase, $An_{80\text{-}95}$.

UREILITES

FIGURES 6-32, 6-33

ALH82106 (35.1 g), 82130 (44.6 g).—Patches of black fusion crust cover much of the surfaces of these two specimens. Exposed interior surfaces are black with moderate to heavy oxidation. Well-developed crystal faces are obvious. The thin sections show an aggregate of anhedral to subhedral grains (0.3–1.8 mm across) of olivine (about 60%) and pyroxene (about 30%), with about 10% of opaque material that is in part disseminated throughout and in part concentrated along grain boundaries. Both olivine and pyroxene show undulose extinction, suggesting that the specimens have been shocked. Olivine grains are gray from submicroscopic opaque inclusions, whereas pyroxene grains are clear but are extremely fractured. The opaque material along grain boundaries consists of graphite and secondary iron oxides. Microprobe analyses give the following compositions: olivine is somewhat variable, with a range of $Fa_{0\text{-}5}$ and a mean of Fa_3; pyroxene is essentially uniform, $Wo_5En_{91}Fs_4$, although one grain of sub-calcic augite was analyzed that has the composition $Wo_{36}En_{62}Fs_2$. The mineralogy and textures of these two stones are typical of ureilites, but the minerals have higher Mg/Fe ratios than those in any ureilite so far described.

ALH82130 is essentially identical to ALH82106 in all respects and can confidently be paired with it.

Goodrich and Berkley (1985) have reported precise determinations for Ti, Al, Cr, Mn, Ca, P, and Ni in the cores of olivine crystals from this meteorite.

ALH83014 (1.3 g).—Weathered fusion crust covers part of this small ureilite (1 × 0.5 × 0.5 cm). Well-developed crystal faces are apparent on other surfaces. The overall color is reddish brown. The thin section shows an aggregate of rounded to subhedral grains (0.6–3 mm across) of olivine with minor pyroxene. Small platy crystals of graphite are present in carbonaceous rims around the silicate grains. Trace amounts of troilite and nickel-iron are present, the latter being largely altered to translucent brown limonite. Microprobe analyses show olivine of uniform composition (Fa_{18}) with notably high CaO (0.4%) and Cr_2O_3 (0.7%) contents; the pyroxene is a pigeonite of composition $Wo_8En_{77}Fs_{15}$. This meteorite appears

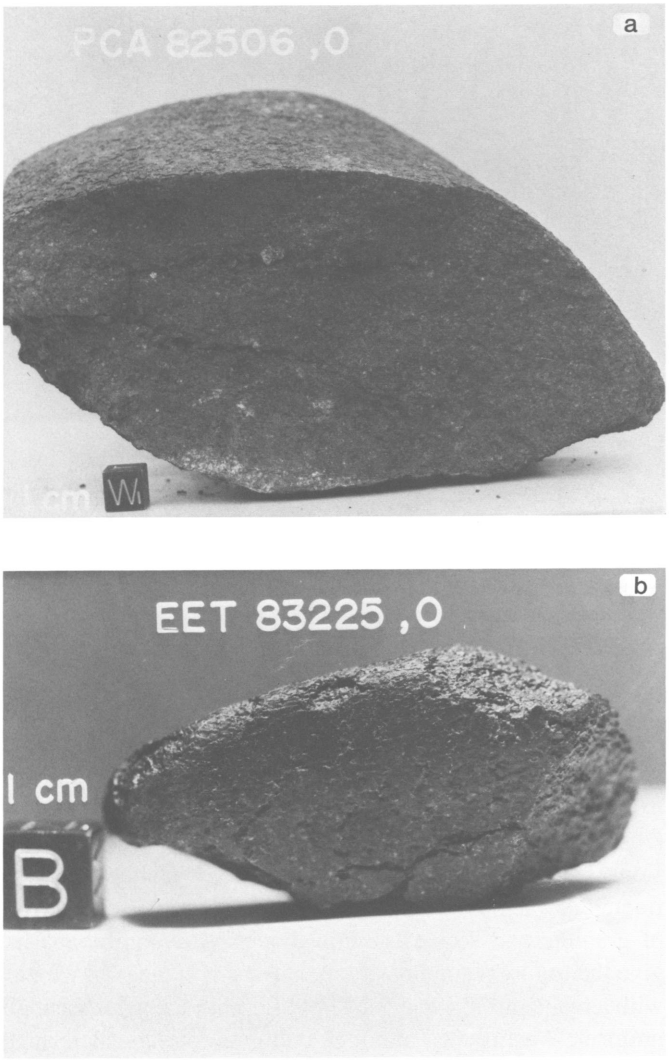

FIGURE 6-32.—Ureilites.

to be relatively unshocked compared to most ureilites.

PCA82506 (5316 g).—Patches of fusion crust cover 75% of the surface of this large achondrite (22 × 16 × 9 cm); in places this fusion crust has a blistery texture. Areas with little fusion crust are greenish to brown; the interior is grayish green to brown. The matrix has a blocky texture and many crystal faces are evident. The thin section shows an aggregate of anhedral to subhedral grains (0.6–3 mm across) of olivine and pyroxene. Individual grains are rimmed by carbonaceous material, included within which are thin stringers of troilite. Trace amounts of nickel-iron have been largely weathered to limonite. Microprobe analyses show olivine of uniform composition (Fa_{21}) with notably high CaO content (0.3%); the pyroxene is pigeonite with composition $Wo_6En_{76}Fs_{18}$. Some grains show undulose extinction but this meteorite is otherwise relatively unshocked compared to most ureilities.

Goodrich and Berkley (1985) have reported precise determinations of Ti, Al, Cr, Mn, Ca, P, and Ni in the cores of olivine crystals from this meteorite. Berkley and Goodrich (1985) described cohenite-bearing metallic spherules. Miyamoto et al. (1985) have estimated a cooling rate of 10°/hour from an initial temperature of 1200° ± 50° C down to a final temperature of 800° C.

EET83225 (44.0 g).—The surface of this meteorite (5 × 2.5 × 2.5 cm) is covered with a very thin and smooth fusion crust, which is brownish black with a dull sheen. Well-developed crystals make up the interior, which is heavily oxidized to a reddish brown color. The thin section reveals a medium- to coarse-grained ureilite composed of generally clear crystals of olivine (Fa_{11}) and pyroxene ($Wo_{10}En_{77}Fs_{13}$), with the pyroxene predominant in abundance. Grain boundaries are coated with dark material containing vein-like metal, graphite, and a yellow/red cathodoluminescent phase that is probably diamond. Tiny metallic inclusions occur in some olivine and pyroxene grains. The section shows a distinct, dimensionally-dependent, preferred orientation of both pyroxene and olivine, suggesting cumulus structure.

AUBRITES

FIGURE 6-34

ALH83009 (1.7 g), 83015 (3.1 g).—These two small white specimens appear visually to be identical, and this is confirmed by petrographic examination. Both consist almost entirely of orthopyroxene clasts up to 5 mm in size set in a comminuted groundmass of the same mineral. One grain was found that has *inclined extinction and appears to be clinoenstatite.* Accessory minerals include olivine, plagioclase, nickel-iron, troilite, daubreelite, and alabandite. Rusty haloes surround the metal grains. Microprobe analyses show that the olivine and pyroxene are essentially pure magnesium silicates: olivine FeO ~0%–0.06%; pyroxene FeO ~0%–0.17%; CaO ~0.05%–0.46% with a mean of 0.26%. Plagioclase is $An_{90}Or_3$. Silicon was not detected in the metal. ALH83009 differs from ALHA78113 in not having the dark clasts observed in the latter meteorite.

DIOGENITES

FIGURES 6-35, 6-36

ALHA81208 (1.6 g).—An evaporite deposit coats the oxidized fusion crust that totally covered this small stone (2.1 × 1 × 0.5 cm). The stone crumbled when it was chipped, revealing the interior to be completely weathered. The thin section consists almost entirely of orthopyroxene clasts, ranging up to 3 mm in maximum dimension, with accessory chromite. The individual clasts are rimmed by dark brown to black material, which consists in part of limonite. Remnants of fusion crust are present in the thin section, and have an outer crust of brown limonite. Microprobe analyses show that the

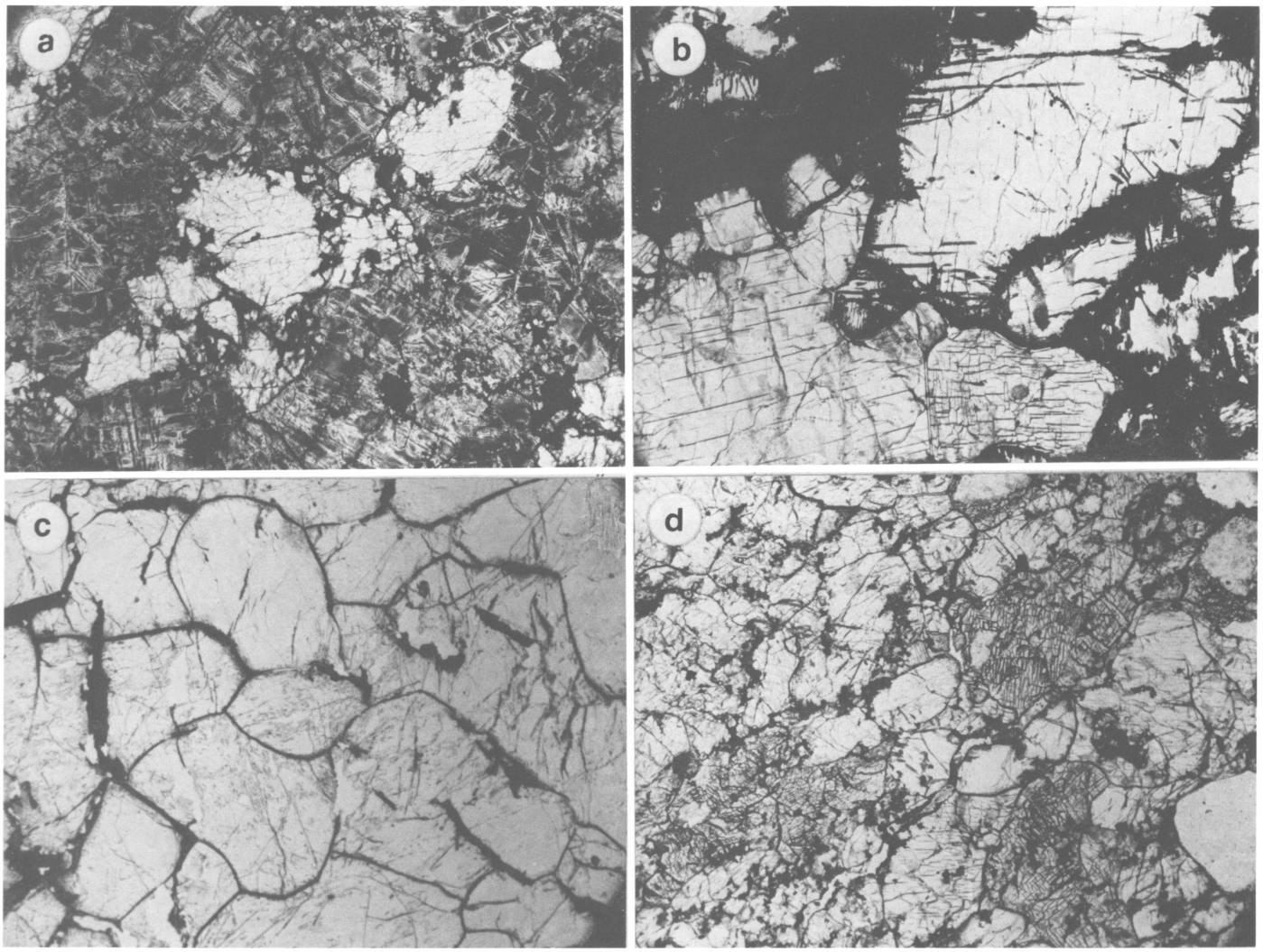

FIGURE 6-33.—Photomicrographs of thin sections of ureilites (each field of view is 3 × 2 mm): *a*, ALH82106; *b*, PCA82506; *c*, ALH83014; *d*, EET83225. Note the distinctly different textures in these four ureilites.

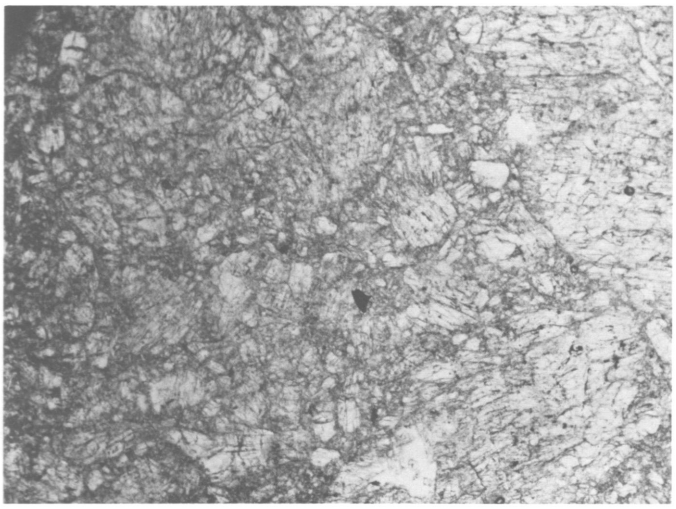

FIGURE 6-34 (*Left*).—Photomicrograph of thin section of the aubrite ALH83015 (field of view is 3 × 2 mm). This is a microbreccia consisting almost entirely of enstatite crystals.

pyroxene is essentially uniform in composition, except for some variation in calcium content (CaO 1.2%–2.5%); the mean composition is $Wo_3En_{72}Fs_{25}$, with 0.7% Al_2O_3, 0.14% TiO_2, and 0.6% MnO. The meteorite is classified as a diogenite, although the amount of limonite suggests that it may be a silicate fragment from a mesosiderite. It is therefore listed in the Appendices to this volume as a diogenite/mesosiderite.

TIL82410 (18.8 g).—A dull, blistery fusion crust covers one surface and is present in patches on other surfaces of this stone (3 × 2.5 × 1.5 cm). Areas without fusion crust have a pinkish tinge. Mineral clasts up to 5 mm in longest dimension are abundant, as are gray veins (1–5 mm wide), which stand out

in relief relative to the surrounding material. A single green crystal and several reddish brown grains are present. The thin section shows angular clasts of pyroxene, up to 3 mm in greatest dimension, in a groundmass of comminuted pyroxene. The only other minerals noted were rare grains of plagioclase and trace amounts (less than 1%) of nickel-iron. Remnants of fusion crust are present along one edge. The section is stained brown with limonite. Microprobe analyses show the pyroxene to be uniform in composition: $Wo_2En_{74}Fs_{24}$, with 0.47% Al_2O_3, 0.64% MnO, and 0.07% TiO_2.

EET83246 (48.3 g).—Shiny patches of fusion crust cover one surface and dull pitted fusion crust covers the opposite surface of this meteorite (4 × 3.5 × 2 cm). A highly polished

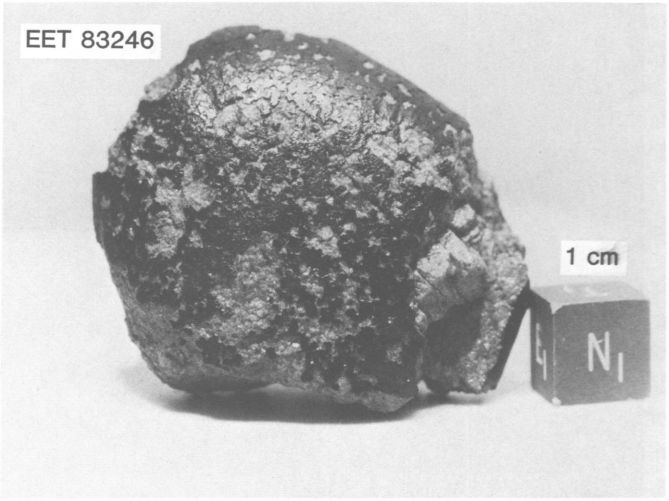

FIGURE 6-35 (*Right*).—Diogenite. Areas of black fusion crust have flaked off, revealing coarsely crystalline orthopyroxene.

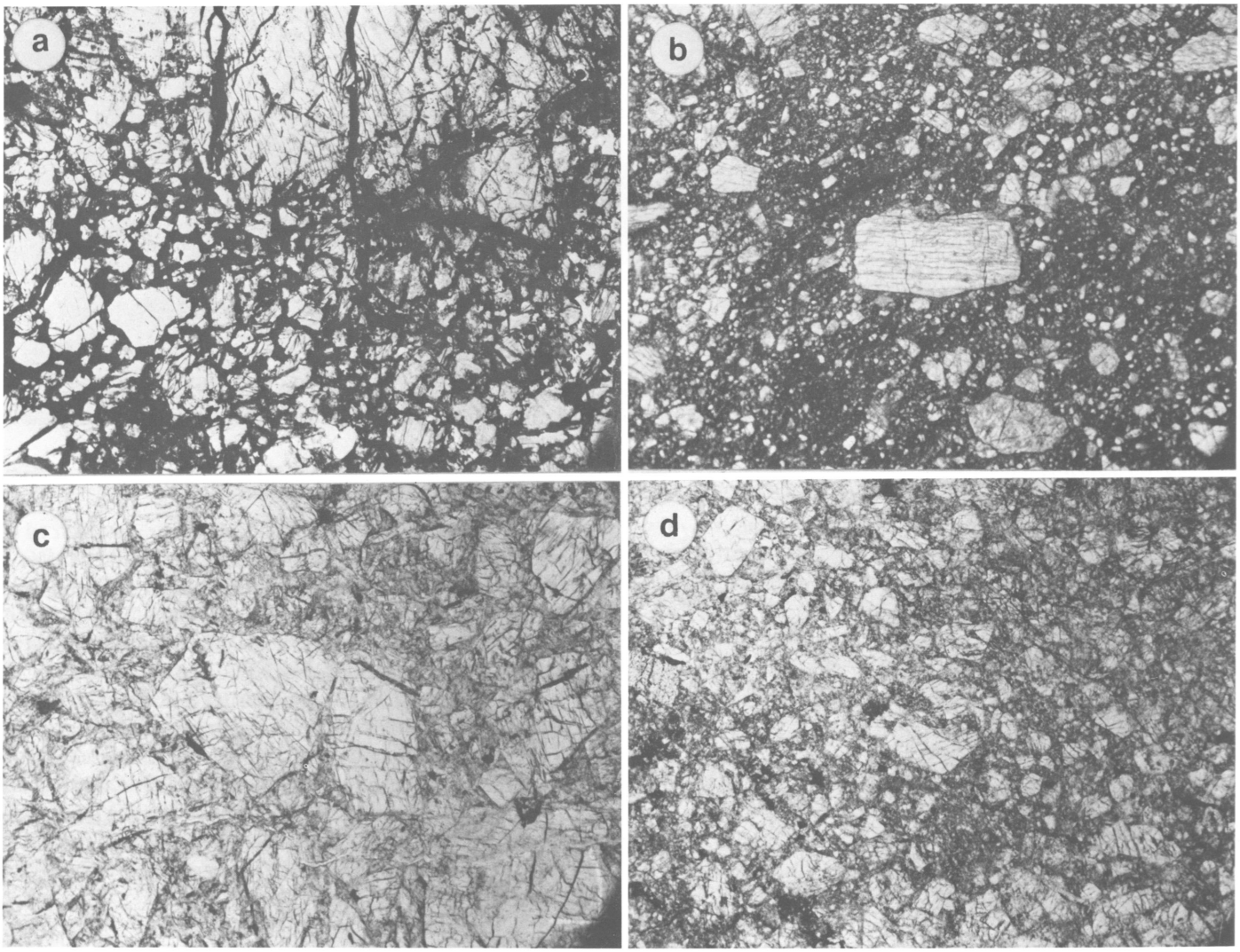

FIGURE 6-36.—Photomicrographs of thin sections of diogenites (each field of view is 3 × 2 mm): *a*, ALHA81208; *b*, TIL82410; *c*, EET83246; *d*, EET83247. Note the distinctly different textures in these four diogenites.

fracture surface exposes the greenish gray crystalline interior. Many clasts are visible, the largest of which is 1 cm long. The thin section shows clasts of orthopyroxene up to 9 mm long, in a groundmass of comminuted pyroxene and accessory chromite, troilite, and nickel-iron. The pyroxene is very uniform in composition, $Wo_{2.6}En_{73.4}Fs_{24}$, with 0.7% Al_2O_3 and 0.5% MnO.

EET83247 (22.5 g).—Shiny black fusion crust covers about one quarter of the surface of this specimen (4 × 2.5 × 1.5 cm). About half of the exterior surface has weathered to a reddish brown, and the remainder is medium gray with large cream-colored clasts. One fine-grained black clast was also noted. Most of the exposed interior has been heavily oxidized. The thin section shows a cataclastic texture, and there is a continuous range in clast size from less than 0.1 mm to 2 mm. The meteorite consists almost entirely of orthopyroxene, with accessory amounts of chromite, troilite, and nickel-iron. Brown limonitic staining pervades the section. The pyroxene is uniform in composition, $Wo_2En_{75}Fs_{23}$, with 0.6% Al_2O_3 and 0.5% MnO.

These two EET diogenites are not paired, and appear to be different from the other Elephant Moraine diogenite, EETA79002.

ACHONDRITE, UNCLASSIFIED

FIGURE 6-37

ALHA81187 (40.0 g).—Several cracks penetrate the mostly weathered interior of this stone (4.5 × 2.5 × 2 cm). Fusion crust covers two surfaces, one of which shows remnants of flow features. The thin section shows an aggregate of anhedral to subhedral grains, 0.05–0.6 mm across, of pyroxene to olivine, with about 20% of disseminated nickel-iron and minor amounts of plagioclase, troilite, and schreibersite. The proportion of pyroxene to olivine is estimated at 4:1. Weathering is extensive, with veinlets and small areas of brown limonite throughout the section. Microprobe analyses give the following compositions: olivine, Fa_4; pyroxene, $Wo_3En_{90.5}Fs_{6.5}$; plagioclase, An_{18}. The meteorite is tentatively considered to be an achondrite (unclassified), but it may belong to the small group of forsterite chondrites (Graham et al., 1977).

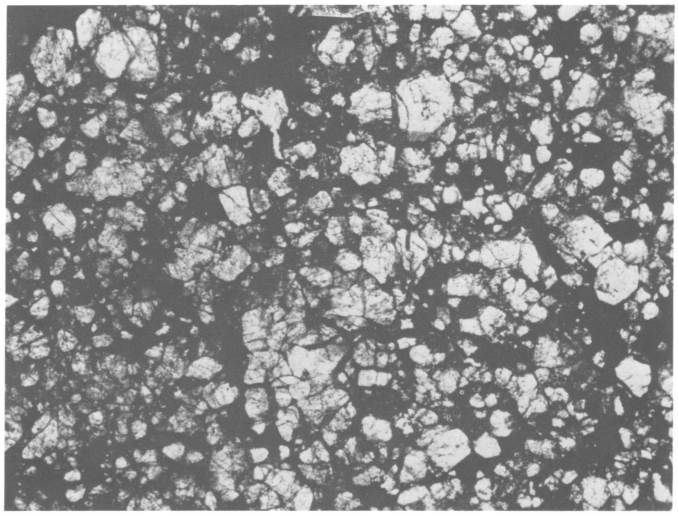

FIGURE 6-37.—Photomicrograph of thin section of the unclassified achondrite ALHA81187 (field of view is 3 × 2 mm). It consists mainly of olivine and orthopyroxene, with minor plagioclase (white to gray), some nickel-iron and troilite.

Literature Cited

Antarctic Meteorite Newsletter, 6(2).

Antarctic Meteorite Newsletter, 8(1).

Antarctic Meteorite Newsletter, 8(2).

Berkley, J.L., and C.A. Goodrich
1985. Cohenite-bearing Metallic Spherules in Ureilites: Petrology and Implications. In *Lunar and Planetary Science XVI*, pages 49-50. Houston: The Lunar and Planetary Institute.

Dodd, R.T., Jr., W.R. Van Schumus, and D.M. Koffman
1985. A Survey of the Unequilibrated Ordinary Chondrites. *Geochimica et Cosmochimica Acta*, 31:921–951.

Goodrich, C.A., and J.L. Berkley
1985. Minor Elements in Ureilites: Evidence for Reverse Fractionation and Interstatial Silicate Liquids. In *Lunar and Planetary Science XVI*, pages 280–281. Houston: The Lunar Planetary Institute.

Graham, A.L., A.J. Easton, and R. Hutchison
1977. Forsterite Chondrites; the Meteorites Kakangari, Mount Morris (Wisconsin), Pontlyfini, and Winona. *Mineralogical Magazine*, 41:201–210.

Lovering, J.F.
1975. The Moama Eucrite—A Pyroxene-Plagioclase Adcumulate. *Meteoritics*, 10:101–114.

Miyamoto, M., H. Toyoda, and H. Takeda
1985. Thermal History of Ureilite as Inferred from Mineralogy of Pecora Escarpment 82506. In *Lunar and Planetary Science XVI*, pages 567–568. Houston: The Lunar and Planetary Institute.

Palme, H., L. Schultz, B. Spettel, H.W. Weber, H. Wanke, M. Christophe Michael-Levy, and J.C. Lorin
1981. The Acapulco Meteorite: Chemistry, Mineralogy and Irradiation Effects. *Geochimica et Cosmoshimica Acta*, 45:727–752.

Scott, E.R.D.
1985. Further Petrologic Studies of Metamorphosed Carbonaceous Chondrites. In *Lunar and Planetary Science XVI*, page 748. Houston: The Lunar and Planetary Institute.

Van Schumus, W.R., and J.A. Wood
1967. A Chemical-Petrographic Classification System for the Chondritic Meteorites. *Geochimica et Cosmochimica Acta*, 31:747–765.

Wieler, R., H. Baur, Th. Graf, and P. Signer
1985. He, Ne, and Ar in Antarctic Meteorites: Solar Noble Gasses in an Enstatite Chondrite. In *Lunar and Planetary Science XVI*, pages 902–903. Houston: The Lunar Planetary Institute.

7. Descriptions of Some Antarctic Iron Meteorites

Roy S. Clarke, Jr.

This chapter provides brief descriptions of three octahedrites and two ataxites that were collected during the 1983 field season. The descriptions are preliminary and are based on material prepared for publication in the *Antarctic Meteorite Newsletter*. Previously unpublished chemical values by Eugene Jarosewich are included for three of the specimens.

Octahedrites

EET83245 (59 g).—This specimen (5.5 × 2.5 × 1.3 cm) from Elephant Moraine has a smoothly curved top surface that meets a flat bottom surface at one side, and an irregular narrow surface that is perpendicular to the bottom surface on the opposite side. The shield-shaped specimen is completely covered with a reddish brown coating of terrestrial iron oxides. No remnant fusion crust was visible. The curved surface appears to have been an exposed surface during weathering: wind ablated, polished, and slightly pitted. The other two surfaces are more deeply corroded.

A slice from near one end of the specimen yielded a 1.4 cm^2 metallographic section of mainly kamacite. The wind-ablated surface was also an ablation surface during atmospheric passage, as it has a heat-altered zone extending at least 1 mm into the interior. Fusion crust, however, has been removed by weathering. The bottom surface appears to consist of either weathered fusion crust or, more likely, weathered melt material that filled a crack during atmospheric heating. Some interior material along this bottom surface is also heat altered. Microrhabdites occur in abundance throughout, with occasional rhabdites and very thin lamellar schreibersites along subgrain boundaries. One grain boundary contains schreibersite and heat-altered taenite. The presence of taenite in what appears to be a relatively large mass of kamacite suggests that this specimen is a fragment of a coarsest octahedrite. A bulk value of 6.1 weight percent Ni is consistent with a IIB chemical classification.

EET83333 (188 g).—This specimen (5 × 4 × 2.5 cm) from Elephant Moraine is irregularly shaped, weathered and pitted, and mostly covered with a reddish brown coating of secondary oxides. Tiny areas of remnant fusion crust have been preserved in several depressions. Silicates are exposed at the bottoms of other depressions, the largest silicate area measuring 10 × 5 mm. Ablative melting of inclusions appears to have caused other surface depressions.

A median section through the specimen provided an area of approximately 8 cm^2 for examination (Figure 7-1). The surface is silicate-rich, containing a number of millimeter-sized silicate regions as well as numerous smaller individual crystals unevenly distributed in the metal. Silicate associations comprise 5%–10% of the surface area, two clusters having maximum dimensions of 5 mm. The metal is polycrystalline kamacite with individual crystals in the millimeter-size range. Longest dimensions are normally less than 5 mm, and the shortest normally more than 1 mm. Taenite and pearlitic plessite areas are distributed along grain boundaries and at junctions of three or more kamacite grains. A striking feature of this meteorite, readily visible on the etched surface shown in Figure 7-1, is a continuous and unusually thick circumferential heat-altered zone. The thickness of the α_2 structure averages about 5 mm and ranges from 2 to 7 mm. About half of the area of the slice is heat altered. Although small areas of fusion crust were tentatively identified in surface depressions, none was recognized in polished section. Weathering is most obvious near the surface and has penetrated into the interior along grain boundaries.

Interior kamacite areas contain numerous straight Neumann bands and numerous curved subboundaries. Subboundaries are populated with occasional schreibersites, some of which have distinct rhabdite morphologies. Kamacite areas tend to be mottled, suggesting the presence of unresolvable microrhabdites. Large schreibersites occur along crystal boundaries, and several areas of massive schreibersite occur in association with silicate-graphite-troilite areas. Schreibersite also occurs at taenite borders. The plessite has a well-developed pearlitic structure and is present in abundance, consistent with a medium or coarse octahedrite. A distinct Widmanstatten pattern is not sufficiently well developed to obtain reliable band widths.

Silicate areas contain coarse (0.1 to 0.5 mm), colorless, and transparent crystals associated with abundant troilite and traces

Roy S. Clarke, Jr., Department of Mineral Sciences, National Museum of Natural History, Smithsonian Institution, Washington, D.C. 20560.

FIGURE 7-1.—Polished and etched surface of EET83333. The mottled gray rim zone is atmospherically heat-altered to a depth of 7 mm at one point. The dark gray inclusions are silicate-graphite-troilite areas. Kamacite grain boundaries and areas of Widmantatten pattern may also be seen. The maximum width of the slice is 4 cm.

of included kamacite and taenite. Graphite occurs in some of the silicate areas, generally at silicate/metal interfaces, and it is coarse-grained where present. All the troilite in this section occurs with silicates. Survey electron microprobe examination of the silicates identified plagioclase (An_9), olivine (Fa_5), and pyroxene (Fs_7).

This individual is a silicate-rich octahedrite, probably a Group I iron. The unusually thick heat-altered zone suggests an atypical passage through the atmosphere.

EET83390 (15.1 g).—This specimen (2 × 1.8 × 1 cm) from Elephant Moraine is irregular in shape and deeply weathered. The surface is covered with reddish brown secondary oxides, and contains several small depressions that may have resulted from atmospheric melting.

A median section provided an area of 1 cm^2 for examination. The structure revealed is that of a heat-affected octahedrite, either a medium or coarse octahedrite. The few structures available for band width measurements indicate a 1 to 1.5 mm range. Throughout the section kamacite has been transformed to α_2 by atmospheric heating. Most of the rim of the section is coated with layered secondary oxides from 0.1 to 1 mm thick.

Taenite and comb plessite areas also appear to have been somewhat heat-affected. Microrhabdites are present, and several remant Neumann bands are suggested by linear arrays of microrhabdites. Major grain boundaries are populated over much of their lengths by either grain boundary schreibersite or secondary iron oxides that have invaded the interior. Some schreibersite is associated with taenite-plessite areas.

This specimen appears to be a small individual that was severely heated upon passage through the atmosphere. It is an octahedrite and may prove on further study to be a Group III iron.

Ataxites

EET83230 (530 g).—This specimen (5.5 × 5 × 5 cm) from Elephant Moraine is a rounded, and roughly equidimensional individual, reminiscent of a small cobble. It is completely covered with a secondary reddish brown coating of iron oxides, and no traces of fusion crust remain. The surface that has been recently exposed to wind ablation in our atmosphere is slightly smoother than the other surfaces, having rounded edges and a slightly distorted rectangular outline.

A slice through one side of the specimen produced a 15 cm^2 surface for examination. The matrix is martensitic, containing a few widely dispersed kamacite spindles. An occasional spindle will contain a very small schreibersite. The section's most interesting feature is a concentration, in one half of the slice, of about a dozen mm-sized iron phosphate crystals (Figure 7-2), some with euhedral outline and/or enclosed troilite. These inclusions are partially bordered by thin kamacites.

This individual is an unusual phosphate-rich ataxite with a bulk value of 16.1 weight percent Ni.

ILD83500 (2523 g).—This specimen (13.5 × 12 × 4 cm) was found near Inland Forts by Bob Ackert of the University of Maine at Orono. It was found "imbedded in loose sandy till with abundant pebbles and cobbles of the Beacon Sandstone and dolorite. The glacial deposit overlies the Beacon Sandstone. The top of the white evaporite deposit marks the depth at which the iron was buried" (Figure 7-3). The specimen is flat with an outline similar to that of a policeman's badge. It has three distinct surface types. The exposed surface as found is slightly irregular and covered with a scaley reddish brown to dark reddish brown iron oxide coating. This surface is bordered on the sides by a ≤1 cm thick band of cream-colored soil and clay. The sides and bottom of the specimen below this band have a much different appearance. These surfaces are rough, range in color from black to reddish brown, and have numerous adhering soil particles and sand grains.

A metallographic surface of 9 cm^2 was prepared for examination. The most prominant features in the martensitic matrix are centimeter-long lamellar inclusions that appear to be oriented according to parent taenite crystallography. They have thin kamacite borders that occasionally enclose schreibersite. Most appear to have contained very thin cores that have been replaced by oxides due to weathering. The best preserved of these lamellae contain cores of chromite a few microns thick. The matrix contains a high concentration of ~50 μm-sized schreibersite grains surrounded by kamacite. The orientation of the kamacite seems to have been controlled by schreibersite precipitation. Several troilites are present in association with lamellar and/or equidimensional chromite. A very small crystal tentatively identified as tridymite was found within troilite, at its border with kamacite.

This specimen is an unusual ataxite with a bulk value of 18.9 weight percent Ni.

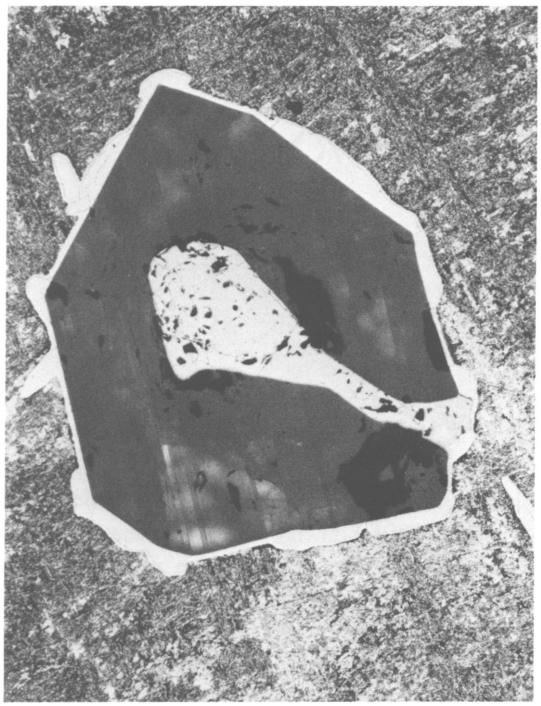

FIGURE 7-2.—A large crystal of $Fe_3(PO_4)_2$ in EET83230 photographed in reflected light. A martensitic matrix surrounds the phosphate, as does a thin rim of kamacite. Troilite intrudes into the center of the crystal. The maximum length between crystal edges is 0.7 mm.

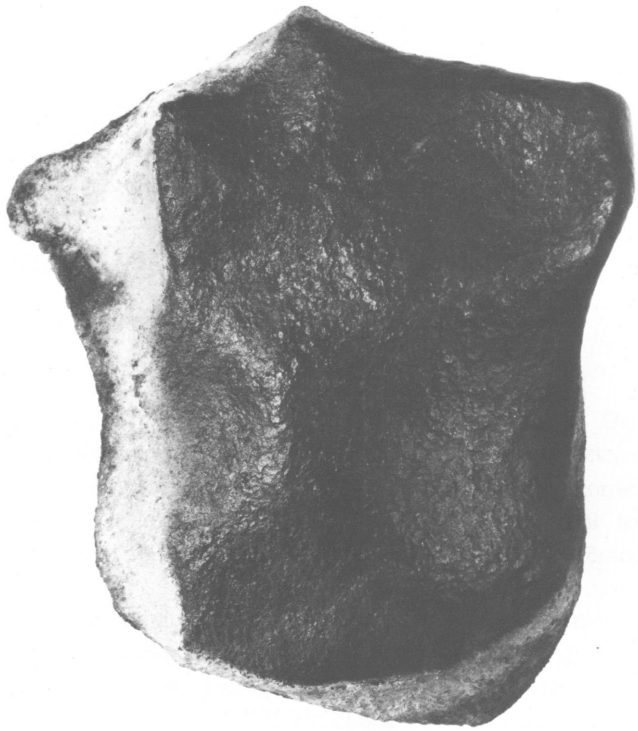

FIGURE 7-3.—ILD83500 was found partially within soil near Inland Forts. The dark surface area is typical of weathered meteoritic iron that has been exposed to the atmosphere, developing a thin coating of pitted, reddish brown iron oxides. The light-colored areas along the left side and bottom of the photograph were in soil. Weathering was more severe and soil particles still adhere. Maximum length is 15 cm.

8. Overview of Some Achondrite Groups

Jeremy S. Delaney and Martin Prinz

Introduction

Many meteorites have been collected in Antarctica during every field season between 1976 and 1984 (Table 8-1). Prior to 1969, only four meteorites from Antarctica were known (Hey, 1966; Hutchison et al., 1977), but since then nearly 6700 samples have been collected from several sites all over the Antarctic continent. Most of the samples collected are ordinary chondrites, but numerous achondritic samples have also been collected (Table 8-2).

Achondritic meteorites have been collected at localities near the Transantarctic Mountains from latitudes 76°S in Victoria Land to 80°30'S in the Thiel Mountains–Pecora Escarpment region. For brevity, all the meteorites collected by American expeditions to Antarctica are described as "Victoria Land" achondrites since most of the meteorite deposits (away from the Yamato Mountains area) are in Victoria Land. Studies of meteorite suites are reviewed and some emphasis is given to new samples from the 1983 season that have not yet been widely studied. The Victoria Land achondrites sample all the known achondritic meteorite suites and include several unique meteorite types. (Note that the terms "sample" and "meteorite" are not used interchangeably in this study. A sample is taken to mean one individual fragment that has been or can be assigned a sample number such as those in Table 8-3. A meteorite, however, is taken to consist of one sample or several samples that are parts of the same original fall. The number of samples available is, therefore, larger than the number of meteorites that are represented by these samples.)

The most common achondrite samples are the basaltic achondrites (44 samples). Of these, the polymict achondrites are the most abundant (31 samples). There are only seven eucrites and five diogenites. Ureilites are the next most abundant type (11 samples) and other achondrite groups are represented by smaller numbers of samples. Specimens of the shergottite-nakhlite-chassingite group have been collected in Victoria Land but are omitted from this review. Table 8-3 includes the mesosiderite sample numbers, since these stony irons have a basaltic achondrite silicate fraction. The 70 achondrite samples in Table 8-3 do not represent 70 meteorites. Many samples may be grouped as a single meteorite. In particular, the polymict basaltic achondrites appear to be samples of four to six meteorite showers, each represented by one to many samples (Delaney, O'Neil, et al., 1984).

The problem of determining the number of meteorite falls has been addressed using several different techniques: field relations (Marvin, 1984), petrography (Delaney, Takeda, Prinz, et al., 1983; Delaney, O'Neil, et al., 1984a; Delaney, Prinz, et al., 1984), chemical composition (Reid and Le Roex, 1984; Fukuoka, 1984), terrestrial ages (Webster et al., 1982; Schultz and Freundel, 1984). The total number of samples associated with each fall is presently unknown, but the achondrite specimens from the Victoria Land sites (Table 8-3) are probably samples of fewer than 30 meteorites, distributed among eight achondrite types. More than half of the specimens are polymict eucrites.

Basaltic Achondrites

The number of basaltic achondrite samples (eucrites, polymict eucrites, howardites, diogenites) from Victoria Land continues to grow rapidly. The number of well-distinguished meteorites is, however, fairly small as most samples may almost certainly be grouped as members of showers or as fragments of broken meteorites.

The Victoria Land basaltic achondrites are generally similar to the non-Antarctic meteorites. The most abundant non-Antarctic suites are eucrites and polymict achondrites and these are also the most important Victoria Land suites. Diogenites, members of a closely related achondrite group, are also represented in both suites. Statistical analyses comparing the number of non-Antarctic falls with Victoria Land finds for each achondrite group suggest that the Antarctic samples are derived from a similar population to the present day meteorite influx. In general, similarities between the Antarctic meteorite collections and the non-Antarctic collection seem to be increasing as the number of Antarctic meteorites increases.

Jeremy S. Delaney and Martin Prinz, Department of Mineral Sciences, American Museum of Natural History, New York, New York 10024.

TABLE 8-1.—Number of meteorite specimens collected at Antarctic localities.

Year	Allan Hills	Bates Nun.	Belgica Mtn	Derrick Peak	Inland Forts	Elephant Moraine	Meteorite Hills	Mount Baldr
1969	–	–	–	–	–	–	–	–
1973	–	–	–	–	–	–	–	–
1974	–	–	–	–	–	–	–	–
1975	–	–	–	–	–	–	–	–
1976	9	–	–	–	–	–	–	2
1977	307	–	–	–	–	–	–	–
1978	262	4	–	9	–	–	28	–
1979	54	–	5	–	–	10	–	–
1980	32	–	–	–	–	–	–	–
1981	315	–	–	–	–	–	–	–
1982	145	–	–	–	–	17	–	–
1983	102	–	–	–	1	84	–	–
1984	17 +	–	–	–	–	–	–	–
Total	1243	4	5	9	1	111	28	2

Year	Outpost Nun.	Pecora Esc.	Purgatory Peak	Reckling Peak	Taylor Glac.	Thiel Mtn	Yamato Mtn
1969	–	–	–	–	–	–	9
1973	–	–	–	–	–	–	12
1974	–	–	–	–	–	–	663
1975	–	–	–	–	–	–	307
1976	–	–	–	–	–	–	–
1977	–	–	1	–	–	–	–
1978	–	–	–	4	–	–	–
1979	–	–	–	15	–	–	3676
1980	1	–	–	68	–	–	13
1981	–	–	–	–	–	–	133
1982	–	29	–	–	1	16	211
1983	–	–	–	–	–	–	42
1984	–	–	–	–	–	–	58
Total	1	29	1	87	1	16	5124

NOTES.—Achondrite classes not represented in Antarctica: 1, nakhlites; 2, angrites; 3, chassignites. Nun. = Nunatak; Glac. = Glacier; Esc. = Escarpment; Mtn = Mountains. Meteorites found before 1969: Adelie Land; Lazarev; Thiel Mtn; Neptune Mtn.

TABLE 8-2.—Number of achondritic meteorites from Victoria Land.

Type	Allan Hills	Elephant Moraine	Reckling Peak	Pecora Escarp.	Thiel Mtn
Lunar	1	–	–	–	–
Shergottites	1	1	–	–	–
Aubrites	3	–	–	–	–
Ureilites	–	1	1	1	–
Winonaites	1	–	–	–	–
Eucrites	1	1	2	2	1
Diogenites	1	3	–	–	1
Polymict eucrites	2–3	2–3	–	–	–

TABLE 8-3.—Victoria Land achondrites sample numbers.

Type	Numbers
Lunar	A81005
Winonaites	A81187
Aubrites	A78113, A83009, A83015
Shergottites	A77005, E79001
Diogenites	A77256, E79002, T82410, E83246, E83247
Eucrites	R80204, R80224, A81011(?), A81313(?), T82403, P82501, P82506, E83236
Ureilites	A77257, A78019, A78262, R80239, A81101, P82506, A82106, A82130, A83014, E83225
Mesosiderites	A77219, R79015, R80229, R80246, R80258, R80263, R81059, R81098(?), A81028
Polymict eucrites	A76005, A77302, A78006(?), A78040, A78132, A78158, A78165, A79017, A80102, A81001(?), A81006, A81007, A81008, A81009(?), A81010, A81012, E79004, E79005, E79006, E79011, E82600(?), E83212, E83227, E83228, E83229, E83231, E83232, E83234, E83235, E83251, E83283

NOTES.—Numbers followed by (?) have been given different classifications in *Antarctic Meteorite Newsletters*. A, E, P, R, T, are Allan Hills, Elephant Moraine, Pecora Escarpment, Reckling Peak, Thiel Mountains, respectively.

COMPARISON OF ANTARCTIC AND NON-ANTARCTIC BASALTIC ACHONDRITES

Although there are overall similarities, there are some differences in detail, between the Antarctic and non-Antarctic samples. The most important of these are between the suites of polymict achondrites. These meteorites sample a continuum of breccias that represent the crust and regolith of at least one basaltic achondrite parent body, and are dominated by two lithological components that are present in varying proportions: orthopyroxenites and mafic rocks. Minor amounts of other rock types are also present. The presence and amount of these two main components is used as a basis for classifying the polymict basaltic achondrites and, therefore, a brief description of each is given.

ORTHOPYROXENITES.—This component is represented by mineral clasts of orthopyroxene with compositions similar to diogenetic pyroxene (En_{70-75}) and very rare lithic clasts of orthopyroxenite containing variable but minor amounts of olivine, chromite, troilite, and metal. The range of pyroxene compositions (En_{70-86}) sampled by the polymict achondrites is, however, greater than that of the diogenites. The orthopyroxenite component of these meteorites, therefore, cannot be simply equated with the diogenites as they are represented by the present meteorite collections. Study of pyroxene-rich achondrites from the Yamato collections of Antarctic achondrites has extended the range of compositions in pyroxenitic meteorites toward more iron rich pigeonitic compositions (En_{60-70}) (Takeda and Mori, 1984). Some of these Yamato samples are comparable with the Binda pyroxene-rich cumulate and appear to represent a transitional facies between the orthopyroxenite and mafic components of polymict achondrites (Takeda and Mori, 1984). There are no unbrecciated or monomict achondrites as magnesian as the most magnesian orthopyroxenes (En_{80+}) found in polymict achondrites.

MAFIC CLASTS.—The most common type of mafic clast in polymict achondrites is eucritic and has approximately equal volumes of pigeonite and plagioclase with compositions similar to the eucrites ($En_{30-40}Wo_{4-15}$ and An_{80-92}, respectively). There is, however, a great variety of mafic clast types present in these meteorites. This variability is not as well documented as the typical eucritic meteorites. Numerous studies have recognized, however, that these clasts represent an additional important suite of mafic rocks from the basaltic achondrite parent body (Bunch, 1976; Delaney et al., 1981; Dymek et al., 1976; Simon and Papike, 1983; Treiman and Drake, 1984). These clasts extend the compositional ranges for the major minerals beyond the limited range of clasts in the eucrites, and provide greater insight into the nature of the solid-liquid fractionation on the basaltic achondrite parent body than is available by studying the eucrites alone.

Prior to the discovery of polymict achondrite breccias in Antarctica, the non-Antarctic polymict breccias were generally referred to as howardites, and all the non-Antarctic examples contain clasts of both orthopyroxenitic and mafic material. Some of the first polymict achondrites found at both Yamato Mountains and Allan Hills in Antarctica differ from those previously known, however, as they contain a variety of mafic, or eucritic, clast types but no orthopyroxenite component (Miyamoto et al., 1978; Takeda et al., 1978; Olsen et al., 1978). For this reason, they were called polymict eucritic breccias or, more commonly, polymict eucrites. Further study revealed rare orthopyroxene grains in some of the Yamato samples, and when the first Elephant Moraine samples were studied a small orthopyroxenite component was recognized in EET79005 and 79006 (Simon and Papike, 1983; Delaney et al., 1982). As more Antarctic samples become available, it is clear that these polymict basaltic achondrites have continuously variable amounts of the two main components. The most orthopyroxene-rich meteorite appears to be Yamato 7308 (with 76% vol. opx.) and the most mafic clast-rich meteorite is the Allan Hills I meteorite represented by ALHA 76005, 77302, 78040, and numerous other specimens. This Allan Hills meteorite contains no orthopyroxenite component. Delaney, Takeda, and Prinz (1983a) suggest that those meteorites containing more than 90% (vol.) of eucritic, or mafic, material be called polymict eucrites and those with less than 90% be called howardites. Mason (1983b) suggests, alternatively, that meteorites containing any orthopyroxenite component should be called howardites.

As a group, the non-Antarctic polymict achondrites all contain an orthopyroxenite component and most have more than 10% (vol). The Victoria Land polymict achondrites, in contrast, contain either no orthopyroxene or less than 10% (vol.). Polymict achondrites with abundant orthopyroxene are, however, found in Antarctica at Yamato Mountains, especially

in the 1979 collections (Takeda et al., 1984; Delaney, Prinz, et al., 1984). Indeed, the Victoria Land and Yamato collections together sample a greater variety of polymict basaltic achondrites than do the non-Antarctic collection.

A number of clast types in the Antarctic samples has been described by Delaney, O'Neil, et al. (1984). All of these clast types have been recognized in both non-Antarctic howardites and polymict eucrites. At present, no clast type is known that occurs only in meteorites from one part of the world. The Victoria Land, Yamato, and non-Antarctic polymict basaltic achondrites are, therefore, believed to be a part of a continuum of breccias that sample a significant part of the regolith of their parent body or bodies.

NEW SAMPLES.—Samples of all the basaltic achondrite types are represented in the Victoria Land collections but the polymict eucrites are by far the most abundant. In the 1983 season, 13 basaltic achondrites were collected at the Elephant Moraine meteorite deposit. Two diogenites (EET83246; 83247), one eucrite (83236), and 10 polymict basaltic achondrites were collected (Table 8-1). Preliminary descriptions of these samples are given in *Antarctic Meteorite Newsletter*, 8(1), 1985.

Diogenites

The two new Elephant Moraine diogenites increased the number of Victoria Land samples to five (Table 8-3). This is a small number of samples compared with the 35, or more, diogenite samples recovered at Yamato Mountains (Takeda et al., 1981). Because the total number of meteorites represented both at Yamato Mountains and Victoria Land is either four or five, there is a similar number of meteorites available from each site. Unlike the Yamato diogenites, however, the Victoria Land samples are similar to most non-Antarctic diogenites as they are brecciated orthopyroxenites dominated by En_{70-75} pyroxene.

Eucrites

The eucrite EET 83236 is the eighth recovered from Victoria Land and Thiel Mountains localities. It is a typical eucrite containing lithic fragments with ophitic to radiate textures. It is mineralogically similar to the other Antarctic and the non-Antarctic eucrites (Tables 8-3 and 8-4, Figure 8-1, cf. Delaney, Takeda, and Prinz, 1984).

The Victoria Land eucrites appear to represent eight different meteorite falls as all have distinctive textures or mineral compositions, or are separated by long distances from similar meteorites. The eucrites, therefore, differ significantly from the polymict achondrites as they are not found as groups of samples at a single locality. Each of the Antarctic eucrites has uniform Fe/(Fe+Mg) in its pyroxene and thus has been thermally processed in the same way as most non-Antarctic eucrites. Allan Hills 81011 is unique as it appears to be a genomict breccia (Mason, 1983a). Treiman (1984) describes 81011 as a polymict eucrite having equilibrated basaltic clasts in a vesicular glass matrix, and as representing a major impact on the parent body. Allan Hills 81313, which contains maskelynite and was described as a shergottite, is also significantly different. Other eucrites (e.g. Padvarninkai; Reckling Peak 80204) contain variable amounts of maskelynite and, because mineral compositions in ALH81313 are identical to those in typical eucrites and quite different from any shergottite, it is suggested that this sample be classified as an eucrite.

Allan Hills 81001 was classified as an anomalous eucrite as it differs from most eucrites in several ways (Mason, 1983a). This sample closely resembles the fine-grained eucritic clasts typically found in Allan Hills polymict eucrites. It may be a large clast that separated from the Allan Hills I polymict eucrite shower during atmospheric descent and landed on the Antarctic ice as a separate object (Delaney, 1984). Whether this sample should be treated as a separate meteorite fall or grouped with the Allan Hills I polymict eucrite is not clear. Both approaches to classifying this sample have disadvantages. Perhaps further study can demonstrate that Allan Hills 81001 should be treated as a unique meteorite, but we assume here that it is a member of the Allan Hills polymict eucrites.

There are eight Victoria Land eucrites, represented by eight samples. In contrast, there are four to six Victoria Land polymict eucrites represented by at least 32 samples. Similar sample/meteorite ratios are calculated for the Yamato achondrites. Delaney (1984) has suggested that the eucrites were strong meteorites that are represented by individual falls whereas the polymict eucrites were friable and fell as showers. Statistics for known eucrite falls support this suggestion as showers are uncommon among the known eucritic falls.

Polymict Achondrites

Polymict basaltic achondrites are the most abundant Victoria Land achondrites. Of the 40 or more samples known, 16 are from Allan Hills and 16 from Elephant Moraine (Table 8-3). The Allan Hills and Elephant Moraine suites together appear to represent four or five meteorites that have been called Allan Hills I, Allan Hills II, Elephant Moraine I, and Elephant Moraine II by Delaney, O'Neil, et al. (1984). The samples collected at Elephant Moraine during the 1983 field season represent both Elephant Moraine I and II meteorites on the basis of their textures and mineral composition. Feldspar Na_2O contents and pyroxene compositions, generated by electron microprobe modal analysis, for the Elephant Moraine 1983 series are given in Figures 8-2 and 8-3. These data were generated under the same conditions as the data presented by Delaney, O'Neil, et al. (1984) for all the polymict eucrite suites previously identified and may be compared directly with those results (Figures 8-4 and 8-5).

Most polymict eucrites have pyroxene and feldspar of

TABLE 8-4.—Modes of Victoria Land 83-series achondrites (A = aubrite, alab = alabandite, D = diogenite, db = daubreelite, E = eucrite, gyps = gypsum or anhydrite, nd = not detected, PA = polymict basaltic achondrite, tr = trace, unrep = unrepresentative sample).

Number	Oliv	Opx	Pig	Aug	Feld	SiO_2	Ilm	Chr	Phos	Troil
83009 A	0.4	99.0	0.2	nd	0.2	nd	nd	nd	nd	
83015 A	2.96	95.1	0.4	nd	1.04	nd	nd	nd	nd	
83212 PA	0.3	15.2	43.8	4.7	33.5	2.0	0.17	0.26	nd	tr
83227 PA	nd	19.2	28.5	6.2	41.7	3.7	0.31	0.50	0.05	tr
83228 PA	0.10	19.7	33.3	7.3	36.0	3.0	0.57	0.05	0.05	tr
83229 PA	nd	13.1	33.7	8.3	38.1	4.9	1.3	0.30	nd	0.3
83231 PA	nd	26.8	16.1	11.8	40.0	4.0	1.1	0.05	0.11	tr
83232 PA	0.25	24.6	14.2	12.8	39.3	6.6	1.05	tr	nd	0.4
83235 PA										
83236 E	nd	24.6	12.0	14.0	40.9	7.4	0.69	0.05	0.05	0.27
83237 PA										
83246 D	nd	98.2	0.63	0.21	nd	0.8	nd	0.21	nd	nd
83247 D	nd	98.7	nd	nd	0.1	1.0	nd	0.2	nd	nd
83251 PA	0.43	22.6	29.6	8.2	34.3	3.2	0.37	0.11	0.05	
83283 PA	nd	22.7	30.4	7.9	35.5	2.9	0.24	0.06	nd	nd

Number	Kam	Taen	Others	Area (mm^2)
83009 A	0.2		db, alab	
83015 A	0.3		db, alab	
83212 PA	nd	nd	unrep	92
83227 PA				
83228 PA	nd			103
83229 PA				48
83231 PA	nd	nd		107
83232 PA				91
83235 PA				
83236 E	nd	nd		117
83237 PA				
83246 D	nd	nd		118
83247 D	nd	nd		136
83251 PA			gyps	150
83283 PA	nd	nd		86.7

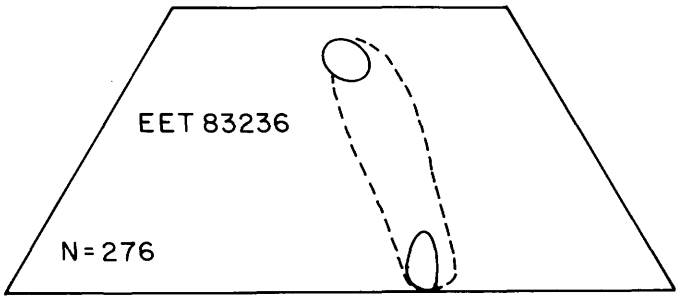

FIGURE 8-1.—Modal distribution of pyroxene composition in the eucrite EET83236, shown in a standard pyroxene quadrilateral. Dotted contour includes 95% of modal analyses; solid line includes 50% of analyses.

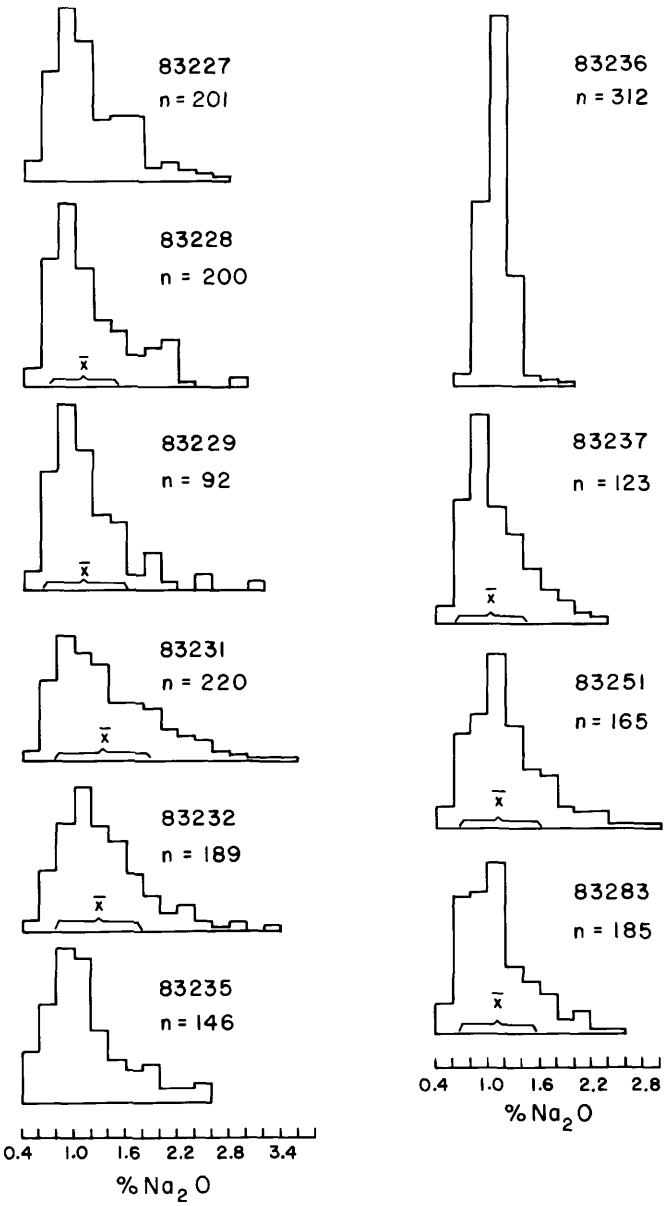

FIGURE 8-2.—Modal distribution of Na_2O in basaltic achondrite feldspar. Data are generated by a rapid electron microprobe modal technique and are of low precision. Area of each histogram totals 100%.

variable composition (Delaney, O'Neil, et al., 1984). The feldspar usually varies between An_{80} and An_{95} with most having compositions near An_{90} (Na_2O ~1.0–1.2% wt.). The pattern of feldspar composition distribution can be used to distinguish between the more sodic Yamato and the more calcic Victoria Land polymict eucrites (Delaney, O'Neil, et al., 1984), but among the Victoria Land suites only Allan Hills I and Allan Hills II may be distinguished on the basis of feldspar composition alone (Figure 8-5). The two Elephant Moraine groups recognized by Delaney, O'Neil, et al. (1984) have indistinguishable feldspar distributions (Figures 8-2 and 8-5). The pyroxene distributions in these meteorites are distinct, however, and are used to assign the samples to the appropriate suites.

Delaney, O'Neil, et al. (1984) described pyroxene from the Allan Hills I suite as dominated by homogeneous, eucritic pyroxene (i.e., lying on tie lines, between orthopyroxene and pigeonites ($En_{30-40}Wo_{1-6}$) and augites (~Wo_{40-45}) (Figure 8-4), with compositions appropriate for equilibration at 800°–900° C (Lindsley and Andersen, 1983). In addition, Allan Hills I contains minor zoned pigeonite of the "Pasamonte-type" (Takeda, 1979). Allan Hills II (78006) differs in having almost no zoned pigeonite. Instead, it contains about 2%–4% of homogeneous magnesian orthopyroxene (plus olivine), similar to diogenitic pyroxene, and small amounts of pyroxene with compositions between the eucritic and diogenitic ranges (Figure 8-4).

The two Elephant Moraine suites have different pyroxene distribution patterns (Figure 8-4). Elephant Moraine I is dominated by compositionally homogeneous pyroxene (En_{40-45}) with minor amounts of the other pyroxene components described by Takeda (1979) and Delaney, O'Neil, et al. (1984). This suite has a variety of pyroxene textural types in its mineral and lithic clasts. All but a few clasts appear to contain homogenized (with respect to Fe and Mg) pyroxene that reflects the influence of a late metamorphic overprint (Delaney et al., 1982). The Elephant Moraine II suite has much more variable pyroxene compositions. This suite has the textural and compositional variability of the most abundant non-Antarctic polymict achondrites, the howardites. All the textural types described by Takeda (1979) and Delaney, O'Neil, et al. (1984) occur in Elephant Moraine II, and the entire pyroxene compositional range from $En_{85}Wo_1$ to $En_{20}Wo_{40}$ is present. This suite differs from the howardites, however, as it contains in excess of 90% of eucritic components and only 2%–7% of diogenitic pyroxene. It, therefore, falls within the modal composition range of polymict eucrites as defined by Delaney, Takeda, and Prinz, 1983b, and Delaney, Takeda, Prinz, et al., 1983.

The 10 new polymict achondrites from the 1983 Elephant Moraine collections appear to fit into the two previously described suites from this locality. Three samples have distribution patterns for their pyroxene compositions that are similar to Elephant Moraine I. The modal pyroxene data for these samples are given in Figure 8-3. (EET83212 is omitted, as the original thin section studied is dominated by a single mafic clast and is, therefore, unrepresentative). The Elephant Moraine I suite is dominated by pyroxene compositions scattered about tie lines based at En_{40-45} Wo_{1-4} with a sparsely populated tail toward more magnesian compositions (Figure 8-4) (Delaney, Takeda, and Prinz, 1984). This distribution is seen in EET83235, 83237, and 83283 (Figure 8-3).

The modal compositions of many polymict eucrite samples are given by Delaney, Takeda, and Prinz (1984) and modes of the Elephant Moraine-83 series are given for comparison

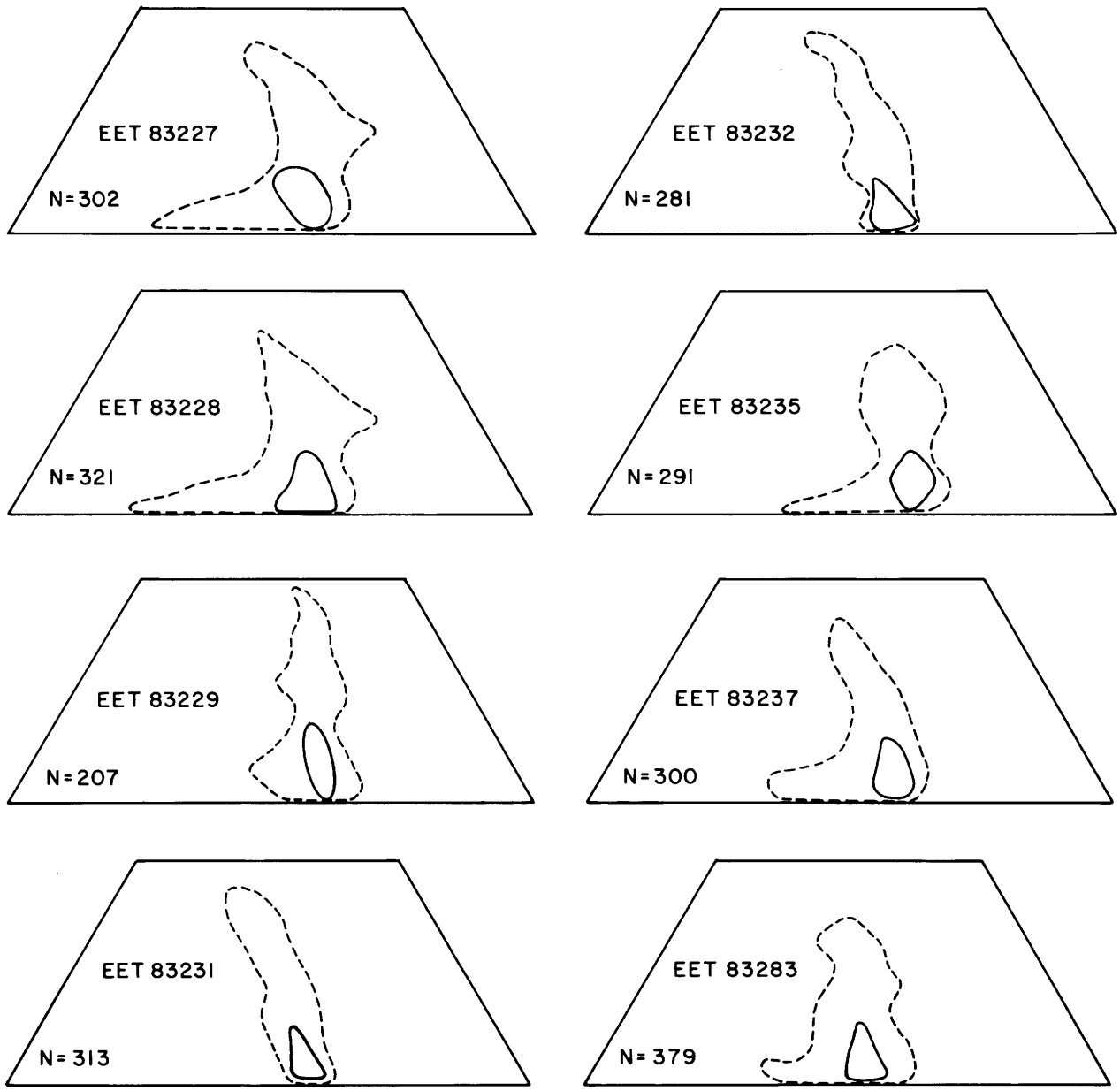

FIGURE 8-3.—Modal distribution of pyroxene compositions in the 1983 Elephant Moraine polymict eucrites. (Low precision data from automated modal program.) Contours as in Figure 8-1.

(Table 8-4). No major differences exist between the 83-series samples and the previously described samples (Delaney, Takeda, and Prinz, 1984). It is difficult to distinguish Elephant Moraine I and II on the basis of the modal abundance of the minerals alone (Table 8-4) although the distribution of pyroxene compositions is distinct in the two suites (Figures 8-3 and 8-4). The new samples extend the modal ranges of the two Elephant Moraine suites and confirm the indications that modal heterogeneity exists within each suite as seen previously within the Allan Hills I suite of polymict eucrites (Delaney, Takeda, and Prinz, 1984).

On the scale of a thin section there are detectable modal differences between different samples in all the Victoria Land suites, but when the distribution of mineral compositions within individual thin sections are compared, each suite has a coherent signature from sample to sample. The data presented for the Elephant Moraine 1983 samples, however, seem to lessen the differences between Elephant Moraine I and II. All of these samples may, therefore, be fragments of a single heterogeneous meteorite, with variable degrees of metamorphism detectable in different samples rather than two distinct meteorites, as previously suggested (Delaney et al., 1984c).

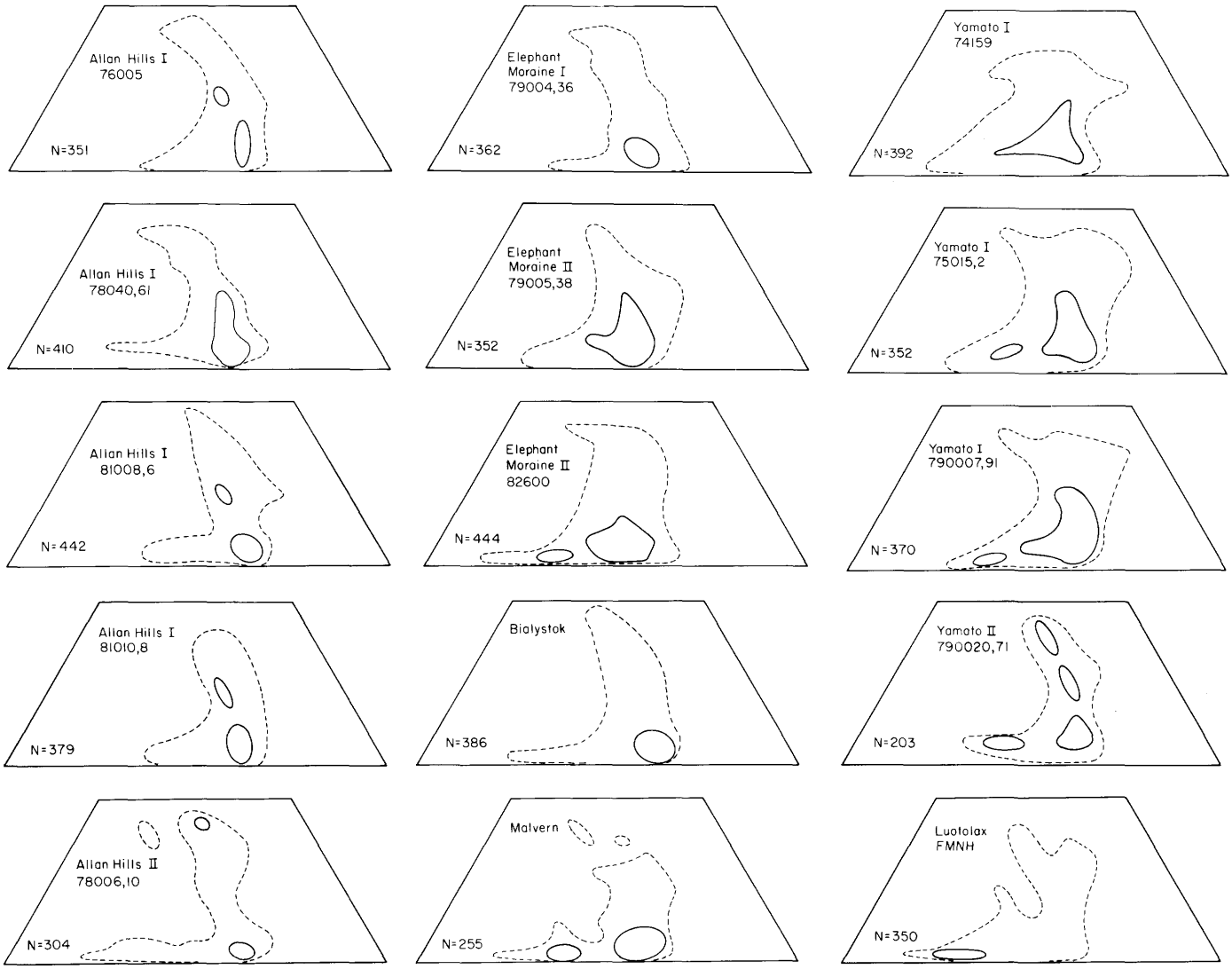

FIGURE 8-4.—Modal distribution of pyroxene compositions in suites of Antarctic polymict eucrites. Figure includes three non-Antarctic polymict achondrites for comparison. Contours as in Figure 8-1.

In general, all the Victoria Land samples are heterogenous when compared on the scale of a thin section (2.5 cm diameter), but comparison of chemical analyses of larger samples (e.g., Reid and Le Roex, 1984) may indicate that they are chemically uniform at the "hand sample" scale.

Because the polymict basaltic achondrites sample a continuum of breccias made up of several lithic components, the assignment of a rigidly constrained rock name is difficult. Two names are presently in common use: polymict eucrite and howardite. No consensus presently exists with regard to the usage of these terms, but polymict eucrites are dominated by clasts of various eucritic components while howardites contain additional pyroxenitic (or diogenitic) components. Using the nomenclature scheme of Delaney, Takeda, Prinz, et al. (1983) all the Elephant Moraine 83-series samples are "polymict eucrites." Using the Mason (1983b) scheme, the samples of Elephant Moraine II are "howarditic." Similar ambiguities (caused by the different nomenclature schemes) occur when the various nomenclatures are applied to other Victoria Land, Yamato, and non-Antarctic polymict basaltic achondrites.

Comparison of the Victoria Land polymict achondrites with the Yamato Mountains collection and the non-Antarctic specimens reveals several differences from suite to suite. All three collections of meteorites contain polymict achondrites containing a variety of clast rock types. In both of the major Antarctic collections (Yamato Mountains and Victoria Land) the vast majority of lithic clasts may be descibed as eucritic. Pyroxenitic material is rare or uncommon. The non-Antarctic collection, on the other hand, contains many meteorites with a large proportion of pyroxenitic clasts (10%–50% of the

original meteorite) while those dominated by eucritic material are less common. Only about 25% of all non-Antarctic polymict basaltic achondrites are dominated by eucritic clasts (i.e., contain more than 90% of eucritic material). The most characteristic lithic clast type in the Antarctic meteorites is unequilibrated eucritic, described by Takeda et al. (1978) as "Pasamonte-type." These clasts, which are usually less than 1 cm in diameter, are found in all the Antarctic suites but are not as common in the non-Antarctic collections. The non-Antarctic polymict breccias generally have not been characterized as well as the Antarctic samples. Small lithic clasts of unequilibrated eucritic material have been recognized in many non-Antarctic polymict achondrites but they do not appear to be as abundant or as large as in the Antarctic collections.

Ureilites

Two new ureilites (ALH83014 and EET83225) were collected in the 1983 field season. There are now 10 ureilites from Victoria Land (with a total mass of 7.6 kg). Modes of nine Victoria Land samples are given in Table 8-5 along with the mean mode and standard deviation of the non-Antarctic ureilites described by Berkley et al. (1980). The range of modal composition in the Victoria Land ureilites is essentially identical to that of non-Antarctic ureilites. EET83225 is one of the most pyroxene-rich, having similar olivine/pyroxene ratios to Dingo Pup Donga and the paired ureilite samples ALHA82106 and 82130. ALH83014 is a ureilite having a generally unshocked texture with euhedral to subhedral graphite crystals present in veins between the silicates (Figure 8-6). Texturally and modally (Table 8-5) ALH83014 is similar to ALHA78019. It has less metal + sulfide + graphite, however, and the cores of silicate mineral grains are more magnesian than in 78019. ALH83014 may be the second relatively unshocked ureilite found with euhedral graphite blades but pairing with ALH78019 may be demonstrated by further work. Detailed chemical and petrographic study of these two samples should provide useful constraints on the origin of the intensely shocked ureilites. Olivine cores in 83014 are generally Fo_{81-83} with forsterite rims (Fo_{90-98}) while pigeonite cores are $En_{76-78}Wo_{8-9}$.

EET83225 has a well-developed preferred orientation of its olivine and pigeonite grains with carbonaceous material, including diamond, limited to the grain boundaries. Unlike other pyroxene-rich ureilites (e.g., ALHA82106 and 82130) EET83225 does not contain any augitic pyroxene. None of the Victoria Land ureilites resembles the augitic ureilite Yamato 74130 described by Takeda et al. (1979). Some of the Victoria Land ureilites contain only pigeonitic pyroxene whereas others have more variable pyroxene compositions indicating that some exsolution and possibly some inversion to orthopyroxene occurred. (Note that the assignment of pyroxene "polymorphs" in Table 8-4 is based only on composition and does not imply that three polymorphs have been identified crystallographically. Indeed some of the "pigeonite" identified by this program may represent analyses of overlapping orthopyroxene and augite. See Delaney, O'Neil, et al. (1984) for more detail of methods applied.)

Compositional variation of the olivine in the Victoria Land ureilites is summarized in Figure 8-7. These data are of low precision as they are generated by electron microprobe modal analysis but they are consistent with published analyses and provide an unbiased estimate of the modal olivine compositional range. Only two of the analyzed ureilites have the same olivine distribution pattern (ALHA82106, 82130) suggesting that these are the only paired samples in this group (Mason, 1984). Study of the distribution of pyroxene compositions is in progress. Ureilites generally have olivine in the Fo_{80} to Fo_{90} range with a few more magnesian compositions present. These patterns reflect the variable reduction of iron-bearing olivine to forsterite plus metal that is typical of these meteorites. Reckling Peak 80239 has a distinctive bimodal distribution with about 25% of its olivine analyses more magnesian than Fo_{95}. This distribution suggests that evidence of reduction reactions is particularly well preserved in this sample. The paired samples, Allan Hills 82106 and 82130, have more magnesian olivine but it is not clear if these compositions were formed by the late redox processes that are typical of ureilites rather than early magmatic reduction processes. The high augite content of these samples (Table 8-4) is, however, consistent with their position on the reverse fractionation trend described by Goodrich and Berkley (1985). They defined Fe-depletion in later formed silicates as a result of reduction by magmatic graphite.

Subhedral-euhedral graphite grains have been described in only two ureilites (ALHA78019 and ALH83014) although all ureilites have interstitial graphite, often containing diamond or lonsdaleite (Berkley and Jones, 1982). The presence of euhedral graphite grains in ALHA78019 has been interpreted as representing crystallization of magmatic carbon. Similarly the presence of round inclusions in olivine, containing kamacite, troilite, and cohenite (Fe_3C), in at least four Victoria Land ureilites (ALHA78019, 77257, 78262, and RKPA 82506) is also believed to support crystallization from a carbon saturated silicate melt (Berkley and Goodrich, 1985). Study of these and other minor phases in ureilites (e.g. Berkley and Goodrich, 1985; Goodrich and Berkley, 1985) should provide useful insight into these meteorites.

Aubrites

The one aubrite found between 1976 and 1982, Allan Hills 78113, is a polymict breccia showing similarities to Cumberland Falls and containing chondritic inclusions that have been described as F-chondritic (Verkouteren and Lipschutz, 1983), as unequilibrated enstatite chondrites (Prinz et al., 1984), and as reduced LL chondrites (Kallemeyn and Wasson, 1985). The

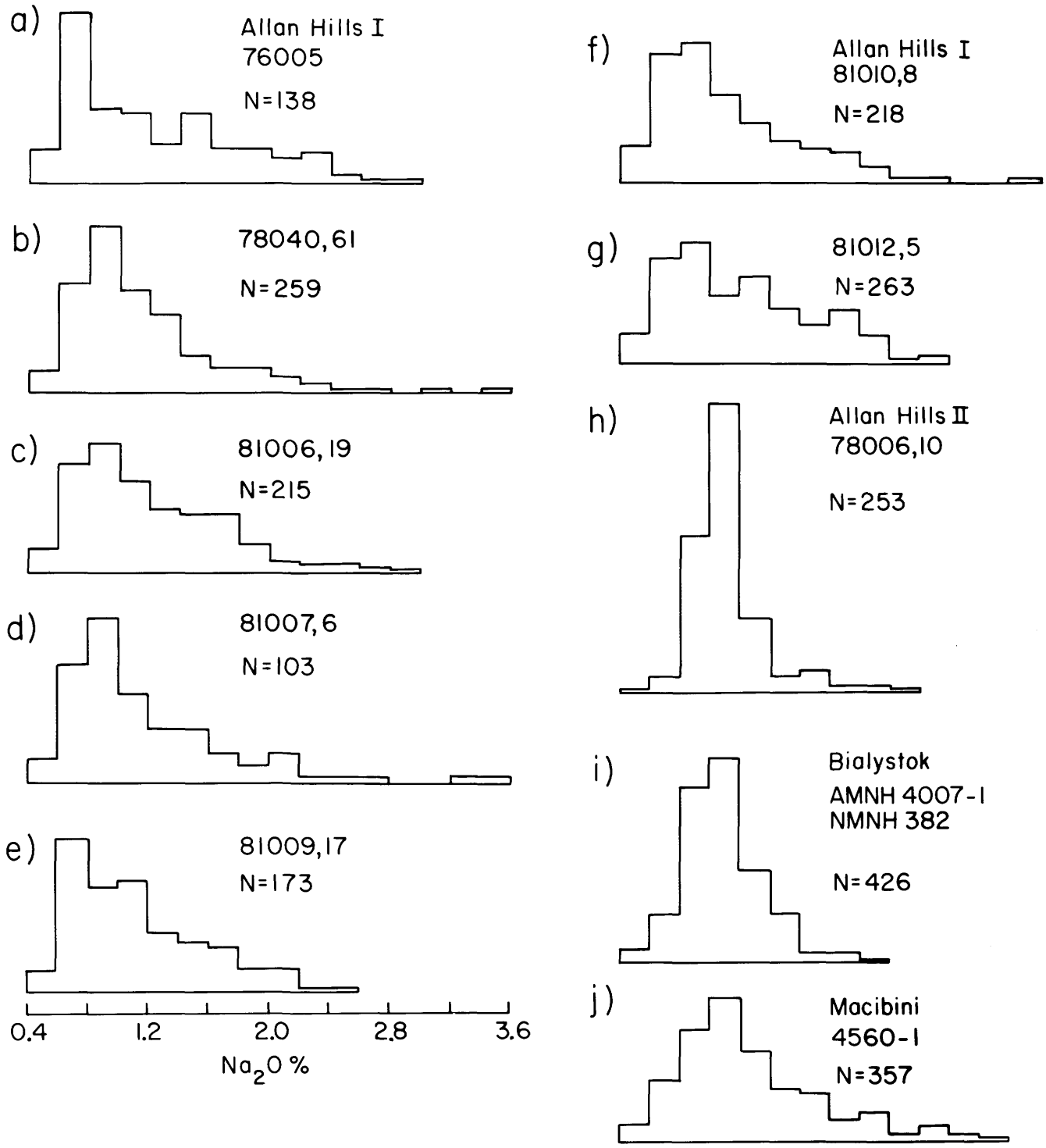

FIGURE 8-5.—Modal distribution of feldspar composition in suites of Antarctic polymict eucrites. Area of histogram is 100%. (Scale bars are the same for all figures, with the left margin at 0.4 in all cases.)

aubritic host was described by Score et al. (1982) and Watters and Prinz (1979). Volatile trace elements were analyzed by Biswas et al. (1981) and Verkouteren and Lipschutz (1983). The mineralogy of the ALHA 78113 host is typical of aubrites.

Two new aubritic samples from Allan Hills were identified in the 1983 collection. These samples (ALHA83009 and 83015) are quite similar to each other but appear to be distinct from ALHA78113.

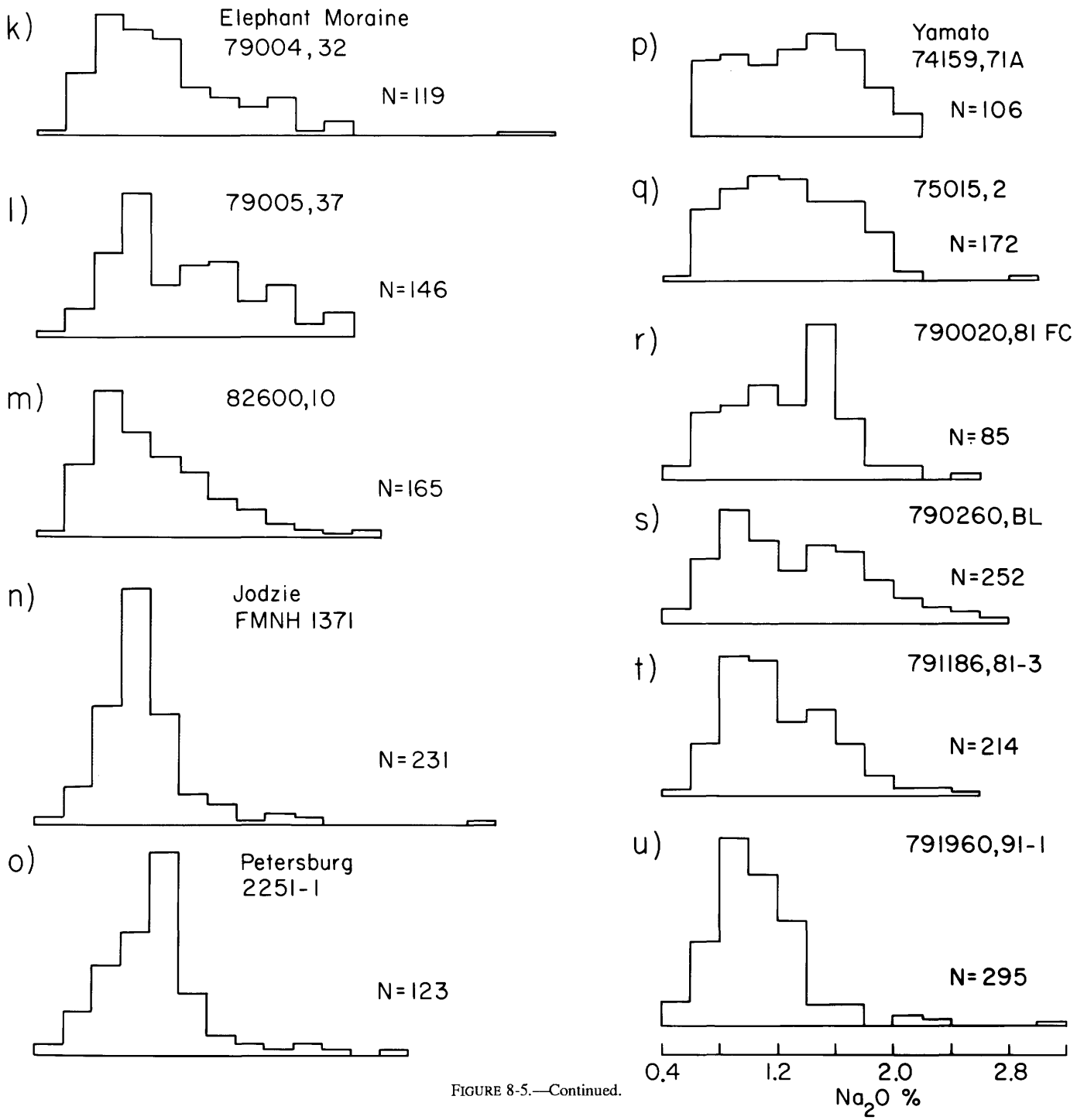

FIGURE 8-5.—Continued.

Summary

The Victoria Land achondrites have provided impetus to research on achondritic meteorites in general, by providing sufficient samples of uncommon meteorite types that detailed study is now easier. Initially, many Antarctic achondrites appeared to be different from the non-Antarctic collections but, as more research is published and more Antarctic meteorites are found, it is clear that the Antarctic and non-Antarctic collections are sampling similar populations of meteorites.

The basaltic achondrite samples increase the known diversity of these meteorites. These meteorites contain clasts of many rock types ranging from magnesian orthopyroxenites ($En_{70-85}Wo_1$) with minor olivine (as magnesian as Fo_{90}) to very iron rich mafic clasts dominated by $En_{30}Wo_{15-30}$ pigeonites and

TABLE 8-5.—Modes of Victoria Land ureilites (nd = not detected, tr = trace. Non-Antarctic data from Berkley et al., 1980.)

Number	Oliv	Opx	Pig	Aug	Feld	SiO_2	Sulf	Metal	Other	Area mm^2	Number points	P.t.s. #[1]
								Combined				
83225	52.1	2.9	40.8	nd	nd	0.1		4.1		60	725	LIB
83014	85.2	1.5	11.3	nd	nd	0.1		1.9		64	879	
82506	67.1	3.6	24.3	nd	nd	0.5		4.5		180	641	,25
82130	46.1	29.2	11.9	7.6	nd	nd		5.1		154	860	,10
82106	47.9	31.8	8.9	6.4	0.1?	nd		5.0		109	990	, 6
81101	58.9	17.1	13.8	0.24	nd	0.5		8.9		162	847	,11
80239	59.0	7.1	29.0	nd	tr?	nd		4.9		74	888	, 6
78019	76.0	4.6	8.8	0.3	nd	nd		10.6		54	828	,15
77257	81.5	7.6	5.8	0.1	0.1?	nd		4.9		36	717	,42
Non-Antarctic ureilites:												
Mean	65.9		31.9		–	0.1	0.9	1.2	–	–	–	–
S.D.	10.4		10.6		–	–	0.6	1.1	–	–	–	–

[1]Catalogue number of polished thin section examined in this study; LIB = Library section.

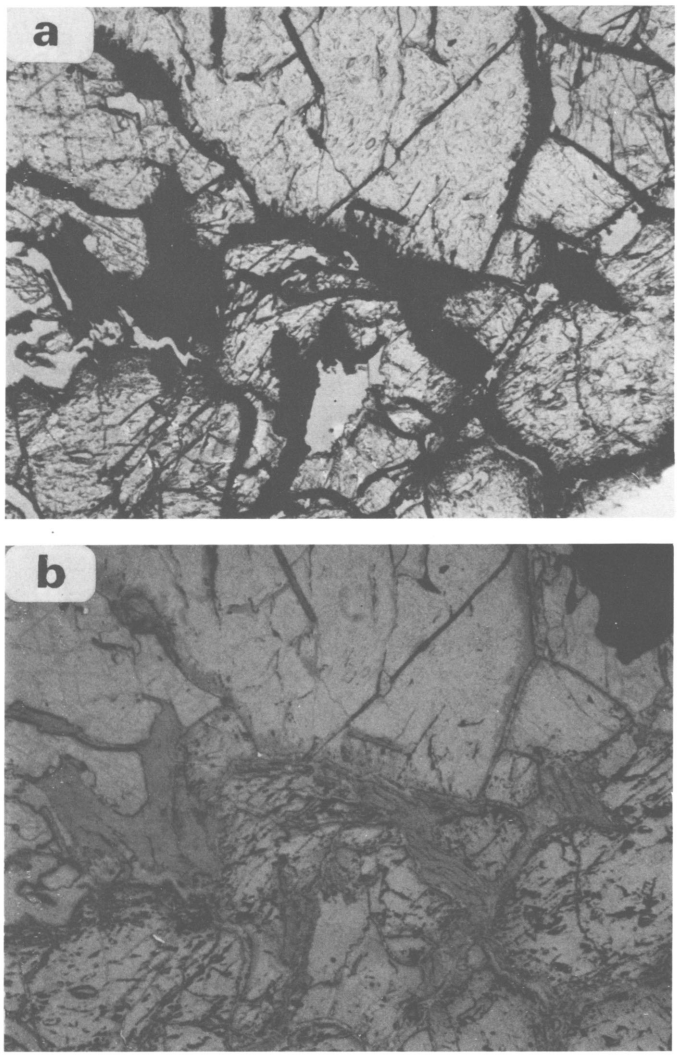

FIGURE 8-6.—Euhedral to subhedral graphite crystals in ALH83014: *a*, transmitted light; *b*, reflected light. Long dimension of photographs is ~2 mm.

augites. The clasts described in numerous studies document continuous trends of Fe/Mg increase with increasing modal abundance of pigeonite, augite, feldspar, and silica. These trends appear to reflect general trends of solid-liquid fractionation on the basaltic achondrite parent body that are independent of the present state of brecciation and mixing of the known samples. Metamorphism is known to have modified the compositions of lithic clasts in many polymict samples from Victoria Land and in most eucrites, but no systematic studies have yet tried to distinguish between unmodified igneous clasts and metamorphosed clasts. Detailed study of the original trends of igneous fractionation from clast to clast requires that metamorphosed clasts be eliminated from this type of study. Similarly, impact-melt clasts in these meteorites have received little attention and definitive tests to distinguish between impact-generated clasts and original igneous clasts are not available. The small samples of the polymict basaltic achondrites in the non-Antarctic collections were generally insufficient for these types of studies to be completed, but the large number of Victoria Land samples presently available makes more complete and detailed study possible. In particular, the identification of large unbrecciated lithic clasts in these breccias is of great importance for the study of rock types that differ from the typical eucrites and diogenites.

The Antarctic ureilite collections have more than doubled the number of samples available and have provided examples of previously unknown types that constrain models of ureilite origin more closely. In general, the popular model of a cumulus origin (Berkley et al., 1980) is supported by evidence from the Victoria Land samples, but controversy about the relationships between the silicate and carbonaceous fractions continues.

The Antarctic aubrites do not differ greatly from the non-Antarctic collection but study of the dark inclusions in these meteorites is revealing chondritic material unlike the previously known chondrite groups. Further study should distinguish between the competing hypotheses that these

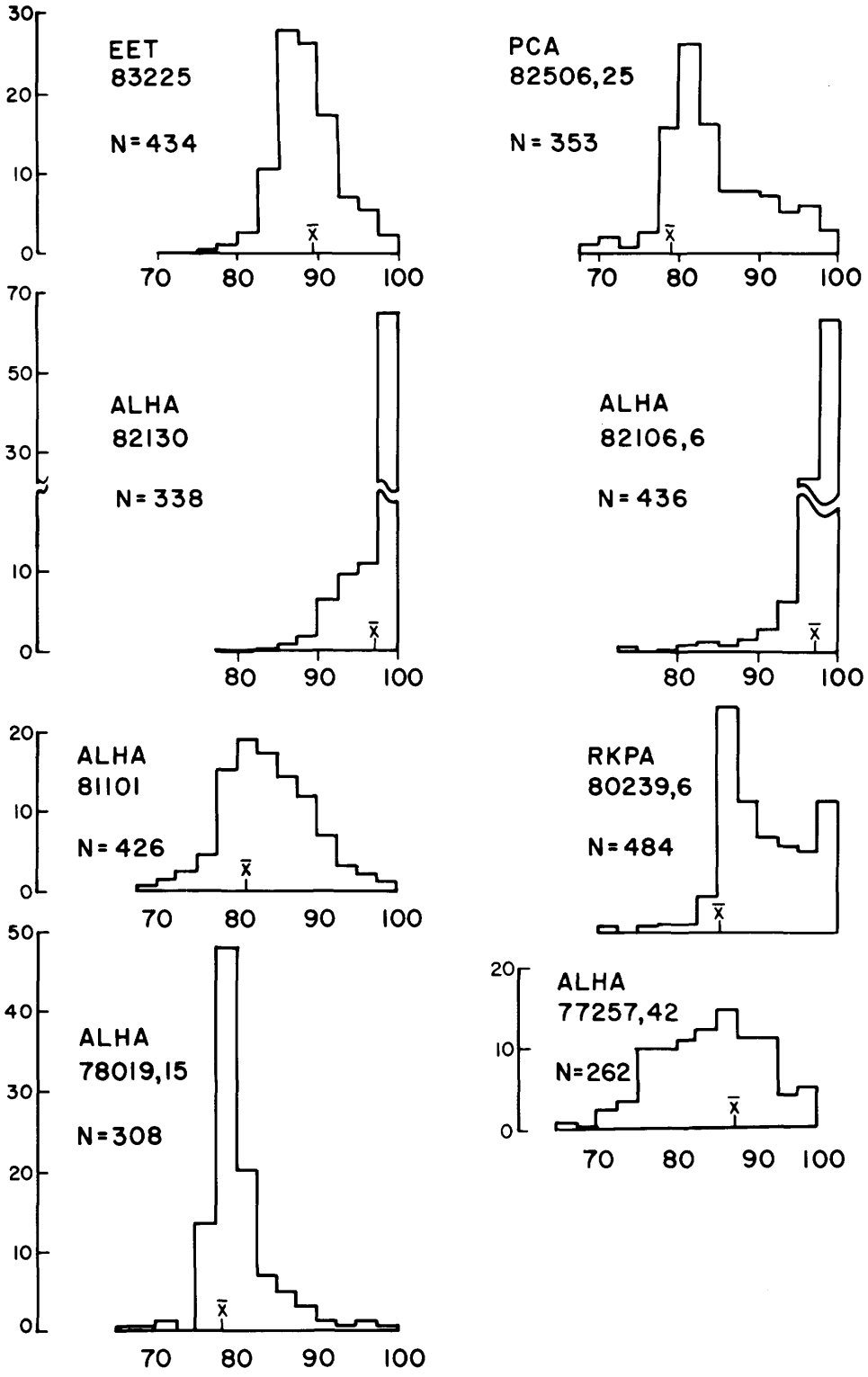

FIGURE 8-7.—Modal distribution of olivine compositions (mole % forsterite) in Victoria Land ureilites. Data are of low precision but provide a consistent criterion of comparison for these meteorites. Area of histogram is 100%.

inclusions represent a new type of chondrite, or that they are actually inclusions of ordinary chondritic material that was subjected to metamorphism and metasomatism after incorporation in an aubritic host.

The discovery of unusual material in the Antarctic achondrites is prompting increasing study of non-Antarctic collections with the result that previously unrecognized material is being identified. With the assured supply of carefully sampled achondrites from Antarctica, the next decades of research on achondritic meteorites should prove very rewarding and fruitful.

Literature Cited

Berkley, J.L., and C.A. Goodrich
1985. Cohenite-bearing Metallic Spherules in Ureilites: Petrology and Implications. In *Lunar and Planetary Sciences XVI,* pages 49–50. Houston: Lunar and Planetary Institute.

Berkley, J.L., and J.H. Jones
1982. Primary Igneous Carbon in Ureilites: Petrological Implications. *Journal of Geophysical Research,* 87(supplement):A353–A364.

Berkley, J.L., G.J. Taylor, K. Keil, G.E. Harlow, and M. Prinz
1980. The Nature and Origin of Ureilites. *Geochimica et Cosmochimica Acta,* 44:1579–1597.

Biswas, S., T.M. Walsh, H.T. Ngo, and M.E. Lipschutz
1981. Trace Elements of Selected Antartic Meteorites—II: Comparison with Non-Antarctic Specimens. *Memoirs of the National Institute of Polar Research* (Japan), special issue, 20:221–228.

Bunch, T.E.
1976. Petrography and Petrology of Basaltic Achondrite Polymict Breccias (Howardites). In *Proceedings of the Sixth Lunar and Planetary Science Conference,* pages 469–492.

Delaney, J.S.
1984. Why Did So Many Polymict Eucrites Land and Survive Only in Antarctica? In *Lunar and Planetary Science XV,* pages 206–207. Houston: Lunar and Planetary Institute.

Delaney, J.S., C. O'Neil, C.E. Nehru, M. Prinz, C. Stokes, H. Kojima, and K. Yanai
1984. The Classification and Reconnaissance Petrography of Basaltic Achondrites from the Yamato 1979 Collection Including Pigeonite Cumulate Eucrites, a New Group. *Memoirs of the National Institute of Polar Research* (Japan), special issue, 35:53–80.

Delaney, J.S., M. Prinz, C.E. Nehru, and G.E. Harlow
1981. A New Basalt Group from Howardites: Mineral Chemistry and Relationships with Basaltic Achondrites. In *Lunar and Planetary Science XII,* pages 211–213. Houston: Lunar and Planetary Institute.

Delaney, J.S., M. Prinz, C.E. Nehru, and C. O'Neil
1982. The Polymict Eucrites Elephant Moraine A79004 and A79011 and the Regolith History of a Basaltic Achondrite Parent Body. In *Journal of Geophysical Research,* supplement, 87:A339–A352.

Delaney, J.S., M. Prinz, C.E. Nehru, and C.P. Stokes
1984. Allan Hills A81001, Cumulate Eucrites and Black Clasts from Polymict Eucrites. In *Lunar and Planetary Science XV,* pages 212–213. Houston: Lunar and Planetary Institute.

Delaney, J.S., H. Takeda, and M. Prinz
1983a. Modal Comparison of Yamato and Allan Hills Polymict Eucrites. *Memoirs of the National Institute of Polar Research* (Japan), special issue, 30:226–233.
1983b. Reply to B. Mason: "Definition of a Howardite." *Meteoritics,* 18:247–248.
1984. The Polymict Eucrites. *Journal of Geophysical Research,* supplement, 89:C251–C288.

Delaney, J.S., H. Takeda, M. Prinz, C.E. Nehru, and G.E. Harlow
1983. The Nomenclature of Polymict Basaltic Achondrites. *Meteoritics,* 18:103–111.

Dymek, R.F., A.L. Albee, A.A. Chodos, and G.J. Wasserburg
1976. Petrography of Isotopically-dated Clasts in the Kapoeta Howardite and Petrologic Constraints on the Evolution of Its Parent Body. *Geochimica et Cosmochimica Acta,* 40:1115–1130.

Fukuoka, T.
1984. Comparison of Chemical Compositions of Yamato Polymict Eucrites. *Meteoritics,* 19:227.

Goodrich, C.A., and J.L. Berkley
1985. Minor Elements in Ureilites: Evidence for Reverse Fractionation and Interstitial Silicate Liquid. In *Lunar and Planetary Science XVI,* pages 280–281. Houston: Lunar and Planetary Institute.

Hey, M.H.
1966. *Catalogue of Meteorites.* lxviii + 637 pages. London: British Museum (Natural History).

Hutchison, R., A.W.R. Bevan, and J.M. Hall
1977. *Appendix to the Catalogue of Meteorites.* xxvii + 297 pages. London: British Museum (Natural History).

Kallemeyn, G.W., and J.T. Wasson
1985. The Compositional Classification of Chondrites: IV Ungrouped Chondritic Meteorites and Clasts. *Geochimica et Cosmochimica Acta,* 49:261–270.

Lindsley, D.H., and D.J. Andersen
1983. A Two-Pyroxene Thermometer. *Journal of Geophysical Research,* supplement, 88:A887–A907.

Marvin, U.B.
1984. Meteorite Distributions on the Main Icefield of the Allan Hills Region, Antarctica. *Meteoritics,* 19:265–266.

Mason, B.
1983a. [Description.] *Antarctica Meteorite Newsletter,* 6:7.
1983b. Definition of a Howardite. *Meteoritics,* 18:245.
1984. [Description.] *Antarctic Meteoritic Newsletter,* 7:10.

Miyamoto, M., H. Takeda, and K. Yanai
1978. Yamato Achondrite Polymict Breccias. *Memoirs of the National Institute of Research* (Japan), special issue, 8:185–197.

Olsen, E.J., A. Noonan, K. Fredriksson, E. Jarosewich, and G. Moreland
1978. Eleven New Meteorites from Antarctica, 1976–1977. *Meteoritics,* 13:209–225.

Prinz, M., C.E. Nehru, M.K. Weisberg, and J.S. Delaney
1984. Type 3 Enstatite Chondrites: A Newly Recognized Group of Unequilibrated Enstatite Chondrites (UEC's). In *Lunar and Planetary Science XV,* pages 653–654. Houston: Lunar and Planetary Institute.

Reid, A.M., and A.P. Le Roex
1984. Compositions of 7 Allan Hills Polymict Eucrites and One Diogenite. *Meteoritics,* 19:299.

Schultz, L., and M. Freundel
1984. Terrestrial Ages of Antarctic Meteorites. *Meteoritics,* 19:310.

Score, R., T.V.V. King, C.M. Schwarz, A.M. Reid, and B. Mason
1982. Descriptions of Stony Meteorites. *In* U.B. Marvin and B. Mason, editors, Catalogue of Meteorites from Victoria Land, Antarctica, 1978–1980. *Smithsonian Contributions to the Earth Sciences,* 24:19–48.

Scott, E.R.D.
1984. Pairing of Meteorites Found in Victoria Land, Antarctica. *Memoirs of the National Institute of Polar Research* (Japan), special issue, 35:102–125.

Simon, S.B., and J.J. Papike
1983. Petrology of Igneous Lithic Clasts from Polymict Eucrites ALHA 76005 and ALHA 77302. *Meteoritics,* 18:35–50.

Takeda, H.
1979. A Layered Crust Model of a Howardite Parent Body. *Icarus,*

40:445–470.

Takeda, H., M.B. Duke, T. Ishii, H. Haramura, and K. Yanai
1979. Some Unique Meteorites Found in Antarctica and Their Relation to Asteroids. *Memoirs of the National Institute of Polar Research* (Japan), special issue, 15:54–76.

Takeda, H., M. Miyamoto, K. Yanai, and H. Haramura
1978. A Preliminary Examination of the Yamato-74 Achondrites. *Memoirs of the National Institute of Polar Research* (Japan), special issue, 8:170–184.

Takeda, H. and H. Mori
1984. The Diogenite-Eucrite Links and the Crystallization History of a Crust of Their Parent Body. *Journal of Geophysical Research,* supplement, 90:C636–C648.

Takeda, H., H. Mori, and K. Yanai
1981. Mineralogy of the Yamato Diogenites As Possible Pieces of a Single Fall. *Memoirs of the National Institute of Polar Research* (Japan), special issue, 20:81–99.

Treiman, A.H.
1984. Polymict Eucrite ALHA 81011: Equilibrated Clasts in a Glassy Matrix. *Meteoritics,* 19:323–324.

Treiman, A.H., and M.J. Drake
1984. Basaltic Volcanism on the Eucrite Parent Body: Petrology and Phase Equilibria of ALHA 80102 and the Discovery of Ferroan Troctolite. In *Lunar and Planetary Science XV,* pages 862–863. Houston: Lunar and Planetary Institute.

Verkouteren, R.M., and M.E. Lipschutz
1983. Cumberland Falls Achondritic Inclusions—II: Trace Elements of Forsterite Chondrites and Meteorites of Similar Redox State. *Geochimica et Cosmochimica Acta,* 47:1625–1633.

Watters, T.R., and M. Prinz
1979. Aubrites: Their Origins and Relationship to Enstatite Chondrites. In *Proceedings of the Tenth Lunar and Planetary Science Conference,* pages 1073–1093.

Weber, H.W. O. Braun, L. Schultz, and F. Begemann
1982. The Noble Gases in Antarctic and Other Meteorites. *Zeitschritt fur Naturforsch,* 38A:267–272.

9. Antarctic Carbonaceous Chondrites: New Opportunities for Research

Harry Y. McSween, Jr.

Introduction

Milestones in the understanding of carbonaceous chondrites reached previously can be traced in a series of reviews on the subject (Mason, 1963; Hayes, 1967; Mason, 1971; Nagy, 1975; McSween, 1979a). One might logically expect that this paper on Antarctic carbonaceous chondrites, most of which have been found since the last review article was published, should provide an updated account of new discoveries and insights. This, unfortunately, is not true, because this subset of carbonaceous chondrites has not yet been thoroughly studied. The Antarctic meteorite bonanza is just too vast to be assimilated quickly, and other classes of meteorites (especially the achondrites) have received more attention. Those major contributions that have been made during the last few years are derived mainly from studies of non-Antarctic carbonaceous chondrites.

The intent of this paper is to describe what kinds of carbonaceous meteorites are available in the Antarctic collections of the United States and Japan, and to summarize briefly what research has been done. Some new data that bear on the question of pairings among Antarctic carbonaceous chondrites will also be presented. The importance of this paper really lies in what it does *not* say—the still available research opportunities that these meteorites offer.

Classification of Carbonaceous Chondrites

The classification used for carbonaceous chondrites is somewhat unwieldy and has evolved in a number of steps. Van Schmus and Wood (1967) distinguished C1, C2, and C3 chondrites based on petrographic and chemical characteristics. This sequence supposedly reflected a sort of decreasing "primitiveness," distinct from the grade of thermal metamorphism described by petrologic types 4 to 6. Van Schmus and Hayes (1974) recognized two groups of C3 chondrites, which they called the Ornans (now abbreviated CO3) and Vigarano (CV3) subtypes. Wasson (1974) stressed that C1, C2, and C3 chondrites were not an isochemical group and devised the names CI (Ivuna type, formerly C1) and CM (Mighei type, formerly C2) to parallel the classification of C3 chondrites into CV and CO groups. McSween (1979a) accepted Wasson's chemical distinctions and added another: CR (Renazzo group). He also suggested a reinterpretation of petrologic types 3 to 1 to reflect increasing degrees of aqueous alteration. A few carbonaceous chondrites have been thermally recrystallized and are assigned to petrologic type 4.

In Table 9-1 are listed carbonaceous chondrites recognized in the Antarctic collections of the Unites States (Victoria Land) and Japan (Queen Maud Land) through 1984. Included are classification, original weights, and the best descriptive references for each. In many cases no descriptive references are available, except in the original newsletter announcements, which are not referenced here. Classifications are the generally accepted assignments published in the newsletters of the Antarctic Meteorite Working Group and the National Institute of Polar Research. Recrystallized chondrites classified as C4 are difficult to assign to a specific group, even if adequate chemical data are available.

Petrologic, Chemical, and Isotopic Studies of Antarctic Carbonaceous Chondrites

CM2 Chondrites

Most of the work on CM chondrites has been done on Yamato samples; the Allan Hills samples are almost untouched. Brief petrographic descriptions are available for Y-74641, Y-74642, Y-74662 (Mason and Yanai, 1983), Y-75293, Y-790123 (Ikeda, 1983a), and Y-793321, Y-790003, Y-791198, Y-791824, B-7904 (Kojima et al., 1984). McSween (1979b) also provided some petrographic data on ALHA77306, and Steele et al. (1985) studied cathodoluminescence zoning of olivines in B-7904. Although some petrographic differences are apparent, these meteorites do not expand the limits of primary petrographic variation already known from non-

Harry Y. McSween, Jr., Department of Geological Sciences, University of Tennessee, Knoxville, Tennessee 37996.

TABLE 9-1.—Antarctic carbonaceous chondrites.

Sample	Classification	Weight (g)	Best descriptive references
Meteorites from Victoria Land			
ALHA77306	CM2	19.9	McSween (1979b)
ALHA78261	CM2	5.1	
ALHA81002	CM2	14.0	
ALHA81004	CM2	4.7	
ALHA81312	CM2	0.7	
ALH82100	CM2	24.3	
ALH82131	CM2	1.0	
ALH83016	CM2	4.1	
ALH83100	CM2	434.6	
ALH83102	CM2	1240.8	
EET83224	CM2	8.6	
EET83226	CM2	33.1	
EET83250	CM2	11.5	
ALH84029	CM2	119.8	
ALH84030	CM2	6.2	
ALH84031	CM2	12.5	
ALH84032	CM2	7.9	
ALH84033	CM2	60.4	
ALH84034	CM2	44.1	
ALH84042	CM2	51.2	
ALH84044	CM2	147.4	
ALHA77003	C03	779.6	Ikeda (1982)
ALHA77029	C03	1.4	McKinley and Keil (1984)
ALHA77307	C03	181.3	Nagahara and Kushiro (1982)
ALH82101	C03	29.1	
RKPA80241	CV3	0.1	Scott (1984)
ALHA81003	CV3	10.1	
ALHA81258	CV3	1.1	
ALHA84028	CV3	735.9	
ALH82135	C4	12.1	Scott (1985)
PCA82500	C4	90.9	Scott and Taylor (1985)

TABLE 9-1.—Continued.

Sample	Classification	Weight (g)	Best descriptive references
Meteorites from Queen Maud Land			
Y-74641	CM2	4.5	Mason and Yanai (1983)
Y-74642	CM2	10.6	Mason and Yanai (1983)
Y-74662	CM2	151	Ikeda (1983a)
Y-75260	CM2	4.0	
Y-75293	CM2	8.1	Ikeda (1983a)
B-7904	CM2	1234	Kojima et al. (1984)
Y-790003	CM2	4.3	
Y-790032	CM2	6.1	
Y-790112	CM2	24.0	
Y-790123	CM2	6.8	Ikeda (1983)
Y-791198	CM2	179.8	Kojima et al. (1984)
Y-791824	CM2	23.3	Kojima et al. (1984)
Y-793331	CM2	379.3	
Y-793332	CM2		
Y-74135	C03	7.7	Kojima et al. (1984)
Y-790992	C03*		
Y-791717	C03	25,3332	Kojima et al. (1984)
Y-75260	CV3	4.0	
Y-6903	CV4	150	Okada and Shima (1979); Scott (1985)
Y-790112	CR2	24.0	
Y-793495	CR2	45.0	

*Y-790992 is listed only as a C3, but I have assigned it to C03 based on inspection of a thin section in the collection of the National Institute of Polar Research. Ikeda (1983a) also noted that this meteorite was similar to ALHA77003.

Antarctic CM chondrites.

High-resolution electron microscope studies of the matrices of ALHA77306 (McKee and Moore, 1980) Y-74662 (Akai, 1982), Y-793321, B-7904 (Akai, 1984) and Y-791198 (Akai and Kanno, 1985) have been reported. These studies have identified a bewildering variety of phyllosilicates with platy, tubular, and poorly crystalline structures, much like those found in non-Antarctic CM chondrites. Ikeda (1983a) reported the chemical compositions of matrix phyllosilicates in Y-790123, Y-75293, and Y-74662 to be similar to other published analyses. Fujimura et al. (1982) documented preferred orientations of phyllosilicates in Y-74642 and Y-74662 by x-ray pole figure goniometry, indicating anisotropic deformation of these meteorites.

Bulk chemical data are available for Y-74642, Y-74662, Y-790032, and Y-791198 (Haramura et al., 1983). Trace element data for Y-74662 were determined by Knab and Hintenberger (1978). Carbon and sulfur determinations have been reported for Y-76442 and ALHA77306 (Gibson and Yanai, 1979) and B-7904, Y-791824, Y-793321 (Gibson et al., 1984). Carbon and nitrogen abundances in Y-791198 were published by Shimoyana et al. (1985). Major element concentrations, including sulfur, are near normal CM levels, but depletions of carbon in some meteorites may reflect exposure to liquid water in the Antarctic environment.

The apparent leaching of carbon in some CM chondrites is a disturbing finding, especially for what it portends for studies of organic compounds. ALHA77306 has significantly lower amino acid concentrations than non-Antarctic CM chondrites (Cronin et al., 1979), and Y-7891824, Y-793321, and B-7904 contain practically none of these compounds (Gibson et al., 1984; Shimoyama and Harada, 1984). However, amino acids in Y-74662 and Y-79118 are at higher concentrations (Shimoyama et al., 1979, 1985). Aspartic acid, serine, glycine, alanine, theonine, glutamic acid, valine, norvaline, and leucine have been identified, as well as aromatic compounds from pyrolysis experiments (Holzer and Oro, 1979; Murae et al., 1983, 1984).

Stable light isotope (N, C, H) compositions reported for Y-790003 and Y-790032 (Grady et al., 1983) indicate that Y-790003 is highly unusual. It is characterized by enrichment of heavy carbon and nitrogen, but not deuterium, and falls outside the known ranges for CM chondrites. Isotopic abundances of noble gases (He, Ne, Ar, Kr, Xe) in B-7904, Y-74662, and Y-791198 are similar to other non-Antarctic CM chondrites (Nagao et al., 1984; 1985); however, a new component of Kr and Xe has been reported in B-7904. No data are available on cosmogenic nuclides.

Magnetic studies of Y-74662 (Nagata, 1980; Brecher, 1980) confirmed its CM2 classification. The magnetic properties of ALHA77306 have been used to estimate its magnetite content at less than 0.8 weight percent (Hyman and Rowe, 1979).

CR2 Chondrites

From inspection of thin sections in the collection at the National Institute of Polar Research in 1982, the author tentatively classified Y-790112 and Y-793495 as CR chondrites, as subsequently reported in the *National Institute of Polar Research* special issue of 1982. Oxygen isotopic analysis of Y-790112 (Clayton et al., 1984) has confirmed this classification. A bulk chemical analysis of this meteorite was given by Haramura et al. (1983). Light element stable isotope analysis is also consistent with the CR assignment (Grady et al., 1983), though data from Y-790112 indicate the CR group is highly variable in its isotopic character. Nothing is known about Y-793495. This is a particularly important pair of meteorites, because so little is known about the CR group with only two non-Antarctic members.

CO3 Chondrites

The two large CO chondrites in the Allan Hills collections (ALHA77003 and 77307) have understandably received most of the attention accorded to this group, although massive Y-791717 offers an exciting opportunity. Petrographic descriptions of ALHA77003 (Ikeda, 1982), ALHA77307 (Nagahara and Kushiro, 1982), and ALHA77029 (McKinley and Keil, 1984) have been published. The latter was found in a collection of pebble-sized meteorites. Scott et al. (1981) and Scott (1984) provided some additional petrographic data on all three meteorites. ALHA77307 appears to be the least metamorphosed of the three chondrites. Brief petrographic descriptions and studies of the alteration of Y-791717 and Y-74135 were presented by Kojima et al. (1984).

Bulk chemical analyses have been performed for ALHA77003 (Rhodes and Fulton, 1980; Jarosewich, 1980; Kallemeyn and Wasson, 1982a), ALHA77029 (Kallemeyn and Wasson, 1982a), ALHA77307 (Biswas et al., 1981; Kallemeyn and Wasson, 1982a), and Y-791717 (Haramura et al., 1983). The chemical composition of ALHA77307 has resulted in some uncertainty about its classification. Biswas et al. (1981) assigned this meteorite to the CV group, based on its high Cd concentration, but Kallemeyn and Wasson (1982b) concluded that its composition was similar in most respects to CO and CM chondrites. They also suggested that weathering may have been a factor in altering its composition. Its thermoluminescence properties are consistent with the CO classification, although it is not a normal member of that group (Sears and Ross, 1983). Petrographic data (Scott et al., 1981) also suggest ALHA77307 is an unusual member of this class, although Kainsaz, which it most resembles, is also unusual.

Organic constituents have been analyzed only in ALHA77307 (Moore et al., 1981; Murae et al., 1983). It contains only traces of amino acids, and pyrolysis experiments indicate highly volatile products.

Wieler et al. (1985) reported isotopic measurements of noble gases in ALHA77307 and ALHA82101. The only cosmogenic nuclide data available for these meteorites is for ALHA77003. Nishiizumi (1984) summarized ^{53}Mn, ^{26}Al, ^{36}Cl, and ^{14}C activities and calculated a cosmic ray exposure age of 20 million years.

CV3 Chondrites

Virtually nothing is known about any of these chondrites, but most are very small, and representative samples may be difficult to obtain. Scott (1984) briefly mentions RKPA80241.

C4 Chondrites

Petrographic descriptions of Y-6903 (Okada and Shima, 1979; Scott, 1985), PCA82500 (Scott et al., 1984), and ALH82135 (Scott, 1985) indicate that these meteorites are recrystallized and resemble Karoonda, though each is distinctive in some ways. The oxygen isotopic composition of Y-6903 is identical to that of Karoonda, and ^{18}O fractionation between plagioclase and magnetite corresponds to an equilibration temperature of 600° C (Clayton et al., 1979).

Bulk chemical analyses of Y-6903 and PCA82500 were reported by Kallemeyn (1985). Y-6903 may be a metamorphosed CVF chondrite, but compositional data for PCA82500 suggest affinities with both the CO and CV groups, as already noted for Karoonda (Kallemeyn and Wasson, 1982b). An analysis for carbon and sulfur in Y-6903 was reported by Gibson and Yanai (1979). Noble gas isotopic abundances for ALH82135 and PCA82500 were determined by Wieler et al. (1985).

Pairing of Antarctic Carbonaceous Chondrites

Very little information exists on which to make pairing assignments for these meteorites. Of both Antarctic collections, the only carbonaceous chondrite for which a terrestrial age has been determined is ALHA77003. Its reported ^{14}C age is $35{,}600 \pm 500$ years (Fireman, 1983), and its ^{36}Cl age is

110,000 ± 70,000 years (Nishiizumi, 1984). Four CM2 chondrites from the Allan Hills (77306, 78261, 81002, and 81004), and two Allan Hills CO3 chondrites (77003, and 82101) have been previously paired, based on petrographic similarities (Antarctic Meteorite Working Group, 1984). However, marked differences in olivine compositions (Scott et al., 1981) and noble gas abundances (Wieler et al., 1985) between ALHA77003 and ALH82101 suggest that these specimens are not paired.

To assist in this thorny problem of pairing assignments, provided below are partial modal analyses of the Victoria Land CM and CO chondrites (except ALH84033), obtained using optical point-counting methods outlined by McSween (1979b). It must be noted that no accurate determination of modal variability within any one meteorite has ever been made; however, point counts by the author on two thin sections for each of two different CO chondrites agreed within about 10 percent. An additional problem hampering accurate modal analyses is brecciation. Both of these meteorite classes are now known to contain clasts with different petrographic properties (McSween, 1979b; Rubin et al., 1984), and these could introduce substantial variations on a thin-section scale within one meteorite. In order to minimize these effects, I have relied only on matrix/chondrule ratios (rather than differences in the relative proportions of inclusions, chondrules, monomineralic fragments, etc.), where chondrules refer to everything that is not fine-grained, opaque matrix. This gross parameter, when combined with subjective assessment of degrees of hydrous alteration in CMs, and oxidation or textural blurring due to thermal metamorphism in COs, provides the basis for the pairings suggested in Table 9-2.

Three possible groupings of CM chondrites are proposed. The relatively unaltered chondrites are subdivided into two groups from the Allan Hills and two unpaired samples from Elephant Moraine based on matrix/chondrule ratios. However, petrographic variability within a large CM chondrite might permit these groupings to overlap. Microprobe defocused beam analyses of matrix would certainly help define these two groups. None of the altered CM chondrites from the Allan Hills are paired because of large differences in matrix/chondrule ratios. None of the Elephant Moraine specimens are paired for the same reason. No modal data are presented for the large group of highly altered CM chondrites from the Allan Hills, but they are paired because of their exceptional petrography. Chondrules and inclusions are so heavily altered that it is difficult to distinguish these from matrix in many cases. This alteration is so distinctive that these meteorites can probably be paired with confidence.

No obvious pairings exist among CO3 chondrites. Based on matrix/chondrule ratios, ALHA77129 and ALHA77307 could be paired, but differences in textural blurring, equilibration seen in olivine histograms (Scott et al., 1981), and bulk compositions (Kallemeyn and Wasson, 1982a) preclude pairing of any of these CO3 chondrites.

TABLE 9-2.—Pairing information.

	Meteorite	Matrix/Chondrule volume ratio	Subjective observations
	CM2		
I	ALHA81002	3.70	relatively unaltered
I	ALHA81004	2.78	relatively unaltered
I	ALH82100	3.33	relatively unaltered
II	ALHA78261	2.27	relatively unaltered
II	ALH82131	low*	relatively unaltered
II	ALH83016	1.96	relatively unaltered
	ALHA77306	4.17	altered
	ALHA81312	1.52	altered
	EET83224	1.75	relatively unaltered
	EET83226	0.65	relatively unaltered
	EET83250	2.50	altered with clasts
III	ALH83100	†	highly altered
III	ALH83102	†	highly altered
III	ALH84029	†	highly altered
III	ALH84030	†	highly altered
III	ALH84031	†	highly altered
III	ALH84032	†	highly altered
III	ALH84034	†	highly altered
III	ALH84042	†	highly altered
III	ALH84044	†	highly altered
	CO3		
	ALHA77003	0.43	metamorphosed, reduced
	ALHA77029	0.79	metamorphosed, reduced
	ALHA77307	0.76	unmetamorphosed, oxidized

I, II, III Tentatively paired groups
*Sample too small for modal analysis
†Sample too highly altered for modal analysis

Conclusions

The Antarctic meteorite collections from Victoria Land and Queen Maud Land contain all of the known classes of carbonaceous chondrites except CI (C1). These specimens greatly enlarge the limited quantities of carbonaceous chondrites in museum collections. Moreover, available pairing information, though limited, suggests that they represent many different falls. Unfortunately, many of these meteorites are small, and work has understandably focused on the larger specimens. Studies of even large Antarctic carbonaceous chondrites are very limited, however, and should be pursued more vigorously.

ACKNOWLEDGMENTS.—This work was partly supported by NASA grant NAG 9-58.

Literature Cited

Akai, J.
1982. High Resolution Electron Microscopic Characterization of Phyllosilicates and Finding of a New Type with 11Å Structure in Yamato-74662. *Memoirs of the National Institute of Polar Research* (Japan), special issue, 25:131–144.

1984. Mineralogical Characterization of Matrix Materials in Carbonaceous Chondrite Yamato-793321 and Belgica-7904 by HREM. [Abstract.] In *Ninth Symposium on Antarctic Meteorites*, pages 59–61. Tokyo: National Institute of Polar Research (Japan).

Akai, J., and J. Kanno

1985. Mineralogical Study of Matrix Phyllosilicates and Isolated Olivines in Yamato-79118 and 79331. [Abstract.] In *Tenth Symposium on Antarctic Meteorites*, pages 47–49. Tokyo: National Institute of Polar Research (Japan).

Antarctic Meteorite Newsletter, 7(1), 1984.

Biswas, S., T.M. Walsh, H.T. Ngo, and M.E. Lipschutz

1981. Trace Element Contents of Selected Antarctic Meteorites—II: Comparison with Non-Antarctic Specimens. *Memoirs of the National Institute of Polar Research* (Japan), special issue, 20:221–228.

Brecher, A.

1980. Meteorites as Magnetic Probes: Recent Results. In *Lunar and Planetary Science XI*, pages 106–108. Houston, Texas: Lunar and Planetary Institute.

Clayton, R.N., T.K. Mayeda, and N. Onumo

1979. Oxygen Isotopic Compositions of Some Antarctic Meteorites. In *Lunar and Planetary Science X*, pages 221–223. Houston, Texas: Lunar and Planetary Institute.

Clayton, R.N., T.K. Mayeda, and K. Yanai

1984. Oxygen Isotopic Compositions of Some Yamato Meteorites. *Memoirs of the National Institute of Polar Research* (Japan), 35:267–271.

Cronin, J.R., S. Pizzarello, and C.B. Moore

1979. Amino Acids in an Antarctic Carbonaceous Chondrite. *Science*, 206:335–337.

Fireman, E.L.

1983. Carbon-14 Terrestrial Ages of Antarctic Meteorites. *Memoirs of the National Institute of Polar Research* (Japan), special issue, 30:246–250.

Fujimura, A., M. Kato, and M. Kumazawa

1982. Preferred Orientation of Phyllosilicates in Yamato-74642 and -74662, in Relation of Deformation of C2 Chondrites. *Memoirs of the National Institute of Polar Research* (Japan), special issue, 25:207–215.

Gibson, E.K., Jr., and K. Yanai

1979. Total Carbon and Sulfur Abundances in Antarctic Meteorites. In *Proceedings of the Tenth Lunar and Planetary Science Conference*, pages 1045–1051. New York: Pergamon Press.

Gibson, E.K., Jr., J.R. Cronin, R.K. Kotra, T.R. Primax, and C.B. Moore

1984. Amino Acids, Carbon and Sulfur Abundances In Antarctic Carbonaceous Chondrites. [Abstract.] In *Ninth Symposium on Antarctic Meteorites*, pages 78–80. Tokyo: National Institute of Polar Research (Japan).

Grady, M.M., I.P. Wright, A.E. Fallick, and C.T. Pillinger

1983. The Stable Isotopic Composition of Carbon, Nitrogen and Hydrogen in Some Yamato Meteorites. *Memoirs of the National Institute of Polar Research* (Japan), special issue, 30: 292–305.

Haramura, H., I. Kushiro, and K. Yanai

1983. Chemical Compositions of Antarctic Meteorites 1. *Memoirs of the National Institute of Polar Research* (Japan), special issue, 30:109–121.

Hayes, J. M.

1967. Organic Constituents of Meteorites: A Review. *Geochimica et Cosmochimica Acta*, 31:1395–1440.

Holzer, G., and J. Oro

1979. The Organic Composition of the Allan Hills Carbonaceous Chondrite (77306) as Determined by Pyrolysis–Gas Chromatography–Mass Spectrometry and Other Methods. *Journal of Molecular Evolution*, 13:265–270.

Hyman, M. and M. W. Rowe

1979. Magnetic Contents of Carbonaceous Meteorites. *Transactions of the American Geophysical Union (EOS)*, 60:308.

Ikeda, Y.

1982. Petrology of ALH-77003 Chondrite (C3). *Memoirs of the National Institite of Polar Research* (Japan), special issue, 25:34–65.

1983a. Alteration of Chondrules and Matrices in the Four Antarctic Carbonaceous Chondrites ALHA-77307 (C3), Y-790123 (C2), Y-75293 (C2), and Y-74662 (C2). *Memoirs of the National Institute of Polar Research* (Japan), special issue, 30:93–108.

1983b. Major Element Chemical Compositions and Chemical Types of Chondrules in Unequilibrated E, O, and C Chondrites from Antarctica. *Memoirs of the National Institute of Polar Research* (Japan), special issue, 30:122–145.

Jarosewich, E.

1980. Appendix 2: Chemical Analyses of Some Allan Hills Meteorites. *In* U.B. Marvin and B. Mason, editors, Catalog of Antarctic Meteorites, 1977–1978. *Smithsonian Contributions to the Earth Sciences*, 23:48.

Kallemeyn, G.W.

1985. Compositional Comparisons of Metamorphosed Carbonaceous Chondrites. In *Tenth Symposium on Antarctic Meteorites*, pages 45–46. Tokyo: National Institute of Polar Research (Japan).

Kallemeyn, G.W., and J.T. Wasson

1982a. Carbonaceous Chondrites from Antarctica. In *Lunar and Planetary Science XIII*, pages 373–374. Houston, Texas: Lunar and Planetary Institute.

1982b. The Compositional Classification of Chondrites, III: Ungrouped Carbonaceous Chondrites. *Geochimica et Cosmochimica Acta*, 46:2217–2228.

Knab, H.-J., and H. Hintenberger

1978. Isotope Dilution Analysis of 20 Trace Elements in 9 Carbonaceous Chondrites by Spark Source Mass Spectrography. *Meteoritics*, 13:522–527.

Kojima, H., Y. Ikeda, and K. Yanai

1984. The Alteration of Chondrules and Matrices in New Antarctic Carbonaceous Chondrites. *Memoirs of the National Institute of Polar Research* (Japan), 35:184–199.

Mason, B.

1963. The Carbonaceous Chondrites. *Space Science Reviews*, 1:621–646.

1971. The Carbonaceous Chondrites—A Selective Review. *Meteoritics*, 6:59–70.

Mason, B., and K. Yanai

1983. A Review of the Yamato-74 Meteorite Collection. *Memoirs of the National Institute of Polar Research* (Japan), special issue, 30:7–28.

McKee, T.R., and C.B. Moore

1980. Matrix Phyllosilicates of the Antarctic C2 Chondrite ALHA77306. In *Lunar and Planetary Science XI*, pages 703–704. Houston, Texas: Lunar and Planetary Institute.

McKinley, S.G., and K. Keil

1984. Petrology and Classification of 145 Small Meteorites from the 1977 Allan Hills Collection. *In* U.B. Marvin and B. Mason, editors, Field and Laboratory Investigations of Meteorites from Victoria Land, Antarctica. *Smithsonian Contributions to the Earth Sciences*, 26:55–71.

McSween, H.Y., Jr.

1979a. Are Carbonaceous Chondrites Primitive or Processed? A Review. *Reviews of Geophysics and Space Physics*, 17:1059–1078.

1979b. Alteration in CM Carbonaceous Chondrites Inferred from Modal and Chemical Variations in Matrix. *Geochimica et Cosmochimica Acta*, 43:1761–1770.

Moore, C.B., J.R. Cronin, S. Pizzarello, M.-S. Ma, and R.W. Schmitt
1981. New Analyses of Antarctic Carbonaceous Chondrites. *Memoirs of the National Institute of Polar Research* (Japan), special issue, 20:29–32.

Murae, T., T. Takahashi, and A. Masuda
1983. Organic Compounds in Carbonaceous Chondrite ALH-77307,51. *Memoirs of the National Institute of Polar Research* (Japan), special issue, 30:452–455.
1984. Pyrolytic Studies of Organic Components in Antarctic Carbonaceous Chondrites Y-74662 and ALH-77307. *Memoirs of the National Institute of Polar Research* (Japan), special issue, 35:250–256.

Nagahara, H., and I. Kushiro
1982. Petrology of Chondrules, Inclusions and Isolated Olivine Grains in ALHA-77307 (CO3) Chondrite. *Memoirs of the National Institute of Polar Research* (Japan), special issue, 25:66–77.

Nagao, K., K. Inoue, and K. Ogata
1984. Primordial Rare Gases In Belgica-7904 (C2) Carbonaceous Chondrite. *Memoirs of the National Institute of Polar Research* (Japan), 35:257–266.

Nagao, K., J. Matsuda, and K. Inoue
1985. Primordial Rare Gases In Carbonaceous Chondrites. [Abstract.] In *Tenth Symposium on Antarctic Meteorites*, page 149. Tokyo: National Institute of Polar Research (Japan).

Nagata, T.
1980. Magnetic Classification of Antarctic Meteorites. In *Proceedings of the Eleventh Lunar and Planetary Science Conference*, pages 1789–1799. New York: Pergamon Press.

Nagy, B.
1975. *Carbonaceous Meteorites*. 238 pages. New York: Elsevier.

National Institute of Polar Research
1982. *Meteorites News; Japanese Collection of Antarctic Meteorites*, 1:1–3.

Nishiizumi, K.
1984. Cosmic-Ray-Produced Nuclides in Victoria Land Meteorites. *In* U.B. Marvin and B. Mason, editors, Field and Laboratory Investigations of Meteorites from Victoria Land, Antarctica. *Smithsonian Contributions to the Earth Sciences*, 26:105–109.

Okada, A., and M. Shima
1979. Yamato-694 Meteorite: Chemical Composition of Silicate. *Memoirs of the National Institute of Polar Research* (Japan), special issue, 12:109–113.

Rhodes, J.M., and C.R. Fulton
1980. Chemistry of Some Antarctic Meteorites. In *Lunar and Planetary Science XII*, pages 880–882. Houston, Texas: Lunar and Planetary Institute.

Rubin, A.E., J.A. James, B.D. Keck, K.S. Weeks, D.W.G. Sears, and E. Jarosewich
1984. The Colony Meteorite and Variations in CO3 Chondrite Properties. *Meteoritics*, 20:175–196.

Scott, E.R.D.
1984. Classification, Metamorphism, and Brecciation of Type 3 Chondrites from Antarctica. *In* U.B. Marvin and B. Mason, editors, Field and Laboratory Investigations of Meteorites from Victoria Land, Antarctica. *Smithsonian Contributions to the Earth Sciences*, 26:73–94.
1985. Further Petrologic Studies of Metamorphosed Carbonaceous Chondrites. In *Lunar and Planetary Science XVI*, page 748. Houston, Texas: Lunar and Planetary Institute.

Scott, E.R.D., and G.J. Taylor
1985. Petrology of Types 4–6 Carbonaceous Chondrites. *In* Proceedings of the Fifteenth Lunar Planetary Science Conference. *Journal of Geophysical Research*, 90(supplement):C699–C709.

Scott, E.R.D., G.J. Taylor, P. Maggiore, K. Keil, S.G. McKinley, and H.Y. McSween, Jr.
1981. Three CO3 Chondrites from Antarctica—Comparison of Carbonaceous and Ordinary Type 3 Chondrites. *Meteoritics*, 16:385.

Sears, D.W.G., and M. Ross
1983. Classification of the Allan Hills A77307 Meteorite. *Meteoritics*, 18:1–7.

Shimoyama, A., and K. Harada
1984. Search for Amino Acids Indigenous to the Yamato-793321 and Belgica-7904 Carbonaceous Chondrites. [Abstract.] In *Ninth Symposium on Antarctic Meteorites*, page 81. Tokyo: National Institute of Polar Research (Japan).

Shimoyama, A., K. Harada, and K. Yanai
1985. Indigenous Amino Acids from the Yamato-791198 Carbonaceous Chondrite. [Abstract.] In *Tenth Symposium on Antarctic Meteorites*, pages 52–54. Tokyo: National Institute of Polar Research (Japan).

Shimoyama, A., C. Ponnamperuma, and K. Yanai
1979. Amino Acids in the Yamato Carbonaceous Chondrites from Antarctica. *Nature*, 282:394–396.

Steele, I., J.V. Smith, and C. Skirius
1985. Cathodoluminescence Zoning and Minor Elements in Forsterites from the Murchison (C2) and Allende (C3V) Carbonaceous Chondrites. *Nature*, 313:294–297.

Van Schmus, W.R., and J.M. Hayes
1974. Chemical and Petrographic Correlations among Carbonaceous Chondrites. *Geochimica et Cosmochimica Acta*, 38:47–64.

Van Schmus, W.R., and J.A. Wood
1967. A Chemical-Petrologic Classification for the Chondritic Meteorites. *Geochimica et Cosmochimica Acta*, 31:737–765.

Wasson, J.T.
1974. *Meteorites*. 316 pages. New York: Springer.

Wieler, R., H. Baur, Th. Graf, and P. Signer
1985. He, Ne and Ar in Antarctic Meteorites: Solar Noble Gases in an Enstatite Chondrite. In *Lunar and Planetary Science XVI*, pages 902–903. Houston, Texas: Lunar and Planetary Institute.

10. The Emerging Meteorite: Crystalline Structure of the Enclosing Ice

Anthony J. Gow and William A. Cassidy

Introduction

While searching for meteorites in the Far Western Icefield of the Allan Hills region during the austral summer of 1982–1983, Carl Thompson discovered a small, walnut-sized meteorite with just its tip protruding above the ice surface (Cassidy et al., 1983). Closer inspection showed that this meteorite was not surrounded by a zone of clear ice as would have been expected if melting and refreezing had occurred around the stone. The meteorite appeared to be still embedded in the original ice and becoming exposed for the first time at the ablation surface. If this interpretation were proved correct, this would be the first example observed in Antarctica of an emerging stone, a discovery of special importance because the terrestrial age of the meteorite would be the same as that of the enclosing ice. Since the terrestrial age of the stone can be determined by measurement of several different nuclides (e.g., ^{26}Al, ^{10}Be, ^{36}Cl, ^{81}Kr, ^{58}Mn, and ^{14}C), such dating would furnish, for the first time, a good measure of the time that has elapsed since the meteorite embedded itself in the Antarctic ice sheet. This, in turn, would provide an independent check on age determination methods currently being developed for dating ancient ice. Because of the potentially unique nature of this meteorite it was left untouched and collected within a block of ice measuring approximately 36 cm long by 30 cm wide and 10 to 20 cm deep. This sample was shipped frozen to the U.S. Army Cold Regions Research and Engineering Laboratory in Hanover, New Hampshire, where the meteorite was removed by sterile procedures and the crystalline structure of the ice in contact with the meteorite was examined in a series of orthogonal thin sections. This study was undertaken to determine if the crystalline properties of the ice were consistent with the notion that the ice enclosing the meteorite is coeval with the terrestrial age of the meteorite.

Anthony J. Gow, U.S. Army Cold Regions Research and Engineering Laboratory, 72 Lyme Road, Hanover, New Hampshire 03755-1290. William A. Cassidy, Department of Geology and Planetary Science, University of Pittsburgh, Pittsburgh, Pennsylvania 15260.

Sample Processing

Prior to processing, the ice block was remeasured and photographed from several different directions. Figure 10-1 shows the disposition of the meteorite in the ice prior to cutting the block with a band saw. A narrow sublimation cavity around the meteorite (Figure 10-2) was rimmed by sublimation crystals and contained sparse grains of a fine, reddish dust which could have been derived from the meteorite, but might be windblown terrestrial contamination. The ice block displayed three mutually perpendicular sets of parallel cracks, which were features observed at the find site.

Saw cuts were made on either side of the meteorite and the block was then split apart by wedging, as illustrated in Figure 10-3. A close-up view of the meteorite still embedded in one wall of the cleaved ice is shown in the Frontispiece. Inspection of the ice in contact with the meteorite showed no trace of melting anywhere along the contact margin. The meteorite was removed with a pair of pre-cleaned tongs (Figure 10-4) and transferred to a polyethylene bag. This bag was then enclosed in a second bag (as is done in the field) and placed in a thick-walled styrofoam container, which was then filled with dry ice and air-shipped to the curatorial facility of the NASA Johnson Space Center, Houston, Texas. The 9.9 kilogram piece of ice (Figure 10-5), from which the meteorite was extracted, was shipped to Dr. K. Nishiizumi at the University of California at San Diego for further processing and dating. As a member of the meteorite-collecting expedition of 1983–1984, Dr. Nishiizumi returned to the site, marked by a flag, where the block had been removed and collected additional ice for his analyses. Crystal structure studies were performed on thin sections cut from slabs V1, V2, and H1 in the region of the mold of the meteorite in the other half of the sawn block (Figure 10-5). Ice from piece V2 was also used to prepare samples for conventional chemical analysis by J. Cragin at CRREL and for stable isotope measurements by S. Epstein at the California Institute of Technology. Results of these investigations together with those of terrestrial age dating of the meteorite are not yet available. The meteorite, ALH82102,

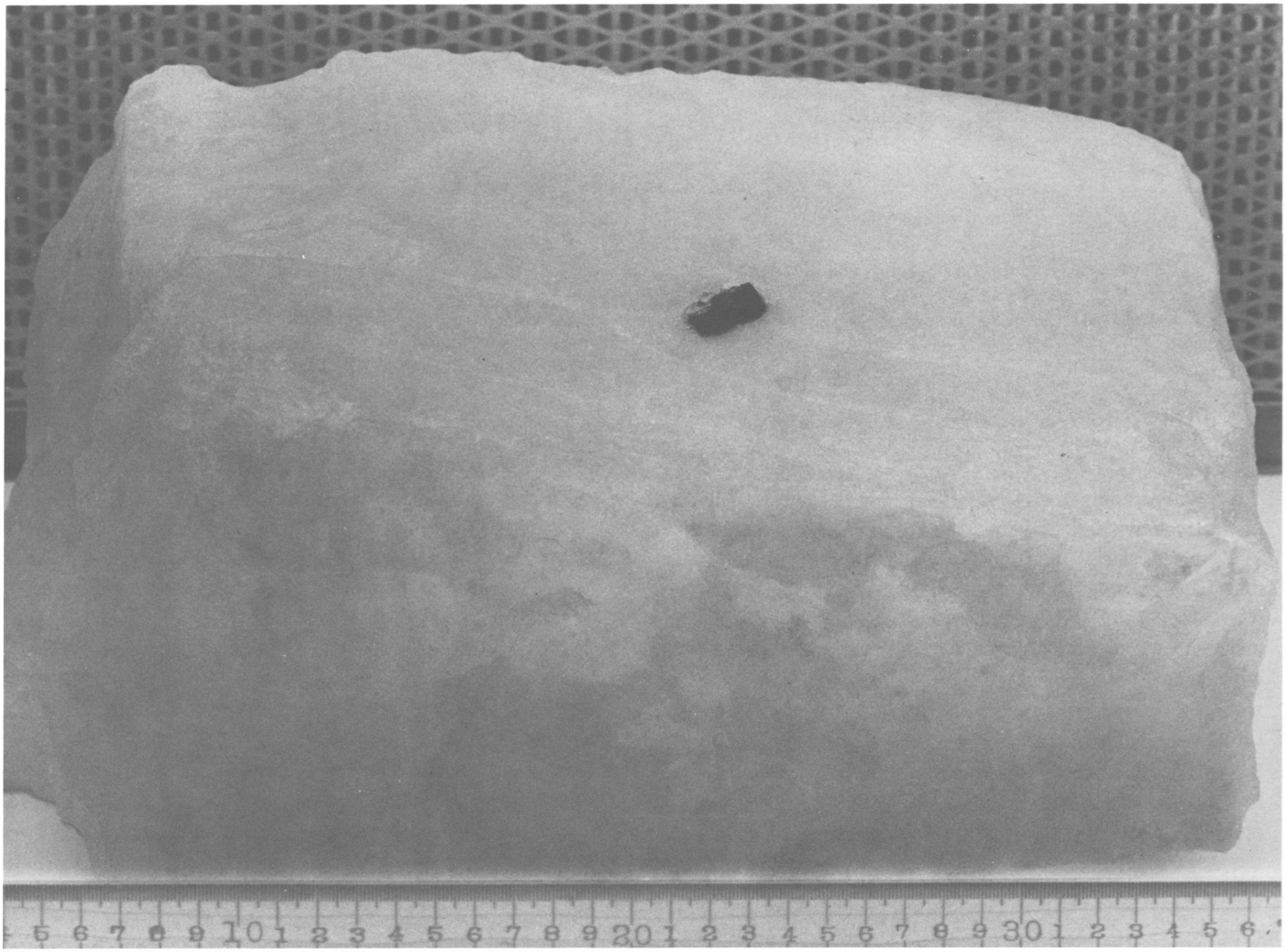

FIGURE 10-1.—Block of ice with enclosed meteorite, collected from the Allan Hills Far Western Icefield and shipped frozen (T = −12° C) to the Cold Regions Research and Engineering Laboratory in New Hampshire. Traces of a dominant fracture plane cross the ice from left to right. (Scale in cm).

a 48 g H5 chondrite with an almost complete fusion crust, is described in the chapter on stony meteorites by Mason et al., Chapter 6.

Ice Structure Analysis

Three thin sections were cut in mutually perpendicular directions. This was done in order to evaluate the three-dimensional picture of the crystal/bubble structure of the ice. Figure 10-6*a* shows a picture of Section V1, a thick (3 mm) slice that was photographed in reflected light to show the extremely bubbly nature of the ice. On average, bubble abundances occur in excess of 100 per cubic centimeter of ice. Bubble sizes seldom exceed 1 mm in diameter though elongated bubbles in some sections of the ice may measure 2 mm or more in length. The generally irregular (non-spherical) shapes of bubbles would suggest that they have been formed by "exsolution," that is, were re-formed from air previously dissolved under pressure in buried ice. Such a process was first documented in deep ice cores from Byrd Station, Antarctica, where bubbles in concentrations exceeding 200 per cm^3 of ice in the top 800 m had completely disappeared by 1100 m depth (Gow et al., 1968; Gow and Williamson, 1975). Such a process is believed to be pressure-induced since "exsolution" or reappearance of non-spherical and generally irregularly shaped bubbles began to occur some days after cores were pulled to the surface. In contrast to exsolved bubbles, original bubbles derived from air trapped between grains of snow in the upper layers of the Antarctic Ice Sheet tend to retain rounded, substantially spherical outlines up to the time they become absorbed in deeper ice.

Considering probable ice temperatures upstream of the find site (the depth at which bubbles are absorbed by the ice depends on temperature as well as pressure), we surmise that the ice

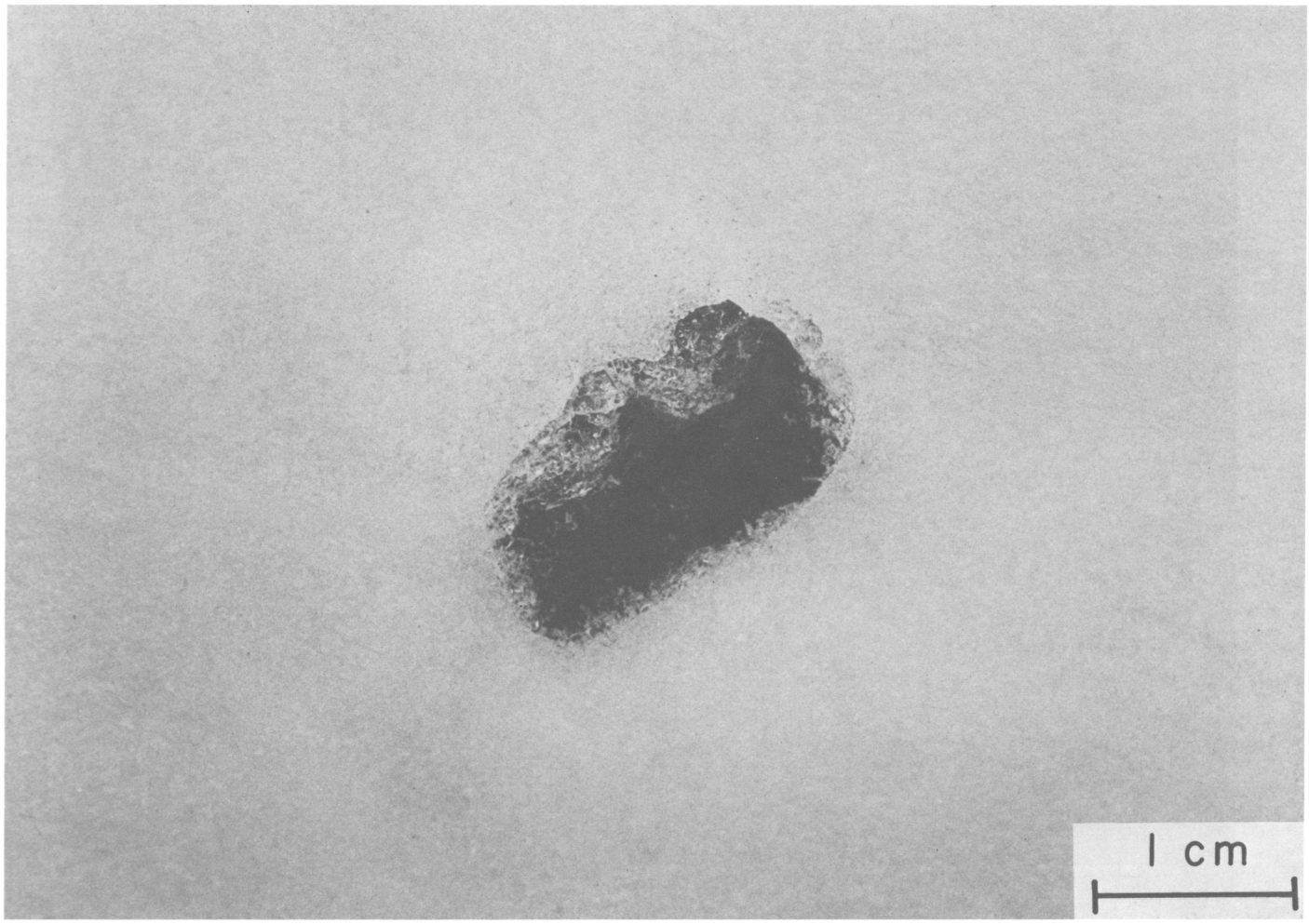

FIGURE 10-2.—Closeup of the meteorite in situ, rimmed by a narrow sublimation cavity in which feathery ice crystals protrude from the ice walls. The cavity and its crystals, observed in the field, survived transport to CRREL.

containing the meteorite must have been buried to a depth of at least 700 m in order for complete dissolution of original air bubbles to have occurred (Miller, 1969, and Gow and Williamson, 1975). Based on our estimate of its burial depth and the time needed for it to have reached the surface by upward flow and ablation, assuming an ablation rate of 5 cm of ice per year (see Nishio et al., 1982), the meteorite is believed to have impacted the surface at least 30,000 years ago. This is somewhat older than the 20,000 years that Nishio et al. (1982) estimate for the age of ice samples located close to Allan Hills. However, our estimate is not in disagreement with minimum ages given by Whillans and Cassidy (1983) for ice reaching the surface in the region of the Far Western Icefield where the meteorite was discovered.

A photograph of the vertical section, taken in cross-polarized light to reveal the outlines of individual crystals, is shown in the Frontispiece of this volume. It shows a general flattening of grains in the horizontal plane with respect to the top surface of the ice block. The only exception is in the immediate vicinity of the meteorite mold where crystals curve upwards. We would attribute this curving upwards of the crystals to reaction between the meteorite and the enclosing ice, most likely as a result of differential deformation of ice due to the presence of the non-deformable meteorite. In the horizontal section (Figure 10-6*b*, Section H1) taken from near the bottom of the ice block the crystals have become more equidimensional. Also, the c-axes of crystals tend to be clustered together in a very broad maximum about the vertical axis, which would be compatible with effects due to horizontal shearing of the ice. Coarser-grained ice in immediate contact with the meteorite exhibited no structural characteristics consistent with melting and refreezing or annealing.

On the basis of the above observations, we conclude that the meteorite was just beginning to emerge at the ablation surface when discovered on 2 January 1983, and that the ice enclosing the meteorite is coeval with the impact age of the meteorite. The terrestrial age measurement of the meteorite therefore will determine the age of the enclosing ice.

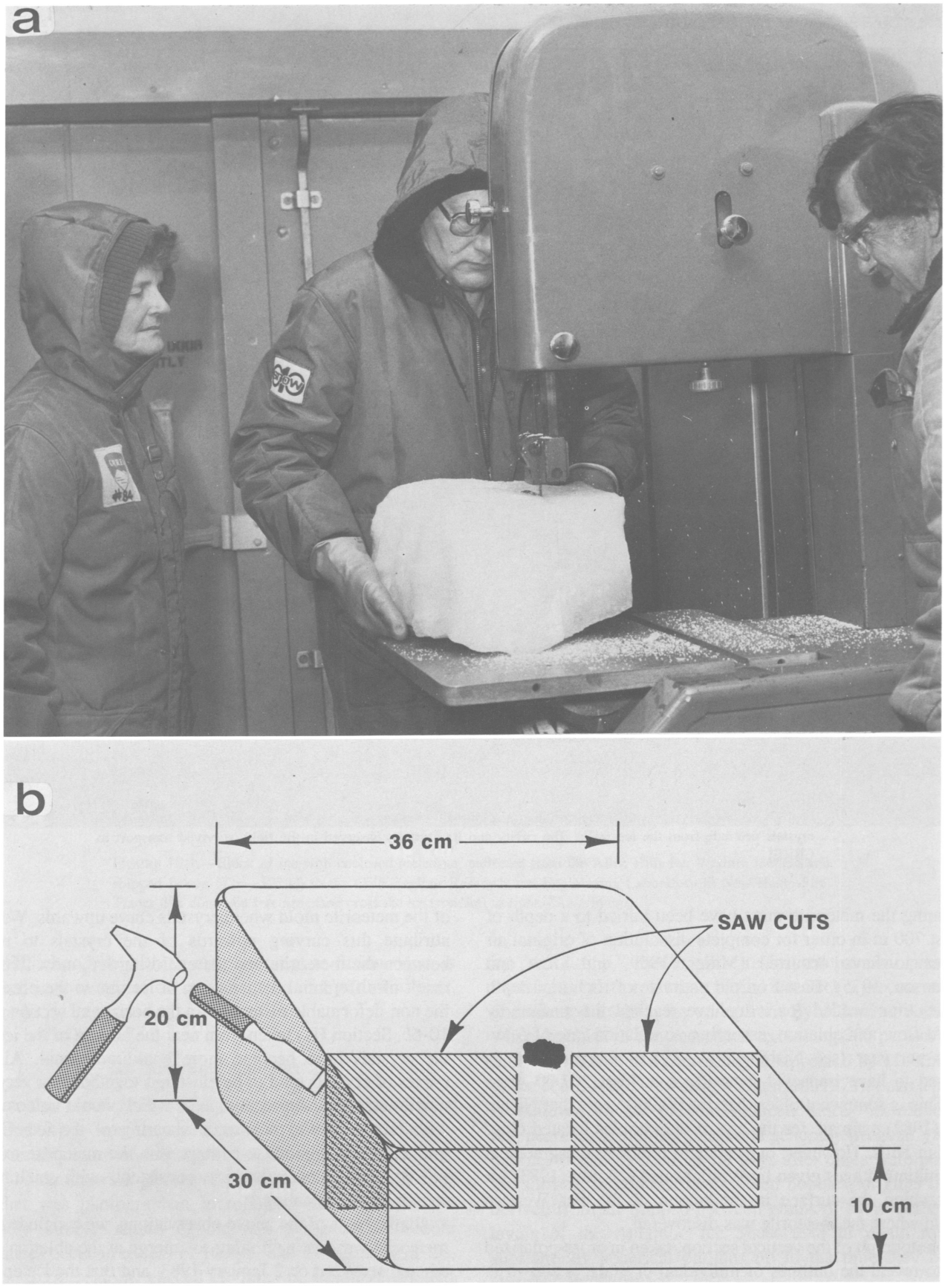

FIGURE 10-3.—Splitting the ice block without touching the meteorite: *a*, Bill Cassidy making the first saw cut from one edge toward the stone. A second cut was made from the opposite edge, a wedge inserted in the cut, and the block split open. Spectators are Ursula Marvin and Tony Gow. *b*, diagram of the sawing and splitting process.

Literature Cited

Cassidy, W.A., T. Meunier, V. Buchwald, and C. Thompson
1983. Search for Meteorites in the Allan Hills/Elephant Moraine Area, 1982–1983. *Antarctic Journal of the United States,* 18(5):81–82.
Gow, A.J., H.T. Ueda, and D.E. Garfield
1968. The Antarctic Ice Sheet: Preliminary Results of Drilling to Bedrock. *Science,* 161:1011–1013.
Gow, A.J., and T. Williamson
1975. Gas Inclusions in the Antarctic Ice Sheet and Their Glaciological Significance. *Journal of Geophysical Research,* 80(36):5101–5108.
Miller, S.L.
1969. Clathrate Hydrates of Air in Antarctic Ice. *Science,* 165:489–490.
Nishio, F., N. Azuma, A. Higashi, and J.O. Annexstad
1982. Structural Studies of Bare Ice near the Allan Hills, Victoria Land, Antarctica: A Mechanism of Meteorite Concentration. *Annals of Glaciology,* 3:222–226.
Whillans, I.A., and W.A. Cassidy
1983. Catch a Falling Star: Meteorites and Old Ice. *Science,* 222:55–57.

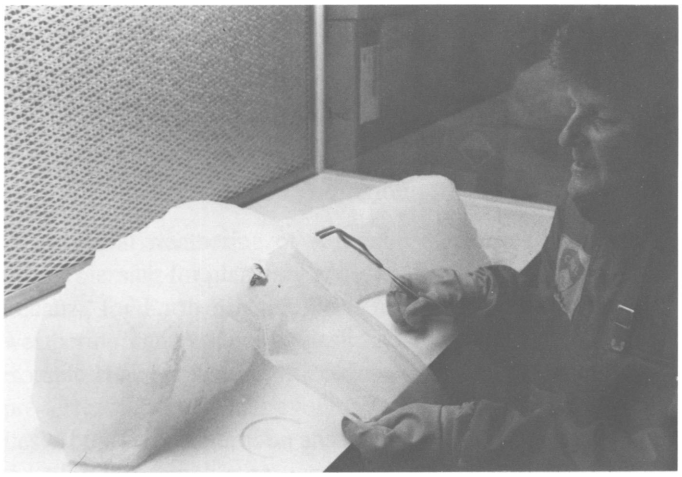

FIGURE 10-4.—Extraction of the meteorite at CRREL, using precleaned stainless steel tongs and a polyethylene bag.

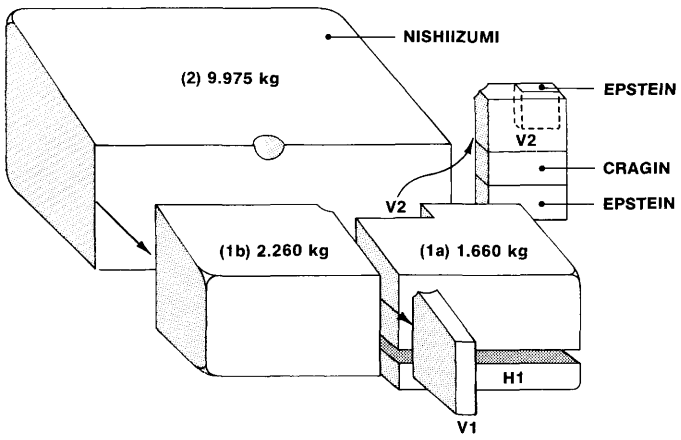

FIGURE 10-5.—Subsamples of the ice block. Portions of samples 1a, 1b, V1, and part of V2 remain at CRREL and are available for further study.

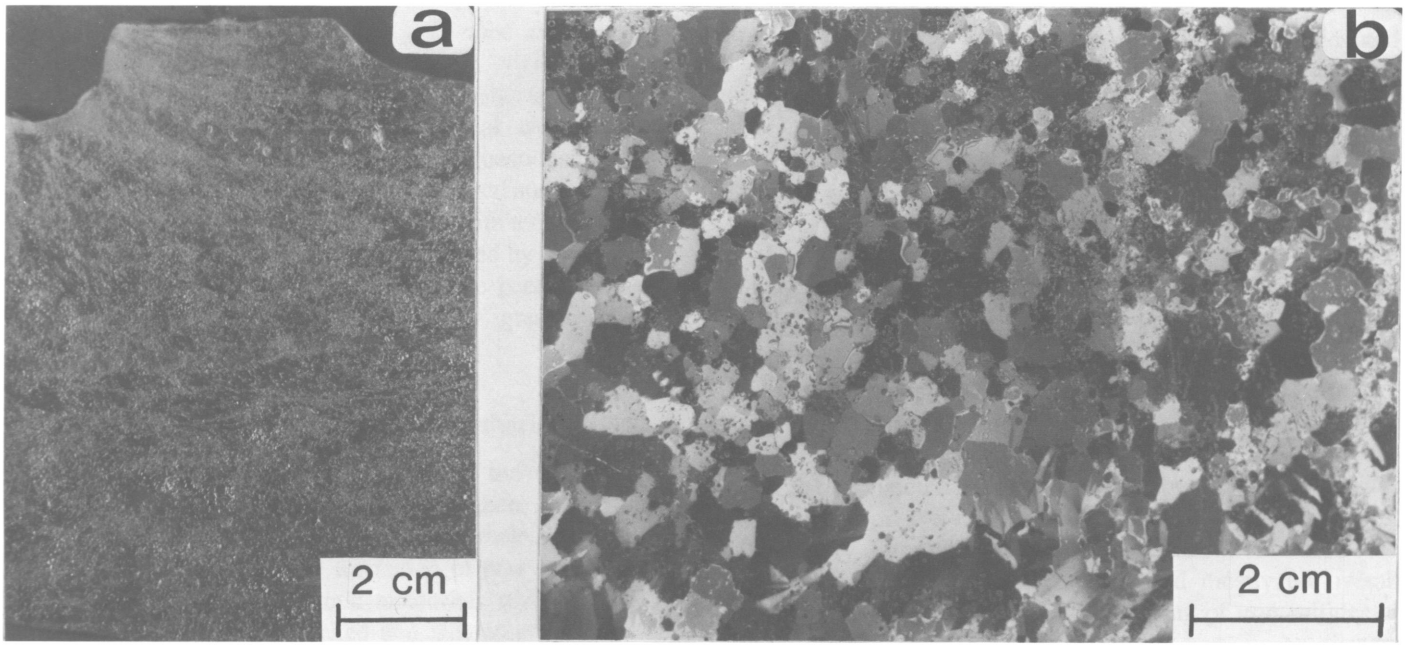

FIGURE 10-6.—Orthogonal sections through the ice: *a,* a vertical thick section (V1), taken in reflected light (scale in cm), showing the very bubbly nature of the ice. The cavity that held the stone is at upper left. A photograph of this same section after thinning, taken in cross-polarized light, is shown in the Frontispiece. *b,* horizontal thin section (H1) in cross-polarized light. The grains are more equidimensional in this section. The small gray inclusions are air bubbles (scale in cm).

11. Significance of Terrestrial Weathering Effects in Antarctic Meteorites

James L. Gooding

Introduction

Terrestrial weathering of Antarctic meteorites represents a mixed blessing for planetary geoscience but may be a potential bonanza for Earth science. With respect to cosmochemistry, weathering can produce undesirable physical, chemical, and isotopic changes that might confuse or obscure the records of pre-terrestrial origin and evolution that are sought in meteorites. At the same time, as an analog in comparative planetology, the ultra-low-temperature weathering of meteorites in an icy "regolith" represents a window into the processes of mineral and rock alteration that have probably operated on icy planetary bodies such as Mars, comets, asteroids, and satellites of Jupiter and Saturn. For Earth science, terrestrial weathering effects in Antarctic meteorites represent distinctive "marker horizons" which, if they can be quantitatively calibrated and correlated with other measurable properties, might yield important information about histories of Antarctic ice sheets.

Major issues surrounding the terrestrial weathering of Antarctic meteorites include the following questions:

1. How can weathering effects be recognized and quantified?
2. Are degrees of weathering correlated with terrestrial ages?
3. How are cosmochemical studies affected by weathering?

To date, answers to these questions have been incomplete and unsatisfying and it is time to apply greater research emphasis to the problem.

Recognition and Quantification of Weathering Effects

In the broadest sense, "weathering" is the collection of processes which, through surface/atmosphere interactions, leads to the decomposition or alteration of rocks, minerals, or mineraloids, and the possible formation of new phases. Even casual observations of Antarctic meteorites reveal that most specimens are rusty and cracked and that outer surfaces are partially eroded and discolored relative to interior surfaces that are exposed upon chipping. Therefore, it is clear that both physical and chemical weathering have affected Antarctic meteorites. Products of chemical weathering include carbonates, sulfates, and hydrous iron oxides (Marvin, 1980; Gooding, 1981) as well as clay mineraloids (Gooding, 1984a,b; 1986b). Aluminosilicate weathering products, in particular, are easily overlooked because of their small grain sizes and their resemblance to primary felsic minerals (Figures 11-1, 11-2). Because rust is so common and conspicuous, however, degree of rustiness has been adopted as the conventional means for expressing the "degree of weathering" of a given specimen.

Under the current curatorial practices that apply to the American collection, preliminary examination and classification of each Antarctic meteorite specimen includes assignment to an A, B, or C weathering type according to the following, generalized definitions:

- A: Minor rustiness; rust haloes on metal particles and rust stains along fractures are minor.
- B: Moderate rustiness; large rust haloes occur on metal particles and rust stains on internal fractures are extensive.
- C: Severe rustiness; metal particles have been mostly, if not totally, converted to rust and the specimen is stained by rust throughout.

Unfortunately, the A-B-C system is only qualitative and its application is largely subjective. In addition, its dependence on meteoritic metal as an index phase makes it difficult, if not impossible, to apply uniformly to all types of meteorites. Not only is it difficult to compare achondrites with chondrites by the A-B-C system, but comparisons within either group can be just as problematical, as exemplified by the case of aubrites vs. eucrites or the case of H-chondrites vs. C-chondrites, respectively. In practice,the A-B-C assignment for a meteorite that contains little or no metal is based mostly on overall rustiness that has developed by weathering of iron sulfides or mafic silicates.

Reflectance spectrophotometry might offer a means of more objectively and quantitatively ranking meteorite specimens according to their degrees of rustiness. As shown in Figure 11-3, there appears to be an inverse correlation between

James L. Gooding, Code SN2, Planetary Materials Branch, NASA/ Johnson Space Center, Houston, Texas 77058.

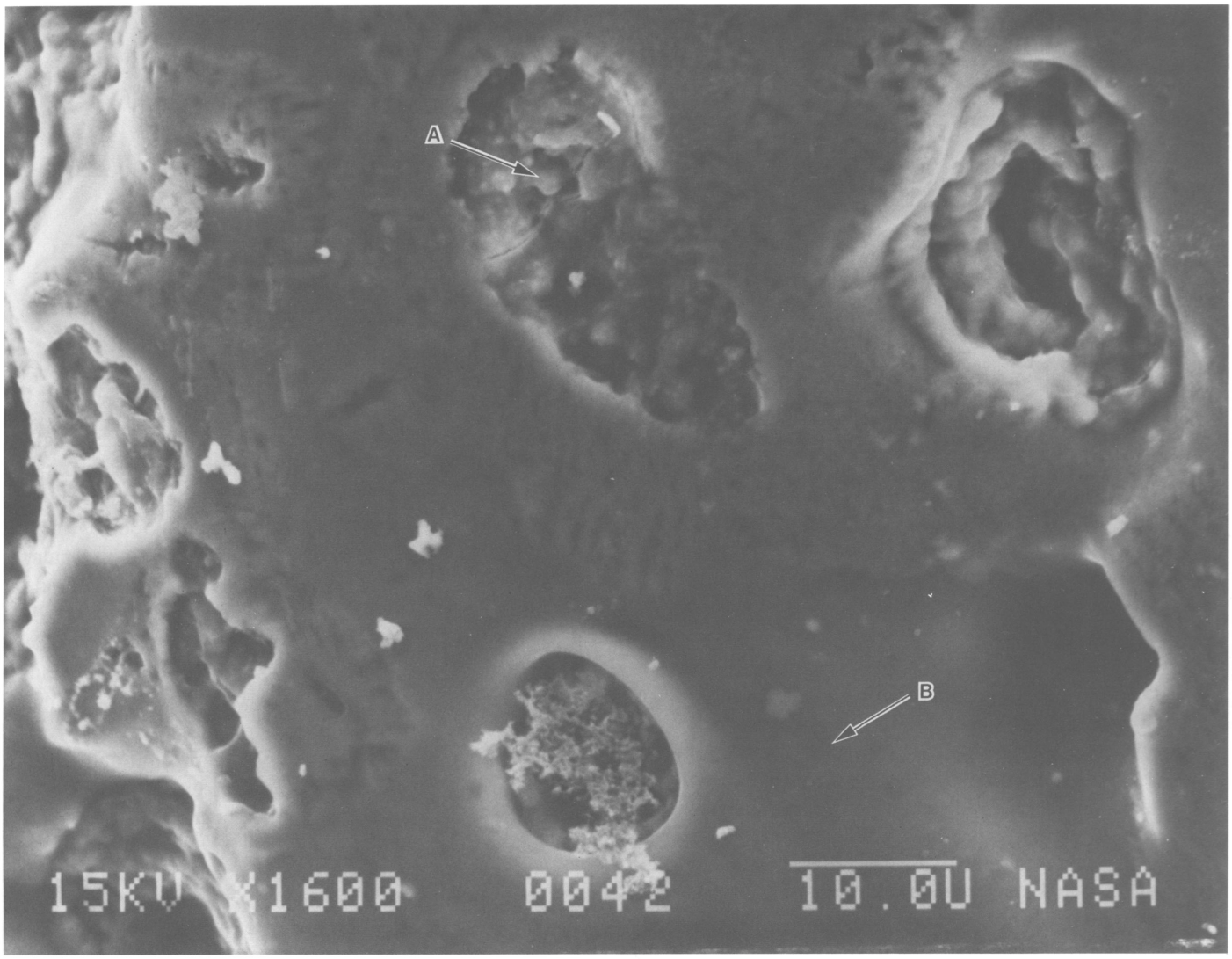

FIGURE 11-1.—Scanning electron image of Antarctic weathering products that fill cavities in the fusion crust of the "emerging stone," ALH82102 (H5 chondrite). The etched appearance of portions of the fusion crust suggests aqueous leaching whereas the vug fillings clearly suggest aqueous precipitation. Points A and B correspond to elemental analyses that are depicted in Figure 11-2. Scale bar is 10 μm.

measurable "redness" and measurable degree of iron oxidation for ordinary chondrites. The trend is most clear for samples of the Holbrook, Arizona chondrite that were recovered at different times after its fall to Earth in 1912. As previously noted (Gibson and Bogard, 1978), the 1931 Holbrook specimen appears to be more weathered than the 1968 specimen even though the same climate prevailed during weathering of both specimens. Therefore, variations among microenvironments (depth of burial in soil, quality of drainage, etc.) that apparently affected weathering of Holbrook specimens must be considered in deducing the weathering histories of Antarctic meteorites. Not only are differences in Antarctic weathering to be expected between meteorites found in moraines and those found on open ice sheets, but differences in degrees of weathering among finds on ice sheets might exist as a function of the time that each specimen spent encased in ice relative to the time that it spent exposed at the ice/atmosphere surface (Gooding, 1986a).

Results for the Antarctic L6 chondrites in Figure 11-3 underscore one of the deficiencies of the A-B-C system. Even though all three L6-chondrite specimens were categorized as transitional A/B in terms of degree of weathering, they yield substantially different values for the spectrophotometric index and possibly also for the rust index (note that a relatively small change in the ratio total-Fe/(FeO + FeS) corresponds to a significant change in oxidation state). Therefore, at least in its present form, the A-B-C system of categorizing degree of weathering should not be considered quantitative and should not be overinterpreted. Indeed, a reliable and quantitative index

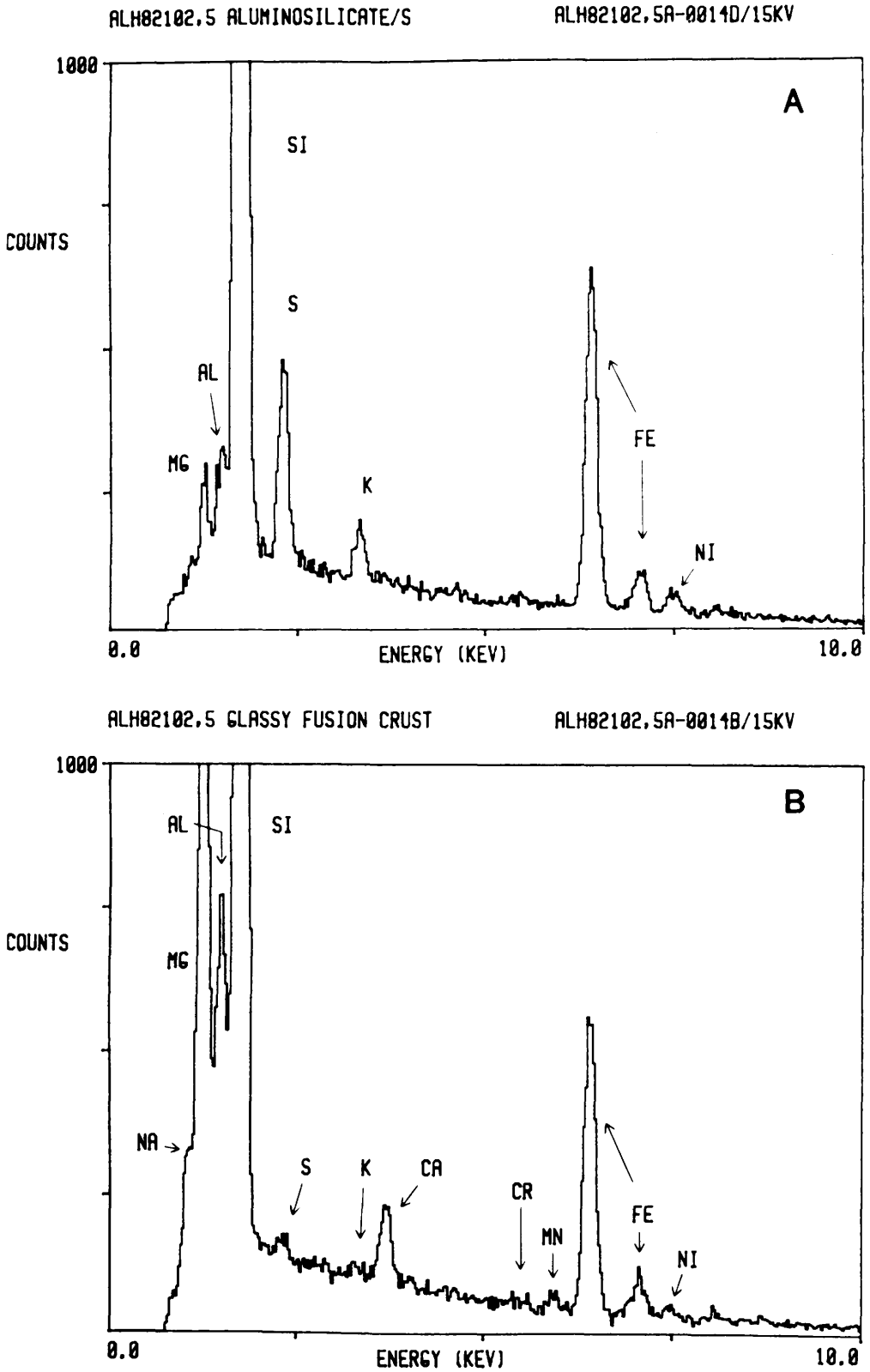

FIGURE 11-2.—Energy-dispersive x-ray emission spectra for areas on the fusion crust of ALH82102 as depicted in Figure 11-1. (A) complex weathering-product assemblage, possibly consisting of silica and/or an aluminosilicate mixed with a sulfate, that fills a cavity. (B) fusion crust, representing approximately the pre-terrestrial bulk major-element composition of the meteorite. Note the elemental fractionations that have occurred during weathering of the fusion crust (i.e., A vs. B).

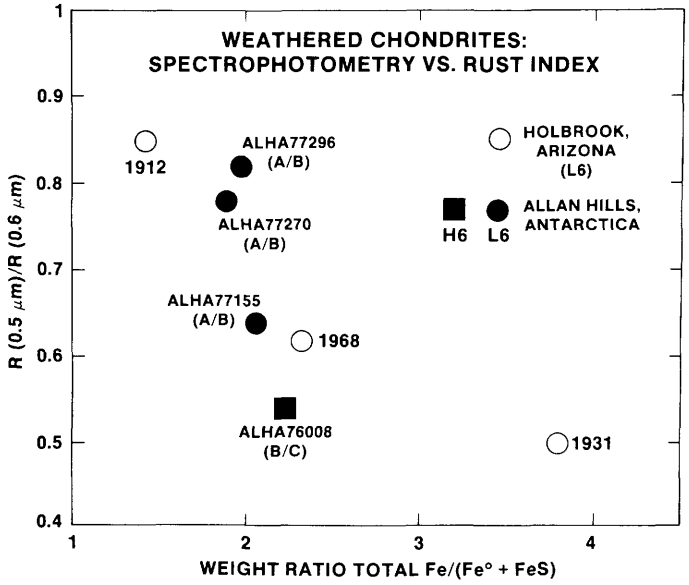

FIGURE 11-3.—Ratio of diffuse spectral reflectance at 0.5 μm wavelength to that at 0.6 μm, as a function of an independently determined "rust index" that is based on the oxidation of meteoritic metal and troilite. Decrease in the value of the spectrophotometric ratio corresponds to an increase in the visually perceptible degree of reddish coloration. Increase in the rust index corresponds to increase in degree of terrestrial oxidation. Each reflectance target was prepared by pulverizing and homogenizing a visually representative sample from the outer 1 cm of the specimen. Spectrophotometric data are from Gooding (1981) whereas chemical data are from Gibson and Bogard (1978) and Jarosewich (1984).

for degree of weathering remains a major need in research on Antarctic meteorites. Attention must be paid to the fact that oxidation of iron is only one of several processes that occur during Antarctic weathering and that, because of the wide variation of metal and total iron contents among meteorites, a simple rust index might not be the best measure of degree of weathering.

Correlations between Weathering and Terrestrial Age

The situation can be stated succinctly: no correlation between degree of weathering and terrestrial residence age has yet been demonstrated for Antarctic meteorites. It is intuitively reasonable to suspect that, at least for a given meteorite type (e.g., L6 chondrite), degrees of weathering among Antarctic specimens might be correlatable with the lengths of time that the specimens have spent on Earth. Either the presence or absence of such a correlation would be of great significance in efforts to identify the mechanisms that are responsible for transportation and concentration of meteorite specimens by Antarctic ice.

Previous conclusions regarding the absence of a correlation between degree of weathering and terrestrial residence age have relied on the fact that no systematic increase in terrestrial age occurs with alphabetic letter among specimens that have been categorized by A-B-C designations (e.g., Nishiizumi, 1986). As discussed above, though, weathering types defined by the A-B-C system cannot be treated as quantitative classifications. Consequently, the apparent lack of correlation between terrestrial age and degree of weathering might only reflect the irreconcilable mixture of quantitative measurements with qualitative estimates. Further progress on this problem cannot be expected until a quantitative index for degree of weathering is developed.

As shown in Figure 11-4, there may exist sensible inverse correlations between the spectrophotometric rust index and terrestrial age. Chondrites from Allan Hills, Antarctica, appear to have rusted much more slowly than did the Holbrook samples, based on the observation that the slopes of their respective trendlines differ by a factor of 10. Not surprisingly, the metal-rich H-chondrites seem to be systematically more rusty than the L6 chondrites among the Antarctic specimens. For the few data that are available, the trends in Figure 11-4 are not impressive but suggest that further work along these lines might produce a much better test of weathering/age correlations than has been made to date.

Possible Consequences for Cosmochemistry

Ultrasensitive analytical techniques and interpretive models that comprise current wisdom in cosmochemistry were developed mostly from experience with lunar samples and freshly fallen meteorites (Allende, Murchison, etc.). However, none of the meteorites recovered from Antarctica can be considered "pristine." Elemental fractionations occur during weathering (Jarosewich, 1984) although the degree to which a particular chemical study is likely to be affected might be determined largely by the samples and methods that are employed. Although untreated aliquots that are isochemically weathered at the scale of sampling may appear undisturbed in bulk analyses, disturbances may become apparent in analyses that sample a meteorite at less than the scale of weathering (e.g., aliquots of a few milligrams) or that depend upon mineralogical or ion-exchange separations or gas extractions. Phase locations and solubilities of analyte species are subject to change by chemical weathering.

Textural relationships between weathering products and their hosts clearly show that aqueous transportation has played a key role during weathering of Antarctic meteorites (Gooding, 1981, 1986b; Figure 11-1). In at least some cases, aqueous leaching and precipitation have produced significant elemental fractionations between the progenitors and products of chemical weathering (Figure 11-2). The same aqueous geochemical processes might be responsible for the uptake or loss, as well as the internal redistribution, of other elements. Pre-terrestrial gases can be lost by solution weathering of their host phases, whereas terrestrial gases can be incorporated during growth of secondary minerals and mineraloids.

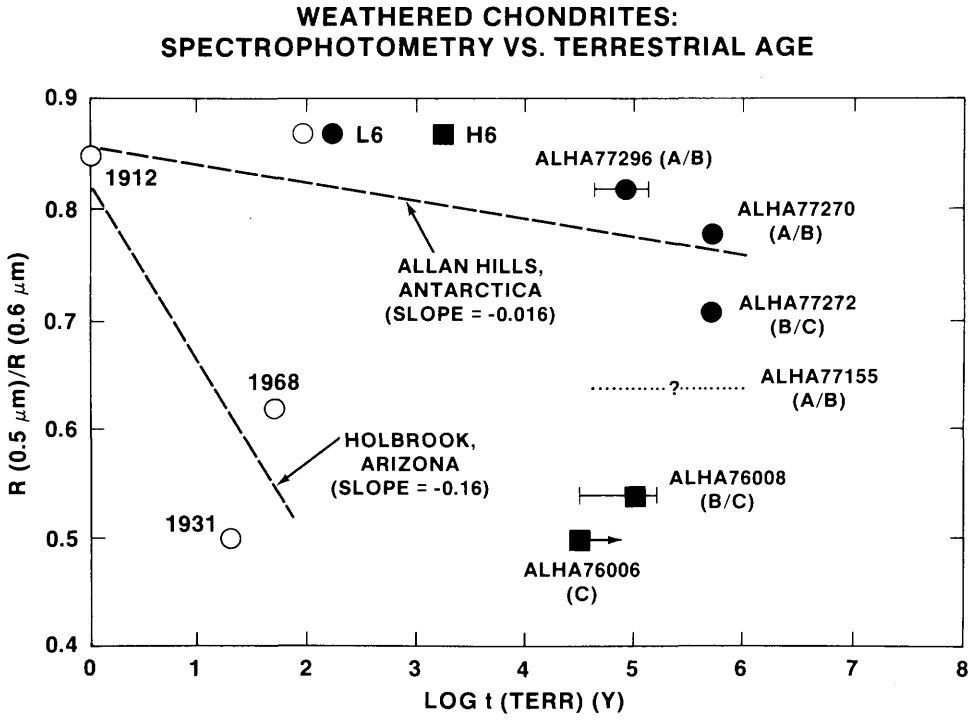

FIGURE 11-4.—Spectrophotometric index (defined in Figure 11-3) as a function of terrestrial residence age. Terrestrial ages of Antarctic specimens are from the compilation by Nishiizumi (1984). Trendlines represent linear least-squares fits through the respective data points. The "Allan Hills" trendline is defined by ALHA77270, ALHA77272, and ALHA77296, assuming Holbrook-1912 as the control point for an unweathered L6 chondrite. No terrestrial age has been published for ALHA77155.

Lipschutz (1982) briefly reviewed published trace-element data for Antarctic meteorites in the context of the weathering problem and concluded that loss of elements by natural leaching is the most serious problem but that, by restriction of work to samples from >1 cm depth in type A specimens, bulk trace-element analyses can be obtained for Antarctic meteorites without interference from weathering effects. Unfortunately, many of the most interesting Antarctic specimens are small (e.g., lunar meteorite ALHA81005: 3 cm maximum dimension) and the 1 cm depth criterion has not been applied during sampling. Furthermore, at least some type A specimens contain non-rusty weathering products (salt minerals, clay mineraloids) that might constitute important sources of interference in other types of analyses, especially isotopic and gas analyses. For example, the shergottites EETA79001 and ALHA77005 were both categorized as type A even though they contain aluminosilicate weathering products of the types that can be expected to be strong and fractionating sorbents of gases (Gooding, 1984b).

Clayton et al. (1984) reported effects of Antarctic weathering in some of their oxygen isotopic analyses and Kaneoka (1984) and Spangler and Warasila (1985) presented clear evidence for disturbance by weathering of K-Ar systematics in both chondrites and achondrites from Antarctica. Disturbance of noble gas abundances occurred during weathering of the Holbrook chondrite (Gibson and Bogard, 1978) but, unfortunately, comparison of results for Holbrook with results for Antarctic specimens might be less straightforward than expected. Although rust in Antarctic L-chondrites is very similar to that in Holbrook (Gooding, 1981), Antarctic specimens also contain non-rusty aluminosilicates and salt minerals (Figures 11-1, 11-2) that are rare to absent in Holbrook. Therefore, effects of Antarctic weathering on cosmochemical properties of meteorites might be significantly different from effects of temperate-latitude weathering.

Ideally, every Antarctic meteorite sample that is destined for a critical cosmochemical analysis should first be mineralogically examined for overall evidence of weathering (not just rustiness) so that problems (and possible data corrections) can be assessed in advance of sample consumption. Such precautions are especially important for studies that attempt to define new meteorite groups or sub-divide previously recognized meteorite groups using elemental or isotopic parameters that might be sensitive to disturbance by weathering.

Summary

The current inadequate understanding of weathering histories of Antarctic meteorites, and their possible effects on

measurable properties of the specimens, stems from a general lack of attention to the problem. A first major element of progress would be to augment or replace the currently used A-B-C system of categorizing degree of weathering with a system that is more objective and quantitative. Reflectance spectrophotometry might be a useful method for quantifying degree of rustiness although other methods may be required to quantify abundances of non-rusty weathering products.

Literature Cited

Clayton, R.N., T.K. Mayeda, and K. Yanai

1984. Oxygen Isotopic Compositions of Some Yamato Meteorites. *In* Proceedings of the Ninth Symposium on Antarctic Meteorites. *Memoirs of National Institute of Polar Research* (Japan), special issue, 35:267–271.

Gibson, E.K., Jr., and D.D. Bogard

1978. Chemical Alterations of the Holbrook Chondrite Resulting from Terrestrial Weathering. *Meteoritics,* 13:277–289.

Gooding, J.L.

1981. Mineralogical Aspects of Terrestrial Weathering Effects in Chondrites from Allan Hills, Antarctica. In *Proceedings of the Twelth Lunar and Planetary Science Conference,* pages 1105–1122. New York: Pergamon Press.

1984a. Low-Temperature Aqueous Alteration in the Early Solar System: Possible Clues from Meteorites Weathered in Antarctica. In *Lunar and Planetary Science XV,* pages 308–309. Houston: Lunar and Planetary Institute.

1984b. Search for "Martian(?) Weathering" Effects in Achondrites EETA79001 and ALHA77005: Complications from Antarctic Weathering. In *Lunar and Planetary Science XV,* pages 310–311. Houston: Lunar and Planetary Institute.

1986a. Weathering of Stony Meteorites in Antarctica. *In* J.O. Annexstad, L. Schultz, and H. Wänke, editors, Workshop on Antarctic Meteorites. *LPI Technical Report,* 86-01:48–54. Houston: Lunar and Planetary Institute.

1986b. Clay-mineraloid Weathering Products in Antarctic Meteorites. *Geochimica et Cosmochimica Acta,* 50:2215–2223.

Jarosewich, E.

1984. Bulk Chemical Analyses of Antarctic Meteorites, with Notes on Weathering Effects on FeO, Fe-metal, FeS, H2O, and C. *In* U.B. Marvin and B. Mason, editors, Field and Laboratory Investigations of Meteorites from Victoria Land, Antarctica. *Smithsonian Contributions to the Earth Sciences,* 26:111–114.

Kaneoka, I.

1984. Characterization of Ar-Degassing from Antarctic Meteorites. *In* Proceedings of the Ninth Symposium on Antarctic Meteorites. *Memoirs of National Institute of Polar Research* (Japan), special issue, 35:272–284.

Lipschutz, M.E.

1982. Weathering Effects in Antarctic Meteorites. *In* U.B. Marvin and B. Mason, editors, Catalog of Meteorites from Victoria Land, Antarctica, 1978–1980. *Smithsonian Contributions to the Earth Sciences,* 24:67–69.

Marvin, U.B.

1980. Magnesium Carbonate and Magnesium Sulfate Deposits on Antarctic Meteorites. *Antarctic Journal of the United States,* XV(5):54–55.

Nishiizumi, K.

1984. Cosmic-Ray-Produced Nuclides in Victoria Land Meteorites. *In* U.B. Marvin and B. Mason, editors, Field and Laboratory Investigations of Meteorites from Victoria Land, Antarctica. *Smithsonian Contributions to the Earth Sciences,* 26:105–109.

1986. Terrestrial and Exposure Histories of Antarctic Meteorites. *In* J.O. Annexstad, L. Schultz, and H. Wänke, editors, Workshop on Antarctic Meteorites. *LPI Technical Report,* 86-01:48–54. Houston: Lunar and Planetary Institute.

Spangler, R.R. and R.L. Warasila

1985. 39Ar-40Ar Ages of ALHA77302, 77256, and 77219. In *Lunar and Planetary Science XVI,* pages 805–806. Houston: Lunar and Planetary Institute.

12. Trace Element Variations between Antarctic (Victoria Land) and Non-Antarctic Meteorites

Michael E. Lipschutz

Studies, mainly of contemporary meteorite falls, reveal that the Earth is today sampling 70–80 parent bodies (Dodd, 1981) and/or source regions. These are far fewer than the 3330 numbered asteroids (Marsden, 1985), let alone the 15,000 discovered by the Infrared Astronomy Satellite (Tedesco, 1984). Even if non-Antarctic finds are considered to be heavily biased toward irons because of their recognition factor and greater resistance to weathering, the number of extraterrestrial sources is not increased markedly. Has the Earth always sampled the same few sources, or has the meteoroid complex varied in time or space?

Until the Antarctic meteorite discoveries, this question could not be addressed, since most witnessed falls have occurred during the most recent 200 years before present (B.P.). Non-Antarctic finds extend this to 1000–10,000 years B.P. but their utility is limited because many meteorites are degraded and contaminated during weathering in warmer latitudes. This is too short an interval in which to expect a detectable temporal source variation. Antarctic meteorites allow a farther look backward since their terrestrial ages generally are 0.1–0.7 Myr B.P. (Bull and Lipschutz, 1982) and, with some caveats, weathering has not reduced their scientific value (Lipschutz, 1982; Dennison and Lipschutz, in prep. a). While terrestrial age distributions for meteorites from Victoria Land and Queen Maud Land overlap, these two major Antarctic sample populations have different mean ages—0.3 and 0.1 Myr B.P., respectively—and mass distributions that differ from each other and from those of non-Antarctic falls (Bull and Lipschutz, 1982). In view of these differences, these three sample populations are treated here as different ones—referring to each by name: the adjective "Antarctic" will be applied when specific sample population designation is unnecessary.

Because relatively few Antarctic meteorite fragments recovered to date (over 1900 by the United States-led Antarctic Search for Meteorites and over 5100 by the Japanese Antarctic Research Expedition teams) can be paired with confidence, the number of distinct meteorite events represented by the Antarctic finds is somewhat uncertain. Many Antarctic specimens are unpaired but a very few have numerous well-established siblings, numbering up to 148 (Mason and Yanai, 1983). Taking an overall average of 5 fragments per fall (estimated as 2–6 per fall by Scott, 1984), the Antarctic population represents about 1400 distinct events. This number is comparable (within a factor of 2) to the 2611 known, distinct non-Antarctic meteorites currently cataloged (Graham et al., 1985).

From the first, it was recognized that the Antarctic population includes a substantial number of meteorites of rare or unique type compared with the non-Antarctic ones (Kusunoki, 1975). Subsequently, recovery and study of such exciting specimens has proven to be very nearly an annual event as, for example, in the cases of lunar and putative Martian meteorites (Marvin, 1983; Yanai and Kojima, 1984). Representatives of some rare types resemble their non-Antarctic congeners but, curiously, often show subtle differerences from them in composition. This seems to reflect preterrestrial processes rather than terrestrial weathering (Biswas et al., 1980, 1981; Lipschutz, 1982). Antarctic and non-Antarctic meteorites differ in other ways. For example, general differences occur in the distribution of iron meteorite chemical groups (Clarke, 1986) and in the textures and mineral compositions of Antarctic and non-Antarctic diogenites and eucrites (Mason and Yanai, 1983). Of course, these comparisons are based on poor statistics since we are dealing with representatives of rare meteorite types.

Subject to inevitable uncertainty because of pairing problems, Antarctic and non-Antarctic populations differ in their constituent meteorite proportions. Considering just the most general classification (Table 12-1), the Victoria Land population (corrected for known pairing) contains fewer irons, LL chondrites, and perhaps stony-irons than do non-Antarctic falls. Furthermore, the high iron to low iron (H/L) chondrite ratio is over 3 in the Victoria Land population and 1 in non-Antarctic falls (and finds). In the only comprehensive study of a single year's (1974) collection in Queen Maud Land, Mason and

Michael E. Lipschutz, Department of Chemistry, Purdue University, W. Lafayette, Indiana 47907.

Yanai's (1983) data yield an H/L chondrite ratio (corrected for paired samples) of 155/54, or nearly 3. These differences cannot reasonably be ascribed to Antarctic weathering; they hint at some major difference in the nature of meteorites landing in Antarctica and those landing elsewhere. Possibly the parent bodies of Antarctic meteorites followed more highly inclined orbits, or, more likely, a temporal change has taken place in the meteorite flux (Dennison et al., 1986).

Indications for differences between meteorite types in Antarctic and non-Antarctic sample populations do not necessarily mean that any given meteorite type will differ in the two sample populations. To identify the significant differences, one must compare parameters known to vary widely and be indicative of meteoritic genetic processes. Volatile and/or mobile trace element contents (Ag, Au, Bi, Cd, Co, Cs, Ga, In, Rb, Sb, Se, Te, Tl, and Zn) provide such a parameter for comparison between non-Antarctic ordinary chondrite falls and Victoria Land chondrites.

Data for a given volatile/mobile trace element in a sample population distribute either normally or lognormally and may be treated as Gaussian in either case (Dennison et al., 1986). Generally, distributions for a given element in two sample populations overlap and one must use standard statistical tests to examine the likelihood that the sample populations derive from the same parent population. If, statistically, this is unlikely for a number of different elements, it may be concluded that the sample populations derive from different parent populations.

As part of a series of systematic studies of equilibrated ordinary chondrites, Dennison et al. (1986) compared volatile/mobile trace element data for 23 Antarctic finds and 20 non-Antarctic H5 chondrite falls. Taking ≥95% confidence level as significant and 90%–94% as possibly so, Dennison et al. (1986) found differences for 8 of 13 elements tested (Table 12-2). This greatly exceeds the proportion expected to arise by chance (1–2 of 13 elements at the ≥90% confidence level). Dennison et al. (1986) and Dennison and Lipschutz (in prep. a,b) extended the comparison to H4-6 chondrites. They considered a variety of more or less plausible explanations for the differences, especially weathering, and concluded that the difference was a real one reflecting preterrestrial genetic differences. More recently, Kaczaral and Lipschutz (in prep.) found that L4-6 chondrites from Victoria Land also differ compositionally from non-Antarctic falls: we take this as additional support for the unimportance of a weathering effect on trace element contents of Antarctic meteorites.

For L6 chondrites, the trace element data suggest, on average, more severe thermal processing (perhaps by shock) for the Victoria Land samples than for non-Antarctic falls (Kaczaral and Lipschutz, in prep.). This suggestion is currently being tested by petrographic and thermoluminescence studies. For H5 chondrites, genetic processes responsible for the compositional differences are less obvious (Dennison and Lipschutz, in prep. b).

TABLE 12-1.—Comparative numbers of selected meteorite types found in Victoria Land and falling in non-Antarctic regions (numbers cited for H, L, and LL chondrites count as part of the total for chondrites).

Meteorite type	Victoria Land*		Non-Antarctic†	
	No.	%	No.	%
Chondrites	756	92.4	784	86.6
H	542	66.3	276	30.5
L	167	20.4	319	35.2
LL	24	2.9	66	7.3
Achondrites	45	5.5	69	7.6
Irons	14	1.7	42	4.6
Stony Irons	3	0.4	10	1.1
Total	818	100.0	905	100.0

*J. Gooding (personal communication, 1985). Data do not include 281 samples paired with ones already classified.

†Graham et al. (1985).

Major and trace element distributions for ordinary chondrites from Victoria Land are more coherent than those for non-Antarctic falls (Fulton and Rhodes, 1984; Dennison et al., 1986; Dennison and Lipschutz, in prep. a,b; Kaczaral and Lipschutz, in prep.), hinting again at preterrestrial compositional differences between Antarctic and non-Antarctic meteorites. Dennison et al. (1986) illustrate one in which meteorite sample populations falling on Earth at specific times in the past could differ in the proportions of constituent types. Such distributions preserved, for example, in the Antarctic ice sheet would constitute "snap-shots in time" of the meteoroid distribution. As yet, we do not know whether the Antarctic sample population is a single one or if the Victoria Land and Queen Maud Land (and others) constitute differing sample populations separated in time, having average ages of 0.3 Myr B.P. (Victoria Land) and 0.1 Myr B.P. (Queen Maud Land) (Bull and Lipschutz, 1982). Another possibility is that Antarctic meteorites preferentially derive from parent bodies in highly inclined orbits.

It seems too optimistic to expect that the Victoria Land population is a "pure" sample of a single parent region (or body) "unsullied" by earlier and later events, and it would be premature to attempt resolution of the near-Earth meteorite flux with only 2 distributions, Victoria Land and non-Antarctic falls. Indeed, it is astonishing that any differences are detectable in chondrite sample populations separated by only 0.2 Myr, when typical cosmic ray exposure ages had been taken to imply an averaging of the chondritic flux over the past 1–10 Myr (Wetherill, 1974).

Nevertheless, the trace element evidence seems compelling that meteorites from Victoria Land sample a population different from that falling today in non-Antarctic regions. Hence, Antarctic meteorites are a more valuable scientific resource than hitherto suspected. Antarctic meteorites may include collision debris from disrupted parent asteroids that was long since swept up and no longer exists among

TABLE 12-2.—Comparison of statistically significant differences in H5 and L6 chondrites from Victoria Land, Antarctica, with contemporary non-Antarctic falls. (Ant. = Chondrites from Victoria Land; Non = non-Antarctic chondrite falls; Sig. = significance level at which it may be concluded that the respective sample populations do not derive from the same parent population. Numbers in parentheses are number of samples analyzed in that population.)

Element	H5			L6		
	Ant. (23)	Non (20)	Sig.	Ant. (13)	Non (25)	Sig.
Co (ppm)*				480	600	97
Au (ppb)*				140	160	90
Sb (ppb)	83	69	97			
Se (ppm)*	9.0	8.2	99			
Rb (ppm)	2.0	2.5	97	2.6	2.2	95
Cs (ppb)				4.02	12.4	99
Te (ppb)				340	380	90
Bi (ppb)	2.8	1.1	98	0.58	2.7	99
Ag (ppb)				45	71	97
In (ppb)	0.21	0.49	96			
Tl (ppb)	0.81	0.24	96			
Zn (ppm)*	43	53	96			
Cd (ppb)	0.72	3.7	99	1.6	14.2	99

*Arithmetric means, all others are geometric means: the specific choice is determined by the data distribution in the populations tested. Further information (e.g., standard deviation, etc.) is in Dennison et al. (1986) and Kaczaral and Lipschutz (in prep.).

contemporary falls elsewhere on Earth. From the standpoint of studies of extraterrestrial materials and processes, Antarctic meteorites offer the potential of an enhanced understanding of planetary surfaces, the genesis, evolution, and composition of meteorite planet bodies, and temporal variations in meteorite and cosmic ray fluxes.

Furthermore, since the fall of Antarctic meteorites can be dated, they provide a potential source of information on the ice sheet region with which they are associated. Ancillary measurements, in concert with meteoritic terrestrial ages, could provide information on the ancient trapped atmosphere, ice sheet dynamics, and oxygen isotopic variations, leading to a predictive model for discovering new meteorite concentrations.

ACKNOWLEDGMENTS.—This research would not have been possible except for the aid of the staff of the University of Missouri Research Reactor, irradiation support through DOE grant DEFG 0280 ERR 10725 and research support by NASA grant NAG 9-48 and NSF grants DPP-8111513 and 8415061.

Literature Cited

Biswas, S., H.T. Ngo, and M.E. Lipschutz
1980. Trace Element Contents of Selected Antarctic Meteorites, I: Weathering Effects and ALH A77005, A77257 and A77299. *Zeitschrift für Naturforschung,* 35a:190–196.

Biswas, S., T.M. Walsh, H.T. Ngo, and M.E. Lipschutz
1981. Trace Element Contents of Selected Antarctic Meteorites, II: Comparison with Non-Antarctic Specimens. *Memoirs of the National Institute of Polar Research (Japan),* special issue 20:221–228.

Bull, C.B.B., and M.E. Lipschutz
1982. Workshop on Antarctic Glaciology and Meteorites. *Lunar and Planetary Institute Technical Report,* 82-03:22.

Clarke, R.S., Jr.
1986. Antarctic Iron Meteorites: An Unexpectedly High Proportion of Falls of Unusual Interest. *In* J.O. Annexstad, L. Schultz, and H. Wänke, editors, Workshop on Antarctic Meteorites. *Lunar and Planetary Institute Technical Report,* 86-01:28–29.

Dennison, J.E., and M.E. Lipschutz
In prep. a. Chemical Studies of H Chondrites—II: Weathering of Antarctic Samples.
In prep. b. Chemical Studies of H Chondrites—III: Antarctic H4-6 Samples.

Dennison, J.E., D.W. Lingner, and M.E. Lipschutz
1986. Antarctic and Non-Antarctic Meteorites for Different Populations. *Nature,* 319:390–393.

Dodd, R.T.
1981. *Meteorites, A Petrologic-Chemical Synthesis.* 368 pages. Cambridge, England: Cambridge University Press.

Fulton, C.R., and J.M. Rhodes
1984. The Chemistry and Origin of the Ordinary Chondrites: Implications from Refractory-Lithophile and Siderophile Elements. *In* Proceedings of the Fourteenth Lunar and Planetary Science Conference. *Journal of Geophysical Research,* 89(supplement): B543–B558.

Graham, A.L., A.W.R. Bevan, and R. Hutchison
1985. *The Catalogue of Meteorites.* 4th edition, 460 pages. London: British Museum.

Kaczaral, P.W., and M.E. Lipschutz
In prep. Chemical Studies of L Chondrites, IV: Antarctic L4-6 Chondrites and Their Origin.

Kusunoki, K.
1975. A Note on the Yamato Meteorites Collected in December 1969. *Memoirs of the National Institute of Polar Research* (Japan), special issue, 5:1–8.

Lipschutz, M.E.
1982. Weathering Effects in Antarctic Meteorites. *In* U.B. Marvin and B. Mason, editors, Catalog of Meteorites from Victoria Land, Antarctica, 1978–1980. *Smithsonian Contributions to the Earth Sciences*, 24:67–69.

Marsden, B.G.
1985. *Minor Planet Circular*, 10063.

Marvin, U.B.
1983. The Discovery and Initial Characterization of Allan Hills 81005: The First Lunar Meteorite. *Geophysical Research Letters*, 10:775–778.

Mason, B., and K. Yanai
1983. A Review of the Yamato-74 Meteorite Collection. *Memoirs of the National Institute of Polar Research* (Japan), special issue, 30:7–28.

Scott, E.R.D.
1984. Pairing of Meteorites Found in Victoria Land, Antarctica. *Memoirs of the National Institute of Polar Research* (Japan), special issue, 35:102–125.

Tedesco, E.F.
1984. IRAS Asteroid Workshop No. 3. *Jet Propulsion Laboratory (Pasadena) Report*, D-1617.

Wetherill, G.W.
1974. Solar System Sources of Meteorites and Large Meteoroids. *Annual Review of Earth and Planetary Science*, 2:303–331.

Yanai, K., and H. Kojima
1984. Lunar Meteorites in Japanese Collection of the Yamato Meteorites. *Meteoritics*, 19:342–343.

13. Pairing of Meteorites from Victoria Land and the Thiel Mountains, Antarctica

Edward R.D. Scott

Introduction

The identification of meteorite specimens that belong to the same fall is useful for a variety of reasons: it minimizes unnecessary duplication of research, waste of specimens, and conserves curatorial resources. It can also improve our understanding of the mechanisms that preserve and transport meteorites in Antarctica. This article reviews what is known about possible pairings among Victoria Land and Thiel Mountains specimens and is based largely on lists of paired specimens in the *Antarctic Meteorite Newsletters* and a previous review (Scott, 1984b). The Newsletter lists were compiled largely by R.A. Score, B. Mason, and C. M. Schwarz from their own petrologic studies of thin sections and specimen exteriors. Estimates of the reliability of these pairings are included here, as well as an assessment of the number of unidentified pairings.

Coordinates of the discovery locations of -76 to -78 specimens have been published by Yanai (1982, 1984). Discovery locations have not been published for other specimens, except for 18 Reckling Peak samples found during the 1979–1980 season (Cassidy and Rancitelli, 1982). However, geographic propinquity is only one guide to pairing as Antarctic specimens found less than a meter apart may belong to different falls, whereas specimens recovered 20 km apart may be paired. In addition, it is likely that strong winds can transport even 200-gram specimens over distances of many kilometers (Scott, 1984b).

Table 13-1 lists all proposed pairings among Victoria Land and Thiel Mountains specimens (excluding typographical errors in the *Antarctic Meteorite Newsletters*). Estimates of the reliability of these pairings were made by evaluating the criteria used for pairing, and by comparing studies of paired specimens using different techniques (Scott, 1984b). For type 3 ordinary chondrites, irons, most achondrites, and carbonaceous chondrites, which are all relatively uncommon, there is general agreement between different investigators. However, for many type 4 to type 6 ordinary chondrites, and some polymict eucrites, mesosiderites, and CM2 chondrites, there are disagreements among petrologists and noble gas and cosmogenic nuclide analysts. In most cases, proposed pairings have not been tested by other investigators, so that there are considerable uncertainties in many of the confidence levels listed in Table 13-1.

With the exception of cosmogenic nuclide studies, there have been few investigations of chemical and mineralogical variations in large (multikilogram) meteorites. This enhances the difficulties in pairing Antarctic specimens, especially for brecciated meteorites such as the polymict eucrites. We do not know whether, for example, a 15% difference in the plagioclase content of then sections of two polymict eucrites or a 40% difference in the Cr concentrations of 2-gram samples of two ordinary chondrites provides good evidence against pairing.

Table 13-1 also includes one to four references for each group of paired specimens; additional references are given in Scott (1984b). Where possible, references are placed opposite the specimens to which they refer, but in some cases a paper may also refer to specimens on different lines of the same pairing group. A numerical list of the specimens in Table 13-1 is given in Table 13-2 together with the pair number and confidence level given in Table 13-1. These tables show that the proportion of specimens with suggested pairings from a given field season has decreased from 1977 to 1981: 75% of the 102 ALHA77- samples classified by Score et al. (1982b) are listed in the pairing tables, but only 22% of the 313 characterized ALHA81- specimens. This is partly because field investigators since Cassidy (1980) have not published suggested pairings, but also because the preliminary examination teams have begun to concentrate their efforts on identifying pairs of the rarer meteorites. This change is reasonable as few researchers study type 4-6 ordinary chondrites, and pairings among rarer meteorites are easier to identify. The proportion of types 4–6 ordinary chondrites among lists of paired specimens is 75% for pairing lists published in 1982 and 1983 (*Antarctic Meteorite Newsletter*, 5(1) and 6(2)), close to the

Edward R.D. Scott, Department of Geology and Institute of Meteoritics, University of New Mexico, Albuquerque, New Mexico 87131.

TABLE 13-1.—Meteorite specimens that have been paired and the confidence levels of these pairings (confidence level: a = high (>95%); b = medium (80%–90%; c = low (50%–75%); x = unpaired or highly uncertain pairing).

Pair number	Specimens	Confidence level	References
UNGROUPED METEORITES			
1.1	ALHA77081, 81261, 81315	a	Mason, 1985
EUCRITES AND HOWARDITES			
2.1	ALHA76005, 77302, 78040, 78132, 78158, 78165, 79017, 81009	a	Score, King, et al., 1982; Schultz, 1985
	80102, 81006–81008, 81010, 81012	b	Delaney et al., 1984
	81001	c	Delaney and Prinz, Chapter 8
2.2a	EETA79004, 79011, 83228, 83229, 83231, 83232, 83234, 83251, 83283	b	Delaney et al., 1984; Delaney and Prinz, Chapter 8
2.2b	EETA79005, 79006, 82600, 83227, 83235	b	Delaney et al., 1984; Delaney and Prinz, Chapter 8
Alternative view			
2.2a	EET83231, 83232	a	Mason et al., Chapter 6
	79004	b	Mason et al., Chapter 6
2.2b	EETA79011, 83229, 83234, 83283	c	Mason et al., Chapter 6
2.2c	EETA79005, 79006, 82600, 83212, 83227, 83228, 83235, 83251	c	Mason et al., Chapter 6
AUBRITES			
3.1	ALH83009, 83015	a	Delaney, 1985; Mason et al., Chapter 6
3.2	ALH84007, 84008, 84011	b	MacPherson, 1985b; Mason et al., Chapter 6
3.3	EET83246, 83247	x	B. Mason, pers. communication
UREILITES			
3.4	ALHA78019, 78262	c	Score et al., 1981; Score, King, et al., 1982; Berkley and Jones, 1982
3.5	ALH82106, 82130	a	Mason, 1984b
MESOSIDERITES			
4.1	ALHA77219, 81059, 81098	b	Mason, 1983a,b; Hewins, 1984
4.2	RKPA79015, 80229, 80246, 80258, 80263	b	Clarke and Mason, 1982
IRONS, GROUP IA			
5.1	ALHA76002, 77250, 77263, 77289, 77290, 77283	a	Clarke et al., 1980
		x	Malvin et al., 1984
IRONS, GROUP IIB			
5.2	DRPA78001–78016	a	Clarke, 1982
CM2 CHONDRITES			
6.1	ALHA81002, 81004, 82100	b	McSween, Chapter 9
	78261, 82131, 83016	c	Mason, 1983a; McSween, Chapter 9
	77306	x	Score, King, et al., 1982
6.2	ALH83100, 83102, 84029–84032, 84034, 84042, 84044	b	MacPherson, 1985a,b
CO3 CHONDRITES			
6.3	ALHA77003, 82101	x	Scott, 1984b; Wieler et al., 1985
CV3 CHONDRITES			
9.10	ALHA81003, 81258	c	Mason, 1985
EH3/4 CHONDRITES			
7.1	ALHA77156, 77295	a	McKinley and Keil, 1984;
	81189	x	Wieler et al., 1985; this work
E6 CHONDRITES			
7.2	ALHA81021, 81260	c	Mason, 1985

TABLE 13-1.—Continued.

Pair number	Specimens	Confidence level	References
H4 CHONDRITES			
8.1	ALHA77004, 77190–77192, 77208, 77223–77226, 77232, 77233	b	Cassidy, 1980
	77221	c	Scott, 1984b
8.2	ALHA77009, 81022	c	Score et al., 1984; Mason, 1983a
	78084	x	Scott, 1984b; Sarafin et al., 1985
8.3	ALHA78193, 78196, 78223	b	Anonymous, 1981
8.4	ALHA80106, 80121, 80128, 80131	c	Mason and Clarke, 1982
8.5	ALHA81041, 81043–81052	c	Score, 1983; Mason, 1983b
8.6	RKPA80237, 80267	b	Mason and Clarke, 1982
	80232	x	Scott, 1984b
H5 CHONDRITES			
9.1	ALHA77014, 77264	c	Cassidy, 1980
9.2	ALHA77021, 77025, 77061, 77062, 77064, 77071, 77074, 77086, 77088, 77102	c	Cassidy, 1980;
		x	Score et al., 1981
9.3	ALHA77118, 77119, 77124	c	Cassidy, 1980
9.4	ALHA78209, 78221, 78225, 78227, 78233	b	Anonymous, 1981
9.5	ALHA79031, 79032	b	Score et al., 1981
9.6	ALHA80111, 80124, 80127, 80129, 80132	c	Mason and Clarke, 1982; Vogt et al., 1985
9.7	RKPA80217, 80218	c	Score, Schwarz, et al., 1982
9.8	RKPA80220, 80223	c	Score, Schwarz, et al., 1982
9.9	RKPA80250, 80251	c	Score, Schwarz, et al., 1982
9.10	TIL82412, 82413	c	Mason, 1984b
9.11	TIL82414, 82415	c	Mason, 1984b
H6 CHONDRITES			
10.1	ALHA77144, 77148	c	Cassidy, 1980
10.2	ALHA77271, 77288	a	Cassidy, 1980; Scott, 1984b
10.3	ALHA78211, 78213, 78215, 78229, 78231	b	Anonymous, 1981
10.4	ALHA80122, 80126, 80130	c	Mason and Clarke, 1982
10.5	ALHA81035, 81038, 81103, 81112	c	Mason, 1983a,b; Anonymous, 1984
10.6	MBRA76001, 76002	a	Weber and Schultz, 1980
10.7	RKPA80203, 80206, 80208, 80211, 80213, 80214, 80221, 80254, 80255, 80265, 80266	b	Mason and Clarke, 1982
	80231, 80262	c	Scott, 1984b
10.8	EET82610, 82615	c	Mason, 1984b
10.9	PCA 82526, 82527	c	Mason, 1984b
11.1	ALHA77011, 77015, 77031, 77033, 77034, 77036, 77043, 77047, 77049, 77050, 77052, 77115, 77140, 77160, 77163–77167, 77170, 77175, 77178, 77185 77211, 77214, 77241, 77244, 77249, 77260, 77303, 78013, 78015, 78017, 78037, 78038, 78041, 78162, 78170, 78176, 78180, 78186, 78188, 78235, 78236, 78238, 78239, 78243, 79001, 79045, 80133, 81025, 81030–81032, 81053, 81060, 81061, 81065, 81066, 81069, 81085, 81087, 81121, 81145, 81156, 81162, 81190, 81191, 81214, 81229, 81243, 81259, 81272, 81280, 81292, 81299	a	McKinley et al., 1981; Scott, 1984b, this work; Nishiizumi et al., 1983; Wieler et al., 1985
11.2	ALHA77215–77217, 77252	a	Score, 1980; Nautiyal et al., 1982
11.3	RKPA79008, 80207	x	Wieler et al., 1985; this work
L4 CHONDRITES			
12.1	RKPA80216, 80242	b	Score, Schwarz, et al., 1982

TABLE 13-1.—Continued.

Pair number	Specimens	Confidence level	References
L5 CHONDRITES			
13.1	ALHA81018, 81023	c	Mason, 1983a
	81017	x	Marvin, Chapter 14
13.2	PCA82504, 82505	c	Mason, 1984a
13.3	RKPA80209, 80228, 80268	c	Mason and Clarke, 1982
L6 CHONDRITES			
14.1	ALHA76003, 76007	x	Weber and Schultz, 1980
14.2	ALHA77001, 77292, 77293, 77296, 77297	b	Cassidy, 1980
	77150, 77180, 77305	x	Anonymous, 1984; Scott 1984b
14.3	ALHA77272, 77273	a	Cassidy, 1980
	77280, 77282	b	Goswami and Nishiizumi, 1983
	77231, 77269, 77270, 77277, 77281, 77284	x	Anonymous, 1984; Scott, 1984b
14.4	ALHA78043, 78045	b	Score et al., 1981
14.5	ALHA78103, 78105	b	Anonymous, 1984
	78104, 78251	x	Scott, 1984a
14.6	ALHA78112, 78114	x	Score et al., 1981; Nishiizumi et al., 1983
14.7	ALHA78126, 78130, 78131	x	Score et al., 1981; Scott, 1984b
14.8	ALHA80101, 80103, 80105, 80107, 80108,	a	Score, Schwarz, et al., 1982; Mason and Clarke, 1982
	80110, 80112–80117, 80119, 80120,	b	Marvin, Chapter 14
	80125, 81017, 81107, 81262		
14.9	ALHA81027–81029	b	Mason, 1983a,b
14.10	BTNA78001, 78002	a	Score et al., 1981; R. Score, pers. communication
14.11	EET82605, 82606	c	Mason, 1984a
14.12	RKPA78001, 78003	b	Score et al., 1981
	79001, 79002, 80202, 80219, 80225,	c	Mason and Clarke, 1982; Scott, 1984b
	80252, 80261, 80264		
LL3 CHONDRITES			
15.1	ALHA76004, 81251	b	Scott, 1984b; Wieler et al., 1985
LL6 CHONDRITES			
16.1	RKPA80238, 80248	a	Mason and Clarke, 1982
	80222	b	Sarafin and Herpers, 1983; Signer et al., 1983

proportion among falls, 68% (Wasson, 1974). However, in two recent lists (*Antarctic Meteorite Newsletter*, 7(2) and 8(1)), the proportion is only 25%.

Another measure of the concentration of effort on the rarer meteorites is the number of proposed pairings of specimens collected in different years. For the types 4-6 ordinary chondrites in Table 13-1, only three of 43 pairing groups contain specimens found in different years. However, for the remaining meteorites, the corresponding figure is 13 out of 23 pairing groups. It is likely that most of the paired specimens among type 3 chondrites (Scott, 1984a), polymict eucrites (Delaney and Prinz, 1984), and other rarer meteorite types have been identified. By contrast, it is certain that for types 4–6 ordinary chondrites, most of the paired specimens have not been recognized.

Justifiably, no attempts have been made to identify paired specimens among the 120 ALHA77- and 21 ALHA78- small specimens of types 4–6 ordinary chondrites that were classified by McKinley and Keil (1984) and by S.J.B. Reed and S.O. Agrell (*Antarctic Meteorite Newsletter* 7(1), 1984).

To illustrate the importance of identifying paired specimens, it is noted that petrologic descriptions of what are very probably a set of paired L3 chondrites have been published under various meteorite names: ALH-77015 (Nagahara, 1981; Fujimake et al., 1981), ALH-77294 (Kimura, 1983), and ALHA77011 (McKinley et al., 1981). The Nomenclature Committee of the Meteoritical Society recommends that the lowest specimen number be adopted as the meteorite name (Graham, 1980). However, in some cases the number of the largest or best-distributed specimen may be a more appropriate meteorite name. To distinguish specimen and meteorite names, it may be useful to italicize the latter. Since no two Antarctic specimens can be paired with complete certainty unless they fit together like pieces of a jigsaw puzzle, it is important that specimen numbers of analyzed paired samples should be published, in addition to the meteorite name.

TABLE 13-2.—Numerical list of meteorite specimens that have been paired and the confidence level of these pairings (confidence level: a = high; b = medium, c = low; x = unpaired or highly uncertain pairing).

Specimen number	Pair number	Confidence level
ALHA		
76002	5.1	a
76003	14.1	x
76004	15.1	b
76005	2.1	a
76007	14.1	x
77001	14.2	b
77003	6.3	x
77004	8.1	b
77009	8.2	c
77011	11.1	a
77014	9.1	c
77015	11.1	a
77021	9.2	c
77025	9.2	c
77031	11.1	a
77033	11.1	a
77034	11.1	a
77036	11.1	a
77043	11.1	a
77047	11.1	a
77049	11.1	a
77050	11.1	a
77052	11.1	a
77061	9.2	c
77062	9.2	c
77064	9.2	c
77071	9.2	c
77074	9.2	c
77081	1.1	a
77086	9.2	c
77088	9.2	c
77102	9.2	x
77115	11.1	a
77118	9.3	c
77119	9.3	c
77124	9.3	c
77140	11.1	a
77144	10.1	c
77148	10.1	c
77150	14.2	x
77156	7.1	a
77160	11.1	a
77163–77167	11.1	a
77170	11.1	a
77175	11.1	a
77178	11.1	a
77180	14.2	x
77185	11.1	a
77190–77192	8.1	b
77208	8.1	b
77211	11.1	a
77214	11.1	a
77215–77217	11.2	a
77219	4.1	b
77221	8.1	c
77223–77226	8.1	b
77231	14.3	x
ALHA (continued)		
77232	8.1	b
77233	8.1	b
77241	11.1	a
77244	11.1	a
77249	11.1	a
77250	5.1	a
77252	11.2	a
77260	11.1	a
77263	5.1	a
77264	9.1	c
77269	14.3	x
77270	14.3	x
77271	10.2	a
77272	14.3	a
77273	14.3	a
77277	14.3	x
77280	14.3	b
77281	14.3	x
77282	14.3	b
77283	5.1	x
77284	14.3	x
77288	10.2	a
77289	5.1	a
77290	5.1	a
77292	14.2	b
77293	14.2	b
77295	7.1	a
77296	14.2	b
77297	14.2	b
77302	2.1	a
77303	11.1	a
77305	14.2	x
77306	6.1	x
78013	11.1	a
78015	11.1	a
78017	11.1	a
78019	3.4	c
78037	11.1	a
78038	11.1	a
78040	2.1	a
78041	11.1	a
78043	14.4	b
78045	14.4	b
78084	8.2	x
78103	14.5	b
78104	14.5	x
78105	14.5	b
78112	14.6	x
78114	14.6	x
78126	14.7	x
78130	14.7	x
78131	14.7	x
78132	2.1	a
78158	2.1	a
78162	11.1	a
78165	2.1	a
78170	11.1	a

TABLE 13-2.—Continued.

Specimen number	Pair number	Confidence level
ALHA (continued)		
78176	11.1	a
78180	11.1	a
78186	11.1	a
78188	11.1	a
78193	8.3	b
78196	8.3	b
78209	9.4	b
78211	10.3	b
78213	10.3	b
78215	10.3	b
78221	9.4	b
78223	8.3	b
78225	9.4	b
78227	9.4	b
78229	10.3	b
78231	10.3	b
78233	9.4	b
78235	11.1	a
78236	11.1	a
78238	11.1	a
78239	11.1	a
78243	11.1	a
78251	14.5	x
78261	6.1	c
78262	3.4	c
79001	11.1	a
79017	2.1	a
79031	9.5	b
79032	9.5	b
79045	11.1	a
80101	14.8	b
80102	2.1	b
80103	14.8	b
80105	14.8	b
80106	8.4	c
80107	14.8	b
80108	14.8	b
80110	14.8	b
80111	9.6	c
80112–80117	14.8	b
80119	14.8	b
80120	14.8	b
80121	8.4	c
80122	10.4	c
80124	9.6	c
80125	14.8	b
80126	10.4	c
80127	9.6	c
80128	8.4	c
80129	9.6	c
80130	10.4	c
80131	8.4	c
80132	9.6	c
80133	11.1	a
81001	2.1	b
81002	6.1	b
81003	6.4	c
ALHA (continued)		
81004	6.1	b
81006–81008	2.1	b
81009	2.1	a
81010	2.1	b
81012	2.1	b
81017	13.1	x
	14.8	b
81018	13.1	c
81021	7.2	c
81022	8.2	c
81023	13.1	c
81025	11.1	a
81027–81029	14.9	b
81030–81032	11.1	a
81035	10.5	c
81038	10.5	c
81041	8.5	c
81043–81052	8.5	c
81053	11.1	a
81059	4.1	b
81060	11.1	a
81061	11.1	a
81065	11.1	a
81066	11.1	a
81069	11.1	a
81085	11.1	a
81087	11.1	a
81098	4.1	b
81103	10.5	c
81107	14.8	b
81112	10.5	c
81121	11.1	a
81145	11.1	a
81156	11.1	a
81162	11.1	a
81189	7.1	x
81190	11.1	a
81191	11.1	a
81214	11.1	a
81229	11.1	a
81243	11.1	a
81251	15.1	b
81258	6.4	c
81259	11.1	a
81260	7.2	c
81261	1.1	a
81262	14.8	b
81272	11.1	a
81280	11.1	a
81292	11.1	a
81299	11.1	a
81315	1.1	a
82100	6.1	b
82101	6.3	x
82106	3.5	a
82130	3.5	a
82131	6.1	c
83009	3.1	a

TABLE 13-2.—Continued.

Specimen number	Pair number	Confidence level
ALHA (continued)		
83015	3.1	a
83016	6.1	c
83100	6.2	b
83102	6.2	b
84007	3.2	b
84008	3.2	b
84011	3.2	b
84029–84032	6.2	b
84034	6.2	b
84042	6.2	b
84044	6.2	b
BTNA		
78001	14.10	a
78002	14.10	a
DRPA		
A78001–78016	5.2	a
EETA		
79004–79006	2.2	b
79011	2.2	b
82600	2.2	b
82605	14.11	c
82606	14.11	c
82610	10.8	c
82615	10.8	c
83227–83229	2.2	b
83231	2.2	b
83232	2.2	b
83234	2.2	b
83235	2.2	b
83246	3.3	x
83247	3.3	x
83251	2.2	b
83283	2.2	b
MBRA		
76001	10.6	a
76002	10.6	a
PCA		
82504	13.2	c
82505	13.2	c
82526	10.9	c
82527	10.9	c
RKPA		
78001	14.12	b
78003	14.12	b
RKPA (continued)		
79001	14.12	c
79002	14.12	c
79008	11.3	x
79015	4.2	b
80202	14.12	c
80203	10.7	b
80206	10.7	b
80207	11.3	x
80208	10.7	b
80209	13.3	c
80211	10.7	b
80213	10.7	b
80214	10.7	b
80216	12.1	b
80217	9.7	c
80218	9.7	c
80219	14.12	c
80220	9.8	c
80221	10.7	b
80222	16.1	b
80223	9.8	c
80225	14.12	c
80228	13.3	c
80229	4.2	b
80231	10.7	c
80232	8.6	x
80237	8.6	b
80238	16.1	a
80242	12.1	b
80246	4.2	b
80248	16.1	a
80250	9.9	c
80251	9.9	c
80252	14.12	c
80254	10.7	b
80255	10.7	b
80258	4.2	b
80261	14.12	c
80262	10.7	c
80263	4.2	b
80264	14.12	c
80265	10.7	b
80266	10.7	b
80267	8.6	b
80268	13.3	c
TIL		
82412	9.10	c
82413	9.10	c
82414	9.11	c
82415	9.11	c

Pairing Notes

Pair Number 2.2

There is some disagreement on the classification and pairing of the 16 eucrites, polymict eucrites and howardites that have been recovered from Elephant Moraine. On the basis of pyroxene analyses, Mason et al. (this volume) believe that 15 specimens come from three different falls; EET83236 may be unpaired. Delaney and Prinz (this volume) argue instead, from their petrographic studies, that 14 of these 15 specimens belong to two falls; they exclude EET83212 because the section studied appeared atypical. Both pairing schemes are listed in Table 13-1. EETA79005, 79006 and 82600, which are paired by both groups, have similar terrestrial and cosmic-ray exposure ages of 0.17–0.19 and 26–28 million years, confirming their pairing (Schultz, 1985). Schultz believes, as do Delaney and Prinz, and Mason et al. that EETA79004 is not paired with these three; its terrestrial and exposure ages are 0.25 and 22 million years.

Pair Number 7.1

Concentrations of spallogenic noble gases in two EH3/4 chondrites, ALHA77156 and ALHA77295, are very similar (Weiler et al., 1985), confirming their pairing on petrographic grounds by McKinley and Keil (1984). Since they were found 18 km apart, this additional evidence for pairing is valuable. Petrologic studies by Prinz et al. (1985) show that ALHA81189 is a highly unequilibrated enstatite chondrite like 77156. However, their modal analyses suggest that 81189 has a much higher abundance of olivine (8% cf. 2% in 77156) and is not paired.

Pair Number 11.1

Confirmation that ALHA77047, 78015, 81030–81032, and 81121 are paired with many other L3 specimens that contain abundant graphite-magnetite aggregates is provided by their concentrations of spallogenic and trapped noble gases (Weiler et al., 1985). These authors also confirm that ALHA81024 is not part of this meteorite shower, even though it also contains abundant graphite-magnetite aggregates (Scott, 1984b). There are seven other unpaired L3 specimens from Allan Hills in United States collections: 77013, 77176, 77197, 78046, 78119, 78133, and 83010. Wieler et al. (1985) have analyzed all but 78046, 78119, and 83010, and their data support this conclusion.

Pair Number 11.3

RKPA79008 and 80207, which were originally classified as L3 chondrites (Score et al., 1982b, 1984), contain similar concentrations of spallogenic ^{21}Ne, and concentrations of solar wind noble gases that are within a factor of two. Since only two other Antarctic and six non-Antarctic L chondrites are known to contain solar wind gases, the suggestion of Wieler et al. (1985) that these two Reckling Peak specimens are paired would appear very likely. However, RKPA80207 is probably an H3 chondrite, as the great majority of its olivine grains have compositions appropriate to equilibrated H chondrites (Scott, 1984a). In RKPA79008, by contrast, most olivines have compositions like those of equilbrated L chondrites. Since chondrites having materials with the compositions of both equilibrated H and L chondrites are not known, it is more likely that these two specimens are not paired.

Pair Number 15.1

The presence of rather similar concentrations of spallogenic and trapped noble gases in the LL3 chondrites, ALHA76004 and 81251, supports their pairing (Wieler et al., 1985). Although petrographically similar, they have very different degrees of weathering, unlike other paired specimens (Scott, 1984b).

ACKNOWLEDGMENTS.—I thank B. Mason, H.Y. McSween, Jr., R.A. Score, P. Signer, R. Wieler, and other members of the Meteorite Working Group for their helpful assistance. This work was partly supported by NASA grant NAG-9-30 to K. Keil.

Literature Cited

Antarctic Meteorite Newsletter, 4(2):9–10.
Antarctic Meteorite Newsletter, 5(1).
Antarctic Meteorite Newsletter, 6(2).
Antarctic Meteorite Newsletter, 7(1):27–29.
Antarctic Meteorite Newsletter, 7(2).
Antarctic Meteorite Newsletter, 8(1).

Berkley, J.L., and J.H. Jones
1982. Primary Igneous Carbon in Ureilites: Petrological Implications. *Journal of Geophysical Research*, 87(supplement):A353–A364.

Cassidy, W.A.
1980. Discussion. *In* U.B. Marvin and B. Mason, editors, Catalog of Antarctic Meteorites, 1977–1978. *Smithsonian Contributions to the Earth Sciences*, 23:42–44.

Cassidy, W.A., and L.A. Rancitelli
1982. The Traverse to Reckling Peak, 1979–1980. *In* U.B. Marvin and B. Mason, editors, Catalog of Meteorites from Victoria Land, Antarctica, 1978–1980. *Smithsonian Contributions to the Earth Sciences*, 24:9–11.

Clarke, R.S., Jr.
1982. The Derrick Peak, Antarctica, Iron Meteorites. *Meteoritics*, 17:129–134.

Clarke, R.S., Jr., and B. Mason
1982. A New Metal-Rich Mesosiderite from Antarctica, RKPA79015. *Memoirs of the National Institute of Polar Research* (Japan), special issue, 25:78–85.

Clarke, R.S., Jr., E. Jarosewich, J.I. Goldstein, and P.A. Baedecker
1980. Antarctic Iron Meteorites from Allan Hills and Purgatory Peak. *Meteoritics*, 15:273–274.

Delaney, J.S.
1985. [Catalog description.] *Antarctic Meteorite Newsletter*, 8 (1).

Delaney, J.S., M. Prinz, and H. Takeda
1984. The Polymict Eucrites. *Journal of Geophysical Research*, 89(supplement):C251–C288.

Fujimaki, H., M. Matsu-ura, I. Sunagawa, and K. Aoki
1981. Chemical Compositions of Chondrules and Matrices in the

ALH-77015 Chondrite. *Memoirs of the National Institute of Polar Research* (Japan), special issue, 20:161–174.

Goswami, J.N., and K. Nishiizumi
1983. Cosmogenic Records in Antarctic Meteorites. *Earth and Planetary Science Letters*, 64:1–8.

Graham, A.L.
1980. Procedures for Naming Antarctic Meteorites. *Meteoritics*, 15:93–94.

Hewins, R.H.
1984. Pairing in Antarctic Mesosiderites. *Meteoritics*, 19:238.

Kimura, M.
1983. Chemical and Petrologic Relations of the Constituent Units in the ALH-77249 Meteorite (L3). *Memoirs of the National Institute of Polar Research* (Japan), special issue, 30:146–167.

MacPherson, G.J.
1985a. [Catalog description.] *Antarctic Meteorite Newsletter*, 8(1).
1985b. [Catalog description.] *Antarctic Meteorite Newsletter*, 8(2).

Malvin, D.J., D. Wang, and J.T. Wasson
1984. Chemical Classification of Iron Meteorites—X: Multielement Studies of 43 Irons, Resolution of Group IIIE from IIIAB, and Evaluation of Cu as a Taxonomic Parameter. *Geochimica et Cosmochimica Acta*, 48:785–804.

Mason, B.
1983a. [Catalog description.] *Antarctic Meteorite Newsletter*, 6(1).
1983b. [Catalog description.] *Antarctic Meteorite Newsletter*, 6(2).
1984a. [Catalog description.] *Antarctic Meteorite Newsletter*, 7(1).
1984b. [Catalog description.] *Antarctic Meteorite Newsletter*, 7(2).
1985. [Catalog description.] *Antarctic Meteorite Newsletter*, 8(1).

Mason, B., and R.S. Clarke, Jr.
1982. Characterization of the 1980–81 Victoria Land Meteorite Collections. *Memoirs of the National Institute of Polar Research* (Japan), special issue, 25:17–33.

McKinley, S.G., and K. Keil
1984. Petrology and Classification of 145 Small Meteorites from the 1977 Allan Hills Collection. *In* U.B. Marvin and B. Mason, editors, Field and Laboratory Investigations of Meteorites from Victoria Land, Antarctica. *Smithsonian Contributions to the Earth Sciences*, 26:55–71.

McKinley, S.G., E.R.D. Scott, G.J. Taylor, and K. Keil
1981. A Unique Type 3 Ordinary Chondrite Containing Graphite-Magnetite Aggregates—Allan Hills A77011. In *Proceedings of the Twelfth Lunar and Planetary Science Conference*, pages 1039–1048. New York: Pergamon Press.

Nagahara, H.
1981. Petrology of Chondrules in the ALH-77015 (L3) Chondrite. *Memoirs of the National Institute of Polar Research* (Japan), special issue, 20:145–160.

Nautiyal, C.M., J.T. Padia, M.N. Rao, T.R. Venkatesan, and J.N. Goswami
1982. Irradiation History of Antarctic Gas-Rich Meteorites. In *Lunar and Planetary Science XIII*, pages 578–579. Houston: Lunar and Planetary Institute.

Nishiizumi, K., J.R. Arnold, D. Elmore, X. Ma, D. Newman, and H.E. Gove
1983. ^{36}Cl and ^{53}Mn in Antarctic Meteorites and ^{10}Be-^{36}Cl Dating of Antarctic Ice. *Earth and Planetary Science Letters*, 62:407–417.

Prinz, M., M.K. Weisberg, C.E. Nehru, and J.S. Delaney
1985. ALHA81189, A Highly Unequilibrated Enstatite Chondrite: Evidence for a Multistage History. *Meteoritics*, 20:731–732.

Sarafin R., and U. Herpers
1983. Spallogenic ^{26}Al and ^{53}Mn in Antarctic Meteorites and Determination of Exposure and Terrestrial Ages. *Meteoritics*, 18:392.

Sarafin, R., M. Bourot-Denise, G. Crozaz, U. Herpers, P. Pellas, L. Schultz, and H.W. Weber
1985. Cosmic Ray Effects in the Antarctic Meteorite Allan Hills A78084. *Earth and Planetary Science Letters*, 73:171–182.

Schultz, L.
1985. Terrestrial Ages of Antarctic Meteorites: Implications for Concentration Mechanisms. In *Abstracts for Workshop on Antarctic Meteorites*, pages 41–43. Houston: Lunar and Planetary Institute.

Score, R.
1980. Allan Hills 77216: A Petrologic and Mineralogic Description. *Meteoritics*, 15:363.
1983. [Catalog description.] *Antarctic Meteorite Newsletter*, 6(2).

Score, R., T.V.V. King, C.M. Schwarz, A.M. Reid, and B. Mason
1982. Descriptions of Stony Meteorites. *In* U.B. Marvin and B. Mason, editors, Catalog of Meteorites from Victoria Land, Antarctica, 1978–1980. *Smithsonian Contributions to the Earth Sciences*, 24:19–48.

Score, R., C.M. Schwarz, T.V.V. King, B. Mason, D.D. Bogard, and E.M. Gabel
1981. Antarctic Meteorite Descriptions 1976–1977–1978–1979. *Curatorial Branch Publication 54, JSC 17076*. 144 pages. Houston: Johnson Space Center.

Score, R., C.M. Schwarz, and B. Mason
1984. Descriptions of Stony Meteorites. *In* U.B. Marvin and B. Mason, editors, Field and Laboratory Investigations of Meteorites from Victoria Land, Antarctica. *Smithsonian Contributions to the Earth Sciences*, 26:23–47.

Score, R., C.M. Schwarz, B. Mason, and D.D. Bogard
1982. Antarctic Meteorite Descriptions 1980. *Curatorial Branch Publication 60, JSC 18170*. 55 pages. Houston: Johnson Space Center.

Scott, E.R.D.
1984a. Classification, Metamorphism, and Brecciation of Type 3 Chondrites from Antarctica. *In* U.B. Marvin and B. Mason, editors, Field and Laboratory Investigations of Meteorites from Victoria Land, Antarctica. *Smithsonian Contributions to the Earth Sciences*, 26:73–94.
1984b. Pairing of Meteorites Found in Victoria Land, Antarctica. *Memoirs of the National Institute of Polar Research* (Japan), special issue, 35:102–125.

Signer, P., H. Baur, Ph. Etique, and R. Wieler
1983. Light Noble Gases in 15 Meteorites. *Meteoritics*, 18:399.

Vogt, St ., U. Herpers, R. Sarafin, P. Signer, R. Wieler, M. Suter, and W. Wölfli
1985. Cosmic Ray Records in Antarctic Meteorites. In *Abstracts for Workshop on Antarctic Meteorites*, pages 55–57. Houston: Lunar and Planetary Institute.

Wasson, J.T.
1974. Meteorites—Classification and Properties. 316 pages. Heidelberg: Springer-Verlag.

Weber, H.W., and L. Schultz
1980. Noble Gases in Ten Stone Meteorites from Antarctica. *Zeitschrift für Naturforschung*, 35a:44–49.

Wieler, R., H. Baur, Th. Graf, and P. Signer
1985. He, Ne, and Ar in Antarctic Meteorites: Solar Noble Gases in an Enstatite Chondrite. In *Lunar and Planetary Science XVI*, pages 902–903. Houston: Lunar and Planetary Institute.

Yanai, K.
1982. Antarctic Meteorite Distribution Map of Allan Hills Victoria Land, Antarctica—Allan Hills-76, -77 and -78 Meteorites. Tokyo: National Institute of Polar Research.
1984. *Locality Map Series of Antarctic Meteorites, Sheet 1, Allan Hills: Explanatory Text of Local Map of Allan Hills-76, Allan Hills-77 and Allan Hills-78 Meteorites*. Tokyo: National Institute of Polar Research.

14. Meteorite Distributions at the Allan Hills Main Icefield and the Pairing Problem

Ursula B. Marvin

Paired meteorite specimens are fragments of a single body that exploded during flight through the atmosphere and fell to Earth as two or more pieces. All fragments, which may number in the thousands, of the same body are cataloged as a single meteorite. Observations in many parts of the world have shown that fragments from a given meteorite shower fall over an elliptical area in which the largest and heaviest specimens travel farthest along the line of flight to the outer limit of a so-called strewnfield. Outside Antarctica, specimens belonging to the same class of meteorite found in a well-defined strewnfield can be paired with confidence. On the Antarctic stranding surfaces, however, strewnfields emerged from depth will be compressed and deformed to some degree and their specimens mixed with those from other falls. The extent to which distribution patterns can aid in pairing specimens of a given meteorite class on the Antarctic icefields has not previously been investigated.

My approach to this problem was to plot the locations of meteorite fragments on a composite map representing six seasons of collecting on the Allan Hills Main Icefield. I also examined thin sections of tentatively paired specimens and combed the literature on pairing. I found that only on rare occasions is pairing easy in Antarctica. When two or more fragments fit together like pieces of a jigsaw puzzle, as was the case with the pieces in Figure 14-1, they are paired in the field and assigned the same specimen number. Specimens are sometimes paired in the field if they look similar and lie within a few meters of one another without actually fitting together. In general, however, the pairing of Antarctic specimens is fraught with uncertainty. Distribution patterns facilitate pairing mainly by indicating which groups of specimens should be scrutinized for similarities in petrography, trace element compositions, solar flare tracks, or other diagnostic features. Frequently, such scrutiny indicates that specimens found lying side by side are not members of the same shower. In at least one case, however, the opposite proved true: the location of a specimen led to its reclassification as a member of a paired group.

Ursula B. Marvin, Smithsonian Astrophysical Observatory, 60 Garden Street, Cambridge, Massachusetts 02138.

Field Maps

Perhaps the main difficulty in mapping specimen distribution patterns on the Allan Hills Main Icefield, is the lack of a single, accurate base map. For the present study, I compiled distributions from two maps. The first map was published by Yanai (1982) with an explanatory text by Yanai (1984). Yanai plotted approximate specimen locations, from field notes made during the 1976–1977, 1977–1978, and 1978–1979 seasons, on a base prepared from an enlarged satellite photograph of the Allan Hills region. The second base map was an unpublished chart, 1.6 meters long with a scale of about 1:8000, prepared by John O. Annexstad and John W. Schutt to show specimen locations of the 1979–1980, 1980–1981, and 1981–1982 seasons. They measured angular directions from each specimen to flags in the geodetic network described by Annexstad and Annexstad (Chapter 4), and measured distances on snowmobile odometers. Together, the maps of Yanai and of Annexstad and Schutt show the locations of about 900 meteorites on the Main Icefield, a number fully adequate for testing the usefulness of distribution patterns.

Unfortunately, the two maps have no common reference point that can be used to superimpose them precisely. Yanai marked latitudes and longitudes on his map but Annexstad and Schutt did not. The latter authors based their map on a coordinate system measured in meters from geodetic network Stations 1 and 2, which were anchored in bedrock and tied by triangulation to peaks in the Allan Hills. They used a satellite photograph, different from Yanai's, to draw in the outlines of the Allan Hills. Both maps show distortion due to the obliqueness of the satellite photographs. After photocopying the two maps to the same scale, I tested several methods of superimposing them and selected the one that produced the least distortion in the southern and central part of the Main Icefield. These regions are shown in Figures 14-2 to 14-6. In those figures on which all specimens are plotted from either

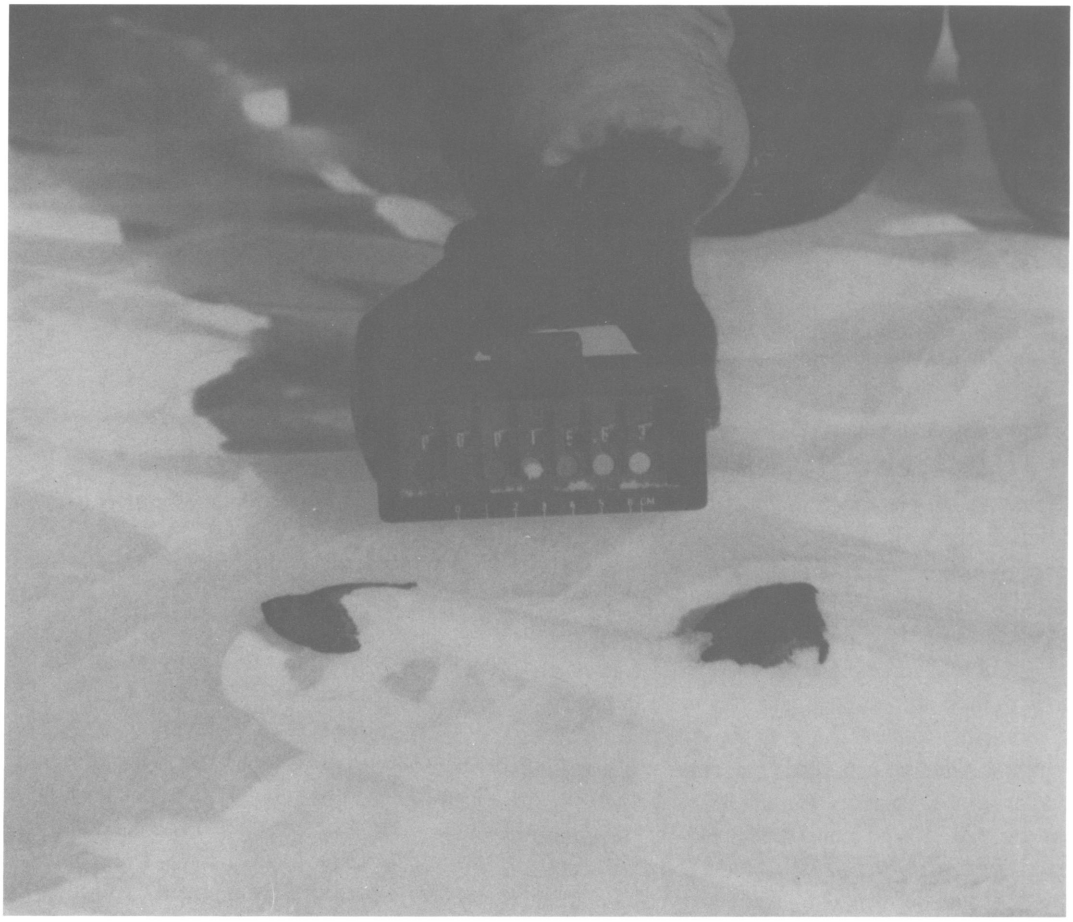

FIGURE 14-1.—Meteorite fragments paired in the field. The two pieces of Allan Hills 81029, a 153 gram L6 chondrite, fitted tightly together along a fractured surface.

Yanai's map or the one by Annexstad and Schutt, the location of each specimen is probably accurate to within a radius of about 100 meters. On those with specimen locations taken from both maps the uncertainty may well involve a radius of up to 2 kilometers. Even with errors of that magnitude, however, it is possible in most cases to see which meteorite fragments occur in clusters and which lie far apart. Figures 14-2 to 14-6 illustrate the distribution patterns of eucrites, ureilites, irons, L3, and L6 chondrites on the Main Icefield, and Figure 14-7 shows that of three mesosiderites found on the Near Western Icefield. Various proposed pairing schemes are indicated and referenced.

Meteorite Distributions

EUCRITES

Beginning in the 1976–1977 season with the discovery of ALHA76005, a 1.4 kg polymict eucrite, a total of 16 eucrite specimens were collected within an area of only about 3.5 × 4.5 kilometers on the Main Icefield (Figure 14-2). Their distribution suggests that all of these fragments belong to the same fall. Some petrologic studies tend to support this interpretation. Delaney, Takeda, and Prinz (1983) tentatively paired 12 of the 16 specimens as polymict eucrites (containing 90% or more of eucritic components) belonging to a group they designated as Allan Hills I. Their second group, Allan Hills II, consisted solely of 78006, a howardite in which no single component makes up 90% of the breccia. Further petrographic analyses led Delaney, Prinz, and Stokes (1984) to designate a third group, Allan Hills III, made up of 81006, 81007, and 81008, specimens they found to contain less feldspar and more pyroxene than they observed in the other members of Group I, and lithic clasts of an apparent pigeonite cumulate not observed in any other eucrites.

Score, Schwarz, and Mason (1984) listed 12 of the 16 specimens as polymict eucrites and paired them on the basis of external appearance and thin section petrography. They tentatively designated 81009 and 81012 as a separate pair because they differ from the other 12 specimens in the range

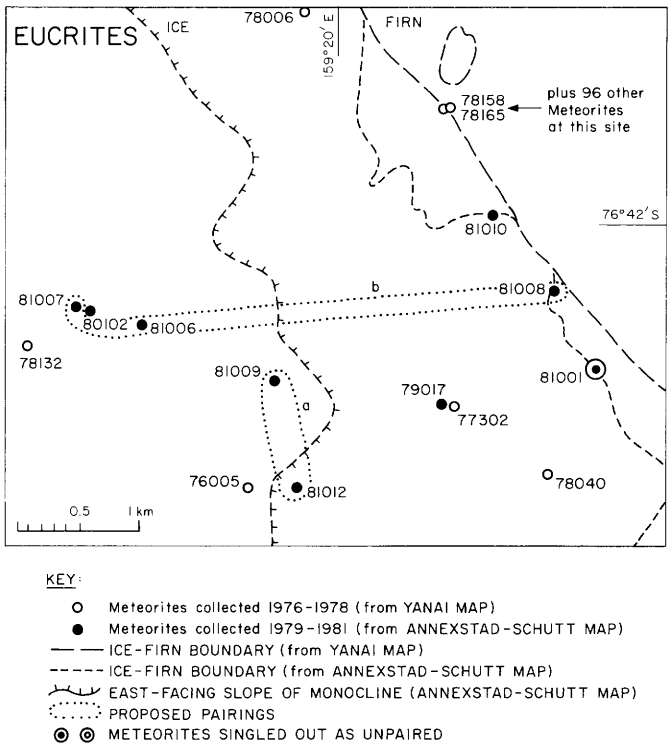

FIGURE 14-2.—The distribution of 16 eucrite specimens and one howardite (78006) on the Main Icefield. Areas outlined by dots include tentatively paired specimens; the shapes of the areas are of no other significance. Pair "a" was proposed by Score, Schwarz, and Mason (1984); pair "b" was proposed by Delaney, Prinz, and Stokes (1984), but later incorporated by Delaney, Prinz, and Takeda (1984) into Allan Hills Group I, which includes all specimens on this map except 81001, the felty glass, and 78006, the howardite. Many specimens belonging to other meteorite classes were also found in this area. For example, the arrow at upper right indicates a site where two eucrites and 96 other stones were collected.

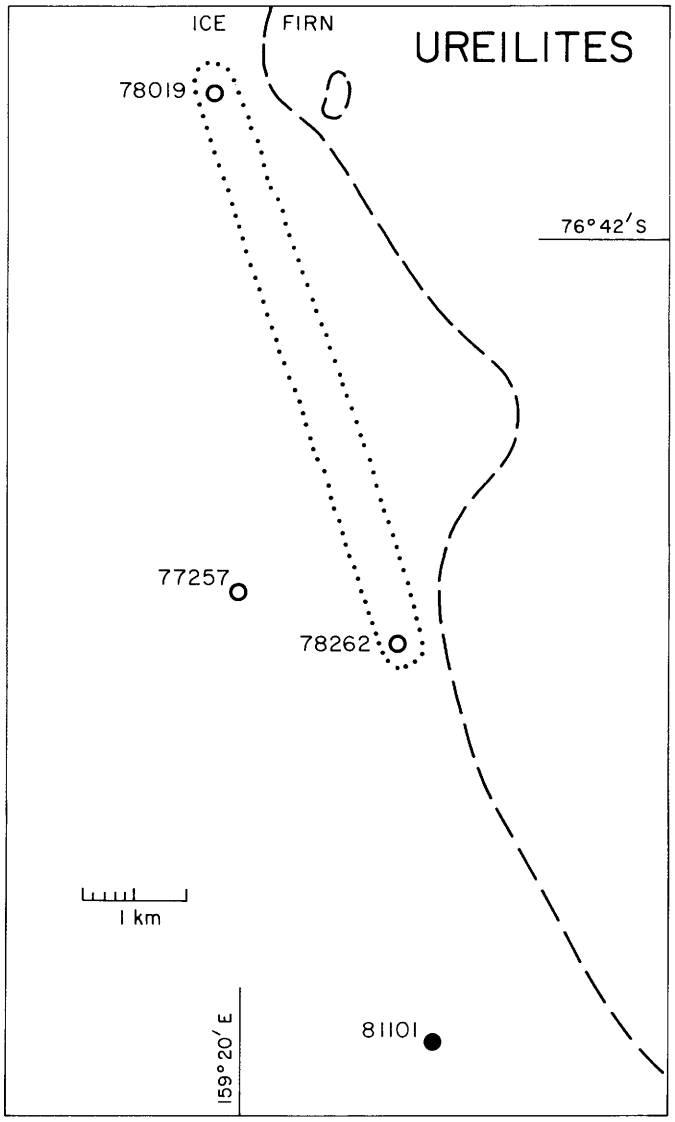

FIGURE 14-3.—Locations of four Allan Hills ureilites. The two closest stones, 77257 and 78262, have not been paired, but 78019 and 78262 were paired by Score et al. (1981). This pairing is disputed by Berkley and Jones (1982). If it is invalid, all four specimens represent separate falls.

and distribution of their pyroxene compositions. The same authors listed 81001 as anomalous, and 81011 (the location of which was not mapped) as a eucritic breccia. They described the anomalous stone, 81001, as consisting of smoky gray glass crowded with felty pyroxene prisms (Score, Schwarz, and Mason, 1984:44, and their figure 49*a*). The bulk composition resembles that of an average eucrite, but no other eucrite has such a texture. However, small clasts of similar material are found within some polymict eucrites. The other unusual stone, 81011, has eucritic clasts up to 1 cm long embedded in a matrix of dark glass and finely crushed plagioclase and pyroxene. The stone looks polymict, but uniform compositions of the plagioclase and pyroxene suggest that it is monomict.

After reviewing the evidence, Delaney, Prinz, and Takeda (1984) concluded that all but two of the eucrites at the Allan Hills probably belong to Group I, a heterogeneous suite in which they included 81009 and 81012 and to which they reassigned 81006, 81007, and 81008. They excluded only the glassy stone, 81001, and the breccia, 81011. Possibly even 81001 should be paired with the main group; its glassy texture may simply represent the chilled margin of a flow or layered body from which the other eucrites originally crystallized.

UREILITES

Four ureilite specimens were found on the Main Icefield by the end of the 1981–1982 season. Without knowledge of their field occurrence, Score et al. (1981) designated 77257 and 78262 as separate falls and paired 78262 with 78019 on the basis of similar external appearance, textures, and olivine and

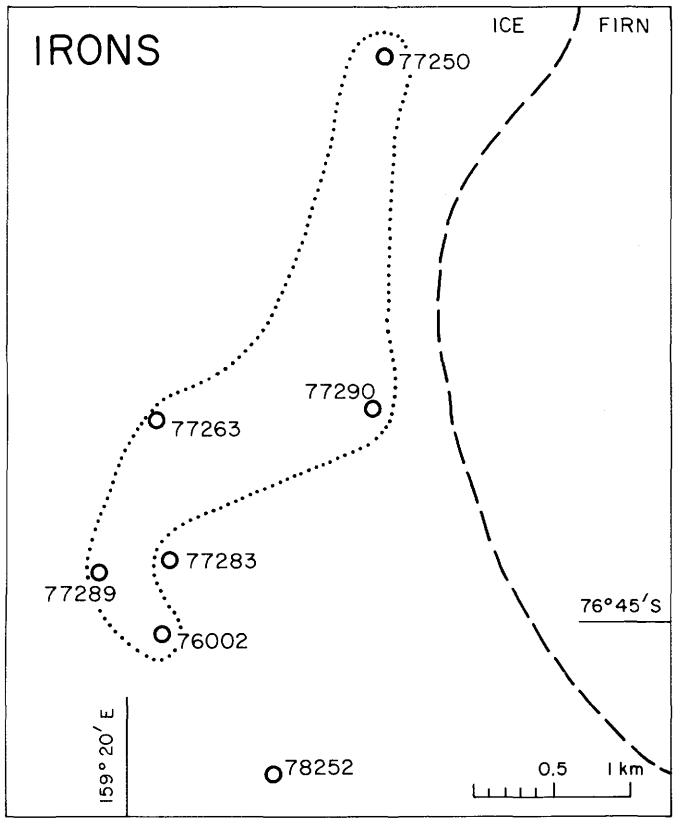

FIGURE 14-4.—Locations of seven iron meteorite specimens. All except 78252 were paired in the field by Cassidy (1980) and later proved to be coarse octahedrites of group IA. Clarke et al. (1980) paired the five irons within the dotted area but separated out 77283 because, although it belongs to the same chemical group, it contains clumps of shock-produced diamond and lonsdaleite. ALHA78252 is a group IVA iron.

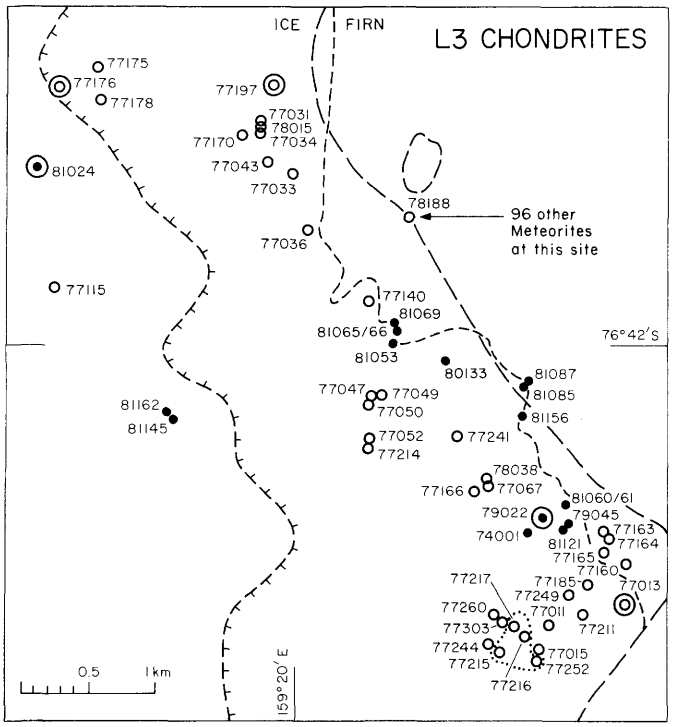

FIGURE 14-5.—The distribution of L3 chondrites on the central and southern portion of the Main Icefield. Other L3 specimens lay farther north, off this map. Unpaired specimens are indicated by extra rings; all others are paired (and designated as the 77011 shower) except for the four specimens lying within the dotted area at lower right, which differ from the others petrographically (Score, 1980; Score et al., 1981) and in containing solar flare tracks (Nautiyal et al., 1982).

pyroxene compositions. Figure 14-3 shows that the first two were found only 1.5 kilometers apart, although in different seasons, and the paired stones were found nearly 5.8 kilometers apart in the same season. Pair 78262 and 78019 is listed in Appendix C, but Berkley and Jones (1982) disputed its validity, arguing that the olivines and pyroxenes in the two stones differ slightly but consistently, and that diamond occurs in 78262 but not in 78019. Petrographic differences between the other stones indicate that, if these two are not paired, then all four ureilites represent individual falls—a surprising situation for such unusual meteorites on a small area of the Icefield, when only about 20 other ureilites have been found throughout the world. Field distribution was of no aid in this case where, if any stones are paired, they are not the two found closest together.

IRONS

Seven specimens of irons were found within the 1.5 × 4.5 km area shown in Figure 14-4. Cassidy (1980) tentatively paired six of them (all except 78252, which lay farthest south) on the basis of their field locations. All of the six are coarse octahedrites belonging to chemical group IA, but Clarke et al. (1980), paired only the five specimens outlined in Figure 14-5, on the basis of identical textures and compositions. The adjacent unpaired specimen, 77283, contains masses of minute shock-produced diamonds admixed with lonsdaleite. The only other iron meteorite known to contain diamonds is Canyon Diablo, a huge body that impacted northern Arizona with sufficient energy to excavate a crater 1.4 kilometers in diameter. The Allan Hills iron, in contrast, is a 10-gram specimen with a thin surficial, heat-altered zone, which shows that it entered the atmosphere as a small body that would have made a soft landing. The diamonds must have formed during a preterrestrial collision in space.

The seventh specimen, 78252, is a group IVA iron. The distribution of these iron meteorites suggested a pairing scheme close to, but not identical with, the one indicated by compositions and textures.

L3 CHONDRITES

Seventy-five L3 chondrite specimens (56 mapped finds and 19 unmapped pebbles) were collected within a 6 × 3 km ellipse on the Main Icefield. The larger fragments were clustered near the southern end of the ellipse and smaller pieces lay at the

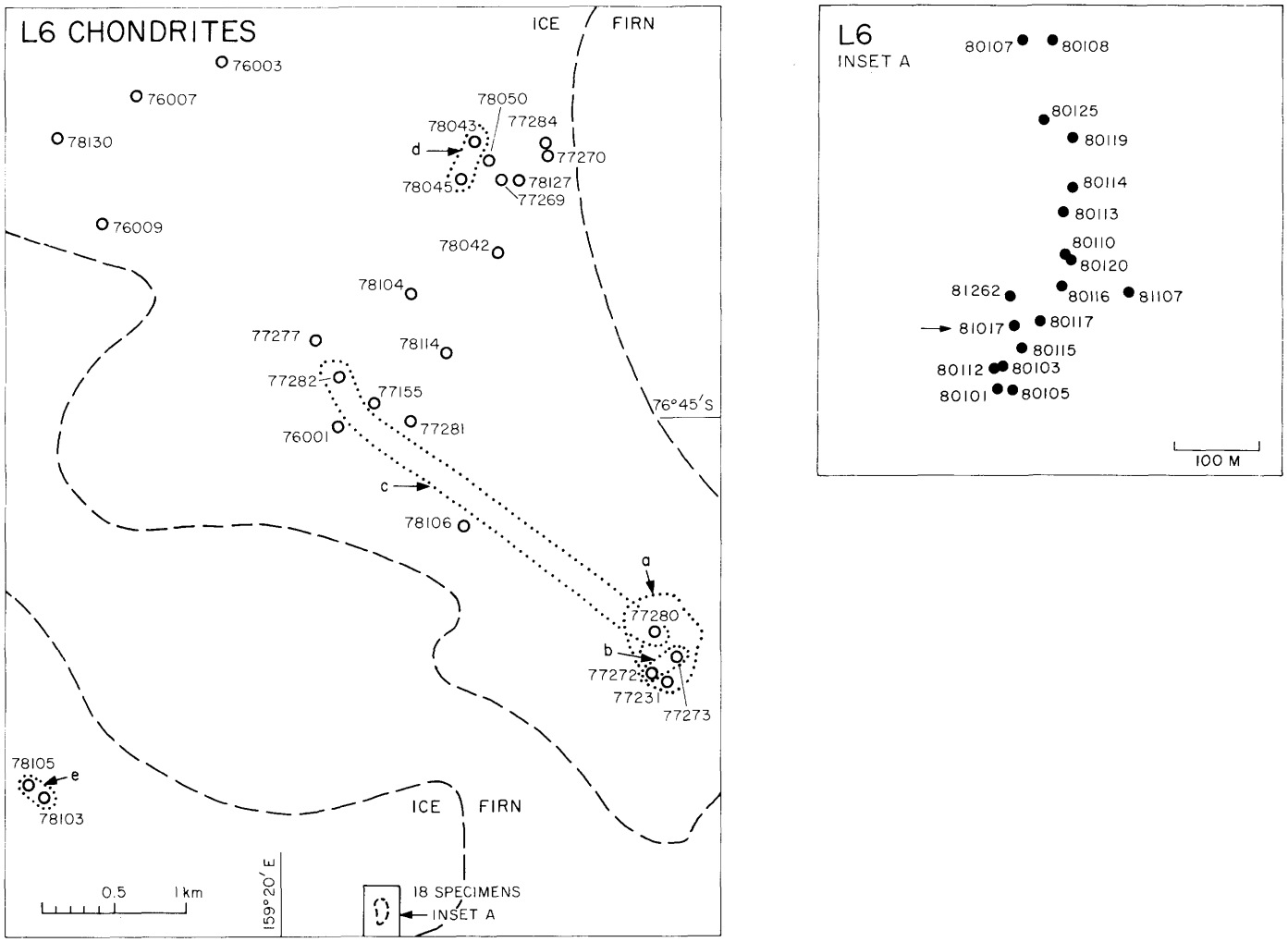

FIGURE 14-6.—The distribution of 44 L6 chondrite specimens that were collected on the central and southern portion of the Main Icefield. Several (but not all) of the proposed pairing schemes are shown. Pair "a" consists of four specimens, 77231, 77273, 77272, and 77280, tentatively paired in the field by Cassidy. All were rather large specimens lying near one another. Pair "b" was separated out on the basis of similar petrography and concentrations of cosmogenic nuclides by Nishiizumi (1984). Specimens 77231 and 77280 differ in nuclide concentrations and cannot be paired with 77272 and 77273; however, Goswami and Nishiizumi (1983) proposed pair "c," 77280 and 77282. Pair "d" was proposed by Score et al. (1981) on petrographic similarities. Pair "e," 78103 and 78105, were found close together in a remote location and they have similar concentrations of ^{26}Al (Evans, Reeves, and Rancitelli, 1982). Inset A shows the location of 18 specimens collected in 1980 and 1981 beyond the southern edge of the Main Icefield. All were classified on petrographic evidence as L6 chondrites, except 81017 (arrow), which was first classed as an L5 and later reclassified as an L6.

ice-firn border at the northern end. This size distribution suggested a strewnfield created by a southbound fireball; however, as noted by Scott (1984) it is more likely that the small fragments were blown to the northern edge of the Icefield by the powerful katabatic winds that course down the surface of the ice sheet from the southern reaches of the polar plateau.

The great majority of these L3 chondrites, large and small, contain distinctive graphite-magnetite aggregates and so were paired by McKinley et al. (1981). However, within a group of nine relatively large specimens lying within an area only 500 meters across, four were shown to belong to a separate fall on the basis of petrography (Score, 1980), and the presence of solar flare tracks (Nautiyal, et al., 1982). Specimen distributions would never suggest the existence of this separate fall (Figure 14-5). Several distinctive, unpaired L3 specimens lie scattered amid the large group.

L6 CHONDRITES

Eighty-five L6 chondrites were collected during the first six seasons on the Main Icefield. Numerous pairing schemes have been proposed and almost all of them are disputed. The map

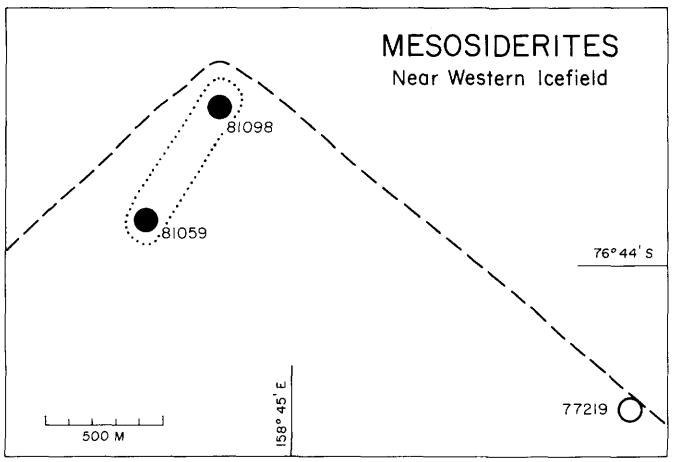

FIGURE 14-7.—The only mesosiderites found in the Allan Hills region lay within 2.25 kilometers of each other on the Near Western Icefield. 81098 consisted of two adjacent pieces that were paired in the field; 81059 was added to the pair after laboratory examination. Although mesosiderites tend to be markedly inhomogeneous, 77219 is regarded as a separate fall.

in Figure 14-6*a*, which includes only the area toward the southern end of the field, shows find locations of 44 specimens and five of the proposed pairings. The four specimens (77272, 77273, 77231, and 77280) at the southeastern part of the field were tentatively paired in the field by Cassidy (1980). Six others (77282, 77269, 77270, 77277, 77281, and 77284) were paired with these four in the *Antarctic Meteorite Newsletter*, 7(1) (1984). Two specimens (77272 and 77273) of Cassidy's original four are still accepted as a pair, but differences in ^{53}Mn concentrations and cosmic-ray track densities, measured by Goswami and Nishiizumi (1983), indicate that 77273 and 77280 cannot be paired with each other even though they were found only 200 meters apart. Without being aware of the field distribution, the same authors using the same criteria paired 77280 with 77282, which were separated by a distance of nearly three kilometers. This leaves one of Cassidy's original four, 77231, unpaired. Two other specimens, 78043 and 78045, were paired on petrographic evidence by Score et al. (1981), and 78103 and 78105, which were were found only about 100 meters apart in a remote part of the field, were paired in the *Antarctic Meteorite Newsletter* (1984). For evaluations of other proposed pairings, see Scott (1984, and Chapter 13).

At the southern extremity of the map, separated from the Main Icefield by a wide band of snow, a group of specimens occupied an area about 500 meters long and 200 meters wide (see Inset A, Figure 14-6). Fifteen specimens were collected there in 1980 and identified as L6 chondrites by Score et al. (1982), who, with no knowledge of their field occurrence, paired them on the basis of identical textures, mineralogy, and degrees of weathering. Three more specimens were picked up in 1981. When thin sections of these were studied, again without knowledge of their field locations, 81107 and 81262 were classed as L6, but 81017 was classed as an L5 chondrite. The anomalous presence of an L5 in this tight cluster of L6 specimens, prompted me to request a reexamination of the thin section of 81017. Mason (personal communication) complied, and shortly afterward reported that he had originally classed the specimen as an L5 because he had noted no plagioclase in the section. On the second examination he found traces of plagioclase and, as the difference between classes 5 and 6 is often very uncertain, he reclassified 81017 as an L6 chondrite belonging with the rest of the group. L6 chondrites are actually so much alike that a case might be made for pairing these 18 specimens with the main group lying farther north. However, the tightly clustered field distribution provides strong evidence of a separate fall of L6 fragments.

MESOSIDERITES

Three mesosiderite specimens have been found in the Allan Hills region, all of them on the Near Western Icefield (Figure 14-7), which lies about 15 kilometers from the Main Icefield. Specimen 77219 was found during a brief helicopter reconaissance in the 1977 season; the other two, 81059 and 81098, were collected on snowmobile traverses in the 1981 season. Specimen 81098 actually consisted of two fragments that were paired in the field. Clarke (1984) suggested pairing 81059 and 81098 on the basis of their mineralogy, texture, and degree of weathering, but he regarded 77219 as a separate fall. Inasmuch as mesosiderites are among the rarest of meteorites (stony-irons of all types make up only 1.5% of falls), the occurrence of these three specimens within 2.5 kilometers of each other at one end of the small Near Western Icefield would suggest a common source. Their distribution alone would not be sufficient for pairing them, but analyses of their isotopic or trace element content or particle track densities might yield conclusive evidence for or against pairing.

Conclusions

This study shows that distribution patterns of specimens on the Antarctic ice sheet can be a helpful guide to meteorite pairings, but one that always must be used in conjunction with other types of evidence. Laboratory examinations confirmed the main outlines of field pairings for some of the seven meteorite classes discussed herein, but produced numerous surprises when adjacent specimens proved not to belong to the same fall and widely separated ones showed strong evidence that they did belong together. Meteorites that fall close together are, in general, expected to remain close together while being transported within a large ice sheet. Confusion begins when they emerge from the ice and and are mixed with other meteorites on stranding surfaces that are compressed against mountain barriers by the persistent push of the oncoming sheet. Furthermore, the powerful storm winds of Antarctica can send specimens up to cobble size—and probably boulder size—skittering across the ice to new locations, and drifts of snow

cover and uncover different groups of specimens from season to season. Despite all the factors that disturb the orderly patterns of strewnfields, specimen distributions are of sufficient aid in pairing to make mapping worth the effort.

Since the 1982–1983 season, mapping techniques have been speeded up and made more accurate by use of an infrared distance measuring device to determine geodetic positions of meteorite specimens relative to known points. There will be no further need for painstaking attempts like this one to superimpose maps in order to locate find sites. However, the first six seasons at the Allan Hills Main Icefield yielded a unique body of data that demanded analysis.

ACKNOWLEDGEMENTS.—I wish to thank John Annexstad and John Schutt for kindly furnishing me with their map of meteorite distributions on the Allan Hills Main Ice Field, and Robbie Score and Ed Scott for critical readings of this manuscript. This work was supported in part by NASA Grant NAG 9-29 and in part by SAO allocation 86400040-P12P11-4P50.

Literature Cited

Antarctic Meteorite Newsletter, 7(1), 1984.

Berkley, J.L., and J.H. Jones
1982. Primary Igneous Carbon in Ureilites: Petrological Implications. *Journal of Geophysical Research*, 87 (supplement):A353–A364.

Cassidy, William A.
1980. List of Possible Pairings of ALHA77 Meteorites. *In* U.B. Marvin and B. Mason, editors, Catalog of Antarctic Meteorites, 1977–1978. *Smithsonian Contributions to the Earth Sciences*, 23:44–46.

Clarke, Roy S., Jr.,
1984. Descriptions of Iron Meteorites and Mesosiderites. *In* U.B. Marvin and B. Mason, editors, Field and Laboratory Investigations of Meteorites from Victoria Land, Antarctica. *Smithsonian Contributions to the Earth Sciences*, 26:49–53.

Clarke, R.S., Jr., E. Jarosewich, J.I. Goldstein, and P.A. Baedecker
1980. Antarctic Iron Meteorites from Allan Hills and Purgatory Peak. *Meteoritics*, 15:273–274.

Delaney, J.S., M. Prinz, and C.P. Stokes
1984. The Allan Hills 81-series of Polymict Eucrites. In *Lunar and Planetary Science XV*, pages 214–215. Houston: Lunar and Planetary Institute.

Delaney, J.S., M. Prinz, and H. Takeda
1984. The Polymict Eucrites. *Journal of Geophysical Research*, 89 (supplement):C251–C288.

Delaney, J.S., H. Takeda, and M. Prinz
1983. Modal Comparison of Yamato and Allan Hills Polymict Eucrites. *Memoirs of the National Institute of Polar Research* (Japan), special issue, 30:206–223.

Evans, J.C., J.H. Reeves, and L.A. Rancitelli
1982. Aluminum-26 Survey of Victoria Land Meteorites. *In* U.B. Marvin and B. Mason, editors, *Smithsonian Contributions to the Earth Sciences*, 24:70–74.

Goswami, N.N., and K. Nishiizumi
1983. Cosmogenic Records in Antarctic Meteorites. *Earth and Planetary Science Letters*, 64:1–8.

McKinley, S.G., E.R.D. Scott, G.J. Taylor, and K. Keil
1981. A Unique Type 3 Ordinary Chondrite Containing Graphite-Magnetite Aggregates—Allan Hills A77011. In *Proceedings of the Twelfth Lunar and Planetary Science Conference*, pages 1039–1048. New York: Pergamon Press.

Nautiyal, C.M., J.T. Padia, M.N. Rao, T.R. Venkatesan, and J.N. Goswami
1982. Irradiation History of Antarctic Gas-Rich Meteorites. In *Lunar and Planetary Science XIII*, pages 578–579. Houston: Lunar and Planetary Institute.

Nishiizumi, K.
1984. Cosmic-ray Produced Nuclides in Victoria Land Meteorites. *In* U.B. Marvin and B. Mason, editors, *Smithsonian Contributions to the Earth Sciences*, 26:105–109.

Score, R.
1980. Allan Hills 77216: A Petrologic and Mineralogic Description. [Abstract.] *Meteoritics*, 15:363.

Score, R., C.M. Schwarz, T.V.V. King, B. Mason, D.D. Bogard, and E. M. Gabel
1981. Antarctic Meteorite Descriptions 1976–1977–1978–1979. *Curatorial Branch Publication, 54, JSC 17076*. 144 pages. Houston: Johnson Space Center.

Score, R., T.V.V. King, C.M. Schwarz, A.M. Reid, and B. Mason
1982. Descriptions of Stony Meteorites. *In* U.B. Marvin and B. Mason, editors, Catalog of Meteorites from Victoria Land, Antarctica, 1978–1980. *Smithsonian Contributions to the Earth Sciences*, 24:19–48.

Score, R., C.M. Schwarz, and B. Mason
1984. Descriptions of Stony Meteorites. *In* U.B. Marvin and B. Mason, editors, Field and Laboratory Investigations of Meteorites from Victoria Land, Antarctica. *Smithsonian Contributions to the Earth Sciences*, 26:23–47.

Scott, E.R.D.
1984. Pairing of Meteorites Found in Victoria Land, Antarctica. *Proceedings of the Ninth Symposium on Antarctic Meteorites. Memoirs of National Institute of Polar Research*, special issue, 35:102–125.

Yanai, K.
1982. *Antarctic Meteorite Distribution Map of Allan Hills, Victoria Land, Antarctica—Allan Hills-76, -77, -78 Meteorites*. Tokyo: National Institute of Polar Research.
1984. *Locality Map Series of Antarctic Meteorites, Sheet 1 Allan Hills: Explanatory Text of Locality Map of Allan Hills-76, Allan Hills-77, and Allan Hills-78 Meteorites*. Tokyo: National Institute of Polar Research.

Appendix

Tables of ANSMET Meteorites

Terminology

Class and type: A = achondrite, unique; Au = aubrite; C = carbonaceous chondrite; Di = diogenite; E = enstatite chondrite; EH = enstatite high-iron chondrite; Eu = eucrite; Ho = howardite; H = high-iron chondrite; I = iron (IA, IIA, IIB, IVA = iron groups); L = low-iron chondrite; LL = low-iron low-metal chondrite; M = mesosiderite; Sh = shergottite; Ur = ureilite. Chondrite petrologic type is indicated by digit following the abbreviation.

Olivine composition in mole percent Fe_2SiO_4 (Fa).

Pyroxene (orthopyroxene or low-Ca clinopyroxene) composition in mole percent $FeSiO_3$ (Fs).

Degree of weathering: A = minor; metal flecks have inconspicuous rust haloes, oxide stain along cracks is minor. B = moderate; metal flecks show large rust haloes, internal cracks show extensive oxide stain. C = severe; specimen is uniformly stained brown, no metal survives.

Degree of fracturing: A = slight; specimen has few or no cracks and none penetrate the entire specimen. B = moderate; several cracks extend across the specimen, which can be readily broken along the fractures. C = severe; specimen has many extensive cracks and readily crumbles.

Locations: ALH = Allan Hills; BTN = Bates Nunatak; DRP = Derrick Peak; EET = Elephant Moraine; ILD = Inland Forts; MBR = Mount Baldr; MET = Meteorite Hills; OTT = Outpost Nunatak; PCA = Pecora Escarpment; PGP = Purgatory Peak; RKP = Reckling Peak; TIL = Thiel Mountains; TYR = Taylor Glacier.

Classification by S.J.B. Reed and S.O. Agrell (*); by S.G. McKinley and K. Kiel (†); by C.B. Moore (+).

Abbreviations: n.d. = no data.

NOTE: The following meteorites were characterized after the manuscript had been submitted:

H5 META78009, 010, 011, 012, 018
H6 META78006, 007, 013, 014, 016, 017, 019, 020, 022, 023, 024, 025, 026, 027
L6 META78002, 003, 004, 005, 021, 028

The possibility of pairings within each group should be considered. Classifications by Brian Mason.

TABLE A.—Meteorites listed by source area in numerical sequence (fractions of grams in weight dropped unless total weight is less than 1 gram).

Specimen number	Weight (g)	Class and type	% Fa in olivine	% Fs in pyroxene	Degree of weathering
ALH					
76001	20151	L6	25	21	A
76003	10495	L6	25	21	A
76004	53	LL3	0–34	0–53	A
76002	307	I			
76005	317	Eu	37–57		A
76006	271	H6	18	16	C
76007	79	L6	24	21	B
76008	281	H6	19	17	B/C
76009	3950	L6	24	21	B
77001	252	L6	25	21	B
77002	235	L5	25	22	B
77003	780	C3O	4–48	2–25	A
77004	2230	H4	17–20	15–27	C
77005	483	Sh	28	23	A
77007†	99	H5	19.1	16.7	B
77008†	93	L6	24.6	20.6	A
77009	236	H4	18	16	C
77010	296	H4	18	15–18	C
77011	292	L3	4–36	1–33	C
77012	180	H5	18	16	C
77013†	23	L3	9–28	1–35	B
77014	309	H5	18	17	C
77015	411	L3	1–21	4–24	C
77016†	78	H5	18.6	17.1	B
77017†	78	H5	18.8	16.3	B
77018†	52	H5	19.0	17.0	B/C
77019†	60	L6	24.9	21.4	B/C
77021	17	H5	18	17	C
77022†	16	H5	19.1	17.0	A
77023†	21	H5	19.1	16.8	B
77025	19	H5	18	17	C
77026†	20	L6	24.3	20.7	B/C
77027†	4	L6	25.0	21.5	B/C
77029†	1	C3O	23.0	2.6	A/B
77031†	0.5	L3	n.d.	n.d.	B/C
77033	9	L3	8–38	8–9	C
77034†	2	L3	n.d.	n.d.	B/C
77036†	8	L3	n.d.	n.d.	B
77038†	19	H5	19.0	17.1	A/B
77039†	8	H5	18.5	16.3	A/B
77041†	17	LL6	30.7	25.1	A
77042†	20	H5	19.0	16.6	A/B
77043†	11	L3	1–37	1–28	B/C
77045†	18	H5	18.7	17.0	A
77046†	8	H6	19.0	16.7	A/B
77047†	20	L3	n.d.	n.d.	C
77049†	7	L3	n.d.	n.d.	B/C
77050†	84	L3	n.d.	n.d.	B/C
77051†	15	H5	18.8	16.5	A
77052†	112	L3	n.d.	n.d.	B/C
77054†	10	H5	18.5	16.9	B
77056†	12	H4	18.8	16.3	A/B
77058†	4	H5	18.8	16.1	B
77060†	64	LL5	28.1	23.2	A
77061	13	H5	18	17	B
77062	17	H5	18	17	B
77063†	3	H5	18.0	16.8	B
77064	6	H5	18	17	B
77066†	5	H5	19.0	17.4	A
77069†	0.8	L6	25.4	21.4	B/C
77070†	18	H5	18.4	16.8	B
77071	11	H5	18	17	B
77073†	10	H5	18.8	17.7	A/B
77074	12	H5	18	17	B
77076†	2	H5	19.5	16.1	B
77078†	24	H5	19.5	16.7	B
77079†	8	H5	18.2	15.8	A
77081	9	"H(?)" * *(Acapulco-like)	11	11	B
77082†	12	H5	19.3	16.5	A/B
77084†	44	H5	18.8	16.8	A/B
77085†	46	H5	18.8	17.6	B
77086	19	H5	19	17	C
77087†	31	H5	19.0	16.7	B
77088	51	H5	19	17	C
77089†	8	L6	25.5	21.4	B
77091†	4	H5	18.9	16.1	B/C
77092†	45	H5	18.5	16.5	A
77094†	7	H5	18.5	16.2	B
77096†	2	H5	18.7	17.1	A
77098†	8	H5	18.7	16.7	B
77100†	18	H5	19.2	16.4	A/B
77101†	4	H5	18.6	17.0	B
77102	12	H5	19	15	B
77104†	6	H5	18.9	16.9	A
77106†	8	H5	18.8	16.5	A/B
77108†	0.7	H5	18.5	15.9	A/B
77111†	52	H6	19.0	16.6	A/B
77112†	22	H5	18.7	16.7	A
77113†	2	H5	18.7	17.2	B
77114†	45	H5	19.6	17.2	B
77115†	154	L3	n.d.	n.d.	B/C
77117†	21	L5	24.4	21.0	A/B
77118	8	H5	19	17	C
77119	6	H5	18	17	C
77120†	4	H5	18.5	16.0	A/B
77122†	5	H5	19.1	16.8	B
77124	4	H5	19	17	C
77125†	19	H5	17.2	15.5	A/B
77126†	25	H5	18.3	16.2	A/B
77127†	4	L5	25.0	21.1	B
77129†	2	H5	18.9	16.6	B
77130†	25	H5	18.9	16.5	A
77131†	26	H6	19.2	16.8	A/B
77132†	115	H5	19.0	16.9	A/B
77133†	19	H6	19.0	17.0	A
77134†	19	H6	18.9	16.7	A
77136†	4	H5	19.1	16.4	A/B
77138†	2	H5	19.2	17.0	A
77140	79	L3	8–44	2–17	B

TABLE A.—Continued.

Specimen number	Weight (g)	Class and type	% Fa in olivine	% Fs in pyroxene	Degree of weathering	Specimen number	Weight (g)	Class and type	% Fa in olivine	% Fs in pyroxene	Degree of weathering
77142†	3	H5	18.9	17.1	A/B	77209†	32	H6	18.8	16.4	B
77143†	39	H5	18.7	16.2	A/B	77211†	27	L3	n.d.	n.d.	B/C
77144	8	H6	19	17	B	77212†	17	H6	18.9	17.0	A/B
77146†	18	H6	18.9	16.9	A/B	77213†	8	H5	18.6	16.5	A
77147†	19	H6	19.0	16.6	A/B	77214	2111	L3	1–49	4–23	C
77148	13	H6	18	16	C	77215	820	L3	22–26	9–21	B
77149†	26	H6	19.1	16.9	A/B	77216	1470	L3	15–35	14–23	A/B
77150	58	L6	25	22	C	77217	413	L3	17–25	9–26	B
77151†	17	H5	18.9	16.4	A	77218†	45	L5	23.4	19.1	A
77152†	18	H5	18.7	16.9	A	77219	637	M	26	24–28	B
77153†	12	H5	19.2	16.7	A	77220†	69	H5	17.7	16.0	B
77155	305	L6	24	20	A/B	77221	229	H4	15	13–15	C
77156†	18	EH4	0.8	1.5	B	77222†	125	H4	18.0	15.3	A/B
77157†	88	H6	18.6	15.7	A/B	77223	208	H4	17	15–23	C
77158†	20	H5	18.9	16.9	B	77224	787	H4	19	17	C
77159†	17	L6	24.4	20.8	A/B	77225	5878	H4	17	16	C
77160	70	L3	3–46	6–40	C	77226	15323	H4	18	16	C
77161†	6	H5	19.3	17.1	B	77227†	16	H5	18.9	16.6	A
77162†	29	L6	25.3	20.9	A	77228†	19	H5	18.5	16.3	B
77163†	24	L3	n.d.	n.d.	B/C	77230	2473	L4	22–25	18–29	C
77164	38	L3	6–39	3–41	C	77231	9270	L6	24	21	A/B
77165	31	L3	8–33	6–35	C	77232	6494	H4	17	15	C
77166†	139	L3	n.d.	n.d.	C	77233	4087	H4	14–21	15–17	C
77167	611	L3	2–41	3–17	C	77235†	5	H5	18.9	16.7	A/B
77168†	25	H5	19.0	16.5	B	77237†	4	H5	18.5	15.8	A
77170†	12	L3	n.d.	n.d.	B/C	77239†	19	H6	18.7	15.9	B
77171†	24	H5	18.9	17.0	A/B	77240†	25	H5	18.8	16.0	A
77173†	26	H5	19.1	17.0	B	77241†	144	L3	n.d.	n.d.	C
77174†	32	H5	18.3	16.0	A	77242†	56	H5	18.8	16.2	B
77175†	23	L3	n.d.	n.d.	B/C	77244†	40	L3	n.d.	n.d.	B/C
77176†	55	L3	0.3–34	1–37	B	77245†	33	H5	19.2	17.2	A/B
77177	368	H5	18	16	C	77246†	42	H6	19.2	16.5	B
77178†	6	L3	1–36	2–40	B/C	77247†	44	H5	18.8	16.4	A/B
77180	191	L6	24	20	C	77248†	96	H6	18.7	16.7	B/C
77181†	33	H5	20.0	17.3	B	77249	504	L3	7–35	2–25	C
77182	1135	H5	19	17	C	77250	10555	I			
77183	288	H6	19	16	C	77251†	69	L6	25.0	21.3	B
77184†	128	H5	17.8	15.9	B	77252	343	L3	22–28	2–22	B
77185†	28	L3	n.d.	n.d.	A/B	77253†	24	H5	19.2	16.9	A/B
77186†	122	H5	18.8	16.0	A/B	77254	246	L5	23	20	A/B
77187†	52	H5	18.1	16.3	A/B	77255	765	I			
77188†	109	H5	18.1	16.1	A/B	77256	676	Di		23	A/B
77190	387	H4	17–19	15–22	C	77257	1996	Ur	13	12	A
77191	642	H4	16–18	14–16	C	77258	597	H6	18	16	B/C
77192	845	H4	16–18	15–21	C	77259	294	H5	18	15	C
77193†	7	H5	19.0	15.7	A	77260	744	L3	7–23	1–28	C
77195†	5	H5	18.9	16.4	A	77261	412	L6	24	21	B
77197†	20	L3	10–27	4–21	A/B	77262	862	H4	15–19	13–16	B/C
77198†	7	L6	24.4	20.6	B	77263	1669	I			
77200†	0.9	H6	19.7	17.6	C	77264	11	H5	19	16	A/B
77201†	15	H5	18.8	15.3	A	77265†	18	H5	17.6	15.9	B
77202†	3	H5	18.6	16.6	B	77266†	108	H5	19.6	17.7	B
77205†	3	H5	18.8	16.7	B	77267†	104	L5	24.7	20.9	A
77207†	5	H5	17.8	16.7	A/B	77268	272	H5	18	16	C
77208	1733	H4	17	14	C	77269	1045	L6	24	22	B

TABLE A.—Continued.

Specimen number	Weight (g)	Class and type	% Fa in olivine	% Fs in pyroxene	Degree of weathering	Specimen number	Weight (g)	Class and type	% Fa in olivine	% Fs in pyroxene	Degree of weathering
77270	589	L6	24	21	A/B	78028	4	H5	18	16	
77271	610	H6	18	16	C	78029+	4	H4	19.2		B
77272	674	L6	24	20	B/C	78031	5	H5	18	16	
77273	492	L6	24	20	B	78033+	5	H4	19.2		B
77274	288	H5	18	16	C	78035	2	H6	18	16	
77275†	25	H5	18.3	15.6	A	78037+	0.5	L3	7–38		B
77277	143	L6	24	20	A/B	78038	363	L3	4–42	2–19	C
77278	313	LL3	11–29	9–21	A	78039	299	L6	24	21	B
77279†	175	H5	18.8	17.1	A	78040	212	Eu		33–52	A
77280	3226	L6	24	21	B	78041+	118	L3	0–41		B
77281	1231	L6	24	20	B	78042	214	L6	24	20	B
77282	4127	L6	24	20	B	78043	680	L6	25	21	B
77283	10510	I				78044	164	L4	23–25	19–24	B/C
77284	376	L6	25	21	A/B	78045	397	L6	25	21	B/C
77285	271	H6	18	16	C	78046	70	L3	8–25	8–20	
77286	246	H4	17	12–16	C	78047*	130	H5	18.8		B
77287	230	H5	18	16	C	78048	191	L6	24	21	A/B
77288	1880	H6	19	17	C	78049+	96	H5	19.4		B
77289	2186	I				78050	1045	L6	23	20	B
77290	3784	I				78051	120	H4	18	15–18	
77291†	6	H5	18.9	15.9	A	78052*	97	H5	17.9		C
77292	200	L6	24	20	B	78053	179	H4	17	16	C
77293†	110	L6	24.7	20.9	B	78055+	14	L6	25.5		B
77294	1351	H5	17	15	A	78057	9	H4	18	16	
77295†	141	EH4	0.8	1.7	B	78059+	9	L6	21.5		B
77296	963	L6	24	21	A/B	78062	11	LL6	29	24	
77297	952	L6	24	20	A	78063+	77	LL6	29.1		A
77299	261	H3	11–21	15–20	A	78065+	7	H6	18.0		B
77300	235	H5	18	16	C	78067	8	H6	18	16	
77301†	55	L6	24.9	20.9	A	78069+	4	H6	19.1		B
77302	236	Eu		37–64	A	78070	10	L4	23	13–25	
77303†	79	L3	n.d.	n.d.	B/C	78074	200	L6	24	21	B
77304	650	L4	18–27	13–19	B	78075	281	H5	18	16	B/C
77305	6444	L6	24	21	B/C	78076	276	H6	18	16	B
77306	20	C2	1–45	1	A	78077	331	H4	19	15–18	C
77307	181	C3	1–30	1–12	A	78078	290	L6	24	20	A/B
						78079	5	H5	18	16	
78001+	85	H5	18.6		B	78080	25	H5	18	16	
78002+	11	H6	19.0		A	78081*	18	H5	19.1		
78003	125	L6	24	20	C	78082+	24	LL6	27.7		A
78004*	36	H5	19.2			78084	14280	H4	18	8–24	B/C
78005+	28	H5	19.3		B	78085	219	H5	18	16	B
78006	8	Ho		25–61	A	78086*	9	H6	19.0		
78008	7	H5	18	16		78088*	5	H5	18.8		
78010+	1	H5	19.4		B	78090*	8	H5	18.7		
78012	38	H5	18	16		78092*	16	H5	19.0		
78013	4	L3	11–45	1–31		78094*	4	H5	19.1		
78015*	35	LL(?L)3	8–35			78096*	7	H5	18.9		
78017+	3	L3	3–43		B	78098*	2	H5	18.9		
78018+	18	H5	19.2		F	78100	85	I			
78019	30	Ur	22	18	B/C	78101	121	L6	24	21	
78021	17	H5	18	16		78102	337	H5	18	17	B/C
78023	10	H5	18	16		78103	590	L6	24	20	B
78025+	8	H5	18.9		A	78104	672	L6	24	20	B
78027*	29	H5	19.3			78105	942	L6	23	20	B

TABLE A.—Continued.

Specimen number	Weight (g)	Class and type	% Fa in olivine	% Fs in pyroxene	Degree of weathering
78106	465	L6	24	20	A/B
78107	198	H5	18	17	C
78108	173	H5	18	16	B
78109	233	LL5	28	23	A/B
78110	161	H5	18	16	B/C
78111	127	H5	18	16	B/C
78112	2485	L6	25	20	B
78113	299	Au			A/B
78114	808	L6	25	20	B/C
78115	848	H6	18	16	B
78116*	128	H5	18.7		B
78117+	4	H5	18.5		A
78119+	103	L3	0–28		A
78120	44	H4	18	16	
78121*	30	H5	19.2		
78122	5	H6	19	17	
78123+	18	H5	19.3		B
78124	28	H6	17	15	
78125*	19	L6	25.0		B
78126	607	L6	25	21	B
78127	195	L6	24	20	B/C
78128	155	H5	19	17	C
78129+	128	H5	19.4		B
78130	2733	L6	25	21	B/C
78131	269	L6	25	21	B/C
78132	656	Eu		40–68	A
78133	60	L3	1–34	1–16	
78134	458	H4	18	15–20	B/C
78135*	131	H6	19.0		B
78136+	52	H5	19.1		A
78137	70	H6	17	15	
78138+	11	LL3	0–35		B
78139*	17	H5	19.3		
78140+	17	H4	18.4		B
78141	24	H5	18	16	
78142*	32	L5	24.2		
78145+	34	H6	19.6		A
78146	17	H5	18	16	
78147*	31	H5,6	19.4		
78149+	23	L3	18–31		B
78150	16	H5	18	16	
78152	5	H6	18	16	
78153	152	LL6	29	24	B/C
78154+	12	H5	19.3		B
78156	9	L6	24	21	
78157+	63	H4	19.0		B
78158	15	Eu		40–68	A
78159	23	H5	18	16	
78160*	16	H5	19.3		
78162+	33	L3	2–30		B
78163+	10	H5	18.7		B
78164	25	H5	18	16	
78165	21	Eu		37–61	A
78168+	34	H4	19.2		B
78169+	22	H6	19.2		B
78170+	21	H3	3–36		B
78171+	23	L6	25.4		B
78172+	29	H4	19.7		B
78173+	20	H5	19.7		B
78174+	13	H5	18.2		B
78176+	8	L3	8–26		B
78178+	7	H5	19.0		B
78180+	8	L3	2–33		B
78182	10	H5	18	16	
78184	8	H6	18	16	
78186	3	L3	3–36	3–24	
78188	0.9	L3	1–34	5–29	C
78189	23	H6	18	16	
78190	20	H5	18	16	
78191	20	H6	18	16	
78193	13	H4	18	16	B/C
78194	25	H5	18	16	
78196	11	H4	18	16	B/C
78197	20	H5	18	16	
78199	13	H5	18	16	
78201	10	H5	18	16	
78203	11	H5	18	16	
78205	9	H5	18	16	
78207	8	H6	19	17	
78209	12	H5	18	15	B/C
78211	11	H6	18	16	B
78213	10	H6	18	15	B
78215	6	H6	18	16	B/C
78217+	8	H5	18.8		B
78219+	8	H5	19.4		B
78221	5	H5	18	16	B
78223	6	H4	18	16	B
78225	5	H5	18	16	B
78227	2	H5	18	16	B/C
78229	2	H6	18	15	B
78231	2	H6	18	16	B/C
78233	1	H5	18	16	B/C
78235+	19	L3	8–28		B
78236	14	L3	2–37	3–26	
78238	10	L3	2–34	3–21	
78239+	16	L3	1–34		B
78241	7	H5	18	16	
78243	2	L3	1–36	3–30	
78245	4	H5	18	16	
78247	3	H5	18	16	
78249	4	H6	18	16	
78251	1312	L6	23	20	B
78252	2789	I			
78253+	7	H5	18.9		B
78255+	3	H5	19.4		A
78257+	2	H5	19.2		B
78259+	6	H5	19.7		A
78261	5	C2	0–50	1–8	A
78262	26	Ur	22	19	B/C

TABLE A.—Continued.

Specimen number	Weight (g)	Class and type	% Fa in olivine	% Fs in pyroxene	Degree of weathering
79001	32	L3	6–39	2–31	C
79002	223	H6	16	18	C
79003	5	LL3	10–38	5–26	B
79004	35	H5	16	14	B/C
79005	60	H6	18	16	B
79006	41	H5	18	15	B/C
79007	142	L6	23	19	A/B
79008	12	H5	17	15	B
79009	76	H5	18	15	C
79010	25	H5	17	15	B/C
79011	14	H5	18	16	B/C
79012	192	H5	17	15	C
79013	28	H5	18	16	C
79014	11	H5	18	16	B
79015	64	H5	17	15	B
79016	1146	H6	17	15	B/C
79017	310	Eu	28–53		A
79018	121	L6	23	20	B/C
79019	12	H6	17	15	B
79020	4	H6	17	15	B/C
79021	29	H5	18	17	B
79022	31	L3,4	1–28	9–22	A/B
79023	68	H4	17	14–17	B/C
79024	22	H6	17	15	C
79025	1208	H5	17	15	C
79026	572	H5	18	16	B
79027	133	L6	24	20	B
79028	16	H6	18	16	B
79029	506	H5	18	16	C
79031	3	H5	16	14	C
79032	3	H5	16	14	C
79033	281	L6	24	20	B
79034	13	H6	18	16	B
79035	38	H4	17	14–18	B
79036	20	H5	18	16	B
79037	15	H6	18	16	B
79038	50	H5	17	15	C
79039	108	H4	16	15	B
79040	13	H5	18	15	B
79041	20	H5	18	16	B
79042	11	H5	18	16	B
79043	62	L6	23	20	C
79045	115	L3	2–38	2–29	C
79046	90	H5	18	15	B
79047	19	H5	18	15	B
79048	37	H5	18	16	B
79049	54	H6	18	16	C
79050	27	H5	18	15	C
79051	24	H5	18	15	C
79052	23	L6	23	20	B/C
79053	86	H5	17	15	B/C
79054	36	H5	18	16	B
79055	15	H6	18	16	B/C
80101	8725	L6	24	20	B
80102	471	Eu		34–52	A
80103	536	L6	24	20	B
80104	882	I			
80105	445	L6	24	20	B
80106	432	H4	19	16–19	C
80107	178	L6	24	20	B
80108	125	L6	24	20	B
80110	168	L6	24	20	B
80111	42	H5	18	16	B
80112	331	L6	24	20	B
80113	313	L6	24	20	B
80114	233	L6	24	20	B
80115	306	L6	24	20	B
80116	191	L6	24	20	B/C
80117	89	L6	24	20	B
80118	2	H6	17	15	B
80119	34	L6	24	20	B
80120	60	L6	24	20	B
80121	39	H4	19	17	B/C
80122	50	H6	18	16	B/C
80123	28	H5	18	16	C
80124	12	H5	18	16	B
80125	139	L6	24	20	B/C
80126	35	H6	19	17	A/B
80127	47	H5	18	16	B
80128	138	H4	18	15–20	B
80129	93	H5	18	15	B
80130	5	H6	18	16	B/C
80131	20	H4	19	16–22	B
80132	153	H5	18	16	B
80133	4	L3	1–35	5–30	B
81001	53	Eu		59	A
81002	14	C2	0–52	0–2	A
81003	10	C3V	0–60	1	A/B
81004	5	C2	0–52	0–2	A/B
81005	31	A	11–40	7–47	A/B
81006	255	Eu		35–60	A
81007	164	Eu		38–55	A/B
81008	44	Eu		32–59	A/B
81009	229	Eu		30–63	A
81010	219	Eu		31–57	A
81011	406	Eu		33–60	A/B
81012	37	Eu		33–62	A/B
81013	17727	I			
81014	188	I			
81015	5489	H5	19	16	B
81016	3850	L6	25	21	B
81017	1434	L5	25	21	B
81018	2237	L5	24	21	B
81019	1051	H5	19	16	B/C
81020	1353	H5	19	16	B
81021	695	E6		0–1	A
81022	913	H4	19	17	B/C
81023	418	L5	25	21	B

TABLE A.—Continued.

Specimen number	Weight (g)	Class and type	% Fa in olivine	% Fs in pyroxene	Degree of weathering	Specimen number	Weight (g)	Class and type	% Fa in olivine	% Fs in pyroxene	Degree of weathering
81024	798	L3	3–28	2–24	C	81079	7	H6	19	16	C
81025	379	L3	1–41	3–40	C	81080	17	H5	19	17	A/B
81026	516	L6	25	21	B	81081	5	H5	19	17	B
81027	3835	L6	25	21	C	81082	6	H5	19	17	B
81028	80	L6	25	21	B	81083	7	H5	19	16	B
81029	153	L6	25	21	C	81084	16	H5	19	16	B
81030	1852	L3	1–49	5–33	B/C	81085	16	L3	1–39	2–25	C
81031	1595	L3	1–43	3–35	C	81086	6	H6	19	16	B
81032	727	L3	0–42	2–14	C	81087	8	L3	2–29	3–31	B/C
81033	252	H5	18	16	C	81088	4	H5	19	17	B
81034	255	H5	19	17	B	81089	11	H5	19	17	B
81035	256	H6	19	17	C	81090	10	H5	19	16	B
81036	252	H5	19	17	C	81091	12	H5	19	16	B
81037	320	H6	20	17	B	81092	16	H4	19	17	B
81038	229	H6	19	17	C	81093	271	H6	20	17	A/B
81039	206	H5	19	17	A/B	81094	152	H6	19	16	C
81040	195	L4	25	21	B/C	81095	59	H4	18	16	B/C
81041	729	H4	18	15–23	C	81096	83	H6	19	17	B
81042	534	H5	19	17	C	81097	80	H4	18	16	B
81043	106	H4	18	15	B/C	81098	71	M		28	C
81044	387	H4	18	16	C	81099	152	L6	25	21	A/B
81045	90	H4	18	16	C	81100	155	H5	19	17	B
81046	17	H4	18	16	C	81101	119	Ur	10–22		A/B
81047	82	H4	18	16	B/C	81102	196	H6	19	17	B/C
81048	191	H4	18	16	B/C	81103	136	H6	19	17	B/C
81049	9	H4	18	16	B/C	81104	184	H4	19	17	C
81050	26	H4	18	16	C	81105	93	H4	18	16	C
81051	43	H4	18	16	B/C	81106	48	L6	24	20	B
81052	29	H4	18	16	C	81107	140	L6	24	21	B
81053	3	L3	1–29	1–42	C	81108	69	H5	18	16	B
81054	2	H6	19	17	B	81109	1	H4	19	17	B
81055	5	H6	19	16	B	81110	3	H5	19	17	B/C
81056	1	H4	19	17	B	81111	210	H6	19	17	B/C
81057	8	H4	19	13–21	B	81112	150	H6	19	17	B/C
81058	66	H4	18	15	C	81113	111	H5	18	16	B/C
81059	540	M	28	25–32	C	81114	79	H4	18	16	B/C
81060	28	L3	2–28	5–27	C	81115	155	H5	19	17	C
81061	24	L3	3–33	5–27	B/C	81116	2	H5	19	17	B
81062	0.5	H5	18	16	C	81117	33	H4	18	14–21	B
81063	5	H5	18	16	B/C	81118	85	H5	19	16	B/C
81064	191	H5	18	15	C	81119	107	L4	24	21	B
81065	13	L3	10–41	5–24	B/C	81120	14	H5	18	16	B/C
81066	9	L3	1–44	1–25	C	81121	88	L3	8–40	1–24	B
81067	228	H5	19	17	C	81122	21	L6	25	21	B
81068	24	H4	19	16	B	81123	2	LL6	30	25	B
81069	7	L3	4–38	1–31	B/C	81124	9	H5	19	17	B
81070	4	H5	19	17	B/C	81125	10	H5	19	17	B
81071	2	H5	19	17	B	81126	22	H5	19	16	B
81072	3	H5	19	17	B/C	81127	15	H6	19	17	B/C
81073	3	H4	19	8–18	B/C	81128	16	H5	19	17	B/C
81074	8	H4	19	16	B	81129	32	H5	18	16	A/B
81075	16	H5	19	17	B	81130	30	H5	18	16	B
81076	10	H6	19	16	B	81131	13	L6	25	22	A/B
81077	4	H5	19	17	B	81132	5	H5	18	16	B
81078	6	H6	19	16	B/C	81133	21	H5	18	16	B

TABLE A.—Continued.

Specimen number	Weight (g)	Class and type	% Fa in olivine	% Fs in pyroxene	Degree of weathering	Specimen number	Weight (g)	Class and type	% Fa in olivine	% Fs in pyroxene	Degree of weathering
81134	15	H6	18	16	B/C	81189	3	E4	2	3	C
81135	10	H5	19	16	B	81190	48	L3	0.3–32	4–28	C
81136	1	H5	20	17	B	81191	30	L3	2–29	1–30	C
81137	9	H6	19	17	B/C	81192	9	H5	19	16	A/B
81138	4	H5	19	17	B	81193	13	H6	18	16	B
81139	7	H5	19	17	B/C	81194	17	H5	19	16	B
81140	14	H4	19	17	B/C	81195	5	H5	18	16	B
81141	1	H5	19	17	B/C	81196	9	H6	18	16	B
81142	1	H4	18	16	B/C	81197	68	H5	17	15	B/C
81143	13	H5	18	16	B/C	81198	0.9	L5	24	21	B/C
81144	3	H5	19	16	B	81199	16	H4	19	16	C
81145	21	L3	5–40	3–23	B	81200	9	H4	19	17	B/C
81146	24	H6	18	16	C	81201	7	H5	18	16	B/C
81147	2	H4	19	16	B	81202	5	H5	19	17	C
81148	13	H5	19	17	B	81203	4	L6	25	21	C
81149	9	H4	19	16	B	81204	7	H6	18	16	B
81150	2	L6	25	22	C	81205	3	L6	25	23	B
81151	5	LL5	28	23	B/C	81206	4	H4	18	15–21	B/C
81152	10	H5	18	16	B	81207	14	H5	18	16	C
81153	4	L5	24	21	B	81208	2	Di/M		25	C
81154	1	H6	19	17	B	81209	14	H5	18	16	B/C
81155	5	H5	19	17	A/B	81210	0.6	H6	19	17	B
81156	20	L3	4–42	1–30	B/C	81211	7	H5	18	16	B
81157	12	H4	19	17	B/C	81212	11	H4	18	16	B/C
81158	2	H5	19	17	B/C	81213	3	H5	19	17	B/C
81159	10	L6	25	21	B/C	81214	4	L3	0.2–38	0.1–45	B/C
81160	12	H6	19	17	C	81215	11	H5	18	16	A
81161	122	H5	19	16	C	81216	2	H5	18	17	C
81162	59	L3	1–40	4–20	C	81217	5	L6	24	20	C
81163	82	H5	19	17	C	81218	6	H5	19	16	C
81164	20	H5	18	16	B	81219	24	H5	19	17	B
81165	6	H5	19	16	B	81220	3	H5	18	16	B/C
81166	26	H5	19	16	B	81221	9	L6	25	21	C
81167	59	L6	25	22	B/C	81223	10	H6	18	16	A/B
81168	8	H5	19	17	C	81224	14	H6	19	17	B/C
81169	6	H5	18	16	B	81225	14	H6	19	17	B
81170	59	H5	19	17	B	81226	3	H5	19	17	C
81171	24	H5	19	17	B/C	81227	11	H5	19	17	B
81172	33	L6	24	21	C	81228	8	H5	18	16	B/C
81173	26	H5	19	16	A/B	81229	40	L3	7–32	2–30	C
81174	33	H5	19	17	B	81230	13	H5	18	16	B
81175	13	H5	19	17	A/B	81231	9	H4	19	16	B/C
81176	95	H5	19	17	B	81232	5	H5	18	16	B
81177	17	H4	19	16	B/C	81233	25	H5	19	17	C
81178	30	H5	19	17	B/C	81234	5	H4	18	16	C
81179	14	H5	19	17	B	81235	7	L6	25	21	C
81180	17	H6	18	16	C	81236	41	H5	18	16	A/B
81181	15	L6	25	22	B	81237	27	H5	18	16	B
81182	5	H5	18	16	B	81238	24	H5	19	16	C
81183	104	H5	17	15	C	81239	32	H5	19	17	B
81184	17	L4	24	20	A/B	81240	41	H5	19	18	C
81185	65	LL6	30	25	A/B	81241	34	H5	17	14	B
81186	23	H5	18	16	B	81242	20	H5	18	17	B/C
81187	40	A	4	6.5	B/C	81243	15	L3	5–44	6–31	C
81188	9	H5	19	17	A/B	81244	5	H5	19	17	B

TABLE A.—Continued.

Specimen number	Weight (g)	Class and type	% Fa in olivine	% Fs in pyroxene	Degree of weathering
81245	4	H5	19	17	B/C
81246	3	H5	19	17	C
81247	104	L6	25	21	A/B
81248	5	H6	18	16	C
81249	10	H5	18	17	B/C
81250	17	H6	18	16	B
81251	158	LL3	1–29	2–28	B/C
81252	2	H5	18	16	B
81253	10	H6	18	16	A/B
81254	9	H6	18	16	C
81255	12	H5	18	16	B
81256	28	H5	18	15	C
81257	29	L6	24	21	B
81258	1	C3V	0–28	0–1	B
81259	10	L3	0–22	0–29	C
81260	124	E6		0.3	A/B
81261	12	"H(?)"* *(Acapulco–like)	11	11	A/B
81262	55	L6	25	21	A/B
81263	6	H5	18	16	B
81265	8	H5	19	17	B/C
81266	12	L6	24	21	A/B
81267	27	H4	18	15–22	C
81268	18	H6	18	16	C
81269	5	H5	18	16	B/C
81270	4	H5	18	16	C
81271	28	H6	18	16	B
81272	23	L3	2–36	3–22	C
81273	43	H6	19	17	C
81274	19	H5	18	16	A/B
81275	11	H5	18	16	B
81276	42	H5	18	16	C
81277	7	H5	18	16	B
81278	1	L6	24	21	B
81279	27	H4	17	16	C
81280	55	L3	1–32	2–24	C
81281	46	H5	18	16	B
81282	31	L6	24	21	A/B
81283	0.6	H5	18	16	B/C
81284	10	H5	19	17	B/C
81285	20	LL6	27	23	C
81286	28	H5	19	17	B
81287	78	H5	17	15	C
81288	20	H6	18	16	B
81289	4	L6	24	21	A
81290	2	H4	18	17	B
81291	4	H6	18	16	B
81292	13	L3	11–34	2–31	C
81293	2	H5	18	16	B
81294	9	H5	18	16	B
81295	105	H5	19	16	C
81296	13	H5	17	15	B/C
81297	20	H5	18	16	B
81298	16	H6	19	17	B
81299	0.5	L3	1–37	2–16	C
81300	10	H5	19	16	A/B
81301	12	H5	19	16	B/C
81302	4	H5	18	16	B/C
81303	4	H6	18	16	B/C
81304	42	L6	24	21	A/B
81305	1	H5	18	16	B/C
81306	7	H5	19	17	B
81307	57	L6	24	21	B
81308	19	H5	18	16	B/C
81309	0.6	H4	18	16	C
81310	0.7	H6	19	17	B
81311	0.9	L6	24	21	B
81312	0.7	C2	1–35	1–31	A
81313	0.5	Eu(?)		38	
81314	3	H5	18	16	B
81315	2	"H(?)"* *(Acapulco–like)	11	11	A/B
82100	24	C2	1–47	1–2	A
82101	29	C30	1–50	1–10	A
82102	48	H5	18	16	B/C
82103	2529	H5	17	16	B
82104	399	L5	25	21	A
82105	363	L6	24	21	A/B
82106	35	Ur	3	4	B
82107	9	L5	22	19	B/C
82108	14	H5	18	16	B/C
82109	47	H5	18	16	B/C
82110	39	H3	1–24	4–27	B/C
82111	63	L6	24	21	A/B
82112	28	H5	17	16	C
82113	61	H6	18	16	A/B
82114	41	H5	17	15	A/B
82115	48	H5	18	16	A/B
82116	18	H6	18	16	B
82117	4	L5	25	22	B
82118	111	L6	24	20	A/B
82119	24	H5	18	16	B/C
82120	7	H5	19	17	B
82121	2	L6	24	20	A
82122	142	H5	18	16	B
82123	111	L6	25	20	B
82124	26	H6	18	16	C
82125	178	L6	24	20	C
82126	140	H4	18	15	B/C
82127	5	H6	18	16	A/B
82128	15	H4	18	16	B/C
82129	14	H5	18	17	B/C
82130	45	Ur	3	4	B
82131	1	C2	0.3		A
82132	6	E4		0.4	C
82133	20	H4	18	16	B/C
82134	28	H5	16	15	B/C
82135	12	C4	27	24	A
82136	4	H4	18	5–20	B

TABLE A.—Continued.

Specimen number	Weight (g)	Class and type	% Fa in olivine	% Fs in pyroxene	Degree of weathering
82137	11	L5	23	20	B
82138	5	H6	19	17	B
82139	0.2	L6	24	20	B
82140	0.3	L6	25	20	C
82141	0.6	H5	19	17	C
82142	20	L6	25	21	C
82143	3	H6	18	16	C
82144	7	H5	19	17	B
83001	1569	L4	23–28	20–32	B
83009	2	Au			A/B
83010	395	L3	4–31	2–28	B
83014	1	Ur	18	15	B
83015	3	Au			A/B
83016	4	C2	0.3–30	0–1	A/B
83100	863	C2			B
83101	639	L6	25	23	A
83102	1241	C2	0–2		B/C
84001	1931	Di		27	A/B
84004	9000	H4	17–18	16–19	B
84006	16000	H4,5	18	17–18	B/C
84007	706	Au			A
84008	302	Au			A/B
84011	138	Au			A
84025	5	A	32–33	11	A/B
84027	8	LL7(?)	27	23	B
84028	736	C3V	0–50	2	A
84029	120	C2	0–2		A
84030	6	C2	0–2		A
84031	12	C2	0–2		A
84032	8	C2	0–2	2	A
84033	60	C2	0–1	2	A
84034	44	C2	0–2		A
84042	51	C2	0–2		A
84044	147	C2	0–2		A
BTNA					
78001	161	L6	24	21	B
78002	4301	L6	24	20	B
78004	1079	LL6	30	24	B
DRPA					
78001	15200	I			
78002	7188	I			
78003	144	I			
78004	134	I			
78005	18600	I			
78006	389	I			
78007	11800	I			
78008	59400	I			
78009	138100	I			
EETA					
79001	7942	Sh	23–27	16–67	A
79002	2843	Di	24–25	22	B
79003	436	L6	24	20	B
79004	390	Eu		30–61	B
79005	451	Eu		30–61	A
79006	716	Ho		19–57	B
79007	200	H5	18	16	B
79009	140	L5	24	20	B
79010	287	L6	24	20	B
79011	86	Eu		30–61	B
EET					
82600	247	Ho		22–53	A
82601	150	L3	2–39	1–35	B/C
82602	1824	H4	19	16	B
82603	8210	H5	19	17	B
82604	1571	H5	19	16	B/C
82605	625	L6	25	21	B
82606	982	L6	25	21	B
82607	165	L6	23	20	B/C
82608	95	LL6	28	23	A/B
82609	326	H4	18	17	B/C
82610	42	H6	19	17	B
82611	13	L4	24	21	B
82612	32	L6	25	21	A
82613	4	L4	24	20	B
82614	8	H5	18	16	A/B
82615	29	H6	19	17	B
82616	2	H4	18	16	B/C
83200	779	H5	17–18	17–19	B/C
83201	1060	H6	18–20	18	B/C
83202	1213	L6	24–25	22–23	A/B
83203	546	H5	20	18–21	B/C
83204	377	LL6	29–31	27	A
83205	471	L6	25	22	A/B
83206	462	L6	24	22	B
83207	1238	H4	18	16–18	B
83208	263	H5	17–19	16–17	B/C
83209	520	L6	25	22–23	B/C
83210	426	L6	24–25	22	A/B
83211	543	H4	18–20	16–20	B/C
83212	402	Eu			B
83213	2727	L3	13–30	3–26	B
83214	1398	L6	24–25	22–24	B
83215	510	H6	18	19	B/C
83224	9	C2	0.2–41	0–1	A/B
83225	44	Ur			B/C
83226	33	C2	0.5–69	0.6–10	A/B
83227	1973	Eu			B
83228	1206	Eu			B
83229	313	Eu			B
83230	530	I			
83231	66	Eu			B
83232	211	Eu			B
83234	181	Eu			B
83235	255	Eu			B
83236	6	Eu			B

TABLE A.—Continued.

Specimen number	Weight (g)	Class and type	% Fa in olivine	% Fs in pyroxene	Degree of weathering
83237	883	L6	25–26	23–25	B
83245	59	I			
83246	48	Di			A/B
83247	22	Di			B/C
83250	11	C2	0.3–22	2–14	B
83251	261	Eu			B
83283	57	Eu			B
ILD					
83500	2523	I			
MBRA					
76001	1096	H6	18	16	B
76002	13773	H6	18	16	B
META					
78001	624	H4	17	14–21	B/C
78002	542	L6	23	20	B
78003	1726	L6	24	21	B
78005	172	L6	24	20	B
78006	410	H6	18	15	C
78007	175	H6	19	17	B/C
78010	234	H5	19	17	B
78028	20657	L6	25	21	B
OTTA					
80301	36	H3	17–19	4–19	B/C
PCA					
82500	91	C4	31		B
82501	54	Eu		41–57	A
82502	890	Eu		36–61	A
82503	8308	L6	24	20	A
82504	3094	L5	23	20	A/B
82505	3086	L5	23	20	B
82506	5316	Ur	21	18	A/B
82507	480	LL6	30	25	A
82508	389	L6	23	20	A/B
82509	286	L6	25	21	B
82510	254	L5	24	20	A
82511	149	H4	17	14	B
82512	55	H6	18	16	B
82513	239	L5	24	20	A/B
82514	130	L4	23	11–22	B
82515	7	H4	17	14	B
82516	16	H6	18	16	B/C
82517	41	H5	19	17	B/C
82518	22	E4	0.8		B
82519	125	L5	24	21	B
82520	23	H3	15–22	2–19	B/C
82521	1	H5	18	16	C
82522	46	H5	18	16	B/C
82523	11	H6	19	16	A
82524	114	H4	18	16	A/B
82525	40	L6	24	20	B
82526	25	H6	18	16	B
82527	3	H6	18	16	A
82528	51	L6	25	21	B/C
PGPA					
77006	19068	I			
RKPA					
78001	235	L6	23	20	C
78002	8483	H4	18	15	B
78003	1276	L6	23	20	C
78004	167	H4	17	14–21	A
79001	3006	L6	23	20	B
79002	204	L6	24	20	B
79003	182	H6	18	16	B
79004	371	H5	18	16	B/C
79008	73	L3	1–29	2–28	B
79009	55	H6	18	16	C
79012	13	H6	18	16	B
79013	11	L5	23	20	B/C
79014	78	H5	18	16	B/C
79015	10022	M		24	A/B
80201	813	H6	19	16	B
80202	545	L6	24	20	B
80203	4	H6	19	17	C
80204	15	Eu		52–57	A
80205	54	H3	17–20	5–13	B
80206	47	H6	19	17	C
80207	18	L3	15–29	6–28	C
80208	10	H6	19	17	B
80209	10	L5	25	21	C
80210	11	H5	19	16	B/C
80211	2	H6	19	17	C
80213	19	H6	19	17	B/C
80214	5	H6	19	17	C
80215	9	L6	24	20	C
80216	44	L4	23	20	B
80217	8	H5	18	15	C
80218	7	H5	18	15	C
80219	21	L6	25	21	B
80220	124	H5	18	16	B/C
80221	52	H6	19	17	C
80222	7	LL6	28	23	B
80223	25	H5	18	16	C
80224	8	Eu	54		A/B
80225	8	L6	25	21	C
80226	160	I			
80227	8	H5	19	16	B/C
80228	11	L5	23	19	C
80229	14	M		24	C
80230	58	H5	18	16	B
80231	238	H6	18	16	C
80232	80	H4	18	16	B

TABLE A.—Continued.

Specimen number	Weight (g)	Class and type	% Fa in olivine	% Fs in pyroxene	Degree of weathering	Specimen number	Weight (g)	Class and type	% Fa in olivine	% Fs in pyroxene	Degree of weathering
80233	414	H5	18	16	B/C	80262	32	H6	19	17	C
80234	136	LL5	26	22	B	80263	17	M		24	C
80235	261	LL6	30	24	A/B	80264	24	L6	24	20	B
80236	16	H5	18	16	B/C	80265	8	H6	19	17	C
80237	22	H4	18	16	C	80266	10	H6	19	17	B/C
80238	18	LL6	28	23	A/B	80267	24	H4	19	16	C
80239	6	Ur	16	15	B	80268	3	L5	24	20	B/C
80240	61	H5	18	16	C						
80241	0.6	C3V	1–6	1–8	B	TIL					
80242	7	L4	22	19	B/C	82400	221	L5	25	21	A/B
80243	3	H5	18	16	C	82401	282	L6	25	21	A/B
80244	14	H5	18	16	C	82402	476	LL6	29	24	A/B
80245	37	H5	18	16	B/C	82403	50	Eu		43–58	A
80246	6	M		24	C	82404	322	L4	23	20	B
80247	1	H5	18	16	C	82405	1116	H6	19	17	B
80248	11	LL6	27	23	A/B	82406	152	L4	23	19	B
80249	10	H5	17	15	B/C	82407	221	L4	23	20	B/C
80250	4	H5	17	15	B/C	82408	80	LL3	1–29	2–21	B
80251	29	H5	17	15	B	82409	231	H5	18	16	B
80252	11	L6	24	20	A/B	82410	19	Di		24	A
80253	5	LL5	27	22	A/B	82411	180	L4	24	21	A/B
80254	68	H6	19	17	C	82412	35	H5	17	16	C
80255	7	H6	19	17	C	82413	18	H5	17	16	C
80256	153	L3	20–25	10–26	B	82414	15	H5	17	15	B
80257	9	H5	17	15	B/C	82415	70	H5	17	15	A/B
80258	4	M		17–21	B/C						
80259	20	E5		0–1	B/C	TYR					
80260	8	H5	18	16	C	82700	892	L4	24	15–23	B
80261	62	L6	24	20	B						

TABLE B.—Meteorites listed by class and source area in numerical sequence (fractions of grams in weight dropped unless total weight is less than 1 gram).

Specimen number	Weight (g)	Class and type	Degree of weathering	Degree of fracturing	Specimen number	Weight (g)	Class and type	Degree of weathering	Degree of fracturing
				CHONDRITES					
ALHA77306	20	C2	A	A	ALHA77056†	12	H4	A/B	
ALHA78261	5	C2	A	A	ALHA77190	387	H4	C	C
ALHA81002	14	C2	A	B	ALHA77191	642	H4	C	B/C
ALHA81004	5	C2	A/B	A	ALHA77192	845	H4	C	C
ALHA81312	0.7	C2	A	A	ALHA77208	1733	H4	C	C
ALH 82100	24	C2	A	A	ALHA77221	229	H4	C	A
ALH 82131	1	C2	A	B	ALHA77222†	125	H4	A/B	
ALH 83016	4	C2	A/B	B/C	ALHA77223	208	H4	C	C
ALH 83100	863	C2	B	B/C	ALHA77224	787	H4	C	C
ALH 83102	1241	C2	B/C	C	ALHA77225	5878	H4	C	C
ALH 84029	120	C2	A	B	ALHA77226	15323	H4	C	C
ALH 84030	6	C2	A	B/C	ALHA77232	6494	H4	C	C
ALH 84031	12	C2	A	B	ALHA77233	4087	H4	C	B
ALH 84032	8	C2	A	A	ALHA77262	862	H4	B/C	B
ALH 84033	60	C2	A	B	ALHA77286	246	H4	C	B
ALH 84034	44	C2	A	A	ALHA78029+	4	H4	B	
ALH 84042	51	C2	A	B	ALHA78033+	5	H4	B	
ALH 84044	147	C2	A	B	ALHA78051	120	H4		
EET 83224	9	C2	A/B	B	ALHA78053	179	H4	C	B
EET 83226	33	C2	A/B	B	ALHA78057	9	H4		
EET 83250	11	C2	B	C	ALHA78077	331	H4	C	B
					ALHA78084	14280	H4	B/C	B
ALHA77307	181	C3	A	A	ALHA78120	44	H4		
					ALHA78134	458	H4	B/C	B/C
ALHA77003	780	C3O	A	A	ALHA78140+	17	H4	B	
ALHA77029†	1	C3O	A/B		ALHA78157+	63	H4	B	
ALH 82101	29	C3O	A	A/B	ALHA78168+	34	H4	B	
					ALHA78172+	29	H4	B	
ALHA81003	10	C3V	A/B	A/B	ALHA78193	13	H4	B/C	A
ALHA81258	1	C3V	B	A/B	ALHA78196	11	H4	B/C	B
ALH 84028	736	C3V	A	A	ALHA78223	6	H4	B	B
RKPA80241	0.6	C3V	B	B	ALHA79023	68	H4	B/C	C
					ALHA79035	38	H4	B	B
ALH 82135	12	C4	A	A	ALHA79039	108	H4	B	B
PCA 82500	91	C4	B	C	ALHA80106	432	H4	C	B
					ALHA80121	39	H4	B/C	C
ALHA81189	3	E4	C	B	ALHA80128	138	H4	B	B/C
ALH 82132	6	E4	C	B/C	ALHA80131	20	H4	B	B
PCA 82518	22	E4	B	A	ALHA81022	913	H4	B/C	A
					ALHA81041	729	H4	C	C
ALHA77156†	18	EH4		B	ALHA81043	106	H4	B/C	C
ALHA77295†	141	EH4		B	ALHA81044	387	H4	C	C
					ALHA81045	90	H4	C	B/C
RKPA80259	20	E5	B/C	B	ALHA81046	17	H4	C	B/C
					ALHA81047	82	H4	B/C	B/C
ALHA81021	695	E6	A	B	ALHA81048	191	H4	B/C	B/C
ALHA81260	124	E6	A/B	A/B	ALHA81049	9	H4	B/C	B
					ALHA81050	26	H4	C	C
ALHA77299	261	H3	A	A	ALHA81051	43	H4	B/C	B
ALHA78170+	21	H3	B		ALHA81052	29	H4	C	B
ALH 82110	39	H3	B/C	B	ALHA81056	1	H4	B	A
OTTA80301	36	H3	B/C	B	ALHA81057	8	H4	B	A
PCA 82520	23	H3	B/C	A/B	ALHA81058	66	H4	C	C
RKPA80205	54	H3	B	B	ALHA81068	24	H4	B	A
					ALHA81073	3	H4	B/C	A
ALHA77004	2230	H4	C	C	ALHA81074	8	H4	B	B
ALHA77009	236	H4	C	A	ALHA81092	16	H4	B	A
ALHA77010	296	H4	C	A	ALHA81095	59	H4	B/C	C

TABLE B.—Continued.

Specimen number	Weight (g)	Class and type	Degree of weathering	Degree of fracturing
ALHA81097	80	H4	B	A
ALHA81104	184	H4	C	C
ALHA81105	93	H4	C	B/C
ALHA81109	1	H4	B	A
ALHA81114	79	H4	B/C	B/C
ALHA81117	33	H4	B	B/C
ALHA81140	14	H4	B/C	A
ALHA81142	1	H4	B/C	B/C
ALHA81147	2	H4	B	A
ALHA81149	9	H4	B	B
ALHA81157	12	H4	B/C	B
ALHA81177	17	H4	B/C	B
ALHA81199	16	H4	C	B
ALHA81200	9	H4	B/C	A
ALHA81206	4	H4	B/C	A
ALHA81212	11	H4	B/C	B
ALHA81231	9	H4	B/C	B
ALHA81234	5	H4	C	A
ALHA81267	27	H4	C	B/C
ALHA81279	27	H4	C	B/C
ALHA81290	2	H4	B	A
ALHA81309	0.6	H4	C	A
ALH 82126	140	H4	B/C	A
ALH 82128	15	H4	B/C	A
ALH 82133	20	H4	B/C	A/B
ALH 82136	4	H4		B
ALH 84004	9000	H4	B	B
EET 82602	1824	H4	B	B
EET 82609	326	H4	B/C	A/B
EET 82616	2	H4	B/C	A
EET 83207	1238	H4	B	B
EET 83211	543	H4	B/C	B/C
META78001	624	H4	B/C	B
PCA 82511	149	H4	B	B
PCA 82515	7	H4	B	A/B
PCA 82524	114	H4	A/B	B
RKPA78002	8483	H4	B	A/B
RKPA78004	167	H4	A	A
RKPA80232	80	H4	B	A
RKPA80237	22	H4	C	B
RKPA80267	24	H4	C	A
ALH 84006	16000	H4,5	B/C	B
ALHA77007†	99	H5	B	
ALHA77012	180	H5	C	A
ALHA77014	309	H5	C	B/C
ALHA77016†	78	H5	B	
ALHA77017†	78	H5	B	
ALHA77018†	52	H5	B/C	
ALHA77021	17	H5	C	A
ALHA77022†	16	H5	A	
ALHA77023†	21	H5	B	
ALHA77025	19	H5	C	B
ALHA77038†	19	H5	A/B	
ALHA77039†	8	H5	A/B	
ALHA77042†	20	H5	A/B	
ALHA77045†	18	H5	A	
ALHA77051†	15	H5	A	
ALHA77054†	10	H5	B	
ALHA77058†	4	H5	B	
ALHA77061	13	H5	B	A
ALHA77062	17	H5	B	B
ALHA77063†	3	H5	B	
ALHA77064	6	H5	B	B
ALHA77066†	5	H5	A	
ALHA77070†	18	H5	B	
ALHA77071	11	H5	B	B
ALHA77073†	10	H5	A/B	
ALHA77074	12	H5	B	B
ALHA77076†	2	H5	B	
ALHA77078†	24	H5	B	
ALHA77079†	8	H5	A	
ALHA77082†	12	H5	A/B	
ALHA77084†	44	H5	A/B	
ALHA77085†	46	H5	B	
ALHA77086	19	H5	C	B
ALHA77087†	31	H5	B	
ALHA77088	51	H5	C	B
ALHA77091†	4	H5	B/C	
ALHA77092†	45	H5	A	
ALHA77094†	7	H5	B	
ALHA77096†	2	H5	A	
ALHA77098†	8	H5	B	
ALHA77100†	18	H5	A/B	
ALHA77101†	4	H5	B	
ALHA77102	12	H5	B	B
ALHA77104†	6	H5	A	
ALHA77106†	8	H5	A/B	
ALHA77108†	0.7	H5	A/B	
ALHA77112†	22	H5	A	
ALHA77113†	2	H5	B	
ALHA77114†	45	H5	B	
ALHA77118	8	H5	C	B
ALHA77119	6	H5	C	B
ALHA77120†	4	H5	A/B	
ALHA77122†	5	H5	B	
ALHA77124	4	H5	C	A
ALHA77125†	19	H5	A/B	
ALHA77126†	25	H5	A/B	
ALHA77129†	2	H5	B	
ALHA77130†	25	H5	A	
ALHA77132†	115	H5	A/B	
ALHA77136†	4	H5	A/B	
ALHA77138†	2	H5	A	
ALHA77139†	66	H5	A/B	
ALHA77142†	3	H5	A/B	
ALHA77143†	39	H5	A/B	
ALHA77151†	17	H5	A	
ALHA77152†	18	H5	A	
ALHA77153†	12	H5	A	
ALHA77158†	20	H5	B	
ALHA77161†	6	H5	B	
ALHA77168†	25	H5	B	
ALHA77171†	24	H5	A/B	
ALHA77173†	26	H5	B	
ALHA77174†	32	H5	A	
ALHA77177	368	H5	C	A

TABLE B.—Continued.

Specimen number	Weight (g)	Class and type	Degree of weathering	Degree of fracturing
ALHA77181†	33	H5	B	
ALHA77182	1135	H5	C	B
ALHA77184†	128	H5	B	
ALHA77186†	122	H5	A/B	
ALHA77187†	52	H5	A/B	
ALHA77188†	109	H5	A/B	
ALHA77193†	7	H5	A	
ALHA77195†	5	H5	A	
ALHA77201†	15	H5	A	
ALHA77202†	3	H5	B	
ALHA77205†	3	H5	B	
ALHA77207†	5	H5	A/B	
ALHA77213†	8	H5	A	
ALHA77220†	69	H5	B	
ALHA77227†	16	H5	A	
ALHA77228†	19	H5	B	
ALHA77235†	5	H5	A/B	
ALHA77237†	4	H5	A	
ALHA77240†	25	H5	A	
ALHA77242†	56	H5	B	
ALHA77245†	33	H5	A/B	
ALHA77247†	44	H5	A/B	
ALHA77253†	24	H5	A/B	
ALHA77259	294	H5	C	B
ALHA77264	11	H5	A/B	A
ALHA77265†	18	H5	B	
ALHA77266†	108	H5	B	
ALHA77268	272	H5	C	C
ALHA77274	288	H5	C	A
ALHA77275†	25	H5	A	
ALHA77279†	175	H5	A	
ALHA77287	230	H5	C	A
ALHA77291†	6	H5	A	
ALHA77294	1351	H5	A	A
ALHA77300	235	H5	C	B
ALHA78001+	85	H5	B	
ALHA78004*	36	H5		
ALHA78005+	28	H5	B	
ALHA78008	7	H5		
ALHA78010+	1	H5	B	
ALHA78012	38	H5		
ALHA78018+	18	H5	B	
ALHA78021	17	H5		
ALHA78023	10	H5		
ALHA78025+	8	H5	A	
ALHA78027*	29	H5		
ALHA78028	4	H5		
ALHA78031	5	H5		
ALHA78047*	130	H5	B	B
ALHA78049+	96	H5	B	
ALHA78052*	97	H5	C	B
ALHA78075	281	H5	B/C	B
ALHA78079	5	H5		
ALHA78080	25	H5		
ALHA78081*	18	H5		
ALHA78085	219	H5	B	B
ALHA78088*	5	H5		
ALHA78090*	8	H5		
ALHA78092*	16	H5		
ALHA78094*	4	H5		
ALHA78096*	7	H5		
ALHA78098*	2	H5		
ALHA78102	337	H5	B/C	B
ALHA78107	198	H5	C	A
ALHA78108	173	H5	B	B
ALHA78110	161	H5	B/C	B
ALHA78111	127	H5	B/C	A
ALHA78116*	128	H5	B	B
ALHA78117+	4	H5	A	
ALHA78121*	30	H5		
ALHA78123+	18	H5	B	
ALHA78128	155	H5	C	B/C
ALHA78129+	128	H5	B	
ALHA78136+	52	H5	A	
ALHA78139*	17	H5		
ALHA78141	24	H5		
ALHA78146	17	H5		
ALHA78150	16	H5		
ALHA78154+	12	H5	B	
ALHA78159	23	H5		
ALHA78160*	16	H5		
ALHA78163+	10	H5	B	
ALHA78164	25	H5		
ALHA78173+	20	H5	B	
ALHA78174+	13	H5	B	
ALHA78178+	7	H5	B	
ALHA78182	10	H5		
ALHA78190	20	H5		
ALHA78194	25	H5		
ALHA78197	20	H5		
ALHA78199	13	H5		
ALHA78201	10	H5		
ALHA78203	11	H5		
ALHA78205	9	H5		
ALHA78209	12	H5	B/C	B
ALHA78217+	8	H5	B	
ALHA78219+	8	H5	B	
ALHA78221	5	H5	B	A
ALHA78225	5	H5	B	A
ALHA78227	2	H5	B/C	B
ALHA78233	1	H5	B/C	B
ALHA78241	7	H5		
ALHA78245	4	H5		
ALHA78247	3	H5		
ALHA78253+	7	H5	B	
ALHA78255+	3	H5	A	
ALHA78257+	2	H5	B	
ALHA78259+	6	H5	A	
ALHA79004	35	H5	B/C	B
ALHA79006	41	H5	B/C	B
ALHA79008	12	H5	B	B
ALHA79009	76	H5	C	A
ALHA79010	25	H5	B/C	B
ALHA79011	14	H5	B/C	A
ALHA79012	192	H5	C	B
ALHA79013	28	H5	C	B
ALHA79014	11	H5	B	A
ALHA79015	64	H5	B	B

TABLE B.—Continued.

Specimen number	Weight (g)	Class and type	Degree of weathering	Degree of fracturing	Specimen number	Weight (g)	Class and type	Degree of weathering	Degree of fracturing
ALHA79021	29	H5	B	A	ALHA81125	10	H5	B	A
ALHA79025	1208	H5	C	A	ALHA81126	22	H5	B	A
ALHA79026	572	H5	B	B	ALHA81128	16	H5	B/C	A
ALHA79029	506	H5	C	B/C	ALHA81129	32	H5	A/B	A
ALHA79031	3	H5	C	B	ALHA81130	30	H5	B	B
ALHA79032	3	H5	C	B	ALHA81132	5	H5	B	A
ALHA79036	20	H5	B	B	ALHA81133	21	H5	B	A
ALHA79038	50	H5	C	B	ALHA81135	10	H5	B	A
ALHA79040	13	H5	B	A	ALHA81136	1	H5	B	A/B
ALHA79041	20	H5	B	B	ALHA81138	4	H5	B	A
ALHA79042	11	H5	B	A	ALHA81139	7	H5	B/C	B
ALHA79046	90	H5	B	B	ALHA81141	1	H5	B/C	B
ALHA79047	19	H5	B	B	ALHA81143	13	H5	B/C	A
ALHA79048	37	H5	B	B	ALHA81144	3	H5	B	A
ALHA79050	27	H5	C	B	ALHA81148	13	H5	B	A
ALHA79051	24	H5	C	A	ALHA81152	10	H5	B	A
ALHA79053	86	H5	B/C	B	ALHA81155	5	H5	A/B	A
ALHA79054	36	H5	B	A	ALHA81158	2	H5	B/C	A
ALHA80111	42	H5	B	A	ALHA81161	122	H5	C	C
ALHA80123	28	H5	C	A	ALHA81163	82	H5	C	B/C
ALHA80124	12	H5	B	B	ALHA81164	20	H5	B	A
ALHA80127	47	H5	B	A	ALHA81165	6	H5	B	A
ALHA80129	93	H5	B	A	ALHA81166	26	H5	B	A
ALHA80132	153	H5	B	B	ALHA81168	8	H5	C	B
ALHA81015	5489	H5	B	B	ALHA81169	6	H5	B	B
ALHA81019	1051	H5	B/C	B	ALHA81170	59	H5	B	A/B
ALHA81020	1353	H5	B	A	ALHA81171	24	H5	B/C	B
ALHA81033	252	H5	C	C	ALHA81173	26	H5	A/B	A
ALHA81034	255	H5	B	B	ALHA81175	13	H5	A/B	B
ALHA81036	252	H5	C	A	ALHA81176	95	H5	B	A
ALHA81039	206	H5	A/B	B	ALHA81178	30	H5	B/C	B/C
ALHA81042	534	H5	C	C	ALHA81179	14	H5	B	A
ALHA81062	0.5	H5	C	A	ALHA81182	5	H5	B	A/B
ALHA81063	5	H5	B/C	B	ALHA81183	104	H5	C	B/C
ALHA81064	191	H5	C	A/B	ALHA81186	23	H5	B	A/B
ALHA81067	228	H5	C	B	ALHA81188	9	H5	A/B	A
ALHA81070	4	H5	B/C	A	ALHA81192	9	H5	A/B	A
ALHA81071	2	H5	B	A	ALHA81194	17	H5	B	B
ALHA81072	3	H5	B/C	A	ALHA81195	5	H5	B	A/B
ALHA81075	16	H5	B	A	ALHA81197	68	H5	B/C	B/C
ALHA81077	4	H5	B	A	ALHA81201	7	H5	B/C	A
ALHA81080	17	H5	A/B	A	ALHA81202	5	H5	C	A
ALHA81081	5	H5	B	A	ALHA81207	14	H5	C	B
ALHA81082	6	H5	B	A	ALHA81209	14	H5	B/C	A
ALHA81083	7	H5	B	A	ALHA81211	7	H5	B	A
ALHA81084	16	H5	B	A	ALHA81213	3	H5	B/C	A
ALHA81088	4	H5	B	A	ALHA81215	11	H5	A	A
ALHA81089	11	H5	B	A	ALHA81216	2	H5	C	A
ALHA81090	10	H5	B	A	ALHA81218	6	H5	C	B
ALHA81091	12	H5	B	B	ALHA81219	24	H5	B	A
ALHA81100	155	H5	B	A	ALHA81220	3	H5	B/C	A/B
ALHA81108	69	H5	B	B	ALHA81226	3	H5	C	A
ALHA81110	3	H5	B/C	A	ALHA81227	11	H5	B	B
ALHA81113	111	H5	B/C	C	ALHA81228	8	H5	B/C	A
ALHA81115	155	H5	C	A/B	ALHA81230	13	H5	B	B
ALHA81116	2	H5	B	A	ALHA81232	5	H5	B	A/B
ALHA81118	85	H5	B/C	A	ALHA81233	25	H5	C	B/C
ALHA81120	14	H5	B/C	B	ALHA81236	41	H5	A/B	A/B
ALHA81124	9	H5	B	A	ALHA81237	27	H5	B	B

TABLE B.—Continued.

Specimen number	Weight (g)	Class and type	Degree of weathering	Degree of fracturing	Specimen number	Weight (g)	Class and type	Degree of weathering	Degree of fracturing
ALHA81238	24	H5	C	B	PCA 82517	41	H5	B/C	B
ALHA81239	32	H5	B	B	PCA 82521	1	H5	C	A
ALHA81240	41	H5	C	C	PCA 82522	46	H5	B/C	B
ALHA81241	34	H5	B	A/B	RKPA79004	371	H5	B/C	B
ALHA81242	20	H5	B/C	A	RKPA79014	78	H5	B/C	B
ALHA81244	5	H5	B	A	RKPA80210	11	H5	B/C	B
ALHA81245	4	H5	B/C	A/B	RKPA80217	8	H5	C	A
ALHA81246	3	H5	C	A	RKPA80218	7	H5	C	A
ALHA81249	10	H5	B/C	A	RKPA80220	124	H5	B/C	B/C
ALHA81252	2	H5	B	A	RKPA80223	25	H5	C	B
ALHA81255	12	H5	B	B	RKPA80227	8	H5	B/C	A
ALHA81256	28	H5	C	A	RKPA80230	58	H5	B	B
ALHA81263	6	H5	B	B	RKPA80233	414	H5	B/C	B
ALHA81265	8	H5	B/C	A	RKPA80236	16	H5	B/C	B
ALHA81269	5	H5	B/C	A	RKPA80240	61	H5	C	A
ALHA81270	4	H5	C	A/B	RKPA80243	3	H5	C	A
ALHA81274	19	H5	A/B	A	RKPA80244	14	H5	C	B
ALHA81275	11	H5	B	A	RKPA80245	37	H5	B/C	B
ALHA81276	42	H5	C	B	RKPA80247	1	H5	C	B
ALHA81277	7	H5	B	A	RKPA80249	10	H5	B/C	A
ALHA81281	46	H5	B	B	RKPA80250	4	H5	B/C	A
ALHA81283	0.6	H5	B/C	A	RKPA80251	29	H5	B	B
ALHA81284	10	H5	B/C	A	RKPA80257	9	H5	B/C	B
ALHA81286	28	H5	B	B	RKPA80260	8	H5	C	B
ALHA81287	78	H5	C	B/C	TIL 82409	231	H5	B	A
ALHA81293	2	H5	B	A/B	TIL 82412	35	H5	C	B
ALHA81294	9	H5	B	A	TIL 82413	18	H5	C	B
ALHA81295	105	H5	C	B/C	TIL 82414	15	H5	B	A
ALHA81296	13	H5	B/C	B	T1L 82415	70	H5	A/B	A
ALHA81297	20	H5	B	A					
ALHA81300	10	H5	A/B	A	ALHA78147*	31	H5,6		
ALHA81301	12	H5	B/C	A					
ALHA81302	4	H5	B/C	A	ALHA76006	271	H6	C	B
ALHA81305	1	H5	B/C	A	ALHA76008	281	H6	B/C	B
ALHA81306	7	H5	B	A	ALHA77046†	8	H6	A/B	
ALHA81308	19	H5	B/C	B	ALHA77111†	52	H6	A/B	
ALHA81314	3	H5	B	A	ALHA77131†	26	H6	A/B	
ALH 82102	48	H5	B/C	A	ALHA77133†	19	H6	A	
ALH 82103	2529	H5	B	B	ALHA77134†	19	H6	A	
ALH 82108	14	H5	B/C	A	ALHA77144	8	H6	B	A
ALH 82109	47	H5	B/C	A/B	ALHA77146†	18	H6	A/B	
ALH 82112	28	H5	C	A	ALHA77147†	19	H6	A/B	
ALH 82114	41	H5	A/B	A	ALHA77148	13	H6	C	B
ALH 82115	48	H5	A/B	A	ALHA77149†	26	H6	A/B	
ALH 82119	24	H5	B/C	B	ALHA77157†	88	H6	A/B	
ALH 82120	7	H5	B	A	ALHA77183	288	H6	C	A
ALH 82122	142	H5	B	A	ALHA77200†	0.9	H6	C	
ALH 82129	14	H5	B/C	A	ALHA77209†	32	H6	B	
ALH 82134	28	H5	B/C	A	ALHA77212†	17	H6	A/B	
ALH 82141	0.6	H5	C	A	ALHA77239†	19	H6	B	
ALH 82144	7	H5	B	A	ALHA77246†	42	H6	B	
EETA79007	200	H5	B	B	ALHA77248†	96	H6	B/C	
EET 82603	8210	H5	B	A	ALHA77258	597	H6	B/C	A/B
EET 82604	1571	H5	B/C	B	ALHA77271	610	H6	C	A
EET 82614	8	H5	A/B	A	ALHA77285	271	H6	C	B
EET 83200	779	H5	B/C	B	ALHA77288	1880	H6	C	B
EET 83203	546	H5	B/C	B/C	ALHA78002+	11	H6	A	
EET 83208	263	H5	B/C	B	ALHA78035	2	H6		
META78010	234	H5	B	A	ALHA78065+	7	H6	B	

TABLE B.—Continued.

Specimen number	Weight (g)	Class and type	Degree of weathering	Degree of fracturing	Specimen number	Weight (g)	Class and type	Degree of weathering	Degree of fracturing
ALHA78067	8	H6			ALHA81160	12	H6	C	B
ALHA78069+	4	H6	B		ALHA81180	17	H6	C	B
ALHA78076	276	H6	B	B	ALHA81193	13	H6	B	A
ALHA78086*	9	H6			ALHA81196	9	H6	B	A
ALHA78115	848	H6	B	A	ALHA81204	7	H6	B	A
ALHA78122	5	H6			ALHA81210	0.6	H6	B	A
ALHA78124	28	H6			ALHA81223	10	H6	A/B	A
ALHA78135*	131	H6	B	B	ALHA81224	14	H6	B/C	A
ALHA78137	70	H6			ALHA81225	14	H6	B	A
ALHA78145+	34	H6	A		ALHA81248	5	H6	C	A/B
ALHA78152	5	H6			ALHA81250	17	H6	B	B
ALHA78169+	22	H6	B		ALHA81253	10	H6	A/B	B
ALHA78184	8	H6			ALHA81254	9	H6	C	A
ALHA78189	23	H6			ALHA81268	18	H6	C	B/C
ALHA78191	20	H6			ALHA81271	28	H6	B	B
ALHA78207	8	H6			ALHA81273	43	H6	C	B/C
ALHA78211	11	H6	B	B	ALHA81288	20	H6	B	A
ALHA78213	10	H6	B	B	ALHA81291	4	H6	B	A
ALHA78215	6	H6	B/C	B	ALHA81298	16	H6	B	B
ALHA78229	2	H6	B	B	ALHA81303	4	H6	B/C	A
ALHA78231	2	H6	B/C	B	ALHA81310	0.7	H6	B	A
ALHA78249	4	H6			ALH 82113	61	H6	A/B	A
ALHA79002	223	H6	C	B	ALH 82116	18	H6	B	B
ALHA79005	60	H6	B	B	ALH 82124	26	H6	C	A/B
ALHA79016	1146	H6	B/C	B	ALH 82127	5	H6	A/B	A
ALHA79019	12	H6	B	A	ALH 82138	5	H6	B	A/B
ALHA79020	4	H6	B/C	B	ALH 82143	3	H6	C	A/B
ALHA79024	22	H6	C	B	EET 82610	42	H6	B	A
ALHA79028	16	H6	B	B	EET 82615	29	H6	B	A
ALHA79034	13	H6	B	A	EET 83201	1060	H6	B/C	A
ALHA79037	15	H6	B	B	EET 83215	510	H6	B/C	C
ALHA79049	54	H6	C	B	MBRA76001	1096	H6	B	B
ALHA79055	15	H6	B/C	B	MBRA76002	13773	H6	B	B
ALHA80118	2	H6	B	A	META78006	410	H6	C	B
ALHA80122	50	H6	B/C	B	META78007	175	H6	B/C	B
ALHA80126	35	H6	A/B	A	PCA 82512	55	H6	B	A
ALHA80130	5	H6	B/C	A	PCA 82516	16	H6	B/C	B
ALHA81035	256	H6	C	A/B	PCA 82523	11	H6	A	B
ALHA81037	320	H6	B	A	PCA 82526	25	H6	B	A
ALHA81038	229	H6	C	B	PCA 82527	3	H6	A	A
ALHA81054	2	H6	B	B	RKPA79003	182	H6	B	A
ALHA81055	5	H6	B	A	RKPA79009	55	H6	C	B
ALHA81076	10	H6	B	A	RKPA79012	13	H6	B	B
ALHA81078	6	H6	B/C	B	RKPA80201	813	H6	B	A
ALHA81079	7	H6	C	A	RKPA80203	4	H6	C	A
ALHA81086	6	H6	B	B	RKPA80206	47	H6	C	B
ALHA81093	271	H6	A/B	A/B	RKPA80208	10	H6	B	A
ALHA81094	152	H6	C	B	RKPA80211	2	H6	C	B
ALHA81096	83	H6	B	B	RKPA80213	19	H6	B/C	B
ALHA81102	196	H6	B/C	A/B	RKPA80214	5	H6	C	B
ALHA81103	136	H6	B/C	B/C	RKPA80221	52	H6	C	B/C
ALHA81111	210	H6	B/C	B	RKPA80231	238	H6	C	B/C
ALHA81112	150	H6	B/C	A	RKPA80254	68	H6	C	B/C
ALHA81127	15	H6	B/C	B	RKPA80255	7	H6	C	B
ALHA81134	15	H6	B/C	B	RKPA80262	32	H6	C	B
ALHA81137	9	H6	B/C	A/B	RKPA80265	8	H6	C	B
ALHA81146	24	H6	C	B	RKPA80266	10	H6	B/C	B
ALHA81154	1	H6	B	B	TIL 82405	1116	H6	B	A

TABLE B.—Continued.

Specimen number	Weight (g)	Class and type	Degree of weathering	Degree of fracturing
ALHA81174	33	H	B	B/C
ALHA77081	9	"H(?)" (Acapulco-like)	B	A
ALHA81261	12		A/B	A
ALHA81315	2		A/B	A
ALHA77011	292	L3	C	A
ALHA77013†	23	L3	B	
ALHA77015	411	L3	C	B
ALHA77031†	0.5	L3	B/C	
ALHA77033	9	L3	C	B
ALHA77034†	2	L3	B/C	
ALHA77036†	8	L3	B	
ALHA77043†	11	L3	B/C	
ALHA77047†	20	L3	C	
ALHA77049†	7	L3	B/C	
ALHA77050†	84	L3	B/C	
ALHA77052†	112	L3	B/C	
ALHA77115†	154	L3	B/C	
ALHA77140	79	L3	C	B
ALHA77160	70	L3	C	B
ALHA77163†	24	L3	B/C	
ALHA77164	38	L3	C	C
ALHA77165	31	L3	C	C
ALHA77166†	139	L3	C	
ALHA77167	611	L3	C	B/C
ALHA77170†	12	L3	B/C	
ALHA77175†	23	L3	B/C	
ALHA77176†	55	L3	B	
ALHA77178†	6	L3	B/C	
ALHA77185†	28	L3	A/B	
ALHA77197†	20	L3	A/B	
ALHA77211†	27	L3	B/C	
ALHA77214	2111	L3	C	C
ALHA77215	820	L3	B	B/C
ALHA77216	1470	L3	A/B	B/C
ALHA77217	413	L3	B	B/C
ALHA77241†	144	L3	C	
ALHA77244†	40	L3	B/C	
ALHA77249	504	L3	C	C
ALHA77252	343	L3	B	C
ALHA77260	744	L3	C	C
ALHA77303†	79	L3	B/C	
ALHA78013	4	L3		
ALHA78017+	3	L3	B	
ALHA78037+	0.5	L3	B	
ALHA78038	363	L3	C	C
ALHA78041+	118	L3	B	
ALHA78046	70	L3		
ALHA78119+	103	L3	A	
ALHA78133	60	L3		
ALHA78149+	23	L3	B	
ALHA78162+	33	L3	B	
ALHA78176+	8	L3	B	
ALHA78180+	8	L3	B	
ALHA78186	3	L3		
ALHA78188	0.9	L3	C	B
ALHA78235+	19	L3	B	
ALHA78236	14	L3		
ALHA78238	10	L3		
ALHA78239+	16	L3	B	
ALHA78243	2	L3		
ALHA79001	32	L3	C	A
ALHA79045	115	L3	C	B
ALHA80133	4	L3	B	B
ALHA81024	798	L3	C	B
ALHA81025	379	L3	C	B
ALHA81030	1852	L3	B/C	B/C
ALHA81031	1595	L3	C	B/C
ALHA81032	727	L3	C	A
ALHA81053	3	L3	C	B
ALHA81060	28	L3	C	B
ALHA81061	24	L3	B/C	A
ALHA81065	13	L3	B/C	B
ALHA81066	9	L3	C	B
ALHA81069	7	L3	B/C	A
ALHA81085	16	L3	C	B
ALHA81087	8	L3	B/C	B
ALHA81121	88	L3	B	B
ALHA81145	21	L3	B	B
ALHA81156	20	L3	B/C	B/C
ALHA81162	59	L3	C	C
ALHA81190	48	L3	C	A/B
ALHA81191	30	L3	C	B/C
ALHA81214	4	L3	B/C	A
ALHA81229	40	L3	C	B/C
ALHA81243	15	L3	C	B
ALHA81259	10	L3	C	B
ALHA81272	23	L3	C	B
ALHA81280	55	L3	C	B
ALHA81292	13	L3	C	A/B
ALHA81299	0.5	L3	C	A/B
ALH83010	395	L3	B	A
EET 82601	150	L3	B/C	A
EET 83213	2727	L3	B	A
RKPA79008	73	L3	B	B
RKPA80207	18	L3	C	B
RKPA80256	153	L3	B	A
ALHA79022	31	L3,4	A/B	B
ALHA77230	2473	L4	C	B
ALHA77304	650	L4	B	B
ALHA78044	164	L4	B/C	B
ALHA78070	10	L4		
ALHA81040	195	L4	B/C	A
ALHA81119	107	L4	B	B
ALHA81184	17	L4	A/B	A
ALH 83001	1569	L4	B	A
EET 82611	13	L4	B	B
EET 82613	4	L4	B	A
PCA 82514	130	L4	B	A
RKPA80216	44	L4	B	B
RKPA80242	7	L4	B/C	B
TIL 82404	322	L4	B	B
TIL 82406	152	L4	B	A
TIL 82407	221	L4	B/C	A
TIL 82411	180	L4	A/B	A
TYR 82700	892	L4	B	A

TABLE B.—Continued.

Specimen number	Weight (g)	Class and type	Degree of weathering	Degree of fracturing
ALHA77002	235	L5	B	A/B
ALHA77117†	21	L5	A/B	
ALHA77127†	4	L5	B	
ALHA77218†	45	L5	A	
ALHA77254	246	L5	A/B	A
ALHA77267†	104	L5	A	
ALHA78142*	32	L5		
ALHA81017	1434	L5	B	A
ALHA81018	2237	L5	B	B
ALHA81023	418	L5	B	A/B
ALHA81153	4	L5	B	A
ALHA81198	0.9	L5	B/C	A
ALH 82104	399	L5	A	A/B
ALH 82107	9	L5	B/C	A
ALH 82117	4	L5	B	B
ALH 82137	11	L5	B	A
EETA79009	140	L5	B	B
PCA 82504	3094	L5	A/B	B
PCA 82505	3086	L5	B	B
PCA 82510	254	L5	A	A
PCA 82513	239	L5	A/B	A
PCA 82519	125	L5	B	A
RKPA79013	11	L5	B/C	B
RKPA80209	10	L5	C	B
RKPA80228	11	L5	C	B
RKPA80268	3	L5	B/C	B
TIL 82400	221	L5	A/B	B
ALHA76001	20151	L6	A	A
ALHA76003	10495	L6	A	A
ALHA76007	79	L6	B	A
ALHA76009	3950	L6	B	B
ALHA77001	252	L6	B	B
ALHA77008†	93	L6	A	
ALHA77019†	60	L6	B/C	
ALHA77026†	20	L6	B/C	
ALHA77027†	4	L6	B/C	
ALHA77089†	8	L6	B	
ALHA77150	58	L6	C	B
ALHA77155	305	L6	A/B	A
ALHA77159†	17	L6	A/B	
ALHA77162†	29	L6	A	
ALHA77180	191	L6	C	A
ALHA77198†	7	L6	B	
ALHA77231	9270	L6	A/B	A/B
ALHA77251†	69	L6	B	
ALHA77261	412	L6	B	B
ALHA77269	1045	L6	B	A
ALHA77270	589	L6	A/B	B
ALHA77272	674	L6	B/C	B
ALHA77273	492	L6	B	B
ALHA77277	143	L6	A/B	A
ALHA77280	3226	L6	B	B/C
ALHA77281	1231	L6	B	B
ALHA77282	4127	L6	B	B
ALHA77284	376	L6	A/B	B
ALHA77292	200	L6	B	A
ALHA77293†	110	L6	B	
ALHA77296	963	L6	A/B	A
ALHA77297	952	L6	A	B
ALHA77301†	55	L6	A	
ALHA77305	6444	L6	B/C	B
ALHA78003	125	L6	C	B
ALHA78039	299	L6	B	B
ALHA78042	214	L6	B	A
ALHA78043	680	L6	B	B
ALHA78045	39	L6	B/C	B
ALHA78048	191	L6	A/B	B
ALHA78050	1045	L6	B	B
ALHA78055+	14	L6	B	
ALHA78059+	9	L6	B	
ALHA78074	200	L6	B	B
ALHA78078	290	L6	A/B	A
ALHA78101	121	L6		
ALHA78103	590	L6	B	B
ALHA78104	672	L6	B	A
ALHA78105	942	L6	B	A
ALHA78106	465	L6	A/B	A
ALHA78112	2485	L6	B	B
ALHA78114	808	L6	B/C	B
ALHA78125*	19	L6	B	B
ALHA78126	607	L6	B	B
ALHA78127	195	L6	B/C	B
ALHA78130	2733	L6	B/C	B
ALHA78131	269	L6	B/C	A
ALHA78156	9	L6		
ALHA78171+	23	L6	B	
ALHA78251	1312	L6	B	A
ALHA79007	142	L6	A/B	B
ALHA79018	121	L6	B/C	A/B
ALHA79027	133	L6	B	A
ALHA79033	281	L6	B	A
ALHA79043	62	L6	C	B
ALHA79052	23	L6	B/C	B
ALHA80101	8725	L6	B	B
ALHA80103	536	L6	B	A
ALHA80105	445	L6	B	B
ALHA80107	178	L6	B	B
ALHA80108	125	L6	B	B
ALHA80110	168	L6	B	B
ALHA80112	331	L6	B	B
ALHA80113	313	L6	B	B/C
ALHA80114	233	L6	B	B
ALHA80115	306	L6	B	A
ALHA80116	191	L6	B/C	B
ALHA80117	89	L6	B	A
ALHA80119	34	L6	B	B
ALHA80120	60	L6	B	B
ALHA80125	139	L6	B/C	B
ALHA81016	3850	L6	B	A
ALHA81026	516	L6	B	A
ALHA81027	3835	L6	C	A/B
ALHA81028	80	L6	B	B
ALHA81029	153	L6	C	A
ALHA81099	152	L6	A/B	A
ALHA81106	48	L6	B	B
ALHA81107	140	L6	B	A

TABLE B.—Continued.

Specimen number	Weight (g)	Class and type	Degree of weathering	Degree of fracturing
ALHA81122	21	L6	B	B
ALHA81131	13	L6	A/B	B
ALHA81150	2	L6	C	A
ALHA81159	10	L6	B/C	A
ALHA81167	59	L6	B/C	B
ALHA81172	33	L6	C	B
ALHA81181	15	L6	B	A
ALHA81203	4	L6	C	A
ALHA81205	3	L6	B	A
ALHA81217	5	L6	C	B/C
ALHA81221	9	L6	C	A/B
ALHA81235	7	L6	C	B
ALHA81247	104	L6	A/B	B
ALHA81257	29	L6	B	A
ALHA81262	55	L6	A/B	B
ALHA81266	12	L6	A/B	B
ALHA81278	1	L6	B	A
ALHA81282	31	L6	A/B	A
ALHA81289	4	L6	A	A
ALHA81304	42	L6	A/B	B
ALHA81307	57	L6	B	B/C
ALHA81311	0.9	L6	B	A
ALH 82105	363	L6	A/B	A
ALH 82111	63	L6	A/B	A
ALH 82118	111	L6	A/B	B
ALH 82121	2	L6	A	B
ALH 82123	111	L6	B	A
ALH 82125	178	L6	C	B
ALH 82139	0.2	L6	B	A
ALH 82140	0.3	L6	C	A
ALH 82142	20	L6	C	B/C
ALH 83101	639	L6	A	A
BTNA78001	161	L6	B	B
BTNA78002	4301	L6	B	A
EETA79003	436	L6	B	B
EETA79010	287	L6	B	C
EET 82605	625	L6	B	A
EET 82606	982	L6	B	B
EET 82607	165	L6	B/C	A
EET 82612	32	L6	A	A
EET 83202	1213	L6	A/B	B
EET 83205	471	L6	A/B	B
EET 83206	462	L6	B	A
EET 83209	520	L6	B/C	A
EET 83210	426	L6	A/B	B
EET 83214	1398	L6	B	A
EET 83237	883	L6	B	A/B
META78002	542	L6	B	A
META78003	1726	L6	B	B
META78005	172	L6	B	B
META78028	20657	L6	B	B
PCA 82503	8308	L6	A	B
PCA 82508	389	L6	A/B	B
PCA 82509	286	L6	B	A
PCA 82525	40	L6	B	B
PCA 82528	51	L6	B/C	B
RKPA78001	235	L6	C	B
RKPA78003	1276	L6	C	B
RKPA79001	3006	L6	B	C
RKPA79002	204	L6	B	B
RKPA80202	545	L6	B	A
RKPA80215	9	L6	C	B
RKPA80219	21	L6	B	A
RKPA80225	8	L6	C	A
RKPA80252	11	L6	A/B	A
RKPA80261	62	L6	B	A
RKPA80264	24	L6	B	B
TIL 82401	282	L6	A/B	A
ALHA78015*	35	LL(?L)3		
ALHA76004	53	LL3	A	A
ALHA77278	313	LL3	A	A
ALHA78138+	11	LL3	B	
ALHA79003	5	LL3	B	B
ALHA81251	158	LL3	B/C	B
TIL 82408	80	LL3	B	A/B
ALHA77060†	64	LL5	A	
ALHA78109	233	LL5	A/B	A
ALHA81151	5	LL5	B/C	A
RKPA80234	136	LL5	B	B
RKPA80253	5	LL5	A/B	A
ALHA77041†	17	LL6	A	
ALHA78062	11	LL6		
ALHA78063+	77	LL6	A	
ALHA78082+	24	LL6	A	
ALHA78153	152	LL6	B/C	B
ALHA81123	2	LL6	B	A
ALHA81185	65	LL6	A/B	A/B
ALHA81285	20	LL6	C	A
BTNA78004	1079	LL6	B	A
EET 82608	95	LL6	A/B	A
EET 83204	377	LL6	A	A
PCA 82507	480	LL6	A	A/B
RKPA80222	7	LL6	B	B
RKPA80235	261	LL6	A/B	B
RKPA80238	18	LL6	A/B	A
RKPA80248	11	LL6	A/B	A
TIL 82402	476	LL6	A/B	A
ALH 84027	8	LL7(?)	B	B

TABLE B.—Continued.

CHONDRITE subtotals:	Class and type	Class weight (g)
	C2	2680
	C3	181
	C30	810
	C3V	748
	C4	103
	E4	31
	EH4	159
	E5	20
	E6	819
	H3	433
	H4	83289
	H4,5	16000
	H5	42892
	H5,6	31
	H6	30305
	H	33
	H(?)	23
	L3	19377
	L3,4	31
	L4	7149
	L5	12397
	L6	154434
	LL(?L)3	35
	LL3	619
	LL5	443
	LL6	3170
	LL7(?)	8
Total:		376220

Specimen number	Weight (g)	Class and type	Degree of weathering	Degree of fracturing	Specimen number	Weight (g)	Class and type	Degree of weathering	Degree of fracturing
				ACHONDRITES					
ALHA81187	40	A (unique)	B/C	B	ALHA78158	15	Eu (polymict)	A	A
ALH 84025	5	A (unique)	A/B	A	ALHA78165	21	Eu (polymict)	A	A
					ALHA79017	310	Eu (polymict)	A	A
ALHA81005	31	Anorthositic breccia	A/B	A	ALHA80102	471	Eu (polymict)	A	B
					ALHA81001	53	Eu (anomalous)	A	B
					ALHA81006	255	Eu (polymict)	A	A/B
ALHA78113	299	Au	A/B	A	ALHA81007	164	Eu (polymict)	A/B	A
ALH 83009	2	Au	A/B	A	ALHA81008	44	Eu (polymict)	A/B	A/B
ALH 83015	3	Au	A/B	A	ALHA81009	229	Eu	A	A
					ALHA81010	219	Eu (polymict)	A	A
ALH 84007	706	Au	A	A/B	ALHA81011	406	Eucritic breccia	A/B	A
ALH 84008	302	Au	A/B	A	ALHA81012	37	Eu	A/B	A
ALH 84011	138	Au	A	A/B	ALHA81313	0.5	Eu (?)		
					EETA79004	390	Eu	B	B
EET 83235	255	Basaltic achon.	B	B	EETA79005	451	Eu (polymict)	A	B
					EETA79011	86	Eu (polymict)	B	B
					EET 83212	402	Eu (polymict)	B	B
ALHA77256	676	Di	A/B	A	EET 83227	1973	Eu (polymict)	B	B
ALH 84001	1931	Di	A/B	B	EET 83228	1206	Eu (polymict)	B	B
EETA79002	2843	Di	B	B	EET 83229	313	Eu (polymict)	B	B
EET 83246	48	Di	A/B	A/B	EET 83231	66	Eu (polymict)	B	A/C
EET 83247	22	Di	B/C	B	EET 83232	211	Eu (polymict)	B	A/B
TIL 82410	19	Di	A		EET 83234	181	Eu (polymict)	B	B
					EET 83236	6	Eu	B	A
ALHA81208	2	Di/M	C	B	EET 83251	261	Eu (polymict)	B	A/B
					EET 83283	57	Eu (polymict)	B	B
ALHA76005	317	Eu (polymict)	A	A	PCA 82501	54	Eu (unbrecciated)	A	A
ALHA77302	236	Eu (polymict)	A	A	PCA 82502	890	Eu (unbrecciated)	A	A
ALHA78040	212	Eu (polymict)	A	A	RKPA80204	15	Eu	A	A
ALHA78132	656	Eu (polymict)	A	A	RKPA80224	8	Eu (unbrecciated)	A/B	A

TABLE B.—Continued.

Specimen number	Weight (g)	Class and type	Degree of weathering	Degree of fracturing	Specimen number	Weight (g)	Class and type	Degree of weathering	Degree of fracturing
RKPA80224	8	Eu (unbrecciated)	A/B	A	ALHA77257	1996	Ur	A	B
TIL 82403	50	Eu (brecciated)	A	A	ALHA78019	30	Ur	B/C	C
					ALHA78262	26	Ur	B/C	A
ALHA78006	8	Ho	A	A	ALHA81101	119	Ur	A/B	B
EETA79006	716	Ho	B	B	ALH 82106	35	Ur	B	A
EET 82600	247	Ho	A	B	ALH 82130	45	Ur	B	A
					ALH 83014	1	Ur	B	A
ALHA77005	483	Sh	A	A	EET 83225	44	Ur	B/C	B
EETA79001	7942	Sh	A	A	PCA 82506	5316	Ur	A/B	A
					RKPA80239	6	Ur	B	B

ACHONDRITE subtotals:	Class and type	Class weight (g)
	A (unique)	45
	Anorthositic breccia	31
	Aubrite	1449
	Basaltic breccia	255
	Diogenite	5540
	Diogenite/Mesos.	2
	Eucrite	10266
	Howardite	971
	Shergottite	8425
	Ureilite	7618
Total:		34602

Specimen number	Weight (g)	Class and type	Degree of weathering	Degree of fracturing	Specimen number	Weight (g)	Class and type	Degree of weathering	Degree of fracturing
					IRONS				
ALHA77255	765	Ataxite (anom)			ALHA77290	3784	IA		
ALHA80104	882	Ataxite			PGPA77006	19068	IA		
EET 83230	530	Ataxite							
ILD 83500	2523	Ataxite			ALHA78100	85	IIA		
ALHA81013	17727	Hexahedrite			DRPA78001	15200	IIB		
					DRPA78002	7188	IIB		
ALHA81014	188	Octahedrite			DRPA78003	144	IIB		
EET 83245	59	Octahedrite			DRPA78004	134	IIB		
RKPA80226	160	Octahedrite			DRPA78005	18600	IIB		
					DRPA78006	389	IIB		
ALHA76002	307	IA			DRPA78007	11800	IIB		
ALHA77250	10555	IA			DRPA78008	59400	IIB		
ALHA77263	1669	IA			DRPA78009	138100	IIB		
ALHA77283	10510	IA							
ALHA77289	2186	IA			ALHA78252	2789	IVA		

Total weight (g): 324743

Specimen number	Weight (g)	Class and type	Degree of weathering	Degree of fracturing	Specimen number	Weight (g)	Class and type	Degree of weathering	Degree of fracturing
					STONY-IRON				
ALHA77219	637	M	B	B	RKPA80229	14	M	C	B/C
ALHA81059	540	M	C	B/C	RKPA80246	6	M	C	C
ALHA81098	71	M	C	B/C	RKPA80258	4	M	B/C	B
RKPA79015	10022	M	A/B	A	RKPA80263	17	M	C	B

Total weight (g): 11311

TABLE C.—Meteorites tentatively identified as paired specimens from common falls. Pairing criteria are field relations (t), megascopic physical similarities (v), petrographic and mineral chemical similarities (w), metallography (x), bulk chemistry (y), and trace element chemistry (z). This list is restricted to paired groups listed in the *Antarctic Meteorite Newsletters* and which are assigned pairing confidence levels of over 50% by Scott (Chapter 13). For a more comprehensive discussion of the pairing problem, and a more inclusive list of pairings, see Scott (Chapter 13) and Scott (1984)*.

Pair no.	Paired specimens	Criteria
	AUBRITES	
1	ALH83009, 83015	v,w
	EUCRITES	
2	ALHA81009, 81012	v,w
3	ALHA76005, 77302, 78040, 78132, 78158, 78165, 79017, 80102	v,w
4	ALHA81006, 81007, 81008, 81010	v,w
5	EETA79004, 83228	w
	HOWARDITES	
6	EETA79006, 82600	w
	UREILITES	
7	ALHA78019, 78262	v,w
8	ALH82106, 82130	w
	C2 CHONDRITES	
9	ALHA81002, 81004	w
10	ALH83100, 83102	v,w
	C30 CHONDRITES	
11	ALHA77003, 82101	w
	C3V CHONDRITES	
12	ALHA81003, 81258	w
	EH4 CHONDRITES	
13	ALHA77156, 77295	w
	E6 CHONDRITES	
14	ALHA81021, 81260	w
	"H?" CHONDRITES (Acapulco-like)	
15	ALHA77081, 81261, 81315	w
	H4 CHONDRITES	
16	ALHA77004, 77190, 77191, 77192, 77208, 77223, 77224, 77225, 77226, 77232, 77233	t,w
17	ALHA78193, 78196, 78223	t,x
18	ALHA81041, 81043, 81044, 81045, 81046, 81047, 81048, 81049, 81050, 81051, 81052	w

*Scott, E.R.D. 1984. Pairing of Meteorites Found in Victoria Land, Antarctica. *Memoirs of the National Institute of Polar Research* (Japan), special issue, 35:102–125. Tokyo.

TABLE C.—Continued.

Pair no.	Paired specimens	Criteria
	H5 CHONDRITES	
19	ALHA77014, 77264	t
20	ALHA77021, 77025, 77061, 77062, 77064, 77071, 77074, 77086, 77088	t,w
21	ALHA77118, 77119, 77124	t
22	ALHA78209, 78221, 78225, 78227, 78233	t,x
23	ALHA79031, 79032	w
24	ALHA80127, 80129, 80132	w
25	RKPA80217, 80218	w
26	RKPA80220, 80223	w
27	RKPA80250, 80251	w
28	TIL82412, 82413	w
29	TIL82414, 82415	w
	H6 CHONDRITES	
30	MBRA76001, 76002	w
31	ALHA77144, 77148	t
32	ALHA77271, 77288	t
33	ALHA78211, 78213, 78215, 78229, 78231	t,x
34	ALHA80122, 80126, 80130	w
35	ALHA81035, 81038, 81103, 81112	w
36	RKPA80203, 80206, 80208, 80211, 80213, 80214, 80221, 80231, 80254, 80255, 80265, 80266	w
37	EET82610, 82615	w
38	PCA82526, 82527	w
	L3 CHONDRITES	
39	ALHA77011, 77015, 77031, 77033, 77034, 77036, 77043, 77047, 77049, 77050, 77052, 77115, 77140, 77160, 77163, 77164, 77165, 77166, 77167, 77170, 77175, 77178, 77185, 77211, 77214, 77241, 77244, 77249, 77260, 77303, 78013, 78038, 78186, 78188, 78236, 78238, 78243, 79001, 79045, 80133, 81025, 81030, 81031, 81032, 81053, 81060, 81061, 81065, 81066, 81069, 81085, 81087, 81121, 81145, 81156, 81162, 81190, 81191, 81214	w
40	ALHA77215, 77216, 77217, 77252	t,v,w
	L4 CHONDRITES	
41	RKPA80216, 80242	w
	L5 CHONDRITES	
42	ALHA81017, 81018, 81023	w
43	PCA82504, 82505	w
	L6 CHONDRITES	
44	ALHA77001, 77292, 77293, 77296, 77297	t,v,w
45	ALHA78043, 78045	w
46	ALHA78103, 78105	t,w
47	ALHA80101, 80103, 80105, 80107, 80108, 80110, 80112, 80113, 80114, 80115, 80116, 80117, 80119, 80120, 80125	v,w
48	ALHA81027, 81028, 81029	w
49	BTNA78001, 78002	v,w
50	RKPA78001, 78003	w
51	RKPA79001, 79002, 80202, 80219, 80225, 80252, 80261, 80264	w
52	EET82605, 82606	w

TABLE C.—Continued.

Pair no.	Paired specimens	Criteria
	LL3 CHONDRITES	
53	ALHA76004, 81251	w
	LL6 CHONDRITES	
54	RKPA80222, 80238, 80248	w
	MESOSIDERITES	
55	RKPA79015, 80229, 80246, 80263	w
56	ALHA81059, 81098	w
	IRONS	
57	ALHA76002, 77250, 77263, 77289, 77290	t,x,y,z
58	DRPA78001, 78002, 78003, 78004, 78005, 78006, 78007, 78008, 78009†	t,v,x,y

†Seven additional specimens (DRPA78010–78016), collected at the same time from the same small area, are believed by all workers to be included in this pairing even though they have not been studied in detail. See Scott (Chapter 13) and Clarke, R.S., Jr. 1982. The Derrick Peak, Antarctica, Iron Meteorites. *Meteoritics*, 17:129–134.

☆ U.S. GOVERNMENT PRINTING OFFICE: 1989-181-717/60033